T_3 AS A PRIMARY HEPATIC MITOGEN

Thesis submitted for the degree of Doctor of Philosophy

(PhD)

Anton Bungay MA

2008

UCL Centre for Hepatology

Hampstead Campus

Royal Free and University College Medical School

London

ProQuest LLC
789 East Eisenhower Parkway
P.O. Box 1346
Ann Arbor, MI 48106-1346

ABSTRACT

An exciting therapeutic goal would be to use agents in clinical practice which could increase the size of a patient's functioning hepatic tissue in times of liver disease such as in the recovery phase from liver transplantation. An increase in the size and function of the liver at times such as this would ensure a more rapid recovery and less associated liver related morbidity and mortality.

As a group, the primary hepatomitogens might be employed to this end. Tri-iodothyronine (T_3) is a non carcinogenic agent and a very plausible candidate to be used in this setting.

T_3 is one of a number of drugs which can bring about proliferation of hepatocytes in the adult liver without any preceding cell loss i.e. a process of direct hyperplasia as opposed to the compensatory regeneration one sees following hepatectomy.

The work undertaken in this thesis aims to form a better understanding of the mechanism of action of the hepatomitogen tri-iodothyronine, T_3.

Thus far the mitogenic response is reliably modelled *in vivo* in the rodent but not in hepatocyte culture. This research attempts to demonstrate directly for the first time a mitogenic effect in human liver and starts with exploring T_3 effects in perfused liver and then *in vivo* in the rodent model where gene array studies are performed to identify novel mediators of the hepatic T_3 proliferative response.

Potential mediators have their serial expression profiles studied over time after T_3 stimulation by Real Time PCR.

Finally, the role of mTOR (important in mediating cell growth and proliferative signalling pathways) is identified in mediating the hepatic mitogenic T_3 response.

CONTENTS

FIGURES

TABLES

ACKNOWLEDGEMENTS

I would like to thank the Dunhill Medical Trust and the Liver Group Charity for funding this research project.

I would like to also thank my supervisors, Professor Humphrey Hodgson and Dr. Clare Selden, for their valuable supervision and guidance throughout this PhD project.

Thank you also to the other members of the Liver Group for their support and technical assistance throughout.

The greatest thanks go to my parents and friends who provide enduring and everlasting support. Thank you Anna.

ABBREVIATIONS

Ab	Antibody
Alb	Albumin
APES	Aminopropyl-trimethyl-silane
ATP	Adenosine triphosphate
BCA	Bicinchoninic Acid
BR931	4-chloro-6-(2,3-xylidino)-2-pyrimidinylthio-(N-beta-hydroxyethyl) acetamide
BrdU	Bromodeoxyuridine
BS	'Basingstoke' – local laboratory code for human liver specimen
BSA	Bovine Serum Albumin
BTEB	Basic Transcription Element Binding Protein
CAR	Constitutive Androstane Receptor
CBP	CREB-binding protein
CCl_4	Carbon tetrachloride
CDK	Cyclin dependent kinase
CHO	Chinese hamster ovary
CoA	Co-activator
CoR	Co-repressor
CPA	Cyproterone acetate
DAB	3,3'-diaminobenzidine chromogen solution
DAG	Diacylglycerol
DBD	DNA Binding Domain
DEPC	Diethylpyrocarbonate
DMSO	Dimethyl Sulphoxide
DNA	Deoxyribonucleic Acid
ECM	Extra-cellular matrix
EDB	Ethylene dibromide
EDTA	Ethylenediaminetetra-acetic acid
EGF	Epidermal Growth Factor
ERK	Extra cellular signal-related protein kinase
FBS	Foetal Bovine Serum
FC	Fold change
FCS	Foetal Calf Serum

FDA	Food and Drug administration
FFPE	Formalin Fixed Paraffin Embedded
FGF	Fibroblast Growth Factor
G6P	Glucose-6 phosphatase
GAPDH	glyceraldehyde-3-phosphate dehydrogenase
GF	Growth Factor
GGT	Gamma Glutamyl Transpeptidase
GO	Gene ontology
GSTP	γ-glutamyl transpeptidase
GTF	General Transcription Factors
HAT	Histone acetlytransferase
HCO_3^-	Bicarbonate
H&E	Haematoxylin and Eosin
HCC	Hepatocellular carcinoma
HDAC	Histone deacetylase
HEPES	4-2-hydroxyethyl-1-piperazineethanesulfonic acid
HGF	Hepatocyte Growth Factor
HRP	Horseradish Peroxidase
IFN	Interferon
Ig	Immunoglobulin
IGF	Insulin-like Growth Factor
IL	Interleukin
i/p	intraperitoneal
IP_3	inositol triphosphate
IPRL	isolated perfused rat liver
IRD	Inner Ring De-iodination
K^+	Potassium
KF	Kruppel Factor
LAT1	human system L amino acid transporters
LBD	Ligand – binding domain
LN	Lead nitrate
LPS	Lipopolysaccharide
MAPK	Mitogen Associated Protein kinase C
MCT	monocarboxylate transporter family
MOPS	3-(N-Morpholino)-propanesulfonic acid

mRNA	messenger ribonucleic acid
mTOR	mammalian target of rapamycin
NaOH	Sodium hydroxide
NF-κB	Nuclear Factor- κB
npc	Non-parenchymal cells
NTC	Non template control
NTCP	Na-taurocholate cotransporting polypeptide
OATP1	Na-independent organic anion transporting polypeptide 1
ORD	Outer Ring De-iodination
PBS	Phosphate Buffered Saline
PCNA	Proliferating cell nuclear antigen
pCO_2	Partial pressure of carbon dioxide
PDGF	Platelet-Derived Growth Factor
PDS	Polydimethylsiloxane
pH	potential of hydrogen
PH	Partial Hepatectomy
PI3-kinase	phosphatidylinositol 3-kinase
PIKK	phosphatidylinositol 3-kinase (PI 3-kinase)- related kinase
PKA	Protein kinase A
PKC	Protein kinase C
PLC	Phospholipase C
PMSF	phenylmethylsulphonyl fluoride
pO_2	partial pressure of oxygen
PP	Peroxisome Proliferator
PPAR	Peroxisome Proliferator Activated Receptor
PPR	Peroxisome Proliferator
PPRE	Peroxisome Proliferator response element
pRb	Retinoblastoma protein
PtdIns(4,5)P_2	phosphatidylinositol (4,5)-biphosphate
PtdIns(3,4,5)P_3	phosphatidylinositol (3,4,5)-triphosphate
PTU	Propylthiouracil
PVDF	Polyvinylidene Difluoride
RAR	Retinoic Acid Receptor
RNA	Ribonucleic acid
RNase	Ribonuclease

RT-PCR	Reverse-Transcriptase Polymerase Chain Reaction
RXR	Retinoid X Receptor
s/c	sub-cutaneous
S.D	Standard Deviation
SD	Sprague Dawley
SDS-PAGE	Sodium dodecyl sulphate polyacrylamide gel electrophoresis
SRCs	Steroid receptor co-activators
STAT	Signal Transducer and Activator of Transcription
T_2	Di-iodothyronine
T_3	3,5,3'-L-tri-iodothyronine
T_4	Thyroxine
TAE	Tris Acetic Acid EDTA
TAT	Tyrosine Aminotransferase
TBG	Thyroxine Binding Globulin
TBS	Tris-Buffered Saline
TCPOBOP	1,4-bis [2-(3,5-dichloropyridyloxy)] benzene
TGF	Transforming Growth Factor
THR	Thyroid Hormone Receptor
TNF	Tumour Necrosis Factor
tRA	Trans Retinoic acid
TRα	Thyroid receptor α isoform
TRβ	Thyroid receptor β isoform
TRE	Thyroid Hormone Response Elements
TSC	Tuberous sclerosis complex
TSH	Thyroid Stimulating Hormone
TTR	transthyretin
USW	University of Wisconsin solution
3D	Three-Dimensional

Chapter 1 - General Introduction

1.1 Synopsis

The thyroid hormone tri-iodothyronine (T_3) has been previously studied as a primary hepatic mitogen (Forbes *et al.* 2000; Short *et al.* 1972; Malik *et al.* 2003). It is an attractive candidate as a non-carcinogenic therapeutic agent which may be used in the future to enhance the functioning mass of a patient's liver not only at the time of liver surgery, either following a resection or liver transplantation, but also during an acute chemical or viral liver related illness. A more rapid recovery of functional hepatic mass would lead to speedier patient recovery and quicker resolution of the diseased state.

The proliferative hepatic effect has been well established *in vivo* in the rodent model where one sees a peak in hepatocyte DNA synthesis 24 hours after a sub-cutaneous dose of T_3 has been administered to the animal (Francavilla *et al.* 1994). However no such mitogenic mode of action has been shown *in vitro* in either rodent or human liver samples. The *in vitro* conditions likely do not reflect the more complex and highly regulated physiological state that exists *in vivo*.

The work undertaken in this PhD thesis therefore attempts to more accurately elucidate the T_3 mitogenic mechanism of action and also to demonstrate a direct mitogenic effect of T_3 on perfused human liver pieces and human hepatocytes in cell culture conditions where no such T_3 effect has thus far been successfully demonstrated. A prime goal was to search for an early marker of the mitogenic T_3 effect which could then be used in organ perfusion and hepatocyte cell culture experiments to confirm a mitogenic T_3 effect in human liver.

The **first** chapter is a general introduction.

The **second** chapter outlines the general methods that were utilised in carrying out this research project. More specific methodology relating to individual results chapters are outlined separately within each chapter.

The **third** chapter describes organ perfusion experiments and how it may be possible to model the effects of liver growth factors in an *ex-vivo in vitro* organ perfusion system and to attempt to demonstrate a mitogenic effect of T_3 on human liver samples.

The **fourth** chapter investigates the *in vivo* rodent hepatic response to T_3 by measuring changes in cyclin D1, an important regulator of the cell cycle. An early molecular marker of the T_3 mitogenic effect is searched for to enable T_3 effects to be measured in

the organ perfusion experiments of Chapter 3. The oncogene Bcl-3 is also probed as a potential candidate critically mediating the T_3 mitogenic response by examining the hepatic proliferative response to T_3 in Bcl-3 knockout mice.

The **fifth** chapter uses RNA expression microarray technology to define which genes are up or down regulated in T_3 treated euthyroid rat liver after 1 hour and then after 3 hours, a scenario not previously investigated in the published literature. This is once again in an effort to identify potential novel early candidates as mediators of the mitogenic T_3 effect.

The **sixth** chapter describes using Real Time PCR technology to examine the hepatic expression profile of candidate T_3 responsive genes, identified in Chapter Five, that may mediate the mitogenic response in rodent liver.

The **seventh** chapter investigates the role of the mammalian Target of Rapamycin (mTOR) in mediating the mitogenic hepatic T_3 effect. Other workers have shown it lies at the heart of signal transduction pathways which are T_3 responsive and therefore its role is further scrutinised.

Chapter **eight** outlines a general set of conclusions from this body of work as well as future directions of work.

1.2 Liver's Role

Many vital functions for the body are provided for by the liver and these include synthesis of many of the plasma proteins, incorporation of toxic ammonia into the non-toxic urea, regulation of plasma glucose levels, lipid mobilisation and export, synthesis and export of the bile to the intestine, metabolism of a host of drugs and toxins too. Loss of life results within a few hours of liver removal.

Severe liver damage can result after exposure to a range of toxins such as the xenobiotics acetaminophen and carbon tetrachloride. Liver damage can also occur after exposure to other injurious agents for example viruses and alcohol which can cause massive and acute hepatic damage or over a longer period of time they may cause chronic liver injury leading to eventual fibrosis and then cirrhosis culminating in a diseased and failing liver with a myriad of systemic complications.

1.3 Thyroid hormone production, transport and metabolism

The thyroid hormones have important effects on growth, development and metabolism. During foetal development and early childhood some of these effects are particularly important and this is reflected in the human clinical syndromes such as cretinism where one sees delayed growth for example (Gruters and Krude 2007). In adults the effects of thyroid hormones are seen in changes in oxygen consumption, lipid, protein and carbohydrate metabolism.

The thyroid gland produces two hormones, T_4 (L-thyroxine) and T_3 (L-triiodothyronine). Iodine is an important constituent making up 65% of the weight of T_4 and 58% of the weight of T_3. T_3 has a ten times greater affinity and efficacy than thyroxine for the nuclear receptor. Only a very small fraction of the circulating hormone is free (unbound) and biologically active, as that which is bound to carrier proteins is inactive (Brent 1994).

Intracellular hormone is in equilibrium with free thyroid hormone in serum. Total hormone concentration in serum is kept at a level proportional to the concentration of carrier proteins, and appropriate to maintain a constant free hormone level. It is a minute fraction of the total extra-thyroidal hormone < 0.5% which is available to tissues. The major serum thyroid hormone binding proteins are thyroxine binding globulin (TBG), transthyretin and thyroxine binding pre-albumin and albumin (Kohrle *et al.* 1987).

Thyroid hormone metabolism is regulated through three groups of enzymes termed the de-iodinases (Kohrle 2000). About 80% T_3 is produced outside the thyroid gland by peripheral conversion of T_4 to T_3. The main organs involved in this are liver, muscle and kidneys. T_3 is therefore the bioactive moiety of thyroid hormone and so T_4 is viewed as a pro-hormone that becomes activated by conversion to T_3 (DiStefano, III *et al.* 1982).

Seleno-deiodinases are responsible for inactivation of T_4 to r T_3, conversion of rT_3 and T_3 to T_2 and activation of T_4 to T_3 (Figure 1).

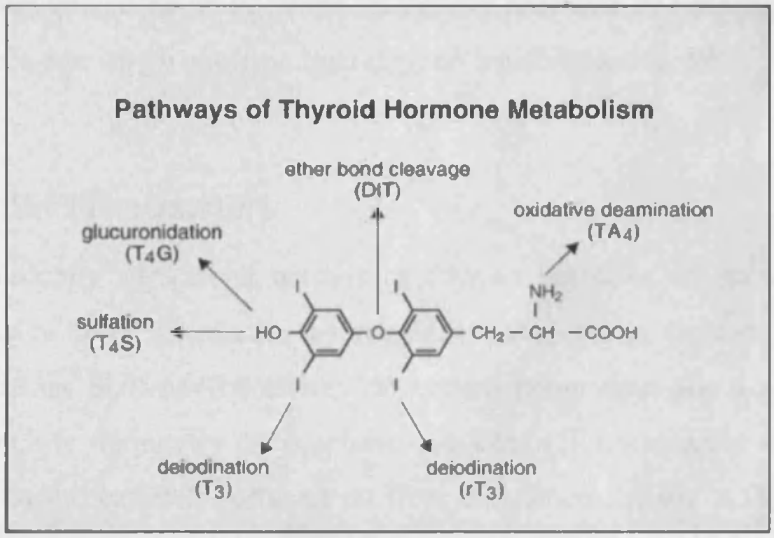

Figure 1. The conversion of thyroxine T_4 to a variety of products by the seleno-deiodinase enzyme system.

About one third of T_4 is converted by ORD (outer ring deiodination) to T_3 and about one third to rT_3. The remainder of the T_4 is metabolised by different pathways using glucuronidation and sulfation. The metabolite 3,3'- T_2 is produced by IRD (inner ring deiodination) of T_3 and ORD of rT_3. Therefore IRD is considered to be a deactivating pathway while ORD is an activating pathway. All three de-iodinases have been cloned and characterised in various species.

Hepatic D1 is largely responsible for the major part of peripheral T_3 production. In clinical practice this is the enzyme inhibited by the anti-thyroid drug propylthiouracil, PTU (Sanders *et al.* 1997).

Type 2 de-iodinase is found in skeletal muscle, pituitary and the CNS and produces about 30 mmol extra-thyroidal T_3. In critical tissues such as the brain, D2 enzyme is required to ensure local conversion of T_4 to T_3 so that intracellular T_3 levels can be regulated independently from variations in plasma T_3 levels (Leonard *et al.* 2000).

Inactivation of T_3 and T_4 can occur with the type 1 and 2 deiodinases but it is type 3 which is the main inactivator, exhibiting mainly inner ring de-iodination. It catalyses the conversion of T_4 to r T_3 and T_3 to T_2, both inactive metabolites, in liver, skin and CNS (Bianco *et al.* 2002).

The first effects of thyroid hormone on metabolic rate were described over 100 years ago by Magnus-Levey in 1895 and since then there have been many proposed models described for its mechanism of action.

The best characterised mode of action of thyroid hormone tri-iodothyronine (T_3) is on its nuclear receptor which acts as a ligand gated transcription factor.

1.3.1 Specific Transporters

For the 'classically' described actions of thyroid hormone to occur on its nuclear receptor it has to cross the plasma membrane. It seems that it crosses the membrane by specific processes that may be energy dependent rather than just a simple process of diffusion which is frequently the mechanism quoted (Hennemann *et al.* 2001). Studies have shown in the isolated perfused rat liver that when hepatic ATP is decreased by fructose, uptake of thyroid hormone into the liver is decreased (de Jong *et al.* 1993). Saturable specific transport of thyroid hormones often found to be energy and sodium dependent has been found in normal human and rat liver cells, as well as in human and rat hepatoma cells.

A variety of specific iodothyronine transporters are now recognised. The Na-taurocholate cotransporting polypeptide (NTCP), and the Na-independent organic anion transporting polypeptide 1 (OATP1) are examples (Friesema *et al.* 2005a; Friesema *et al.* 2005b). The OATP represent a large family of homologous proteins many of which have been shown to transport different iodothyronines. OATP1B2 is expressed in rat liver for example and is involved in transport of T_3 (Cattori *et al.* 2000).

Another class of transporters are the amino acid transporters and since the iodothyronines are composed of 2 tyrosine residues this comes as no surprise. Two identified transporters are LAT1 and LAT2 (human system L amino acid transporters) and their involvement in T_3 transport has been demonstrated extensively in studies using Xenopus oocytes which were injected with the cRNAs for human LAT1 and then the uptake of ^{125}I labelled iodothyronines was examined (Friesema *et al.* 2001).

A T type amino acid transporter, a member of the monocarboxylate transporter family (MCT) identified as MCT8 has been shown to be an active and specific iodothyronine transporter (Friesema *et al.* 2003). In humans there is a clinical syndrome whereby mutations in this transporter lead to severe psychomotor retardation and elevated T_3 levels. The gene is X linked. It seems it is important in neuronal T_3 transport particularly during brain development (Friesema *et al.* 2006).

1.3.2 'Classical' actions of thyroid hormone

The major thyroid hormone receptor is the nuclear receptor for T_3 (Brent 1994). It is part of the nuclear receptor superfamily which includes the glucocorticoid, androgen, oestrogen, progesterone, vitamin D, retinoid X, peroxisome proliferator receptor and retinoic acid receptor (RAR). T_3 binds to its receptor with 10 to 15 times greater affinity than does T_4 (Evans 1988).

There are two major receptor isoforms, TRα and TRβ, located in humans on chromosomes 17 and 3 respectively (Lazar 1993). The thyroid receptors have a central DNA binding domain (DBD) and a carboxy terminal ligand – binding domain (LBD). The DNA binding domains are comprised of two distinct zinc fingers that are separated by a 15-17 amino acid linker sequence. The P-box is a small stretch of amino acids at the base of the first finger and it dictates the DNA sequence specificity of the receptor (Nelson *et al.* 1993).

Multiple isoforms are generated by alternate splicing from each gene, and TRα1 and TRα2 as well as TRβ1 and TRβ2 have all been cloned in humans (Williams 2000).

The TRα1 and TRβ1 isoforms bind thyroid hormone with near equal affinity and are ubiquitously expressed, however TRα1 predominates in the heart (50-70% TR) and TRβ1 in the liver (80% of TR).

Thyroid hormone receptors bind to TH response elements (TREs) in specific target genes and after binding TH, the receptor induces change in gene expression by either increasing or decreasing transcriptional activity (Figure 2).

The consensus sequence recognised by nuclear receptors frequently contains a hexamer AGGTCA known as the half site and two half site sequences are required for functional and efficient binding (Umesono *et al.* 1991). Although TR can bind to certain TREs as a homodimer, it binds to most TREs as a heterodimer with the retinoid X receptor or RXR. These RXR proteins represent its most important heterodimeric partners. They enhance TR binding to the DNA and reduce the rate of receptor dissociation from DNA (Wahlstrom *et al.* 1992).

After binding to DNA, TR alters transcriptional activity by interacting with an array of transcriptional co-factors. In the absence of thyroid hormone, TR represses basal transcription, a phenomenon known as transcriptional silencing. Adding TH reverses basal suppression and increases transcriptional activation.

Co-repressors form a complex with other repressors that have histone deacetylase activity. Local histone deacetylation plays a critical role in the basal repression by unliganded TR/co-repressor complex by maintaining local chromatin structure in a state

that decreases basal transcription. When T_3 binds the TR undergoes a conformational change that dissociates CoRs and recruits a host of co-activators (Shibata *et al.* 1997). The SRC family and CBP proteins are thought to form part of this co-activator complex and these proteins have histone acetlytransferase activity (HAT) (Ribeiro *et al.* 1998). The enzymatic acetylisation of the nucleosome allows for an open chromatin configuration of the TRE on genomic DNA. This open structure facilitates the assembly of the basal transcription machinery and enhances the rate of mRNA transcription of thyroid responsive genes.

Figure 2 Role of co-repressors and co-activators in the control of T_3-regulated genes. In the absence of T_3, the RXR-TR heterodimer recruits co-repressors (CoR), which in turn, assemble additional components of a repressor complex that includes histone deacetylase (HDAC). Deacetylation of histones induce transcriptional repression. In the presence of T_3, the co-repressor complex dissociates and co-activators (CoA) bind to TR. The co-activator complex can include steroid receptor co-activators (SRCs)/p160, CREB-binding protein (CBP), p300/CBP associated factor (P/CAF), and proteins with histone acetyltransferase (HAT) activity. Vitamin D receptor interacting protein/TR associated protein (DRIP/TRAP) complex can also interact with liganded TR, and may cycle with SRC/p160 complex. General transcription factors (GTFs) are also indicated. Acetylation of histones modifies chromatin structure to enhance transcriptional activation (www.thyroidmanager.org).

1.3.3 TRα1 and TRβ1 Receptor specific agonists

Data from knockout mice suggest that TRα1 mediates the effect of thyroid hormone on heart rate and TRβ1 is important in mediating the cholesterol lowering and TSH-suppressant effects of T_3 (Forrest *et al.* 1991).

The advent of thyromimetic agents which can act specifically on one receptor or the other will be useful in reducing any potential harmful cardiac side effects for example tachycardia. This may allow the induction of hyperthyroidism in specific tissues while reducing the effect in others. There has been developed a new class of halogen free thyroid hormone agonists which are highly selective for the TRβ1 receptor. The first molecule in this group is termed GC-1 (Taylor *et al.* 1997).

Columbano (Columbano *et al.* 2006) has looked at the effects of GC-1 on the rodent liver and pancreas. A continuous bromodeoxyuridine (BrdU) labelling index of 48% after 2 days treatment compared to only 9.8% in controls was observed. After 18 hours following a single dose of GC-1 there was a 15 fold increase in the number of positive BrdU hepatocyte nuclei.

The proliferative effect was also noted in the pancreas with significantly increased rates of acinar cell proliferation seen. Consistent with other primary mitogens there is no increase in the immediate early genes c-fos and c-jun seen in compensatory liver regeneration, however as with previous reports there is an early induction of the cell cycle protein cyclin D1 mRNA (after only 2 hours). These molecular processes are discussed later. The results of this study strongly suggest that the proliferative hepatic effect of T_3 is mediated by the TRβ1 receptor, the prevalent isoform in the liver.

1.3.4 'Non Genomic' effects of thyroid hormone

The 'classical' mode of action of T_3 with its nuclear receptor leading to gene transcription events will have a latency response time of hours to days (Bassett *et al.* 2003). There are however a number of T_3 effects which occur in a matter of seconds or minutes and are therefore incompatible with the classic mode of action of T_3 (Losel and Wehling 2003; Wehling and Losel 2006; Wehling *et al.* 2006). These 'non- genomic' or 'non-classical' steroid hormone effects encompass any action that does not directly affect nuclear gene transcription (Davis and Davis 1996; Zhang and Lazar 2000). These are typified by having a short latency, are unaffected by inhibitors of transcription and translation and persist in genetically modified mice that lack the classical nuclear receptors. Generally these non-genomic pathways are mediated by secondary messenger

signalling pathways for example phospholipase C, diacylglycerol, and the MAPK pathway (Kavok *et al.* 2001; Alisi *et al.* 2004). The actions may be mediated by membrane associated isoforms of the thyroid hormone nuclear receptor or by novel receptors which as yet have not have been fully identified.

Non-genomic actions of thyroid hormone have been described at the plasma membrane, in the cytosol and in other cellular organelles. They have included the modulation of Na^+, K^+, Ca^{2+} and glucose transport, activation of PKC, PKA and ERK/MAPK and regulation of phospholipid metabolism by activation of PLC and PLD (Tang *et al.* 2004; D'Arezzo *et al.* 2004).

One of the earliest reports of the non genomic action was to increase 2-deoxyglucose uptake in chick embryo heart cells (Segal *et al.* 1977) and later the same author demonstrated the same effect in various tissues of the rat (Segal 1989a; Segal 1989c; Segal 1989b).

In red blood cells T_4 and T_3 have been shown to stimulate plasma membrane and sarcoplasmic reticulum Ca^{2+} -ATPase, increasing Ca^{2+} efflux from the cytosol (Rubinacci *et al.* 1992). The action on Ca^{2+}-ATPase is likely mediated by PKC, and this follows from activation of PLC which forms DAG from phosphatidylinositol. IP_3 is produced by this reaction and can liberate Ca^{2+} from intracellular stores (Berridge 1993b; Berridge 1993a). The MAPK signal cascade may be driven by T_4, finally exerting multiple effects such as modulating the phosphorylation of STAT, p53 and even TRβ1. This is an example of non-genomic modulation of a nuclear i.e. genomically acting receptor for the same hormone (Shih *et al.* 2001).

In the cardiovascular system T_3 enhances cardiac output and reduces systemic vascular resistance in adult males within 3 minutes (Schmidt *et al.* 2002).

T_3 treatment also lowered the prevalence of atrial fibrillation in artery bypass graft patients, which may be explained by the rapid response of voltage gated K^+ channels to thyroid hormone (Klemperer *et al.* 1996).

Cell culture studies suggest that thyroid hormones rapidly, and non-genomically, regulate the Ca^{2+}ATPase enzyme, the Na^+ channel (I_{Na}) via PKC, the K^+ channel (I_K) via PI3-kinase, the Na^+/H^+ anti-porter via PKC and MAPK and the inward rectifying potassium channel (I_{K1}) (Davis and Davis 2002). Wang showed T_3 has a positive inotropic and arrythmagenic effect by increasing sarcoplasmic reticulum Ca^{2+}, cell shortening, contractility and calcium mediated arrhythmic activity (Wang *et al.* 2003).

In vitro, independent of protein synthesis, T_3 induces IP_3 and calcium signalling and augments the effects of IFNγ via PKC and PKA (Lakatos and Stern 1991; Lin *et al.*

1997). In addition, T_4-linked to agarose, which does not cross the plasma membrane, has been shown to activate MAPK by a pertussis toxin sensitive mechanism suggesting the actions of a G protein-coupled thyroid hormone membrane receptor (Lin *et al.* 1999). *In vivo*, T_4 regulates thermogenesis and the lipolytic activities of catecholamines within 30 minutes (Lynch *et al.* 1985).

Circulating T_3 levels are kept very stable so it may be hard to see how such hormones can bring mediate such rapid and physiologically critical actions. However there is cell type specific regulation of pre-receptor ligand metabolism by the deiodinase enzyme system. D2 has a very short half life and so it may help in rapid regulation of intracellular T_3. As thyroid hormone enters cells through carrier mediated mechanisms then these too represent targets for regulating intracellular thyroid hormone concentrations.

There is emerging evidence that there may be effects on cell proliferation and differentiation by way of these pathways just described. The signals may converge with more classical genomic effects so the cell can respond in an appropriate coordinated fashion, integrating short term and long term needs (Bassett *et al.* 2003).

In further understanding the combination of both non-genomic and classical genomic actions it is proposed that there is a two-step model of steroid hormone action. The rapid non-genomic as well as the delayed genomic actions are comprised together with possible mechanisms of modulation of classic receptor-induced gene transcription by non-genomic signal transduction pathways (Figure 3).

Figure 3 The integration of genomic and non-genomic signalling cascades. In this example steroids act as the ligand for their receptors which sit either at the cell membrane, the cell cytosol and/or the cell nucleus where previously their direct nuclear effects have been classically described. Novel nongenomic second messenger mediated effects are depicted which are initiated at the cell membrane (Wehling and Losel 2006).

1.4 Thyroid hormone membrane receptors

1.4.1 Non classical thyroid hormone receptors

Only recently has the identity of one cell surface thyroid hormone receptor been established (Davis *et al.* 2005), namely on the integrin αVβ3 (Bergh *et al.* 2005; Cody *et al.* 2007). This is linked by transduction cascades involving MAPK to cell membrane transport functions and to MAPK-mediated intra-nuclear events including transcription. Integrins are ubiquitous heterodimeric structural proteins of the cell membrane that can convey signals from the extra-cellular matrix (ECM) to the cell. The integrins are a superfamily of glycoproteins that consist of an α- and β-subunit that associate in defined combinations that yield more than two dozen different mammalian integrin subtypes.

In one study T_4 was found to promote angiogenesis in a chick chorioallantoic membrane model but when it was attached to agarose and therefore unable to enter the cell interior it still had the angiogenic effect (Davis *et al.* 2004). It is clear that T_3 can be associated with membrane initiated events that culminate in the cell nucleus, for example

activation of the phosphatidyl-inositol 3–kinase Akt/protein kinase B signal transduction cascade modulates the transcription of the calcineurin inhibitor ZAKI4A in skin fibroblasts (Cao *et al.* 2005). Whether such activation occurs via αVβ3 or another integrin is not yet clear.

The affinity of this integrin receptor is substantially lower for T_3. However further recent work has shown that T_3 (in higher concentration than T_4) could bring about proliferation of glioma cell lines C6, F98 and GL261 as measured by thymidine incorporation and PCNA accumulation (Davis *et al.* 2006). This effect was inhibited by the T_4 analogue, tetraiodothyroacetic acid, and by an $\alpha_V\beta_3$ RGD recognition site peptide, both of which block T_4 binding to integrin $\alpha_V\beta_3$ but are not agonists.

1.5 The cell cycle

Control of cell proliferation is essential and the cell cycle describes the way in which cells try to achieve this. It is important to note that the vast majority of hepatocytes remain in the resting phase or G_0 phase of the cell cycle and only will emerge from this into the active parts of the cycle following certain stimuli. However after 2/3rds hepatectomy 95% of normally quiescent hepatic cells rapidly re-enter the cell cycle in response to this well established stimulus to bring about compensatory regeneration.

A key step in progression through the cell cycle is that of passing through G_1 having emerged from the resting state and then going past a restriction point allowing DNA synthesis to occur and then cell division.

Cyclin D1 and its associated cyclin dependent kinases are important in the early phase of the cell cycle. Activation through phosphorylation between cyclins and the cyclin dependent kinases (CDKs) leads to cell cycle progression. After a complex chain of events the ultimate substrate is the retinoblastoma protein, pRb which is the major target of the cyclin D1/CDK4 complex. Following its phosphorylation E2F transcription factors are free and can trans- activate genes that allow progression from G_1 to S phase. This is discussed in more detail in chapter four.

1.6 Compensatory and Direct Liver Hyperplasia

Liver regeneration occurs when there is a major loss of hepatic tissue. The liver is noted to possess the remarkable ability to regenerate itself back to an appropriate weight and in so doing to return to a normally functioning hepatic mass appropriate to the size of the organism. This process of liver growth is termed compensatory hyperplasia but in

addition to this process it is recognised that the liver can be made to grow following the application of a mitogenic stimulus without any preceding loss of hepatic mass and this is termed *direct* hyperplasia (Michalopoulos and DeFrances 2005; Michalopoulos and DeFrances 1997).

In the first situation (compensatory hyperplasia), for example following the well known stimulus of partial hepatectomy, cells move from the resting phase of the cycle G_0 to G_1 part of the active cell cycle.

Very briefly the molecular events involve hepatocyte priming by cytokines TNF-α and IL-6 and then activation of the important downstream transcription factors including STAT-3 and NF-κB before activation of the immediate early genes c-fos, c-jun and c-myc (Fausto and Riehle 2005). Delayed gene activation leads to activation of the cell cycle cyclins which allow progression through the cell cycle after passing the G_1 restriction point, having emerged from the resting state G_0 (Columbano and Shinozuka 1996).

In the *direct hyperplasia* response (which occurs without liver cell loss), proliferation comes about without the activation of these transcription factors and early response genes and cyclin D1 activation occurs earlier (within at least 8 hours compared to 16 hours after partial hepatectomy in rodents). A host of 'mitogens' can bring about the direct hyperplasia response including of course T_3 (Fausto 2000; Fausto *et al.* 1995).

1.6.1 Compensatory hyperplasia

The surgical model for partial hepatectomy (PH) leading to compensatory regeneration of the liver was described by Higgins and Anderson in the rat and mouse (Higgins and Anderson 1931). A two thirds PH removes 70% of the liver mass and the residual 30% grows to restore the organ back to its original mass. The growth does not however restore the shape of the liver, and it is now composed of two lobes instead of five. A similar pattern of restoration of hepatic mass is seen in humans in the setting of partial hepatectomy. Following hepatectomy a measurable peak in DNA synthesis is seen in hepatocytes at 24h in the rat and 40h in the mouse and this can even vary between strains. The onset of DNA synthesis is well synchronised beginning around the portal vein and proceeding to the central vein. DNA synthesis in the non parenchymal cells (npcs) peaks at around 36 to 48 hours (Figure 4).

The differences in timing of DNA replication in rats and mice is due to a longer G_1 phase in mice. Studies using thymidine incorporation have shown that more than 90%

of the hepatocytes participate in the regenerative process and so it is not solely due to a subset population. The proliferation begins in hepatocytes around the portal triads and progresses to the central veins by 48h in the rat. However proliferation of the other cell populations proceeds at a different rate, for example endothelial cells start proliferating after three days and peak at day five (Grisham 1962).

Figure 4 Time kinetics of DNA synthesis in different liver cell types during liver regeneration after partial hepatectomy. The four major types of liver cells undergo DNA synthesis at different times. Hepatocyte DNA synthesis peaks at 24 hours, whereas the other cell types proliferate later. Regenerating hepatocytes produce growth factors that can function as mitogens for these cells and it has been suggested that hepatocytes stimulate proliferation of the other cells by a paracrine mechanism (Michalopoulos and DeFrances 1997).

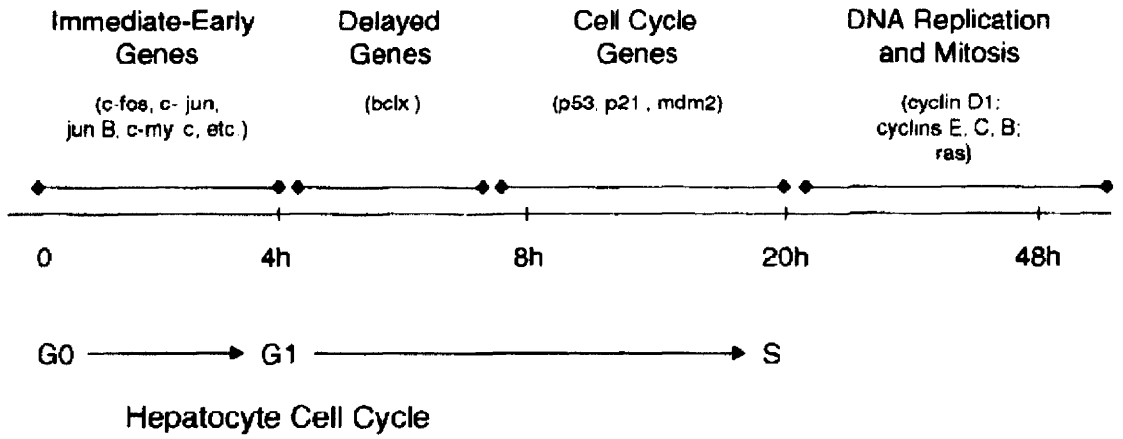

Figure 5 A timeline for the molecular processes involved in compensatory hepatic growth. Immediate early genes are expressed within four hours followed by delayed gene expression up to eight hours later. This parallels progression of the cell cycle from the resting G_0 phase into the active G_1 phase leading eventually to DNA synthesis in S phase.

1.6.1.1 Molecular events during compensatory hyperplasia

A number of genes are either newly expressed or increase their expression after partial hepatectomy (Taub 1996b; Taub 1996a) (Figure 5). The immediate early phase response occurs very rapidly and lasts for about 4 hours. As many as 100 genes participate in this phase (Taub 2004). The events upstream of this are still unclear but certain facts have been determined. Urokinase activity is up-regulated within minutes and the hepatocyte membrane is rapidly depolarised and this persists for more than 3 hours. EGF and HGF receptors are activated by tyrosine phosphorylation within 30 to 60 minutes.

An important group of transcription factors are activated after partial hepatectomy. These include NF-κB, AP-1 and STAT3. Their activation does not require *de novo* protein synthesis. After PH, NF-κB is activated within 30 minutes at the latest and this activation is transient and seen to disappear by 4 hours. Activation occurs through removal of the inhibitor IkB from the NF-κB heterodimer.

STAT3 activation is slower and is detectable in the liver 1 to 2 hours after hepatectomy. STAT3 is activated mainly by IL-6 cytokines (Fausto *et al.* 2006; Michalopoulos and DeFrances 2005; Cressman *et al.* 1995; Cressman *et al.* 1995).

The second phase of gene expression is the delayed gene response. A variety of cell cycle genes become activated including p53, p21, cyclins and cyclin dependent kinases. The induction of cyclin D1 is the most reliable marker of cell cycle progression.

Tumour necrosis factor (TNF) is a potent liver NF-κB inducer and it is hypothesised that the sequence of events after partial hepatectomy is TNF→TNFR-1→ NF-κB →IL-6→STAT3. The TNF-α primes liver cells to be transformed from a quiescent state to an activated G_1 state. Following on there is an increase in IL-6 levels occurring between 2 to 6 hours. This eventually leads to STAT3 activation and the immediate early gene response. IL-6 is produced by non parenchymal cells such as the Kupffer cell and it ligands with its receptor on the hepatocyte membrane. IL-6 bound to gp80 activates its associated gp130 molecule and then there is induction of homo-dimerisation of two gp130 molecules which leads to receptor activation.

It is important to note that hepatic regeneration proceeds eventually in IL6 -/- and TNFR1 -/- mice so other growth factors must compensate in the absence of IL6 and TNF triggered signalling cascades.

Two distinct pathways are seen to operate: a cytokine dependent pathway and a growth factor dependent pathway.

1.6.1.2 Cytokine pathways

TNF-α binds to its Kupffer cell receptor which results in IL-6 up-regulation. IL-6 binds to its receptor on hepatocytes and activates the Janus kinase pathway and this stimulates the STAT3 pathway. STAT3 (which is now active after it has dimerised) translocates to the nucleus where it activates about 36% of the immediate early genes. The activated JAK also stimulates the MAPK pathway.

Lipopolysaccharide (LPS) interacts with its receptor on the Kupffer cells and this may trigger the signalling after PH.

So, during liver regeneration, IL-6 activates two main pathways through the gp130–IL-6R complex — the STAT3 and MAPK signalling pathways. As the STAT3-null phenotype is 'embryonic-lethal', liver-specific STAT3 knockouts (where Alb Alb^+ $STAT3^{fl/fl}$ stands for albumin-driven promoter, and fl stands for floxed, or deleted, allele) were used to test the contribution of STAT3 to the growth response that is mediated by IL-6. Hepatocyte DNA synthesis in Alb^+ $STAT3^{fl/fl}$ livers was impaired after partial hepatectomy, and abnormalities in immediate-early-gene activation largely correlated with, but were not identical to, those seen in $IL\text{-}6^{-/-}$ livers. Normal activation of the MAPK (pERK) pathway in Alb^+ $STAT3^{fl/fl}$ livers supports the idea that not all of the effects of IL-6 on hepatocyte proliferation are mediated by STAT3 (Li *et al.* 2002). Furthermore, this study provided the first *in vivo* evidence that STAT3 promotes cell-

cycle progression and cell proliferation under physiological growth conditions, which implies that the separation between growth-factor- and cytokine-regulated pathways is not absolute.

1.6.1.3 Growth Factor pathways

On the basis of *in vivo* studies and *in vitro* studies in isolated hepatocytes, Transforming Growth factor (TGF-α) and Hepatocyte Growth Factor (HGF) are considered to be two of the most important growth factors. HGF is synthesised by stellate cells and acts in a paracrine manner for hepatocytes (Michalopoulos and Appasamy 1993). HGF and its receptor c-Met are important in many tissues and hence knockout of their genes results in a lethal phenotype. The mitogenic effect is mediated in part at least by TGF-α. However, as a large number of ligands and receptors belong to the TGF and EGF family, the inability to block all of these ligands and receptors simultaneously has made it difficult to prove that the potent hepatocyte mitogens TGF-α and EGF are crucial for regeneration.

1.6.2 Both pathways

HGF and TNF-α-IL-6 signalling are necessary for liver regeneration. It is however not yet fully known how growth factors and cytokines interact to lead to a full regenerative response. For example both HGF and TNF-α can induce cell proliferation and cyclin D1 activation (Schwabe *et al.* 2003; Talarmin *et al.* 1999).

The IL-6–TNF-α and HGF pathways both up-regulate the activity of the various homo- and hetero-dimeric AP1 transcription factors. AP1 activity is required for the activation of a number of proteins that are involved in the growth response

1.7 Direct hyperplasia

Proliferation of liver cells can also come about without preceding cell loss. A group of chemicals which is able to achieve this are known as primary hepatic mitogens (Table 1) and the process they invoke is termed *direct hyperplasia* (Columbano and Shinozuka 1996). The signalling pathways leading to DNA replication differ from those following partial hepatectomy. After nafenopin for example there is no increased activation of NFκβ, however this transcription factor is activated after partial hepatectomy (Menegazzi *et al.* 1997).

The hepatocyte proliferation induced by these agents comes about in the absence of activation of the other transcription factors AP-1, and STAT-3 or changes in the immediate early genes c-jun, c-fos and c-myc which occur following partial hepatectomy.

Table 1 The primary hepatic mitogens

Nuclear Receptor Family Ligands	**Others**
Tri-iodothyronine (T_3)	*Lead nitrate (LN)*
Cyproterone acetate (CPA)	*Ethylene dibromide (EDB)*
9-cis retinoic acid	*Tumour Necrosis Factor-α (TNF-α)*
Peroxisome proliferators e.g. nafenopin and Wy14643 and BR931	*4-Acetylaminofluorane*
1,4-bis [2-(3,5-dichloropyridyloxy)] benzene (TCPOBOP)	*α –Hexachlorocyclohexane*
Oestrogens	*Interleukin-6 (IL-6)*
	Phenobarbital

There is variety between these agents with regards to their mitogenic potency and the time taken to bring about DNA synthesis and cell replication (Ledda-Columbano *et al.* 1993; Ledda-Columbano *et al.* 1994). Importantly after the mitogenic stimulus is withdrawn there is elimination of the excess numbers of cells produced and this is most likely through the process of apoptosis.

A number of studies have shown that the pattern of immediate early gene expression seen after partial hepatectomy is not replicated after stimulation with either LN, EDB, CPA, nafenopin or Wy14643, where there was no increase in expression of for example c-fos (Coni *et al.* 1993; Chevalier *et al.* 1999). After induction of cell proliferation with CPA and nafenopin no changes were observed in either c-jun or c-myc (Menegazzi *et al.* 1997).

Observations thus far indicate that different signalling pathways are involved in triggering hepatocyte proliferation depending on

1) whether the stimulus is direct or compensatory hyperplasia
2) the type of primary mitogen

The different known primary mitogens will now be discussed in more detail.

1.7.1 The Nuclear Receptor Superfamily-RAR, RXR, THR, PPR

Nuclear receptor superfamily	**Ligand**
Thyroid hormone receptor like:	
RAR: RARα RARβ RARγ	Retinoic acid
PPR: PPARα PPARβ PPARγ	Peroxisome proliferators
Vitamin D receptor	Vitamin D
Constitutive androstane receptor CAR	TCPOBOP
THR TRα TRβ	Triiodothyronine
Retinoid X receptor like:	
Hepatocyte nuclear factor 4	
RXR α β γ	

Table 2 The Nuclear Receptor Superfamily

Nuclear hormone receptors comprise a large superfamily of ligand-modulated transcription factors, including the classical steroid and thyroid hormone receptors (TRs) as well as the retinoid hormone receptors (Table 2). These transcription factors classically activate target genes by binding specific DNA sequences located in the promoter of these genes. By comparing amino acid sequences of the first steroid hormone receptors cloned in the mid-1980s, a common structural and functional organization appeared. Four main domains are distinguished: the N-terminal A/B domain that varies in both sequence and length, comprising a ligand-independent transactivation function, called activation function 1 (AF-1); the highly conserved C domain forming an about 70 amino acid long DNA-binding domain (DBD); the D domain or so-called hinge domain, linking the DBD to the ligand-binding domain (LBD); and, the C-terminal E/F domain or LBD, containing a ligand-dependent transactivation function, termed AF-2.

According to the proposed unified nomenclature of nuclear hormone receptors, PPARs form the group C in the subfamily 1 of the superfamily of nuclear hormone receptors, i.e. NR1C. This large subfamily also comprises, for instance, the TRs (NR1A), the all-*trans* retinoic acid receptors, RARs, (NR1B), and the vitamin D3 receptor, VDR, (NR1I) (Germain *et al.* 2006). There are three PPAR isotypes, namely PPARα (NR1C1), PPARβ (NR1C2), and PPARγ (NR1C3), which have been found so far in cyclostoma, teleosts, amphibians, rodents and humans.

Most nuclear receptors will bind to DNA as hetero-dimers with the RXR (Szanto *et al.* 2004). This is thought to enhance affinity and provide greater target gene specificity. Indeed, a hallmark of this receptor family is the DNA binding domain which is folded in two zinc fingers. The DNA response element of nuclear receptors comprises two short hexameric sequence motifs closely related to AGGTCA.

The Retinoic acid receptor (RAR), the retinoid X receptor (RXR), the thyroid hormone receptor and the peroxisome proliferator receptor all possess six domains, two of which are a ligand-binding region and a central region that constitutively binds to DNA. These receptors classically act as ligand activated transcription factors which have a direct effect on gene expression through their DNA response elements (Umesono *et al.* 1988; Columbano and Ledda-Columbano 2003), as described earlier in this chapter.

1.7.2 Peroxisome Proliferators (PPs)

Hypolipidaemic drugs:
clofibrate, clofibric acid, ciprofibrate, WY-14,643, BR-931, methylclofenapate
cyproterone acetate, nafenopin
thiazolidinediones:
pioglitazone and rosiglitazone
Non-steroidal anti-inflammatory drugs:
Indomethacin, ibuprofen

The peroxisome proliferators are a diverse group of chemicals with a host of applications being used in medicine but also in industry and agriculture. In clinical medicine their uses are many, for example the hypolipidaemic fibrates and the insulin sensitising thiazolidinediones, pioglitazone and rosiglitazone (Escher and Wahli 2000). These drugs are so called because they induce peroxisome proliferation in the livers of rats and mice such that peroxisomal volume density is increased and certain

peroxisomal enzyme activities are induced. However they exert another notable effect, that of cell mitosis (Cattley 2003), an effect first noted in the 1960s by Hess.

When BR931, for example, is administered to adult male Wistar rats a wave of DNA replication is seen to start after 12 hours and this peaked at 24 to 36 hours (Ohmura *et al.* 1996). Northern blot analysis shows that there is no induction of HGF, transforming growth factor-alpha, or tumour necrosis factor-alpha mRNAs. In addition no induction of the early growth response genes is seen and gel mobility shift assays reveal no enhanced NFκβ binding to its DNA consensus sequence. The evidence points to the peroxisome proliferator binding directly to its nuclear receptor which then brings about DNA synthesis. This is a key difference in the unfolding molecular events when compared to the stimulus of PH.

The nuclear receptor binds to DNA as a heterodimer with the Retinoid X Receptor (RXR) which acts as the obligate partner for PPARs. The heterodimer binds to a specific response element the PPRE consisting of a direct repeat sequence separated by one oligonucleotide DR-1.

Three receptor isotypes have been identified: PPARα, PPARβ and PPARγ.

PPARα is predominantly expressed in the liver and is important in regulating fatty acid metabolism and the inflammatory response.

PPARβ is expressed ubiquitously in various tissues and is thought to be important in embryo implantation.

PPARγ is highly expressed in adipose tissue and is a potent regulator of adipocyte differentiation.

There is a good correlation between ability of a PP to bind to and/or activate PPARα and the potency of the PP as an inducer of hepatocarcinogenesis. Many, if not all, PP are ligands for PPARα, and it is hypothesised that this receptor is the major cellular target of hepatocarcinogenic PP in the liver.

Ligands have different affinities for the receptor sub-types. For example the fibrates such as Wy 14,643 and clofibrate preferentially activate PPARα but at higher concentrations significant activation of PPARγ does occur. The thiazolidinediones on the other hand show a much higher affinity for PPARγ (Lehmann *et al.* 1995).

PPARα ligands Wy 14,643 and clofibrate, are known to produce liver tumours in mice and rats. Wy 14,643 also induces DNA replication, as assessed by bromodeoxyuridine incorporation *in vivo* in mice and in primary rat hepatocyte cultures. The specific target genes mediating these effects remain unidentified (Peters *et al.* 2005). Clearly the

increased rates of cell proliferation are contributory to the development of hepatic tumours in these rodent models (Corton *et al.* 2000).

In 1990 the PPAR was cloned from mouse liver (Issemann and Green 1990) and eventually a PPARα null mouse was created which did not respond to PP treatment (Lee *et al.* 1995). The knockout animal provided conclusive evidence for involvement of the PPARα receptor. Feeding mice with Wy 14,643 or clofibrate leads to hepatic peroxisome proliferation and hepatocellular neoplasms in the wild-type mice, whereas their knockout counterparts are unaffected. Thus, the PPARα knockout mouse presents a useful animal model to determine the role of this receptor in rodent hepatomegaly and hepatocarcinogenesis.

These observations identify PPARα as a mediator of pleiotropic responses to peroxisome proliferators, which may be partly achieved by H_2O_2 generated through activation of target genes in peroxisomal β-oxidation. PPARα may mediate pleiotropic effects of peroxisome proliferators also by interfering with the cell-cycle. Indeed, a dominant negative PPARα protein prevents the suppression of hepatocyte apoptosis by the peroxisome proliferator nafenopin, suggesting that PPARα can abrogate the commitment of hepatocytes to apoptosis (James *et al.* 1998). However, the respective contribution of peroxisome proliferation and enhanced cell proliferation to hepatocarcinogenesis remains to be evaluated. Furthermore, a link between species-specific hepatic PPARα expression and hepatocarcinogenesis may exist. For instance, hepatic PPARα expression is reported to be lower in human vs. rodents, and no liver tumours are reported in the former upon treatment with peroxisome proliferators. The molecular basis of this strong species difference remains elusive (Corton *et al.* 2000).

In rats treated with PPs the increase in S phase cells has been frequently observed to preferentially occur in the periportal region (Barrass *et al.* 1993). This is observed with WY-14,643, clofibric acid, nafenopin and methylclofenapate. There is an observed increase in mitosis 1 to 2 days after treatment with the drug. The greatest increase in S phase (measured usually by tritiated thymidine incorporation or BrdU incorporation) is seen in the first week in rats fed WY-14,643 in their diet for a year, and there is a corresponding increase in liver weight (Marsman *et al.* 1988). After 1 day 8.8% of hepatocyte nuclei were flash labelled with tritiated thymidine after WY-14,643 and 5.6% after treatment with DEHP, compared to a control of 2.0%.

PPs may exert their effect on proliferation by affecting the expression of cyclins and cyclin dependent kinases. Roberts showed that cyclin E, cyclin D1, CDK4 and CDK2

accumulate upon stimulation with the PP nafenopin (Roberts *et al.* 2002). It has also been shown that PPs have an effect on apoptosis and suppress it (Roberts *et al.* 1995). The basal frequency of apoptosis is low in the rat liver, about 0.03% but after treatment with nafenopin this falls to 0.002%. Again this effect varies between the PPs and even between species whereby CI-924 decreases apoptosis in rat but not mouse liver. This is most likely one of the reasons why one sees the development of pre-neoplatsic foci which can lead to malignant liver tumours. The regression of hyperplasia after withdrawal of the PP comes about through apoptosis, and a rise of almost 6 fold in apoptosis is seen in rat liver after withdrawal of nafenopin.

There is a notable species differences with these drugs. For example in marmosets nafenopin, DEHP or ciprofibrate fail to induce any increase in liver mass. Syrian hamsters are observed to gain liver weight but there is no increase in the number of S phase hepatocytes. Therefore, most of the studies to characterise these agents have been conducted in rats and mice.

1.7.2.1 PPARγ and Liver Regeneration

More recently the role of the PPARγ receptor isotype has been studied in the setting of PH. Liver regeneration has been shown to be impaired in a number of animal models of fatty liver disease (Yang *et al.* 2001). Recent work sought to investigate the role of PPARγ in liver regeneration (Turmelle *et al.* 2006). The results show that thiazolidinediones impair liver regeneration with efficacies corresponding to their relative potencies of PPARγ (i.e. rosiglitazone > pioglitazone > troglitazone) when levels of BrdU incorporation are measured 36 hours following partial hepatectomy in mice pre dosed with one of these agents. The data implicate PPARγ as an important regulator in the hepatic regenerative response, a novel description reflecting the complexities that still exist in describing the molecular events in both direct and compensatory liver hyperplasia.

1.7.3 Retinoic Acid

Retinoids are natural and synthetic vitamin A derivatives which can have marked effects on cellular differentiation and proliferation.

Two classes of receptors mediate the effects of the retinoids, the retinoic acid receptor RAR (RARα, RARβ and RARγ) and the retinoid X receptor RXR (RXRα, RXRβ and

RXRγ). Signal transduction comes about following heterodimerisation of these receptors after ligand binding. Very little data are available on the effect of trans-Retinoic Acid (tRA), a natural metabolite of vitamin A.

Ledda-Columbano has recently studied the effects of tRA on rodent liver *in vivo* (Ledda-Columbano *et al.* 2004b). Mice were fed a diet containing tRA for up to 4 weeks. BrdU added in the drinking water prior to sacrifice enabled them to measure hepatocyte proliferation. At 150mg/kg a BrdU labelling index of 16.5% (against 1.7% of controls) was observed in the first week, when it was maximal. Most labelling was mid-zonal with the areas around zone III being relatively unaffected. DNA synthesis was noted to begin in the first 24 hours with even higher amounts of BrdU incorporation on days 4 and 5. There was no evidence of the mitogen having its effects due to liver damage i.e. compensatory regeneration as the liver enzymes were not raised and neither was the histological mitotic index. After 1 week liver weight and total DNA content was also raised.

After 2 days of treatment with tRA there was a strong induction of cyclin D1 over controls. Cyclin E levels were also increased. It seems this is consistent with the other mitogens which ligand with a nuclear receptor, and in these situations there is an increase in the G1 cyclin, cyclin D1 early on after mitogenic stimulation, earlier than after the stimulus of partial hepatectomy. The evidence from this study again shows the difficulty when interpreting this data with regards to inter-species variations. For example, tRA given shortly before partial hepatectomy in the rat actually inhibits DNA synthesis in the regenerating liver (Ozeki and Tsukamoto 1999).

The effects of tRA are complex as previous work demonstrated a cytostatic effect of tRA in breast cancer (del Rincon *et al.* 2003) but it is thought that this may be as a result of a 're-differentiation effect' on pre-neoplastic nodules. This is borne out with T_3 as well whereby although it can act as a liver mitogen it also inhibits the development of hepatocellular carcinoma and accelerates regression of pre-neoplastic liver nodules (Ledda-Columbano *et al.* 2000a).

1.7.4 1,4-bis [2-(3,5-dichloropyridyloxy)] benzene (TCPOBOP)

The halogenated hydrocarbon 1,4-bis [2-(3,5-dichloropyridyloxy)] benzene (TCPOBOP) is a tumour promoting liver mitogen and a powerful inducer of cell proliferation and a complete carcinogen for mouse liver. It acts by activating the constitutive androstane receptor (CAR) which is another nuclear receptor transcription

factor. Like some other nuclear receptors CAR forms a heterodimer with RXR and this is what binds to gene regulatory elements.

As with other mitogens that have a nuclear receptor, TCPOBOP does not require activation of the transcription factors NF-κB, STAT-3, immediate response genes and does not involve cytokines like TNF-α and IL-6 (Columbano *et al.* 1997).

Mice treated with just one dose of TCPOBOP show levels of BrdU incorporation as high as after two thirds PH and there is a more rapid induction of the cyclins when compared to PH (Ledda-Columbano *et al.* 2000b). Signalling pathways differ once again whereby liver regeneration is severely impaired in TNF-RI and IL-6 knockout mice but the proliferative response to TCPOBOP is normal in these animals.

Eighty per cent of hepatocytes enter S phase within 4 days of treatment and indeed there is an earlier onset of DNA synthesis when compared to partial hepatectomy. After partial hepatectomy cyclin D1 levels are seen to rise after 30 hours whereas after TCPOBOP cyclin D1 mRNA is seen to rise after just 2 hours with the protein rising at 8 hours. It seems that the mitogen TCPOBOP is having two effects i) a very rapid induction of cyclin D1 and ii) a shortening of the G1 phase of the cell cycle, to about 12 to 16 hours.

The cyclin D1 promoter contains an oestrogen responsive region and this may help explain how the gene may be regulated by other ligands which have nuclear receptors.

This cyclin associates with CDK4 and CDK6 which act on pRb which is the cellular substrate for these enzymes. Columbano's group looked at the response to TCPOBOP in mice deficient for the cyclin D1 gene product (Ledda-Columbano *et al.* 2002). They showed that after 24 hours there was less BrdU incorporation compared to normal animals but by 36 then 72 hours there was no difference with the wild type. Lack of cyclin D1 delayed entry into S phase but the hepatocyte response was not ultimately inhibited. It may be hypothesised that other G1 cyclins such as cyclin E can compensate and take over the role of cyclin D1 although this was not proved in the study just described.

This group also looked at the response to TCPOBOP in mice when compared with PH; the early molecular events were examined with the aid of microarray technology (Locker *et al.* 2003). 23 genes were regulated only by TCPOBOP, 57 only by PH and 59 by both. Only 12 regulated genes were associated with the cell cycle directly and given the time between the stimulus and S phase of between 24-36 hours this makes some sense and suggests that cell cycle regulators are not direct targets of CAR or for that matter STAT-3 and NF-κB. TCPOBOP selectively up regulated a set of

detoxification enzymes and like partial hepatectomy elevated anti-apoptotic regulators and down regulated pro-apoptotic regulators.

1.7.5 Interleukin-6 (IL-6)

The multifunctional pro-inflammatory cytokine IL-6 exhibits growth inhibitory, growth stimulatory and differentiation promoting activities depending on the cell type it is targeting (Taga and Kishimoto 1997).

The receptor for this cytokine is called gp130. This complex causes dimerisation of gp130 and subsequent activation of the Janus kinases which tyrosine phosphorylate gp130. This results in the activation of STAT 3 and the MAP kinase pathway.

IL-6 is essential for normal hepatic regeneration in response to partial hepatectomy or injury. Until recently no one had demonstrated a mitogenic role for IL-6 *in vivo*. Zimmers has produced evidence which demonstrates the mitogenic action of IL-6 (Zimmers *et al.* 2003). A CHO cell line was developed which over-expressed human IL-6 and then injected into athymic nude mice. CHO-IL-6 treated mice became wasted during treatment and developed abdominal distension resulting in an enlarged liver seen at post mortem. There was increased liver DNA and protein in CHO-IL6 mice as well as increased expression of cyclin D1 and PCNA. Panlobular hepatocyte hyperplasia was seen histologically with many mitotic figures and increased numbers of cells undergoing DNA synthesis by way of BrdU incorporation. There was no evidence of liver injury.

Furthermore there was a dramatic increase in STAT-3 and following on from this an increase in its target genes c-myc and c-jun. No effect was seen on levels of HGF and EGF or TGF alpha and in fact these pathways appeared to be down regulated.

The long term high dose exposure to IL-6 in this study is thought to have resulted in the increased hepatocyte proliferation which had not been demonstrated before as exposure was too short term and in too low a dose. The application of IL-6 in a clinical environment to augment liver growth may however not be possible given the toxic side effects seen at high dose such as muscle wasting and splenomegaly. Just as with T_3 though if the mechanism of action can be fully elucidated then we may be able to act on members of the IL-6 signalling pathway to bring about specific therapeutic results.

1.7.6 Tumour Necrosis Factor-α (TNF-α)

This cytokine has a well known wide range of biological activities including apoptosis, growth, differentiation and inflammation (Locksley *et al.* 2001). It has two ubiquitously expressed receptors TNFR1 and TNFR2. The transcription factor NF-κB is an essential component of the TNF proliferative pathway and TNF-induced changes in STAT-3, IL-6 and c-myc mRNA are dependent on NF-κB activation.

Iocca and Isom have shown that TNF-α can induce DNA synthesis in long term DMSO culture of rat hepatocytes (Iocca and Isom 2003). They observed maximal induction of DNA synthesis after 24 hours and progression through the cell cycle was confirmed by observing mitotic figures after 96 hours. NF-κB was activated by TNF-α within 1 hour. This is a good demonstration of TNF-α acting as a complete mitogen rather than just a priming factor.

1.7.7 Epidermal Growth Factor/Hepatocyte Growth Factor/Transforming Growth Factor-α

HGF, TGF-α and EGF have been shown to be potent hepatic mitogens *in vitro* and their role in direct hyperplasia has been referred to.

Hepatocyte growth factor (HGF) is the most potent of the hepatic mitogens. First identified in 1984, it is a hetero-dimeric glycoprotein, also known as scatter factor, composed of a 69-kDa α-chain and a 34-kDa β-chain (Nakamura *et al.* 1984). Serine proteases are responsible for the conversion of a single chain precursor form into the two-chain form and this is coupled to its activation. It is made by mesenchymal cells throughout the body. Kupffer, endothelial and Ito cells produce it in the liver. HGF binds with high affinity to its receptor, a transmembrane tyrosine kinase, encoded by the c-Met proto-oncogene (Bottaro *et al.* 1991). The receptor is composed of an extra cellular α-chain and a transmembrane β-chain. HGF activation results in a cascade of signalling involving tyrosine kinases as well as phosphatidylinositol 3-kinase. Met is the only known functional receptor for HGF and HGF is the only natural ligand for Met.

These growth factors have been shown to be complete mitogens for hepatocytes in culture but their *in vivo* role is more difficult to characterise. In culture they act to activate the immediate early genes which leads to DNA synthesis (Band *et al.* 1999). When HGF and EGF are infused directly into the portal circulation in rats using mini osmotic pumps their effects on DNA replication in the liver can be assessed by means of BrdU incorporation into hepatocyte nuclei. When infused alone or even in

combination no more than 10% of hepatocytes are labelled at 24 or 48 hours. When though the animals undergo only 30 % partial hepatectomy and are then given growth factors such as HGF one sees a restoration of a peak of DNA synthesis at 24 hours. This lead to the concept of priming of hepatocytes being necessary prior to these agents being able to exert their full effects on growth (Shiota *et al.* 1994; Fujiwara *et al.* 1993; Webber *et al.* 1994).

Further *in vivo* studies (Fujiwara *et al.* 1993; Patijn *et al.* 1998) suggest that quiescent hepatocytes may divide after more prolonged treatment but they do not respond to the administration of a discrete dose as occurs with some of the other primary mitogens that have been discussed here.

1.7.8 Lead Nitrate (LN)

Columbano's group showed in 1983 that injections of intravenous lead nitrate into male Wistar rats resulted in hepatic enlargement and increased DNA content (Ledda-Columbano *et al.* 1983; Columbano *et al.* 1983; Columbano *et al.* 1984). Increased levels of DNA synthesis were seen as shown by increased amounts of labelled thymidine into hepatic DNA and more mitoses were seen histologically.

Increased labelling with BrdU is seen after an intravenous injection of lead nitrate both in the hepatocytes and in the non parenchymal cells after 12 hours (Shinozuka *et al.* 1994; Shinozuka *et al.* 1996) with a peak at 36 hours. In these studies it was shown that both lead nitrate and TNF-α induced an early proliferative response of the non-parenchymal cells. Lead nitrate enhances the levels of hepatic TNF-α mRNA at a time preceding the onset of hepatocyte DNA synthesis. The peak of hepatocyte proliferation is approximately the same after LN and TNF-α. This is consistent with the observation that TNF-α mRNA is seen to rise within 1 hour after an injection of intravenous LN. Histologically it appears that the induced NPCs are indeed Kupffer cells.

1.7.9 Cadmium nitrate

The effect of a single intravenous injection of cadmium nitrate has been investigated in livers of male Wistar rats (Ledda-Columbano *et al.* 1984). A significant increase in liver weight, accompanied by an elevation of total hepatic DNA content was observed. DNA synthesis as measured by the incorporation of [3H]thymidine, was found to be 6 times greater than the control, at 24 h after treatment, and remained elevated over a period of

72 h. This elevation in DNA synthesis was not a consequence of cell necrosis, since no increase of serum glutamate-pyruvate transaminase (SGPT) activity was observed.

1.7.10 Iron

The role of iron as a hepatic mitogenic stimulus has been investigated because in rodent models of iron overload hepatomegaly is frequently observed. Adult SD rats were administered iron dextran over a 22 week period (Brown *et al.* 2006). Iron loaded livers weighed twice as much and the total DNA content was greater in iron loaded livers. Immunohistochemical staining for PCNA (a marker of S phase) revealed a 3-fold increase in hepatocyte PCNA index in iron loaded livers. Furthermore Western blot analysis revealed significantly increased amounts of cyclin D1 in iron overloaded livers. The study authors propose that iron most likely acts as a direct hepatic mitogen and the response is similar to that seen with lead nitrate.

1.7.11 Ethylene dibromide

Installation of ethylene dibromide (7.5 to 10 mg. per 100 gm. of body weight) into the stomach of nonfasted Wistar rats induces DNA synthesis and cell division in the liver (Nachtomi and Farber 1978; Ledda-Columbano *et al.* 1987). The peak of DNA synthesis, as measured by 3H-methyl thymidine incorporation, was attained at or shortly after 24 hours. The mitotic waves measured with the aid of colchicine occurred at 24 to 30 hours and 48 to 54 hours after ethylene dibromide treatment. Approximately 16 per cent of liver cells entered mitosis.

1.7.12 3,5,3'-L-tri-iodothyronine (T_3) as a primary hepatic mitogen

It was first reported in 1933 that feeding desiccated thyroid tissue to rats enhanced the regenerative hepatic response to partial hepatectomy. By 4 weeks after surgery the liver was 20% larger than in the control group. The control animals also showed an increase in liver weight having been given thyroid tissue but not having undergone surgery (Higgins 1933).

Later on in 1972, Short demonstrated the induction of DNA synthesis in the liver of adult rats after administration of T_3 (Short *et al.* 1972) and again in 1980 (Short *et al.* 1980). In their work an infusate was made called TAGH solution containing

triiodothyronine, amino acids and glucagon. This solution when infused brought about DNA replication in the hepatocytes about half as well as that seen following 70% hepatectomy. Each ingredient of the TAGH solution contributed to the stimulation of DNA synthesis in the rat but the single most important constituent was T_3.

Francavilla further characterised the mitogenic effects of T_3 on rat liver (Francavilla *et al.* 1994). In doses which are many times supra-physiological (40x), there is a peak in hepatic DNA synthesis at 24hr (measured by 3H thymidine incorporation) and in the number of mitoses. There is a return to baseline by 96hr. The cells proliferating at 24 hours after T_3 are predominantly in the hepatic midzone and this compares with the stimulus of PH where the proliferating hepatocytes are predominantly in the periportal region of the liver.

Further work by Malik examined the effects of administering T_3 at the time of PH and in so doing combing the two pathways of liver growth (compensatory and direct hyperplasia) (Malik *et al.* 2003). This study showed that by combining T_3 with PH there were a greater number of hepatocytes undergoing DNA synthesis than after PH alone. There was a larger postoperative liver mass at day 4 with the co-administration of T_3 and there were increases in both total DNA and total protein reflecting the increase in mass was cellular. The BrdU flash labelling index was far greater when T_3 was administered at the time of surgery when compared to partial hepatectomy alone (39.5% $\pm$ 5.0% and 26.5% $\pm$ 2.8% respectively). In addition this study showed that the T_3 caused proliferation in the absence of any liver injury, with serum bilirubin and ALT levels remaining unchanged. Histological sections demonstrated no necro-inflammatory changes.

After T_3 stimulation there is a peak in liver mass at 10 days and the decline in mass thereafter is through a process of hepatocyte apoptosis and in the absence of any histological necro-inflammatory changes in liver sections of experimental rodents, with a return to normal hepatic mass by 14 days (Malik *et al.* 2005). At 10 days after the T_3 dose there is an important observed increase in the metabolic capacity of the liver measured by galactose elimination which rises by between 10 and 15% (Malik *et al.* 2005).

If the T_3 was administered 10 days prior to 70% partial hepatectomy there was a larger remnant liver mass 24 hours after surgery. The liver enhanced in size and function was however shown to have a normal post resection regenerative capacity (Alisi *et al.* 2005; Bockhorn *et al.* 2007).

The precise mechanism by which T_3 mediates hepatocyte proliferation remains elusive. An important molecule to consider is cyclin D1 as the study of its kinetics has gone some way to explain the mechanism of action of T_3. Its expression is increased early after T_3 administration.

Pibiri et al showed that cyclin D1 mRNA levels increase after 2 hours following a T_3 dose and reach a maximum at 4 hours. Increased cyclin D1 protein content also occurs after partial hepatectomy but it is only evident at 12 hours instead of 4 hours seen with T_3. This activation of cyclin D1 by T_3 is not the result of induction of immediate early genes and activation of transcription factors. It is tempting therefore to conclude that the effects on cyclin D1 may be as a result of a direct effect of thyroid receptor on the gene; this is supported by some evidence from using other ligands as mitogens for the nuclear receptor superfamily discussed earlier.

Interestingly, the mitogenic effects of T_3 are not restricted solely to the liver. The pancreas is also a quiescent organ in the adult and it too has the potential for regeneration following resection. Ledda-Columbano has shown that T_3 exerts a strong proliferative effect on pancreatic acinar cells in the mouse and rat and therefore concludes that T_3 is strongly involved in activating cell signal transduction pathways leading to cell cycle entry in different organs (Ledda-Columbano *et al.* 2005). Interestingly other primary mitogens with nuclear receptors notably TCPOBOP, tRA and ciprofibrate did not have the same effect on acinar cell proliferation.

In other work Ledda-Columbano has shown T_3 can stimulate re-entry of adult rat cardiomyocytes (usually these cells lose their proliferative capacity after birth) into the cell cycle leading to DNA synthesis after an increase in the cell's cyclin D1 content (Ledda-Columbano *et al.* 2006). Collectively these data point to the T_3 proliferative effect being quite ubiquitous and therefore unique amongst the group of primary mitogens.

The liver is known to be a major target of thyroid hormone and up to 8% of hepatic genes are regulated by thyroid hormone *in vivo* demonstrated by cDNA microarray technology which has been used to study gene expression in hypothyroid and hyperthyroid mice, six hours after T_3 administration (Feng *et al.* 2000). 55 target genes, 14 up-regulated and 41 down-regulated were identified. Many of these were involved in metabolic pathways such as hepatic lipogenesis but changes in genes involved in cell cycle progression and apoptosis were also observed, including Bcl-3, a known oncogene. Bcl-3 is an IκB related protein which can act as a co-activator for NF-κB

homodimers. It is also co activator for AP-1 and RXR and so may act as a co-activator for the thyroid receptor itself. Its role is further evaluated in chapter four.

1.7.12.1 T_3 Anti tumour properties

Intriguingly although T_3 has this well described effect on hepatocyte proliferation, it has been shown to possess anti tumour properties as well. Ledda-Columbano showed that rats treated with T_3 in their diet for 1 week had a reduction in the number of positive γ-glutamyl transpeptidase (GSTP) lesions, where the GSTP acts as a phenotypic marker of a pre-neoplastic lesion (Ledda-Columbano *et al.* 2000a). Furthermore repeated treatment with T_3 in rats with pre- neoplastic liver lesions led to a 50% reduction in the development of hepatocellular carcinoma (HCC) and a complete inhibition of lung metastasis. The loss of GSTP nodules occurred despite an increase in hepatocyte proliferation within nodules as well as in areas of normal liver. Remodelling (or regression) induced through a re-differentiation program appears to be the most likely explanation for the loss of hepatic nodules caused by T_3. The other very important observation from this study is that cell proliferation *per se* may not necessarily represent a carcinogenic and/or promoting condition. On the other hand, the data suggest that certain proliferative stimuli may play an anti-carcinogenic effect, probably by causing a re-differentiation of pre-neoplastic cells.

1.8 Aim of thesis

Prior to its human use, elucidating the T_3 mitogenic mechanism of action is crucial. To this end, T_3 has been widely studied in the animal rodent model where its mitogenic effects can be readily demonstrated (Malik *et al.* 2005) but so far it has not been possible to demonstrate a direct *in vitro* effect either in monolayer cell culture or in more sophisticated co-culture experiments using adult rodent or human hepatocytes. This may be as a result of several factors, for example the lack of a sophisticated 3-D microenvironment, which one sees *in vivo*, may account for its lack of effect but also it may be acting through intermediaries which are just not present in cell culture conditions. Since previous work in this laboratory has failed to show a mitogenic effect of T_3 in either 3D culture or co-culture with other liver cell types, the primary aim of this research was to further elucidate the T_3 mitogenic mechanism of action and to demonstrate an effect in human liver *in vitro*.

Chapter 2 General Methodology

2.1 Animal Protocols

Materials:

1 ml syringes and needles

NUNC dishes (NUNC Denmark)

Dissection and surgical instruments

Liquid N_2 in a dewar

Formalin filled universal containers labelled

Cryogenic vials

Scalpel blade holder

Size 11 surgical blades

Foil squares

Method:

Male Sprague-Dawley rats (250g) were housed in a temperature- and light-controlled room (12-hour light/dark cycle) with free access to food and water. Animal care and all procedures were compatible with the Animal (Scientific Procedures) Act 1986, UK Home Office.

Animals were sacrificed at the appropriate time points by a schedule one procedure. Liver was harvested and sectioned for histology and pieces were snap frozen in liquid nitrogen and stored at -80°C for later analysis and RNA and protein isolation.

2.2 Histological Analysis

2.2.1 APES coated slides

Aminopropyl-trimethyl-silane (APES)/Silane coated slides

To improve tissue adherence for staining, microscope slides were APES/silane coated.

Materials:

Microscope Slides (BDH).

Acetone (Sigma-Aldrich Ltd.)

3 Aminopropyl-trimethyl-silane (APES), Sigma-Aldrich Ltd., # A1435. , Prepared as a 2 % solution dissolved in acetoneat 4 °C.

Method:

Slides were dipped in acetone for 1 minute, then in 2 % APES/acetone for 2 minutes, and rinsed thoroughly in running tap water, dried overnight before use and stored at room temperature.

2.2.2 Haematoxylin & Eosin staining

Materials:

Haematoxylin (Gill's Haematoxylin, Merck Ltd.)

1 % Eosin (5 % aqueous, Merck Ltd.)

Xylene (BDH)

Aquamount (BDH)

Method:

Formalin fixed sections were stained with haematoxylin and eosin after sequential dewaxing through graded alcohols 100% for 1 minute, 70% for 1 minute and in running tap water for 1 minute. Sections were mounted using aquamount.

2.2.3 Immunohistochemical staining

Materials:

Xylene (3 baths)

Acid alcohol

100% ethanol

70% ethanol

Microwave with a rotating plate

dH_20

1x PBS:

1L dH_2O, 8g NaCl, 0.2g KCL, 1.44g Na_2HPO_4, 0.24g KH_2PO_4. Adjusted to pH 7.4 with a bench top pH meter

0.3% H_2O_2 in 1x phosphate buffered saline (PBS)

Citrate Saline Buffer (0.01M citrate, NaCl 0.15M, pH 6.0)

DAKO pen for immunohistochemistry # S2002

Rabbit serum Sigma-Aldrich # M0744

Goat serum Sigma-Aldrich

Avidin/Biotin blocking system (Vector Labs)

Streptavidin ABC Complex DAKO #K0492

Sigma Fast 3,3-Diaminobenzidine Tablet Sets (DAB Peroxidase Substrate) #D4293

Sigma mouse IgG purified # I 8765

Sigma sheep IgG I-8265

Table 3 Primary and Secondary Antibodies for immunohistochemistry used in this thesis

Primary or secondary antibody	**Product code**	**Dilution/incubation time**	**Secondary antibody dilution/ incubation time**
Mouse anti rat BrdU	DAKO #M0744	1:100 120 minutes	1:200 90 minutes Rabbit biotinylated anti mouse
Rat Ki-67	DAKO	1:100 90 minutes	1:100 biotinylated rabbit anti mouse
Cyclin D1	LabVision #RM-9104-SO	1:50 120 minutes	1:400 30 minutes Goat biotinylated anti rabbit
Mouse monoclonal anti human Ki-67	DAKO #M7240	1:200 60 minutes	1:100 30 minutes Biotinylated rabbit anti-mouse
Rabbit monoclonal anti p-mTOR	Cell Signalling Tech. #2976	1:50 60 minutes	1:400 Goat biotinylated anti rabbit
Mouse monoclonal anti phospho-AKT (Ser 473)	Cell Signalling Technology # 40515	1:2000 4 hours	1:400 Goat biotinylated anti mouse
Mouse	Cell Signalling	1:1000	1:400

monoclonal anti phospho-p70 S6 kinase (Thr 389)	Technology # 9206S	4 hours	Goat biotinylated anti mouse
Anti-BrdU supernatant	Oxford Biotech. #00305	1:100 120 minutes	1:200 90 minutes
Rabbit anti rat immunoglobulin HRP linked	DAKO #PO450		1:200 90 minutes
Rabbit PAP (peroxidase anti-peroxidase)	DAKO #Z0113		1:300 30 minutes
Biotinylated rabbit anti mouse	DAKO #E0464		1:100

Method:

This general method applies to the technique used in this thesis. Where there are specific changes for a particular species or antibody these will be described separately either here or in individual results chapters.

Formalin fixed tissues were embedded in paraffin and 4μm thick sections were cut.

Slides were left to dry overnight at room temperature for at least 12 hours.

Sections were deparaffinised in three baths of xylene and then placed in graded ethanol solutions (100%-70%), 1 minute each prior to re-hydration in running tap water for 1 minute.

Non specific peroxidase activity was blocked by incubation in a 0.3% solution of hydrogen peroxide for twenty minutes. A wax pen was used to draw around the tissue section prior to immersion in citrate saline buffer pH 6.0 (0.01M citrate) and heated in a microwave on high power 800W for twenty minutes to expose antigen. Slides were then washed in cold distilled water and slides were incubated for ten minutes in either goat serum diluted 1:20 or rabbit serum 1:20, to block endogenous immunoglobulins. The blocking serum used was from the same species as the secondary antibody was raised in and so may vary according to which secondary antibody was used.

The serum was gently tapped off and a biotin blocking stage was introduced. Avidin solution was applied for 15 minutes, washed off and a biotin solution was applied for 15 minutes.

The primary antibody, appropriately diluted, was applied at an optimal concentration for incubation in a humid incubator.

The slides were again washed in x1 PBS for ten minutes prior to addition of the ABC complex (streptavadin/biotinylated horseradish peroxidase mixture- DAKO UK) for one hour.

The slides were thoroughly washed in x1 PBS prior to development with DAB solution (Sigma UK) for ten minutes. The sections were counterstained with haematoxylin, dehydrated and mounted ready for viewing under the microscope.

The antibodies used required optimising, varying their concentrations to obtain optimal staining results (Table 3).

2.2.3.1 Negative controls for immunohistochemistry

Non-specific mouse or rabbit IgG controls were used as negative controls for primary antibodies. Both the species and specific IgG concentrations were taken into account.

2.2.4 Mouse BrdU

Materials:

Rat anti-BrdU supernatant (OBT)

DAKO rabbit anti rat immunoglobulin HRP linked

DAKO Peroxidase anti peroxidase (PAP) rabbit polyclonal

Method:

Same as the general method, however after incubation in the secondary HRP-linked antibody at 1:200 dilution for 2 hours, the slides are washed and PAP was applied for 30 minutes at 1:200 dilution. There was no need for a biotin blocking step in this protocol as the detection system did not rely on a biotinylated secondary antibody for detection.

The subsequent steps are the same and detection was with the chromogen DAB applied for 10 minutes.

This method was used in mouse liver tissue to detect BrdU as the antibody product used had an established protocol in the laboratory and was known to work on mouse liver where other antibodies had proven to be less reliable.

2.3 Isolation of RNA

Materials:

Qiagen RNEasy Mini Kit (cat. # 74104) consisting of:

- RNeasy spin columns
- Collection tubes 1.5ml and 2.0ml
- Buffer RLT (guanidine thiocyanate - containing buffer)
- Buffer RW1 (wash buffer)
- Buffer RPE (wash buffer)
- RNase- free water to elute

Rotor Star homogeniser

Method:

The RNeasy procedure uses a silica-gel-based membrane within a column to bind RNA. Firstly, samples of appropriate size are lysed and homogenised in a highly denaturing guanidine isothiocyanate containing buffer, which inactivates RNases to ensure isolation of intact RNA. When applied to the membrane in the column, total RNA binds and contaminants are washed away. The high quality RNA is eluted in water at the very end. RNA molecules longer than 200 nucleotides are isolated and this provides enrichment for mRNA since most other RNAs less than 200 nucleotides are excluded.

The maximum binding capacity of the column is 100μg RNA and it provides an average yield of 40μg of RNA from 10mg of rodent liver tissue.

Samples were removed from -80°C and placed on ice. A piece of liver measuring approximately $3mm^3$ was removed placed in 600μl of buffer RLT and homogenised using a rotor star homogeniser for 40 seconds. Disruption and homogenisation of tissue is an absolute requirement for total RNA isolation.

Tissue lysate was centrifuged for 3 minutes at maximum speed. The supernatant was transferred to a new micro centrifuge tube by pipetting. 70% ethanol (600μl) was added to the lysate and mixed by pipetting. The lysate (700μl) was added to an RNeasy mini column and centrifuged for 15 seconds. The flow through was discarded. Buffer RW1 (700μl) was added to the column and centrifuged for 15 seconds. The flow through was discarded. Buffer RPE (500μl) was added to the column and centrifuged for 15 seconds. A second volume of buffer RPE was added and the process repeated with the flow through discarded again after centrifuging for 2 minutes. The column was placed in a

new collecting tube and eluted with 50µl of RNase-free water. The samples were placed on ice ready for immediate quantitation and aliquoting.

For micro-array work, total RNA was isolated using Promega (Southampton, UK) RNA reagents following the manufacturers protocol.

2.3.1 Determination of RNA yield

Materials:

RNA samples

Glass cuvettes

UVIKON-930 Spectrophotometer

Method:

The yield of RNA was determined spectrophotometrically at 260nm, where 1 absorbance unit (A_{260}) equals 40µg of single stranded RNA/ml. The purity was assessed by the relative absorbances at 260nm and 280nm (A_{260}/A_{280}). The ratio between the readings at 260nm and 280nm provides an estimate of purity of the nucleic acid, with the ratio varying between 1.8 and 2.0 for pure samples.

The spectrophotometer was first set to zero optical density (O.D) value, against a blank cuvette of dH2O, at both 260nm and 280nm. RNA samples were then placed into the cuvette and the O.D value measured at 260nm and 280 nm. The concentration of RNA was calculated using the formula:

$$\frac{A_{260} \times 40 \times \text{dilution factor}}{1000} = \text{conc. } \mu g/\mu l$$

A ratio above 1.8 was obtained for all samples analysed.

A_{260} readings <0.1 and >1.0 lead to considerably lower reproducibility. Readings above 3 are incorrect and this can lead to an underestimation of the amount of RNA. Therefore for reliable spectrophotometric quantification A_{260} readings should lie between 0.1 and 1.0 and this was the case with all samples that were measured.

Immediately following quantitation, the RNA was aliquoted into volumes equivalent to 0.5µg RNA per aliquot. This was done so the same amount of RNA would be used for each sample in the subsequent cDNA synthesis reaction, so reaction efficiencies would

be more uniform across all samples and the problem of overloading the cDNA reaction would be avoided. Samples were stored at -80°C.

2.3.2 RNA Gel Electrophoresis

Materials:

Agarose

Formaldehyde (Sigma)

10x MOPS solution:

200mM MOPS (3-[N-Morpholino] propanesulfonic acid) pH 7.0

80mM sodium acetate

10mM EDTA pH 8.0 Ethylenediaminetetraacetic acid

Diethylpyrocarbonate (DEPC) water

Formamide 1%

Ethidium bromide 1%

Method:

Total RNA was analysed by electrophoresis of RNA samples on a denaturing formaldehyde RNA gel stained with ethidium bromide.

The following agarose gel preparation was used (1.5%):

0.9 g agarose

10.8ml 37% formaldehyde

12ml 5x MOPS (1:2 dilution with DEPC water of 10x MOPS)

37.2ml DEPC water

To each aliquot of RNA (0.5µg in variable volume of water) was added:

5x MOPS	4µl
formaldehyde	3.5µl
formamide	10µl
ethidium bromide 200µg/ml	1µl
DEPC water to make up to:	25µl

The RNA samples were heated to 65°C for 5 minutes and placed on ice just prior to the addition of loading buffer 2.5µl. The gel was pre-run for 10 minutes at 5 Volts per cm length and samples were loaded onto the gel and electrophoresis was performed at 60 Volts, 140mA for approximately 2 hours. RNA was examined under UV light to check the integrity of the RNA. Intact RNA has a sharp 28S and 18S ribosomal RNA bands with a 2:1 ratio (28S:18S).

2.4 cDNA synthesis

Materials:

Fermentas RevertAid™ first strand cDNA synthesis kit (#K1622) containing:

RevertAid M-MuLV reverse transcriptase (200u/µl)

RiboLock Ribonulcease Inhibitor (20u/µl)

5x reaction buffer: 250mM Tris-HCl, 250mM KCl, 20mM $MgCl_2$, 50mM DTT

10 mM dNTP mix

Random hexamer primer

DEPC treated water (DiEthylPyroCarbonate)

Heating block

0.2ml PCR tubes

Method:

To 0.5µg RNA (previously quantitated and aliquoted) was added 1µl random hexamer primer was added and the volume made up to 12µl with DEPC treated water. This was incubated for 5 minutes at 70°C and immediately placed on ice. Once on ice the following components were added:

5x reaction buffer	4µl
RiboLock Ribonuclease Inhibitor	1µl
10mM dNTP mix	2µl

This mixture was incubated at 25°C for 5 minutes.

The enzyme RevertAid M-MuLV reverse transcriptase was added, volume 1µl.

The final volume of 20µl was incubated at 25°C for 10 minutes then at 42 °C for 60 minutes. The reaction was stopped by heating to 70°C for 10 minutes.

This reaction was performed for all samples. The cDNA was stored at - 20°C.

2.5 A Note on Quantitative Real Time PCR

2.5.1 Principles of real-time PCR

Real-time PCR is traditional PCR with incorporation of a fluorescent reporter. Introduction of a fluorescent reporter simplifies the process of producing reproducible quantitation of mRNAs, however, the reaction remains complex as all physical and chemical components of the reaction are interdependent. During PCR, nucleic acids of a target sequence (within a cDNA template) are amplified. Primers anneal to a specific target sequence and synthesise the targeted DNA. The amplicon is then denatured into single strands allowing the primers to anneal again and repeat DNA synthesis. Repetition of this process results in amplified target DNA. The rate of amplification, providing DNA polymerase, dNTPs and primers are in excess, follows a sigmoid relationship. Incorporation of a fluorescent reporter with suitable detection apparatus permits data acquisition during the exponential growth phase, hence the term 'real-time'. The fluorescent reporter signal is measured at every cycle and is proportional to the amount of amplicon generated. The parameter of quantitation is the threshold cycle (C_T) and is defined as the cycle at which a significant increase in fluorescence is detected during the exponential phase of amplicon amplification which correlates to the initial amount of target template (Gibson *et al.* 1996; Higuchi *et al.* 1993).
Various fluorescent reporters are available to monitor DNA amplification; these include DNA-binding agents (SYBR Green I) (Bustin 2000), hydrolysis probes (exemplified by the TaqMan chemistry) (Gibson *et al.* 1996), hybridization probes (Bernard and Wittwer 2000) and hairpin probes (e.g. Molecular Beacons, Scorpions, Sunrise primers and LUX primers.

This thesis uses SYBR Green I (SG) a fluorogenic minor groove binding dye that exhibits little fluorescence when in solution but emits a strong fluorescent signal on binding to double-stranded DNA (Morrison *et al.* 1998). SG is extensively used in real-time PCR as its photophysical properties are temperature stable and selective for double-stranded DNA, allowing for quantification with high sensitivity and once optimized, results in an easy, robust and reliable assay displaying a wide dynamic linear range. However, SG has disadvantages associated with its ability to bind double stranded DNA as it may bind non-specific sequences including non-specific

amplifications and primer-dimer complexes. Hence, SG-based real-time PCR requires extensive optimisation and melt curve analysis to verify SG fluorescence is a direct measure of specific product amplification.

2.5.2 Methods of Quantitation

The advantage of using real-time PCR is the ability to quantify the targeted nucleic acids. Quantitation can be either absolute or relative and these methods have recently been reviewed (Wong and Medrano 2005).

2.5.2.1 Absolute Quantitation

Absolute quantitation determines the total amount of target (expressed as copy number or concentration) using external standards (Bustin 2000). The amplification efficiency of the target and the standards must be equivalent for absolute quantification. The external standards contain sequences equivalent to the target and identical primer binding sites whose absolute concentration is known. There are several criteria for absolute standards (Bustin 2000). Quantitation is achieved by establishing a standard curve (external standard C_T value against log of amount of standard) using a dilution series of the standards from which unknown amounts of initial target (copy number) can be calculated. This copy number must be normalised, typically to the number of cells or total RNA used. The accuracy of absolute quantitation is dependent on the accuracy of the standards.

2.5.2.2 Relative Quantitation

Relative quantitation calculates the ratio between the amount of target and a normaliser. No absolute number is detected. Relative quantitation is the most commonly applied method for gene expression analysis as it accounts for differences in the amount of total RNA that arise between samples that may occur due to variations in efficiency, errors in sample quantitation and loading amounts. As expression of the normaliser should not change in different samples the ratio of the amplicon varies according to the expression level of the target gene. Thus, normalised values can be used to compare differential gene expression in different samples. There are two accepted methods for relative quantitation of gene expression, firstly the comparative C_T method (delta delta C_T) and

secondly the two standard curve method. The comparative C_T method requires the amplification efficiency of the target and normaliser to be identical. Invariably amplification efficiencies are different so relative quantitation using the two standard curve method, one for the target and the other for the endogenous normaliser is preferred. Real time PCR is a developing technology and additional mathematical models for relative quantitation have been described (Pfaffl 2001).

2.5.2.2.1 **Delta Delta C_T Relative Quantitation**

Comparative C_T method (delta delta C_T) does not require the running of standard curves. The amount of template present in an unknown is first normalised by relative comparison to an endogenous control (normaliser). The normalised value is further normalised relative to a calibrator (either a wild-type, untreated control or time zero sample). Reaction efficiencies must be the same and, for results to be valid, quantitation guidelines have been derived.

2.5.2.2.2 **Two Standard Curve Relative Quantitation**

The two standard curve method analyses a sample for the gene of interest and endogenous control (normaliser) in two separate reactions. This method allows for quantification where the amplification efficiencies for the gene of interest and the endogenous control are different. PCR amplifications which proceed at different efficiencies result in unparallel standard curves (slope differences >0.1) therefore the differences in C_T values of the target and normaliser will not be constant when the amounts of target and normaliser are varied. The relative expression of the target of interest to the normaliser in a sample is calculated as the ratio of the resulting amounts of target to the normaliser using their respective C_T values to assign an arbitrary concentration from its corresponding standard curve (standard C_T value against log of estimated amount of standard).

2.5.3 Quantitation

In this thesis expression levels of the gene of interest were determined by *relative* quantitation using the two standard curve method with 18S as the normaliser.

Standard curves for the gene of interest and 18S were constructed using standards, the preparation of which involved several steps; In brief, traditional PCR using specific primers was performed to amplify the target. The amount of amplicon was estimated by on an agarose gel and markers whose intensity using UV quantitation represented product concentration. Serial dilution of the amplified product provided arbitrary standards which were run in an optimised real-time PCR to construct a standard curve.

2.5.3.1 Preparation of standards

Standards were prepared using rodent liver cDNA. Traditional PCR using specific real-time primers amplified the target of interest. The amplified product was electrophoresed in a 2% agarose gel containing ethidium bromide, to ensure the amplicon was a single band of the correct size. The amplicon was excised and extracted from the gel and a known volume was electrophoresed on an agarose gel with Hyperladder IV to ensure amplicon integrity and estimation of amount present. Using Avogadro's constant (6.023×10^{23}) the number of molecules present was estimated to enable preparation of standards.

2.5.4 Rotor-Gene 3000 Real Time PCR machine

This system can detect all available Real-Time chemistries including SYBR Green. It has four light sources, six detection filters ensure no spectral overlap, and flexibility to detect different probes. An LED source illuminates the tube from the side wall and a photomultiplier (PMT) detects the energy from the base of the chamber. For SYBR Green this was an excitation wavelength of 470nm and detection through the 585nm-high pass filter.

The 36 well rotor for 0.2ml tubes was initially used but later a 72 well rotor for 0.1ml strip tubes was used for higher sample through put. All settings and programmes were performed with Rotor-Gene software version 6.0.14.

2.6 Primer design

2.6.1 Primer design rules that were applied:

(i) Should be 15-30 bases in length.

(ii) G + C content should ideally be 30-80%. The run of an identical nucleotide should be avoided (especially for G, where more than 4 is not allowed).

(iii) maximum amplicon size should not exceed 400bp (ideally 50-150 bases). Smaller amplicons give more consistent results as PCR is more efficient and more tolerant of reaction conditions.

(iv) To avoid false positive results due to amplification of contaminating genomic DNA in the cDNA preparation, it is preferable to have primers spanning intron-exon boundaries in the cDNA sequence. By doing this genomic DNA will not be amplified.

Successful real-time PCR requires optimal primer pair design and appropriate primer concentration.

Using GeneBank (http://www.ncbi.nlm.nih.gov) the complete mRNA sequences for the genes of interest were obtained. Forward and reverse primers were designed to comply with the rules set out above with the additional requirement for Real-Time PCR that the size of the amplicon should be no more than 150bp in length. Using the computer software Vector NTI the proposed primers were assessed to ensure that an intron-exon boundary was spanned (to minimize genomic DNA amplification), no potential formation of primer-dimers or secondary structures were predicted, and similar annealing temperatures were appropriate for each primer pair. The primer pairs were screened against the Blast database to ensure specificity to the gene of interest.

Primer sequences were purchased from SigmaGenosys, the sequences for which are given in individual results chapters. An appropriate volume of DEPC-MilliQ water was added to the lyophilized primers to make 100μM stock concentrations from which 10μM working concentrations of primers were made. All primers were stored at -20°C at 100μM concentration for long term storage.

2.6.2 Conventional PCR to check primers

2.6.2.1 Polymerase chain reaction

This is a basic technique central to most modern molecular biology. It is powerful and results in the rapid production of multiple copies of a target DNA sequence. A thermo-stable DNA polymerase enzyme synthesises dsDNA *in vitro* under certain conditions. The other components are:

-Oligo-nucleotides complementary to the sequences flanking the gene to be amplified

-dNTPs- deoxyNucleotideTriphosphates

-salts and buffering to allow enzyme activation

-accurate and rapid temperature control

Amplification specificity of each primer pair was confirmed by traditional PCR.

Materials:

HotStar Taq Mix containing: Taq DNA polymerase (5 units/μL), 2x PCR buffer, 3mM $MgCl_2$ and 400μM of each dNTP (Qiagen)

Forward and reverse oligonulceotide primers (Sigma-Genosys)

DNA template (rat liver cDNA)

DEPC H_2O

Method:

5μl of rat liver cDNA (prepared from 0.5μg RNA) was added to:

HoStar TaqMix	25μl
Forward primer	0.5μl
Reverse primer	0.5μl
DEPC H_2O	19μl

An additional reaction mix was set up with no cDNA to act as a non template control.

The PCR reaction was run on a PCR block:

Step	Number of Cycles		
Hot Start	1	95°C	15 min
Denaturation	35	95°C	30 sec
Annealing		60°C	30 sec
Extension		72°C	30 sec
Extension End	1	72°C	10 min

2.6.3 DNA gel Electrophoresis

Materials:

Agarose (BDH chemicals)

Ethidium bromide (Sigma) stock: 10mg/ml

50x TAE: for 1L in ddH2O242g Tris base, 57.1ml glacial acetic acid, 100ml 0.5M EDTA in ddH_20, pH 8.0

1x TAE: 1 in 50 dilution of 50xTAE stock in ddH_20.

DNA ladder: Hyperladder IV to detect 1000-100 base pairs (Bioline #33029)

Method:

Agarose (0.75g) was dissolved in 50mls TAE buffer and heated to 90°C in a microwave.

After cooling to 50°C, 1µl of ethidium bromide at 10mg/ml was added and poured into a Perspex mould with an appropriate comb already in place and the ends of the tank pre sealed with tape. It was left to set.

20µl of PCR product was added to 4µl loading buffer. The set gel was placed in a tank and this was filled with 1x TAE buffer.

24µl of sample was loaded into each well and electrophoresis was performed at 90V and 140mA for 1 hour. The gel was then visualised under ultraviolet light and an image was captured on computer using the software Labworks 4.6 and a digital camera.

2.6.4 Preparation of standards for Real Time PCR

Materials:

Hotstar Taq MasterMix (Qiagen):

- Hotstar Taq DNA polymerase 5units/µl
- PCR buffer
- dNTPs at concentration of 200µM each

Forward and reverse oligonucleotide primers

Template cDNA

Method:

5µl of cDNA synthesised from 0.5µg RNA in reaction volume of 20µL was used to amplify specific product so standards could be made for the subsequent real time PCR analysis.

The cDNA was added to:

HotStar Taq Mix (Qiagen)	25µl
Forward cyclin D1 primer (10uM)	0.5µl
Reverse cyclin D1 primer (10uM)	0.5µl
Water	19µl

The reaction was performed in a thermal cycler and heated to 95°C to allow separation of double stranded DNA, then a cooling to 60°C to permit the primer to anneal then a rise in temperature to 72°C for extension to take place. The cycle was repeated 35 times as outlined in the table above.
The reaction products were run on a DNA agarose gel as previously described.

2.6.5 Amplicon Excision from DNA Agarose Gel

Materials:

1.5mL microcentrifuge tube
scalpel
UV light box
UV protection

Method:

Wearing UV protection, the agarose gel was placed on a UV light. Using a sterile scalpel the amplicon band was cut out removing as much gel as possible without interfering with the band and placed in a microcentrifuge tube. The microcentrifuge tube was pre-weighed prior to adding the excised band as the weight of the gel was required for extraction reagent volumes using the QIAquick Gel Extraction Kit.

2.6.5.1 Amplicon extraction from agarose gel

Materials:

DNA gel extraction Kit (Qiagen, UK 28704):

Buffer QG: solubilisation and binding buffer (pH ≤7.5)
Buffer PE: ethanol containing wash buffer
Buffer EB: 10mM Tris·Cl (pH 8.5) elution buffer

QIAquick spin column

2mL collection tube

Isopropanol

1.5mL microcentrifuge tube (autoclaved)

Heat block set to 50°C

Microcentrifuge

Method:

DNA adsorbs to the silica-membrane in the presence of high salt while contaminants pass through the column. Impurities are washed away and the pure DNA is eluted with Tris buffer or water.

This extracts DNA (70bp-10kb) from agarose gels in TAE using spin-column technology with the selective binding properties of a silica-gel membrane accompanied with buffers optimized for efficient recovery of DNA. Each spin column can bind up to 10μg DNA.

In a microcentrifuge tube the agarose gel was solubilised by the addition of 3 volumes of Buffer QG per gel volume (100mg ≈ 100μL) and incubating at 50°C for 10 minutes and vortexed intermittently. Isopropanol (1 gel volume) was added to the solubilised gel, mixed by vortex then added to a QIAquick spin column inserted into a 2mL collection tube. The solubilised gel was passed through the column by centrifugation at 14000 rpm for 1 minute at room temperature; the flow through was discarded. Buffer QG (500μL) was added to the column and centrifuged; the flow through was discarded. The column was washed with the addition of 750μL Buffer PE to the column and centrifuged. The flow through was discarded and centrifugation was repeated to remove residual ethanol present in the Buffer PE from the washed column. The column was transferred to a 1.5mL microcentrifuge tube and the DNA was eluted by the addition of 30μL Buffer EB to the centre of the column for 1 minute prior to centrifugation. The eluted DNA was stored at -20°C.

2.7 DNA estimation

Materials:

2% agarose gel

DNA ladder hyperladder IV (Bioline)

TAE buffer

UV light and digital camera/software

Method:

To estimate amplicon amount and ensure integrity following its extraction small volumes were analysed by electrophoresis and compared to Hyperladder IV.

5μL hyperladder IV was run on a 2% agarose gel alongside 1 μL of eluted amplicon and 2μL of eluted amplicon, added to 1μL loading buffer and DEPC water to make a final volume of 6μL. Electrophoresis was performed in 1x TAE buffer for 45 minutes and the separated products visualized under UV light.

2.7.1 Amount of specific product estimation using Avogadro's number

The number of amplicon molecules was calculated using Avogadro's number (6.022 $x10^{23}$), the molecular weight of the amplicon and the estimated concentration of amplicon.

An example of such a calculation for cyclin D1

Amplicon 104 bp

Molecular weight of the amplicon = 330 x (length of the amplicon x 2)

1 mole = 68,640g = 6.022 $x10^{23}$

1ng = $8.77x10^{9}$

From the gel, 2μl = 20ng = 1.75 $x10^{11}$ copies

Standard = 8.75 $x10^{10}$ copies/μl

2.8 Developing a Real Time PCR protocol to quantify candidate gene expression in rat liver

2.8.1 Optimisation Steps

Prior to construction of the necessary standard curves and sample analysis several stages had to be optimised using the Rotor gene machine.

These were: SYBR concentration, primer concentration and magnesium concentration.

Reaction mixtures were set up in individual tubes (HotStar Taq, primers, SYBR Green and DEPC water) and each parameter was then varied while the others remained constant to see which amounts gave the best results.

In each 20µl reaction volume the optimal primer volume was found to be 2µl of 10µM primer stock (which gives a final concentration of 800nM), 1.5µl of 1:3000 SYBR Green equivalent to a final dilution of 1:50 000. It was found that no additional magnesium was required for optimal results.

2.8.2 Standard Curve

For construction of the standard curves, the serially diluted amplified specific product were added in duplicate a volume of 1µl each to the reaction mixture already described and then run on the Real Time PCR machine. Duplicate samples established reproducibility and accuracy of the assay. The Biogene software constructed standard curves for 18S and cyclin D1 at the end of the reaction.

2.8.2.1 Samples

With acceptable standard curves, all samples were run for the target of interest followed by 18S to which the copy numbers per reaction were normalised. Accuracy of the assay was demonstrated by showing reproducibility across more than one Real Time PCR run. Two separate Real Time PCRs were consistently performed each time.

Reaction Mix for ***cyclin D1***:	Hotstar Mix	10µl
	Forward primer	2µl
	Reverse primer	2µl
	SYBR Green	1.5µl
	H_2O	2.5µl
	cDNA	2µl
	TOTAL	20µl

Reaction Mix for 18S:	HotStar Taq Mix	10µl
	Forward primer	0.5µl
	Reverse primer	0.5µl
	SYBR Green	1.5µl
	H_2O	6.5µl
	cDNA	1µl
	TOTAL	20µl

Within each individual Real Time PCR run the appropriate Non Template Controls (NTCs) were included as well as the standards. The standards chosen would lie between the range of fluorescences of the experimental samples and were run in duplicate. At least three standards were included in each reaction. At the completion of each reaction the appropriate standard curve, either for amplicon of interest or 18S, was imported to allow the software to calculate the copy number of amplicon per reaction. This number was then normalised to the 18S copy number per reaction.

2.8.3 cDNA synthesis for the Kruppel Factors (Chapter 6)

Materials:

RNA sample 0.5μg

QuantiTect® Reverse Transcription Kit (Qiagen Cat.#205311) contains:

genomicDNA wipeout buffer 7x

Quantiscript Reverse Transcriptase

Quantiscript RT Buffer 5x

RT primer mix

RNase-free water

Method:

The use of this kit speeds up throughput enabling more efficient handling of a greater number of samples. It was therefore used for the subsequent Real Time PCR analysis of a number of Kruppel Factors discussed in Chapter six.

The RNA sample (variable volume but constant quantity of 0.5μg) was incubated in genomicDNA wipeout buffer at 42^0C for 2 minutes to remove all genomic DNA.

The Quantiscript RT, Quantiscript buffer and RT primer mix were added and the total volume of 20μl was incubated for 15 minutes at 42^0C. Finally to inactivate the reverse transcriptase the reaction was heated to 95^0C for 3 minutes The cDNA was stored until required at -20^0C.

The Quantiscript Reverse Transcriptase has a high affinity for RNA and has been optimised by the manufacturer for efficient and sensitive cDNA synthesis from 10 pg to 1 μg of RNA. This enables high cDNA yields.

2.8.3.1 Real Time PCR for the Kruppel Factors

Materials:

QuantiTect™ SYBR® Green PCR Kit (Qiagen #204143) contains:

HotStar Taq® DNA Polymerase
Quantitect SYBR Green PCR buffer
dNTP mix
SYBR Green
ROX (passive reference dye)
5 mM $MgCl_2$
RNase free water

Method:

The kit provides accurate Real Time quantification of DNA and cDNA targets in an easy to handle format. Optimisation steps previously performed for $MgCl_2$ concentration and SYBR Green concentration were now not required and therefore this method was employed for the remainder of the thesis for quantitation of Kruppel Factor mRNA expression. This method allowed greater sample throughput with better reproducibility across Real Time experimental runs.

A master mix was prepared with each component in the following volumes:

QuantiTect™ Master Mix	10µl
Forward Primer	2 µl
Reverse Primer	2 µl
Water	5 µl

19 µl of this was aliquoted into each PCR strip tube and finally the cDNA was added:

cDNA	1 µl
TOTAL VOLUME	20 µl

Reactions were run in strip tubes in a 72 carousel to enable higher sample throughput. In each Real Time PCR run, the appropriate standards in duplicate were included as well as two NTCs

The PCR reaction used an initial activation step for 15 minutes at 95°C, then 45 cycles of 95°C for 30s, 60°C for 30s, 72°C for 30s, finally 72°C for 10 minutes.

2.9 Isolation of Primary Human Hepatocytes

Normal human liver samples were acquired with patient consent (Ethics ID38-2000 Culture of human liver cells obtained at surgery) from specimens taken during liver resection for colorectal cancer performed at the North Hampshire Hospital. Only tissue considered 'normal' away from tumour margins were used. The weight of the tissue ranged from 29g to 69g. Samples were provided by Mr M. Rees, Department of Surgery, North Hampshire Hospital. These tissue samples have been designated the label BS.

This was carried out by other colleagues.

Materials:

Chelating Buffer (20mM HEPES, 0.5mM EGTA in PBS)

Perfusion Buffer (20mM HEPES in PBS)

Digestion Buffer (20mM Hepes, 1.5g BSA (0.5% w/v), 50µg/ml ascorbic acid and 4µg/ml insulin in 300ml HBSS. Just prior to digestion of the liver 150mg Collagenase Type IV (0.05% w/v) and 30mg DNase I (0.01%w/v) added)

Dispersal Buffer (50ml FCS (10%v/v) and 50mg (0.01% w/v) to 500ml Williams E medium)

Collagenase (Sigma)

Method:

Primary human hepatocytes were isolated from a freshly resected piece of liver by collagenase digestion through the remaining vasculature and differential centrifugation.

2.9.1 Viable cell count by trypan blue exclusion

The viable cell count was performed by trypan blue exclusion. An aliquot of the cells was diluted (1:10) into HBSS (8:10) with trypan blue (1:10) (0.2% Trypan blue in PBS) and kept at room temperature for 2min. The cells were then counted with a haemocytometer. The live cells will exclude the dye, whereas the dead cells have nuclei stained blue.

2.9.2 Preparation of collagen coated plates

Materials:

6-well plates

Sterile HBSS, calcium and magnesium free (Gibco, Invitrogen)

Sterile Saline

Collagen type I prepared from rat tail tendons (1g tendons in 300mls 0.01M sterile acetic acid, stirred at 4°C for 2 days, centrifuged at 800xg for 2 hours and stored at 4°C)

UV lamp

Method:

To a 6 well plate 2ml/well of collagen was added. After 5 minutes the collagen was flicked vigorously out of the wells and rinsed twice with 4mL HBSS. Sterile saline (1.5mL) was added to each well to sufficiently cover collagen. With the lid removed wells were irradiated under UV light. The plates were either used on the same day or stored at 4^0C until use.

2.9.3 Culture of Primary Human Hepatocytes

Materials:

Williams E Medium (Gibco #22551, Invitrogen)

T_3 deplete FCS (final concentration 10%) (Hyclone)

Penicillin/Streptomycin (final concentration 50U/ml) (Gibco)

Fungizone (final concentration 0.292g/L) (Gibco)

L-glutamine (final concentration 1.25µg/ml) (Gibco)

Insulin (final concentration10^{-8}M)

Method:

Williams E medium was made up with all the above supplements. Once isolated, hepatocytes were seeded in collagen coated plates at $1x10^6$cells/ml, with 2ml per well of a six well plate.

Primary hepatocytes were plated at a density of 2 million cells per well on collagen coated tissue culture plates and maintained with William's E medium supplemented with fetal calf serum (10%), penicillin (200U/ml), streptomycin (200U/ml). The culture

plates were maintained in a humidified incubator with an atmosphere of 95% oxygen and 5% carbon dioxide overnight. The next day the wells were washed with HBSS to remove non-viable cells and the culture medium was then replaced with fresh medium prior to the start of the experiments.

2.9.4 T_3 deplete Foetal Calf Serum (FCS)

Materials:

AG 1-X8 resin (Biorad, Richmond CA USA)

dH_2O

50ml NUNC tubes

Filters

Foetal calf serum (Hyclone)

Method:

FCS was incubated at room temperature with 50mg/ml AG 1-X8 resin (Biorad), which had been previously washed three times with distilled water. After 5 hours of incubation under stirring, the resin was removed by centrifugation at 1,000g for 10 minutes. An additional quantity of fresh resin was added at a concentration of 50mg/ml to the residual serum and the serum was incubated for a further 15-18 hours at room temperature. The resin was finally removed by two centrifugation steps at 1,000g for 10 minutes and 30,000g for 20 minutes at room temperature. The serum was then sterilised through a 0.2μm filter and stored at -20°C until required.

2.10 Bicinchoninic Acid (BCA) protein assay

Materials:

96 well plate

Bovine serum albumin stock 100mg/ml

Reagents A and B:

Reagent A: 1 gm sodium bicinchoninate (BCA), 2 g sodium carbonate, 0.16 g sodium tartrate, 0.4 g NaOH, and 0.95 g sodium bicarbonate, brought to 100 ml with distilled water. Adjust the pH to 11.25 with 10 M NaOH.

Reagent B: 0.4 g cupric sulfate (5 x hydrated) in 10 ml distilled water.

Reagent ratio A: B is 50 parts to 1 part

Method:

BSA standards were prepared 1, 0.5, 0.25 and 0.125µg/ml.

Protein samples were first diluted 1:10 in water as they were otherwise too concentrated.

10 µl of standard or sample was pipetted into a well before the BCA reagent volume (A+B ratio 50:1) 200 µl was added.

The plate was then placed in an incubator at 37^0C for 30 minutes.

The absorbance was read at 570nm. A standard curve was generated each time and from this the protein concentration of the samples was determined from the equation of the line.

2.11 Western Blot Protocol

Materials:

NuPAGE Novex Tris-Acetate 3-8% gel (Invitrogen)

RIPA lysis buffer 1x (Autogen-Bioclear # SC24948)

Phenylmethylsulphonyl fluoride (PMSF)

Protease Inhibitor cocktail

Sodium Orthovanadate

Sodium fluoride (50mM final concentration)

Rotor Star Homogeniser

NuPAGE 20X Tris-Acetate SDS Running Buffer (Invitrogen)

Deionised water

NuPAGE Antioxidant (Invitrogen)

Invitrogen gel tank

Methanol (BdH)

1X PBS

Tween

Loading buffer containing SDS

Heating block

Full range 10,000 – 250,000 rainbow molecular weight rainbow marker (Amersham Biosciences)

Polyvinylidene Difluoride (PVDF) membrane Hybond-P PVDF (Amersham)

Whatmann filter paper

Gel tank

Power supply

Ice cold Transfer buffer: 9g TrisBase
43.3g Glycine
1.2g SDS
600ml Methanol
Make this up to a total of 3L with dH2O

Ponceau red

Coomassie reagent

X ray film (Kodak)

ECL plus (Amersham) Solution A contains ECL plus substrate solution in Tris buffer and solution B is stock Acridan solution in Dioxane and ethanol

Cling film wrap

Restore Western Blot Stripping Buffer (Pierce)

Marvel non fat dry milk

Method:

Lysis buffer was prepared by combining 10µl PMSF, 10µl sodium orthovanadate solution and 10µl protease inhibitor cocktail to 1ml of 1X RIPA lysis buffer. To this lysis buffer 50 µl 1M NaF solution was added.

A piece of liver tissue was placed in a 5mL plastic bijou container and the pre-prepared lysis buffer was added in a volume of 1mL. The sample was homogenised for 30 seconds with a rotor star homogeniser while on ice.

The sample was placed on ice for 15 minutes and centrifuged at 1500x g for 10 minutes at 4^0C. The supernatant containing the protein lysate was removed and aliquoted into 100 µl aliquots in labelled 1.5ml centrifuge tubes and stored at -80^0C until further use in quantitation and gel electrophoresis.

2.11.1 Protein electrophoresis

The appropriate volume of sample was added to an equal volume of SDS loading buffer and 1 µl bromophenol blue was added, total volume 20 µl.

Each sample was heated to 100^0C for 5 minutes on a heating block.

The pre-cast gel was mounted into the electrophoresis apparatus and running buffer was added. The molecular weight marker was loaded in the first lane.

The denatured samples were then added to individual lanes.

The electrophoresis apparatus was connected to the electrical supply and a constant voltage of 150V was applied for 60 minutes.

After the samples had run, the gel was removed from the apparatus and immediately prepared for transfer of the polypeptides to the PVDF membrane by western blotting.

2.11.2 Western blotting

Four pieces of Whatmann 3mm paper were cut and soaked in ice cold transfer buffer for five minutes. The blotting tray was then set up as depicted in Figure 6.

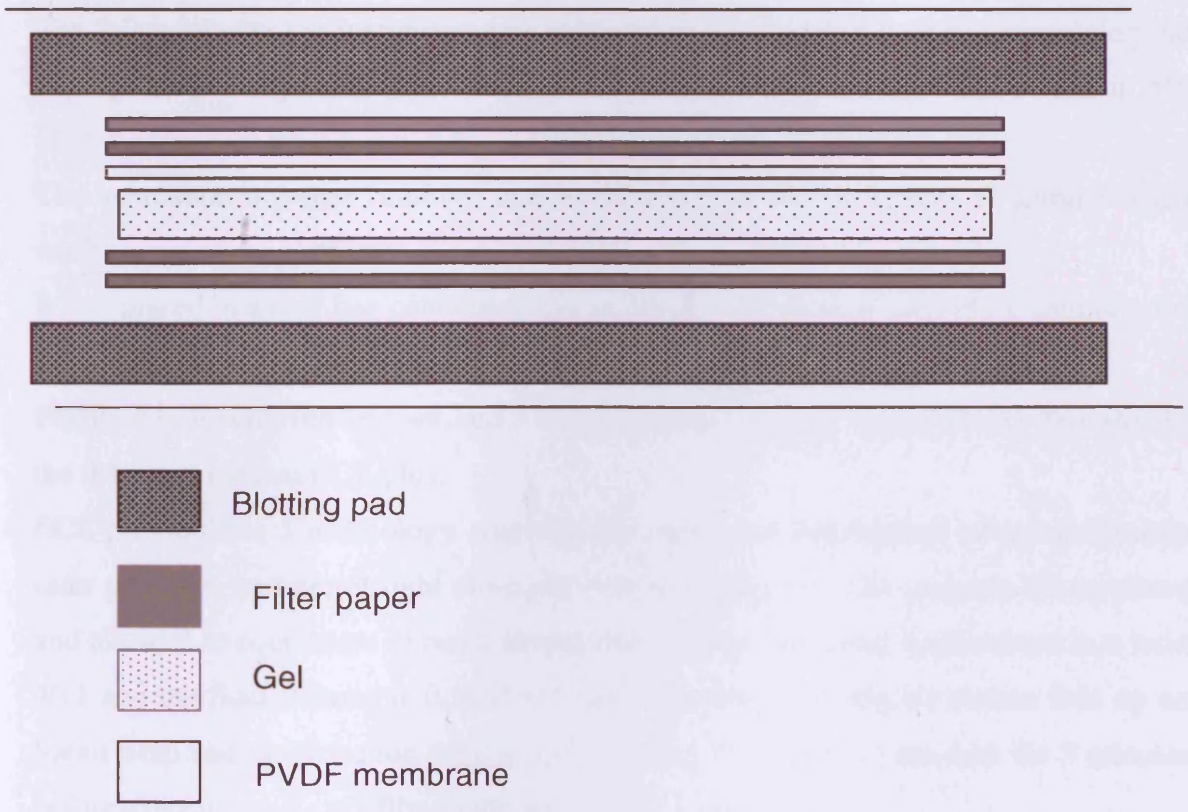

Figure 6 A schematic of the gel and blotting membrane used in the Western blot experiments described in this thesis.

The PVDF membrane was cut to the size of the gel and then activated in cold methanol, washed in water and then soaked in ice cold transfer buffer ready for use and assembly of the blotting apparatus could then take place.

A constant current of 350mA was applied across the assembly for 3 hours to facilitate the transfer of polypeptides from the gel onto the membrane.

2.11.2.1 Staining the membrane

After transfer the membrane was placed in Ponceau Red to demonstrate successful transfer of protein. The gel itself was placed in Coomassie reagent and then washed to demonstrate that no protein bands were visible in the gel i.e. successful transfer to the membrane had taken place.

2.11.2.2 Probing the membrane

The PVDF membrane was placed overnight on a rotating wheel in a sealed bag containing 5% Marvel milk in 1X PBS as a blocking solution at 4^0C.

The following day the membrane was removed and placed in a new bag containing the appropriate primary antibody (Table 4) at a correct dilution in 1x PBS Tween in 5% Marvel. This was for 2 hours at room temperature on a shaking platform

The membrane was then removed and washed in PBS Tween 3 times 15 minutes each wash on a rocking platform.

It was placed in a new bag containing the appropriate dilution of secondary antibody for 90 minutes at room temperature.

Finally it was removed and washed 3 times again in 1X PBS Tween before exposure to the detection reagent ECL plus.

ECL plus utilises a technology whereby the enzymatic degradation of an acridinium ester produces an intense light emission of longer duration. The reagents are removed and allowed to equilibrate to room temperature. Solutions A and B are mixed in a ratio 40:1 and the final volume is 0.1ml/cm^2. The membrane was placed protein side up on Saran wrap and the detection reagent was pipetted on and left in the dark for 5 minutes before exposure to X- ray film in the developing room.

2.11.2.3 Membrane Stripping

Materials:

Restore™ Western Blot Stripping Buffer (Pierce # 21059)

X1 PBS

ECL+ (Amersham)

Kodak film

IgG HRP linked antibody

Method:

So that the PVDF membrane could be probed with a different primary antibody it was stripped using a commercially available stripping buffer.

The buffer was warmed to room temperature. The blot was placed in an adequate volume of buffer for 15 minutes at room temperature. The blot was washed in 1X PBS. To test for complete removal of HRP label, the blot was incubated with new ECL+ and exposed to film. To test for complete removal of primary antibody the blot was incubated with the appropriate secondary HRP labelled antibody, followed by a wash and then incubation in fresh ECL+ and exposed to film.

As no signal was detected at either step of this procedure it was possible to go on and probe the same membrane with another primary antibody.

Table 4 Antibodies used in Western Blot in this thesis

Antibody	Product	Dilution	Secondary
Rabbit anti p-mTOR (Ser 2448)	#2971	1:1000 120 minutes	1:2000 60 minutes
Rabbit monoclonal anti mTOR	Cell Signalling Tech #2983	1:1000 120 minutes	1:2000 60 minutes
Anti rabbit IgG HRP linked secondary	Cell Signalling Tech #7074		1:2000

Chapter 3 Liver Perfusion

3.1 Background

The mitogenic T_3 effect is modelled successfully in rodents *in vivo* but as yet it cannot be used in man until evidence is produced that documents a mitogenic effect in human liver. An important goal therefore is to demonstrate a mitogenic effect of T_3 on human liver tissue prior to its experimental use *in vivo* in man. As yet no mitogenic effect has been demonstrated in hepatocyte culture (either simple monolayer or more complex 3D and co-culture scenarios) in rodent or human hepatocytes. Using therefore an *in vitro* system to model mitogenic effects in the more architecturally sophisticated environment of either an *ex-vivo in vitro* whole rat liver perfusion or in perfusion of pieces of human liver, provides an experimental solution which may offer exciting answers as to whether T_3 exerts a mitogenic effect in human liver.

In this Chapter therefore liver perfusion experiments using rodent and human liver are described in more detail preceded by initial experiments undertaken to define the *in vivo* rodent T_3 proliferative response to better characterise the optimal mitogenic dose and its time course of effect.

3.1.1 Organ perfusion

There is a long history of organ perfusion particularly as a tool to study liver metabolism and the effects of drugs and toxins on the liver and how these agents may be metabolised by the liver (Brauer *et al.* 1951; Bessems *et al.* 2006; Cheung *et al.* 1996) and a lot of work has been done to perfect the technique of the isolated perfused rat liver (IPRL) i.e. an *ex-vivo* perfusion. Numerous studies describe conditions which need to be optimised to enable an optimal perfusion experiment to be completed successfully. The IPRL most closely reflects the *in vivo* scenario, allowing the hepatic response to various xenobiotics to be measured. Oxygen consumption, bile production, liver enzyme levels, pH of perfusate, lactate levels and histological sections are amongst the parameters which have been measured in various publications to date (Cheung *et al.* 1996). Studies thus far have optimally perfused rodent liver for periods of up to 6 hours and the gold standard to assess tissue viability has been the histological appearance on Haematoxylin and Eosin liver tissue sections.

Researchers have for over fifty years used perfusate made up of a buffer with diluted erythrocytes (Brauer *et al.* 1951; Miller *et al.* 1951) or indeed buffer combined with hyperbaric oxygen (Schmucker *et al.* 1975). Early studies found that a haematocrit of 20 % provides the optimal combination of blood flow and oxygen carrying capability whilst maintaining physiological perfusion pressures of about 10 mmHg (Riedel *et al.* 1983).

Mischinger and Starzl (Mischinger *et al.* 1992) describe one technique of organ perfusion although many others have published on how this may be perfected. In their study it was found that the liver could be perfused optimally for up to 3 hours with oxygenated Krebs- Henseleit buffer (KHB) *without* the addition of red blood cells. Changes in hepatocellular enzymes, bile production, and liver histology were measured to determine the best perfusion parameters and it was found that bovine serum albumin (BSA) when added to the perfusate may actually be damaging to the perfused organ.

A separate study (Alexander *et al.* 1998) examined whether using perfusion buffer alone was sufficient in maintaining hepatic function over the time course of the perfusion, typically up to 6 hours. A comparison was made between 6 adult male Sprague Dawley (SD) rat liver perfusions with the addition of rat red blood cells and 6 adult SD male rat liver perfusions without the addition of any red cells. The conclusion from this study was that perfusion using buffer alone was insufficient to maintain optimum liver function.

Many perfusion systems have been cumbersome and required large priming volumes (Alexander *et al.* 1995), and consideration must also be given to the oxygenator which is a crucial part of any successful perfusion circuit, enabling delivery of appropriate oxygen to the tissue which requires it for efficient metabolism and maintenance of as near normal physiological conditions as one can achieve (Alexander *et al.* 1984). Problems described in the past have included the formation of bubbles and foam due to direct contact of the perfusate with the gas phase. An oxygenator therefore needs to be atraumatic, easy to clean and require a small priming volume as a reflection of its oxygen delivery efficiency. The use of a gas permeable membrane allows the avoidance of direct contact of gas with the aqueous phase (Galletti 1971; Robb 1968), and this is one more way in which perfusion circuitry has been improved over the decades.

For this project a perfusion apparatus was designed with the intention of perfusing initially whole rodent liver but then also pieces of human liver, to enable the mitogenic effect of T_3 to be modelled for the first time in human liver tissue.

3.2 Aims

a) To determine the T_3 hepatocyte proliferative dose response and time course of response in rat liver *in vivo.*

b) To develop an *in vitro* organ perfusion system to enable the delivery of growth factors and T_3 to rodent and human liver to model their effects and assess proliferation by means of BrdU incorporation and expression of the cell cycle antigen Ki-67 using histological and immunohistochemical techniques.

3.3 Materials and Method

3.3.1 *In vivo* Rodent T_3 Dose Response and Time course

BrdU is a synthetic thymidine analogue and when administered to the animal at a dose of 50mg/kg solubilised in sterile normal saline at 12.5mg/ml, given intra-peritoneally (i/p), it is incorporated into the DNA of cells undergoing DNA synthesis. Its subsequent detection is achieved using an immunohistochemical technique. It is frequently used in the technique of 'flash labelling', being administered 1 hour prior to animal sacrifice.

T_3 was obtained from Sigma (Poole, England) and dissolved in 1M NaOH at a concentration of 1mg/ml. It was administered to rats (n=3) by subcutaneous injection at a variable dose in 1ml volume (diluted in 960µl normal saline and 40µl 1M NaOH), to determine the T_3 hepatic proliferative effect according to dose (0-10 µg/rat). A second experiment was performed whereby the optimum dose (5µg) was administered to animals (n=3) sacrificed at different time points (14, 18, 24, 26, 30 hours post stimulus) to determine the time of the peak *in vivo* proliferative hepatocyte response. Establishing the most effective *in vivo* T_3 dose and time course of response enables the *in vitro* dose to be estimated.

3.3.2 Whole Rat Liver Perfusions

The perfusion technique was first designed using whole livers from adult male Sprague Dawley rats. Attempts were made to study whether T_3 exerted a mitogenic effect at 24 hours post dose by using BrdU incorporation similar to the *in vivo* scenario which is well established (Francavilla *et al.* 1994) and where one sees a peak hepatocyte proliferative response to T_3 at 24 hours post dose (*see Results*). Given the ready supply of resected pieces of human livers in the laboratory, work promptly moved on to attempt perfusion in these to see if the T_3 effect could be directly demonstrated in human liver. The human liver samples were obtained from a hospital in Basingstoke UK (designated BS) and are described in *General Methods Chapter Two* These livers were also the source of cells for the primary hepatocyte cell work described in *Chapter Seven.*

Materials:

Perfusate 500mls consisting of:

480mls William's E Medium (Gibco)

25mM HEPES buffer (12.5mls of 1M to 500mls Williams E to make 25mM final concentration) (Sigma)

3.5 mls 1M NaOH to a full bottle, filter sterilised, pH 7.4 final

5 mls penicillin/streptomycin

Insulin at a final concentration 10^{-7}M (500µl of a 10^{-4}M stock to 500ml of perfusion buffer)

5 or 20% by volume human red blood cells (when used and obtained from the Royal Free Hospital Blood Bank)

1,000 units heparin

The organ perfusion buffer was prepared under cell culture conditions and was filter sterilised prior to use. It was made fresh the day before a perfusion experiment was performed and stored overnight at 4^0C. Antibiotics were added to ensure the perfusate remained sterile and heparin was added only in the presence of blood to act as an anticoagulant preventing activation of clotting cascades which could have compromised normal perfusion of the liver. HEPES acted as a buffer to maintain pH within a normal physiological range.

Additional materials:

Silicone lid for glass organ beaker (autoclaved)

Watson-Marlow peristaltic pump set at 3 rpm equivalent to a flow rate of 10mls/minute

95% O_2/ 5% CO_2 was at piped into the oxygenator at 500cc/min (BOC gases)

Autoclaved 500ml glass beaker as the organ bath

Water bath at 37^0C

Jelly pads- microwave heated

Mechanical electronic stirrer (Heidolph)

Altec plastic tubing Altesil high strength silicone tubing bore 2.5mm wall 0.5mm (#01-93-1457)

GE Silicone # 03-71-5201

Three way taps (Baxter Healthcare)

22g blue human paediatric cannula (Medisave)

Syringe driver (Baxter Healthcare)

Silicone autoclaved bubble trap tube (Altec)

Hepatocyte Growth Factor (HGF) 10ng/µl and Epidermal Growth Factor (EGF) 10µg/ml (Sigma)

T_3 (Sigma)

BrdU (Sigma)

Hypnorm® containing fentanyl citrate 0.315mg/ml and fluanisone 10mg/ml (VetaPharma UK)

Method:

A diagram of the perfusion apparatus is outlined in Figure 7.

The oxygenator was constructed from a length of hollow polydimethylsiloxane (PDS) tubing. The tubing was wrapped around 2 glass pipettes and held in place with silicone gel. The assembly was then inserted into a glass bottle of volume 1L and in the lid four holes were made using an electric drill. Through these the perfusate tubing could pass, while through another hole oxygen could be introduced from a cylinder at 500cc/min. Oxygen could then be delivered into the beaker and diffuse across the perfusate tubing and into the circulating perfusate.

The perfusion circuit was set up before animal sacrifice and organ harvest. A volume of 500mls perfusate was brought to 37^0C in the incubator and this was used to prime the system in preparation to receive the organ or piece of liver.

The oxygenator bottle was immersed in a warmed water bath and the perfusion beaker sat on a metal support in the water bath so its sides were adequately bathed in water kept at a constant physiological temperature of 37^0C. Perfusate was stirred at a constant rate using an electronic stirrer to ensure proper mixing and therefore even distribution of added drugs such as mitogens and BrdU but also red blood cells which would otherwise sediment out over time.

3.3.3 Perfusate

A volume of 500ml was needed to prime the circuit. Early experiments used packed human red blood cells which were added to the perfusion buffer in an attempt to improve its oxygen carrying and delivery capabilities. The red cells were collected from the Royal Free Hospital Blood Bank and were taken from stocks that were to be discarded for a number of reasons, for example reaching the end of their shelf life.

The ABO blood group and Rhesus antibody status was recorded for all samples and for the human perfusion work an exact match to the perfused liver sample was always sought.

Initial experiments were conducted with 20% red cells by volume and then a concentration of 5% was used before perfusate was eventually utilised with the addition of no red blood cells.

The consequences and reasons for doing this will be discussed in the results and discussion sections.

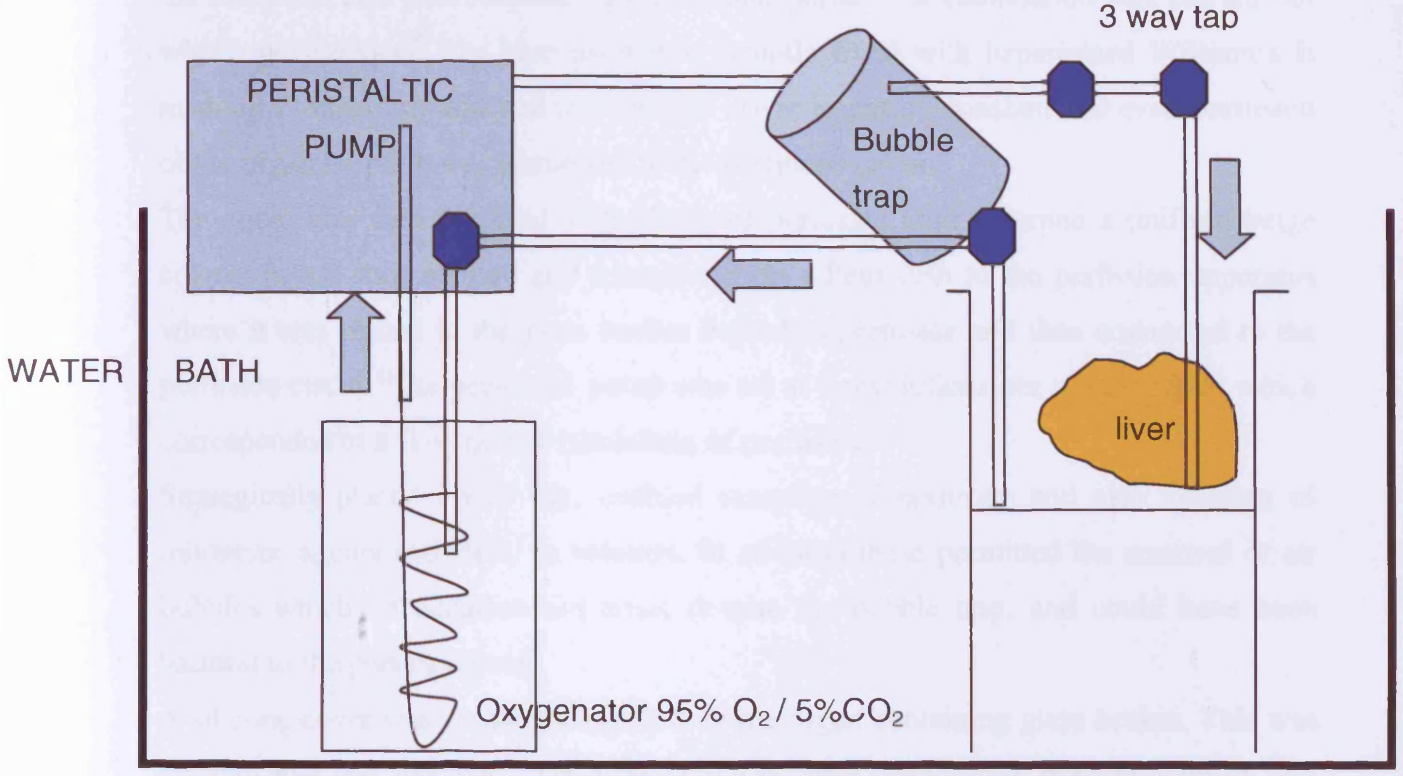

Figure 7 Schematic diagram showing the perfusion circuit. For simplicity and clarity the electronic stirrer is not shown. The entire system was maintained in a water bath held at a constant temperature of 37 ^{0}C. The circuit tubing is composed of Silastic silicone tubing. Strategically placed 3 way taps and a bubble trap allowed the removal or containment of potentially harmful air bubbles.

3.3.4 Animal Protocols

Male Sprague-Dawley rats (250g) were housed in a temperature- and light-controlled room (12-hour light/dark cycle) with free access to food and water. Animal care and all procedures were compatible with the Animal (Scientific Procedures) Act 1986, UK Home Office.

The animal had its weight recorded and was anaesthetised with a dose of 1ml/kg Hypnorm® given IM into a thigh muscle. The drug took about 10 minutes to take effect.

The perfusion apparatus was already set up and primed with warm perfusate as shown in Figure 7. The anaesthetised animal was laid onto the surgical bench placed on top of a warmed jelly bag and a midline laparotomy incision was made to expose the liver fully. The limbs were fixed to the bench using surgical tape.

Heparin was injected through the femoral vein to fully anti-coagulate the animal. Two 3/0 silk ligatures were placed under the portal vein. The organ was mobilised by cutting the falciform and gastrohepatic ligaments and portal vein cannulation was carried out with a polyethylene 22g blue paediatric cannula filled with heparinised William's E medium (2 units/ml) attached to a syringe driver to ensure constant and even perfusion of the organ before it was connected to the perfusion circuit.

The organ was then perfused with 20mls of perfusate until it turned a uniform beige colour. It was then excised and transported on a Petri dish to the perfusion apparatus where it was placed in the glass beaker bathed in perfusate and then connected to the perfusion circuit. The peristaltic pump was set at 3 revolutions per minute (rpm) which corresponded to a flow rate of 10mls/min of perfusate.

Strategically placed 3-way taps enabled sampling of perfusate and also injection of mitogenic agents and BrdU in solution. In addition these permitted the removal of air bubbles which on occasion did arise, despite the bubble trap, and could have been harmful to the perfused liver.

A silicone cover was cut to loosely fit over the organ containing glass beaker. This was autoclavable and therefore sterile and acted to limit evaporation from the system and also to limit access from air-borne microbes. Times were carefully recorded and once the organ was in position and the perfusion circuit was functioning mitogen or vehicle could be introduced to the perfused liver up stream by means of a 3 way tap. Any solution injected was done so carefully to avoid the introduction of air into the circuit.

Perfused liver either received a mitogenic dose of T_3 (*see Chapter 3 Results*), vehicle only or the potent hepatomitogens HGF and EGF.

Twenty three hours after the start of a perfusion BrdU solubilised in normal saline was introduced to the perfusion circuit (final concentration 40μM i.e analogous to the *in vivo* dose of 50mg/kg) to allow cells actively synthesising DNA to be identified at later immunohistochemical analysis.

At the end of each experiment the circuit was switched off and the liver was removed onto a Petri dish. The organ was flushed with fresh formalin and then sectioned and placed in 10% formalin for 24 hours to fix the tissues. Sections were cut from obviously

healthy looking areas of liver and areas which appeared to be poorly perfused so comparisons could be made histologically.

3.3.5 Human Liver Perfusions

Materials:

Human liver designated a BS number

University of Wisconsin (USW) solution

Ice

Cold bag

22g paediatric cannula

Tissue glue (3M)

Cell culture hood

Perfusion buffer already made up and stored at 4^0C but made ready by pre-warming to 37^0C.

Human liver samples were acquired with patient consent (Ethics ID38-2000 Culture of human liver cells obtained at surgery) from specimens taken during liver resection for colorectal cancer performed at the North Hampshire Hospital as described in *Chapter Two General Methods.*

On the day of surgery the liver sample was transported by car to the Centre for Hepatology as soon after surgery as was feasible. It was transported bathed in USW solution and on ice in a cold bag prior to transfer to the cell culture hood. A small piece of pre-perfusion liver tissue was resected on arrival and placed in formalin for later histological analysis.

After successful cannulation of a visible vessel lumen in the liver segment using a 22g human paediatric blue cannula which was secured in place using tissue glue, the liver was flushed with perfusate and transferred to the perfusion beaker and connected to the pump apparatus and perfused for a period which varied between 90 minutes and 48 hours following delivery of T_3 or vehicle only.

3.3.6 T_3 dose for organ perfusion

The optimum *in vivo* T_3 dose was found to be 5μg/250mg rat (*see Results*) to bring about hepatocyte proliferation with the peak *in vivo* response at 24 hours post dose. The assumption made for the perfusion experiments was that 5μg is distributed in the whole blood of the adult rat i.e. 15 mls total circulating blood volume. So for the volume of perfusate the amount needed equates to 166μg T_3 given in 1ml total diluent.
The T_3 was solubilised at 1mg/mL in 1M NaOH and the diluent used was 0.9% normal saline.

3.3.7 HGF/EGF

These potent hepatic mitogens were added to the perfusion circuit in one experiment on human liver, BS10, one hour after the perfusion was started in an attempt to demonstrate a hepatic mitogenic response if a response to less potent mitogens such as T_3 was not demonstrated. The amount administered was 1μg HGF (100μl of 10μg HGF in 1ml water stock) and 10μg EGF (10μg in 1ml water).

3.3.8 Bromodeoxyuridine (BrdU)

BrdU was added to give a final concentration of 40μM based on a dose given to the rodent *in vivo* of 50mg/kg. For 500 ml of perfusate therefore, 270 mg BrdU was solubilised in 5 mls sterile 0.9% sodium chloride solution.

3.3.9 Haematoxylin & Eosin (H&E), BrdU and Ki-67

The quality of the perfusion experiments was assessed by examining tissue sections with Haematoxylin & Eosin, immunohistochemical techniques used to enable detection of the cell cycle marker Ki-67 and to look for the incorporation of BrdU into nuclei of cells undergoing DNA synthesis (*see General Methods Chapter 2*).

3.4 Results

3.4.1 T_3 dose response and time course

The peak proliferative response as assessed by Bromodeoxyuridine (BrdU) incorporation occurs at 24 hours post T_3 when administered at a dose of 5µg per whole animal (Figure 8 and Figure 9). This compares with a peak in response noted by Pibiri et al (Pibiri *et al.* 2001) at 18 hours when using a larger T_3 dose of 20µg/100g body weight.

The dose of T_3 per animal gave the maximal proliferative response was 5µg (Figure 10). The hepatocyte proliferative response is predominantly seen to occur in the midzone region of the hepatic lobule consistent with previous published reports (Malik *et al.* 2003).

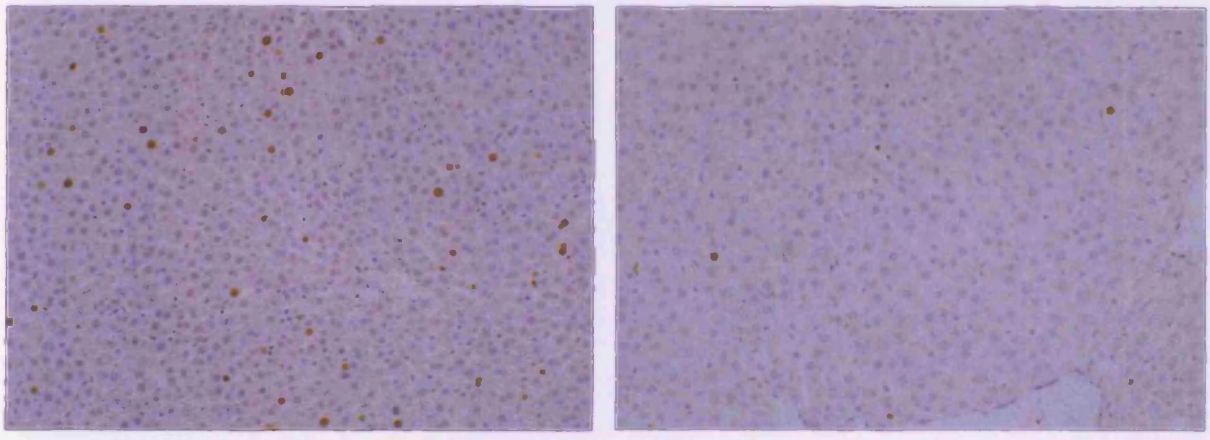

a) *b)*

Figure 8 Histological section of rat liver showing the hepatic proliferative response after mitogenic T_3 as measured by BrdU incorporation (a) after 5µg T_3 and (b) after vehicle only at 24 hours post dose. Cell nuclei within which DNA synthesis is occurring have incorporated BrdU and are stained brown in these tissue sections, x10 objective.

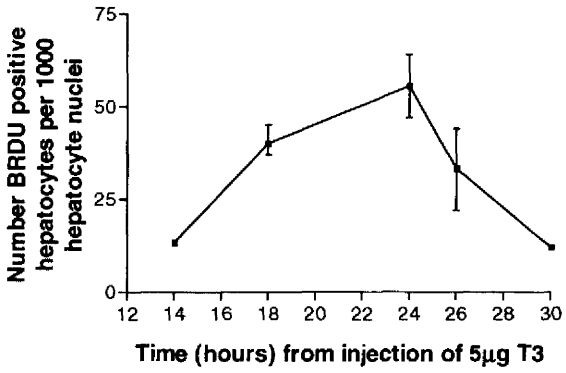

Figure 9 Time course of hepatocyte DNA synthesis in response to T_3 over time in adult male Sprague Dawley rats as measured by BrdU incorporation. Data points represent mean and range, n = 3 per time point. A total of 2,000 hepatocyte nuclei were scored for number of BrdU positive nuclei.

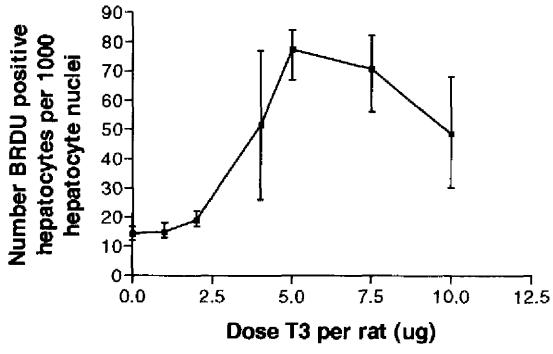

Figure 10 Dose response curve of hepatocyte DNA synthesis after T_3 as assessed by BrdU incorporation in adult male SD rats. At least 2,000 hepatocyte nuclei were scored. Data points represent mean and range, n = 3.

3.4.2 Organ Perfusions undertaken

The overall number of perfusions conducted are summarised in the Table 5. Nine separate rat perfusions were performed in addition to twelve human perfusions.

Table 5 A summary of the rodent and human liver perfusion experiments undertaken. The animal perfusions are designated 'rat' and the human liver perfusions as 'BS'.

LIVER	**PERFUSION TIME (hrs)**	**T_3**	**BrdU**	**Red Blood Cells (RBCs) %**
Rat 1	24	+	+	20%
Rat 2	24	-	+	20%
Rat 3	24	-	+	5%
Rat 4	24	-	+	5%
Rat 5	24	+	+	5%
Rat 6	24	+	+	-
Rat 7	24	-	+	-
Rat 8	24	+	+	5%
Rat 9	24	+	+	5%
BS4	27	+	+	20%
BS5	24	+	+	20%
BS6	24	+	+	5%
BS7	24	-	+	5%
BS8	6	+	-	-
BS9	10	+	-	-
BS10	24	HGF/EGF	+	-
BS13	48	+	+	5%
BS17	48	+	+	5%
BS 33	6	+	-	-
BS 35	6	-	-	-
BS 39 x2	90 minutes	+/-	-	-

The quality of the perfusions was variable but consistently improved upon and the perfusion parameters which affected the outcome are discussed further in the remainder of this results section.

3.4.3 Quiescent Rat Liver

A representative H and E section of quiescent unstimulated adult male Sprague Dawley rat liver is shown to demonstrate the normal hepatic architecture to enable comparisons to be made in the against sections of perfused liver (Figure 11).

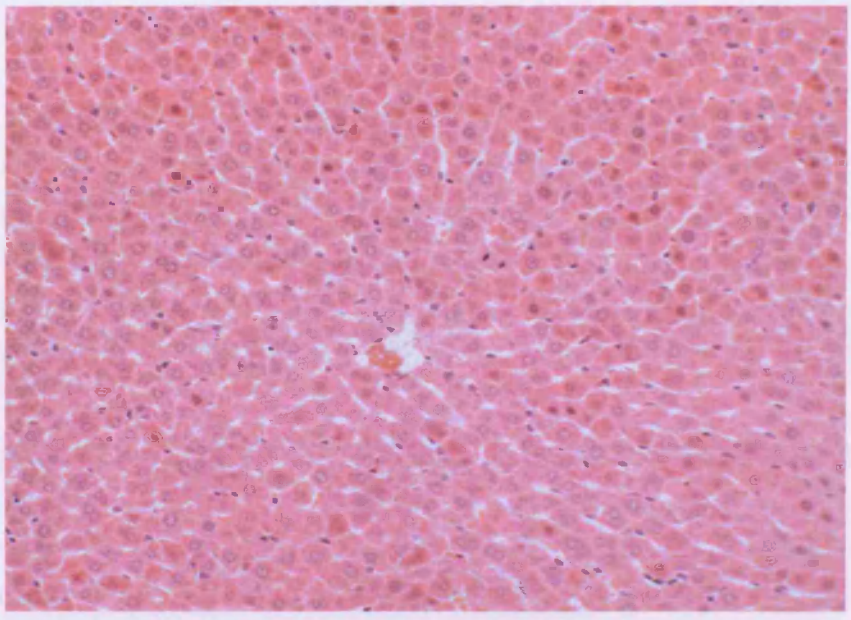

Figure 11 H and E section of unstimulated adult rat liver x20 objective, reflecting the normal hepatic lobular architecture. The vessel seen in the centre of the field is a hepatic vein and a few red blood cells can be seen to occupying its lumen.

3.4.4 Rat liver perfusion with 20% Red Blood Cells

Rat liver perfusion 2 was perfused with perfusate containing 20% RBCs and this resulted in areas of hepatic parenchyma becoming engorged with blood leading to significant architectural distortion (Figure 12). However in the same perfusion a relatively well preserved area of liver can be seen in a different part of the organ (Figure 13) with much less parenchymal red cell engorgement.

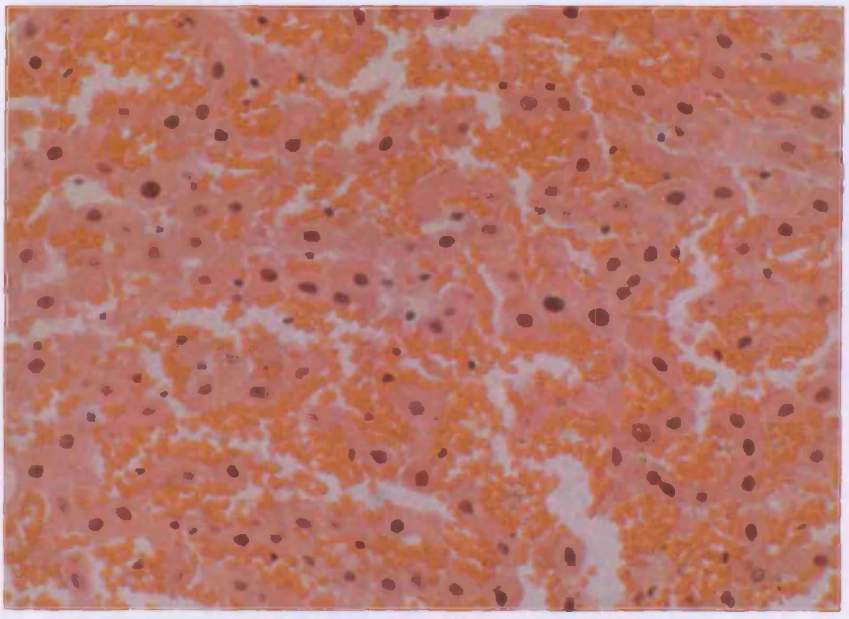

Figure 12 Rat liver histology after 24h perfusion x40 objective H & E section. Perfusate containing 20% red blood cells was used and a perfusion time of 24 hours. Note the architectural disruption and parenchymal engorgement with red blood cells

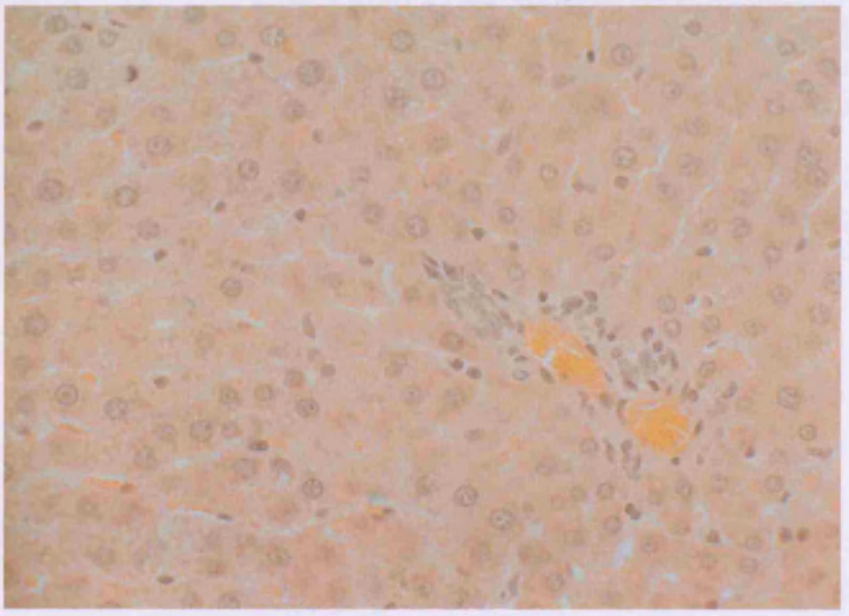

Figure 13 Rat liver histology x40 objective H & E tissue section. Perfused with 20% RBCs over 24 hours. This tissue section shows an area of liver which is better preserved histologically and in which there is no parenchymal engorgement with red cells.

The hepatocytes in the better perfused area look healthy with intact nuclei and intact cell membranes with no signs of vacuolation. In one tissue section there is evidence of a mitotic figure (Figure 14) which suggests that the perfusion conditions were favourable enough to allow this critical process to take place.

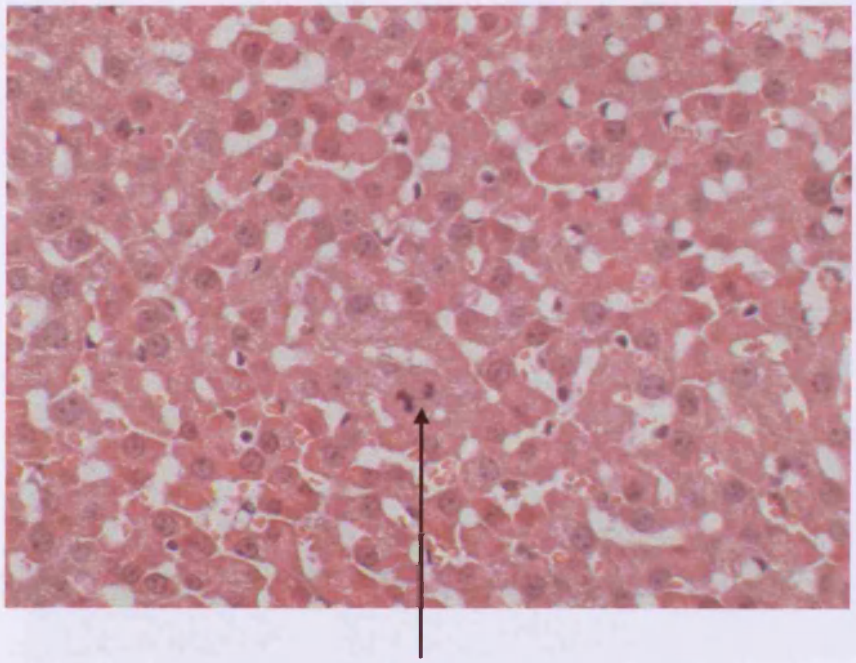

Figure 14 Rat liver histology x40 objective. Perfused with 20% red blood cells over 24 hours. This tissue section contains a single hepatocyte undergoing mitosis (indicated by the arrow).

3.4.5 Rat liver perfusion with 5% Red Blood Cells

Despite a lower concentration of red blood cells there were still significant areas which appeared engorged with blood in these perfusion experiments (Figure 15).

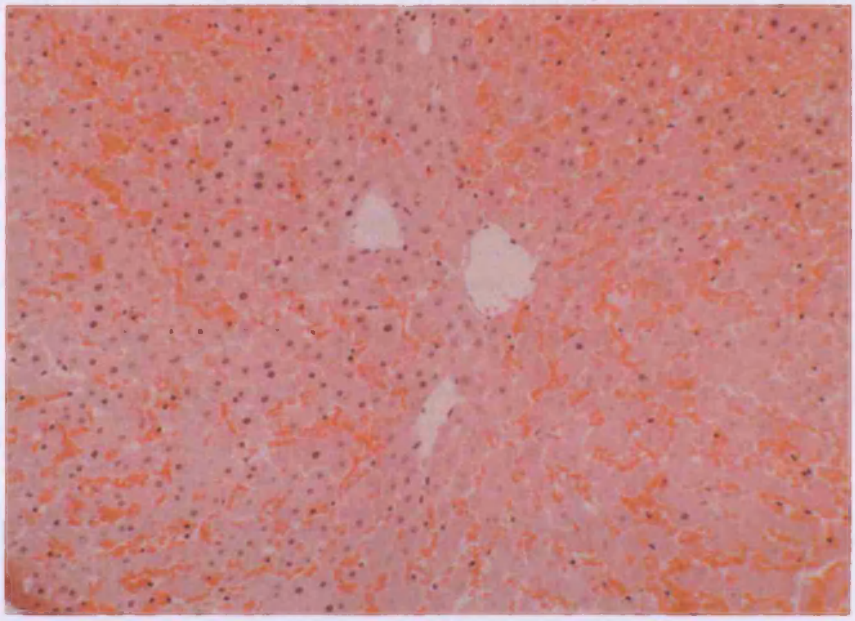

Figure 15 Rat liver histology x20 objective. Perfused with 5% red blood cells over 24 hours H and E section. In this tissue section parenchymal disruption is still apparent despite a lower concentration of red blood cells used in the perfusate.

The addition of red blood cells at concentrations of 5% and 20% led to a picture of engorgement of the hepatic parenchyma and a distorted hepatic architecture and in some areas there was evidence of tissue necrosis and apoptosis. This did not always follow the same pattern. For example it may have been the periphery of the perfused liver which was affected or a more central area or both. These differences depended on which vessel had been cannulated (either portal or hepatic vein) in the human livers and in the whole rat perfusion it indicated that the entire organ was not being equally and adequately perfused at all times despite secure placement of the perfusion cannula in the portal vein. Identifying whether a portal or hepatic vein had been cannulated proved very difficult when examining the human liver specimens but cannulation of a portal vessel was the experimental aim every time.

3.4.6 Rat liver perfusion with addition of no Red Blood Cells

In subsequent organ perfusion experiments conducted without the addition of red blood cells to the perfusate, the parenchymal engorgement with red cells and disruption seen previously was lost and some very well perfused areas of liver can be seen on the H and E sections (Figure 16).

In subsequent perfusion experiments the red blood cells were omitted given the frequency with which engorgement of the parenchyma was noted and appeared to lead to histologically poor areas of liver tissue. The oxygen saturation of the perfusate when measured was satisfactorily maintained (> 90%) despite the omission of red cells and as mentioned in the introduction the published experiences have been very variable but certainly other workers recommend the omission of red cells for short (up to 6 hours) perfusions. Indeed, maintaining a perfusion histologically intact for less than six hours was found to be the most plausible theoretically and experimentally in this thesis.

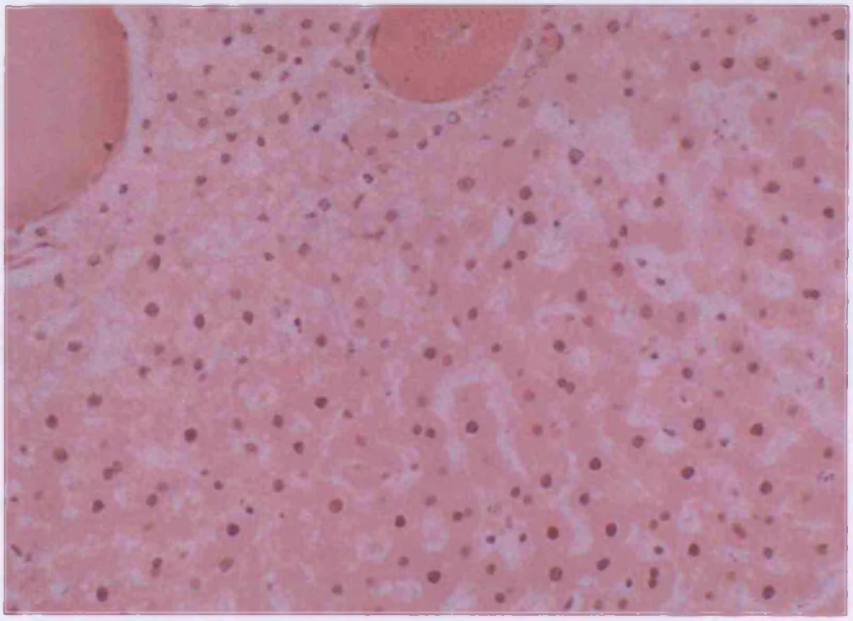

Figure 16 Rat liver histology x40 objective. Organ perfusion with the addition of no red blood cells to the perfusate, H & E section. There is no parenchymal engorgement and this area of liver is well perfused. Perfusate fluid can be seen filling the lumen of two vessels at the top of the tissue section.

3.4.7 BS Human Liver Perfusions

An example of a successful BS human liver perfusion can be seen in Figure 17, with a well perfused area of liver clearly visible under higher magnification.

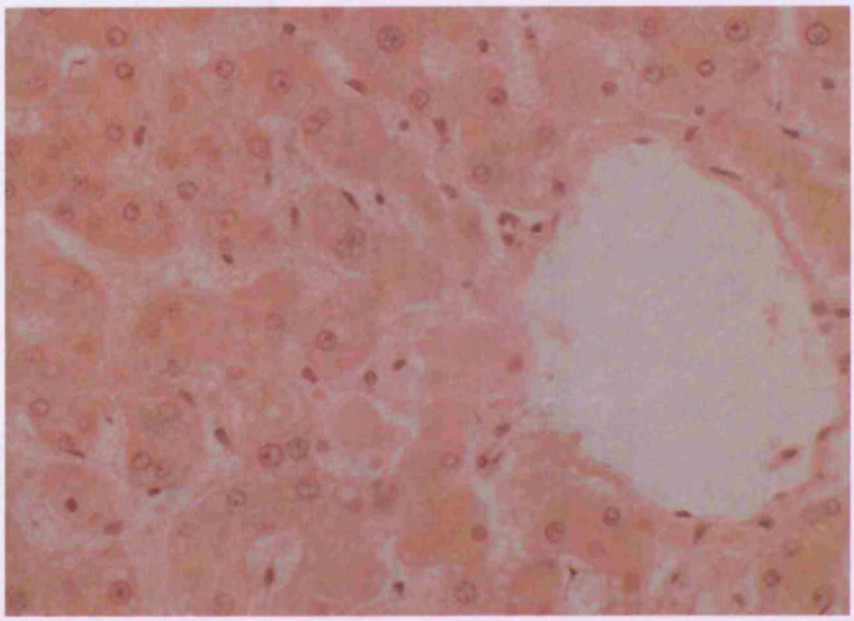

Figure 17 Histological section of human liver perfusion BS8 x40 objective H & E section reflecting a well perfused area of hepatic parenchyma adjacent to a vein. The liver was perfused for 6 hours with no red blood cells added to the perfusate.

3.4.8 Perfusate analysis

On one occasion serial measurements of perfusate fluid were undertaken to assess the change in various parameters such as oxygen saturation and pH using a blood gas analysis machine located within the Royal Free Hospital (Figure 18). Oxygen saturation was adequately maintained but by 18 hours lactate levels had risen sharply and by 24 hours the perfusate pH was almost 7.1, a clearly unacceptable value for normal physiological processes to occur, however it does lie close to rat portal blood pH which is 7.2 (Cheung *et al.* 1996). This analysis further supported the conclusion that perfusions over shorter time periods of only a few hours (0-6 hours) would be more successful.

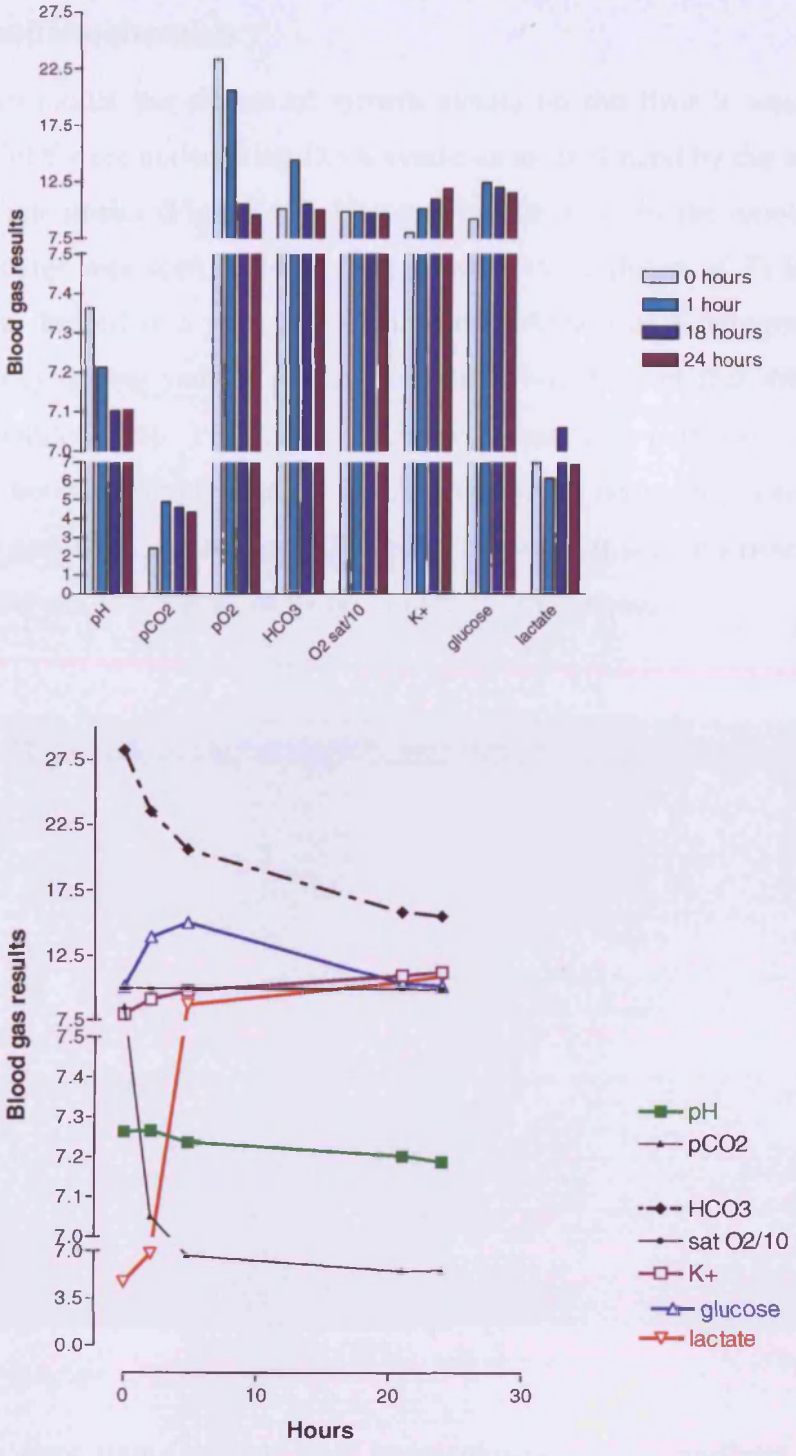

Figure 18 Serial analysis of perfusion parameters during a 24 hour rat liver perfusion experiment. pH is seen to fall and lactate rise after six hours of perfusion. (Normal rat portal blood pH in vivo is 7.2). Units: pCO_2 and pO_2 kilopascal (kPa); glucose, HCO_3, lactate, and K^+ mmol/l. O_2 saturation expressed as % / 10.

3.4.9 Immunohistochemistry

In an attempt to model the effects of growth agents on the liver it was possible to identify cells which were undertaking DNA synthesis as evidenced by the incorporation of BrdU into their nuclei (Figure 19). However no increase in the number of BrdU positive hepatocytes was seen at 24 hours following the addition of T_3 into the liver perfusion circuit. Indeed in a perfusion without the addition of a mitogen there were very few hepatocytes that stained positive for BrdU but the fact that this agent was actually incorporated into cell nuclei reflected that the perfusion milieu was physiologically normal enough to allow DNA synthesis to take place. BrdU was only added when the perfusion was run over 24 hours or more as it is at this time point in the *in vivo* model that one sees a peak of incorporation in hepatocytes.

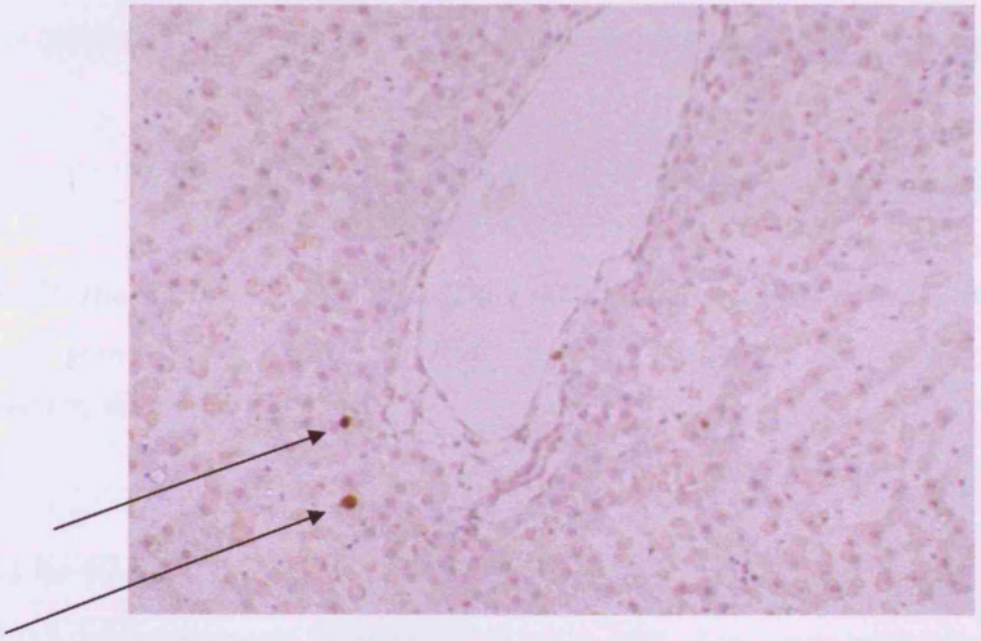

Figure 19 Rat liver tissue section after immunohistochemical analysis showing an example of BrdU incorporation (indicated by the arrows) in the cells of a perfused rat liver x 20 objective.

3.4.9.1 Human BS Liver perfusions

It was possible to demonstrate BrdU incorporation in human hepatocyte nuclei after a perfusion experiment (Figure 20). The number of positive cells was small however and certainly their numbers were not increased following the administration of T_3 into the perfusion circuit.

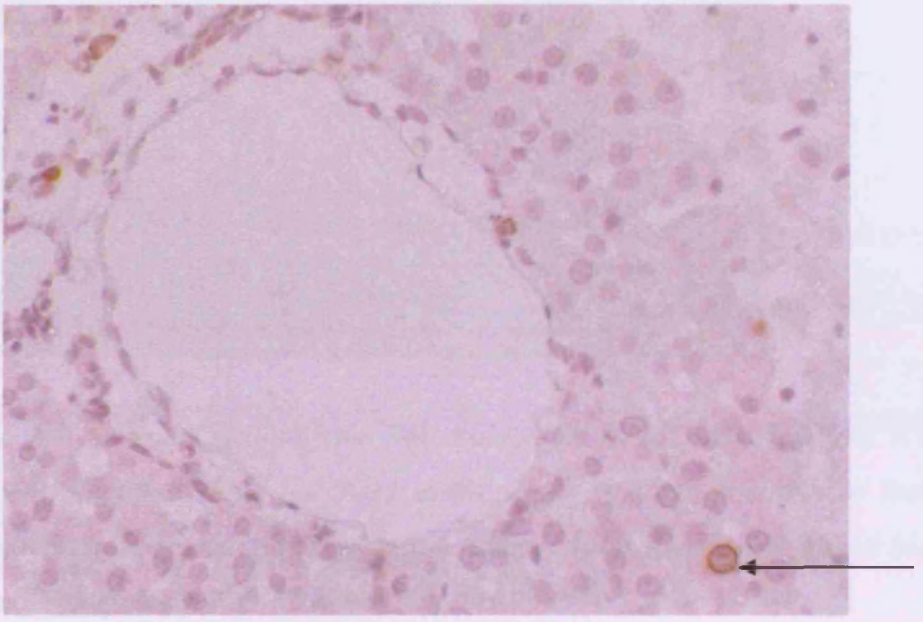

Figure 20 Human liver section from BS6 x 40 objective stained for BrdU. At least 3 cells are seen to stain positive for BrdU. A single hepatocyte positive for BrdU is indicated by the arrow.

3.4.9.2 Ki-67

Ki-67 is a cell cycle protein expressed in all active parts of the cycle but is absent while the cell remains in G_0 (majority of quiescent hepatocytes *in vivo*). Commercial antibodies exist that are directed against human and rat Ki-67. Human liver tissue was stained for Ki-67 to see if the number of positive cells was greater after mitogenic stimulation. In humans, if T_3 is ever to be administered *in vivo* the hepatic proliferative response cannot be measured using BrdU incorporation as this agent may be a potential carcinogen in humans (Gaglio *et al.* 2002; Gerlach *et al.* 1997; Huang *et al.* 2004). It was therefore worthwhile examining human liver sections for this protein as staining for Ki-67 would be useful in the future to assess T_3 treated human liver *in vivo,* for example in biopsy specimens. Unfortunately the numbers of cells positive for Ki-67 were very few and no greater following mitogen administration (Figure 21).

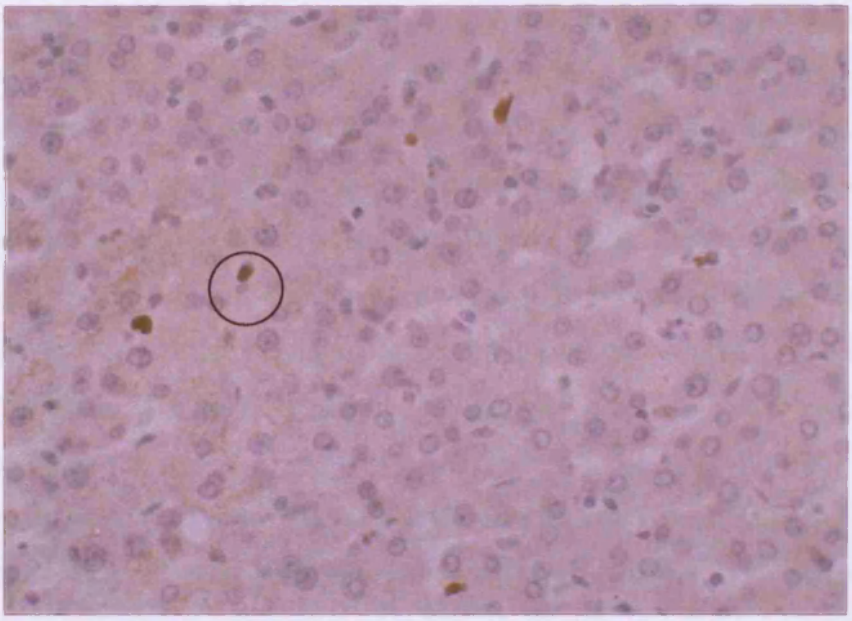

Figure 21 Human liver tissue section from BS6 stained for Ki-67, x40 objective. A non parenchymal cell indicated within the black circle stains strongly positive for human Ki-67 on this human liver section perfused for 24 hours. All the hepatocyte nuclei in this tissue section stain negative for Ki-67.

3.5 Discussion

The successful perfusion experiments achieved here were of short duration (up to 6 hours or less) and therefore this does not enable the more traditional means of identifying cells synthesising DNA, using BrdU incorporation, to be used to ascertain whether T_3 is exerting a proliferative effect on the hepatocytes. Other early markers of the T_3 mitogenic effect have to be sought. The attempts at organ perfusion described in this Chapter were carefully designed but despite the shortcomings in this early work, if the technique was further perfected it could become a very valuable tool in assessing the hepatic response to mitogenic stimuli, including T_3, as long as a marker of such an effect can be found.

There are technical considerations which when addressed might lead to more successful and more prolonged tissue perfusion times but even if this was achieved it remains as yet unclear as to whether the mitogenic agents would exert their desired effects as they are known to do *in vivo*. The *in vitro* perfusion is an attempt at replicating the more subtle and complicated milieu seen in the living organism. T_3 in particular may be acting through intermediate steps which require the interactions of all the animal's major organ systems. In addition even if it does act directly on hepatocytes its mode of action may be exquisitively sensitive to anything other than completely normal physiological conditions and these are difficult to replicate and maintain in the perfusion apparatus described here.

When human liver pieces were perfused it was frequently very difficult to identify the exact nature of the vessel cannulated. Ideally this would have been a portal vein as direction of perfusate flow would have been physiologically normal. However practically speaking the 'best' vessel had to be cannulated and if this was a hepatic vein the direction of perfusate flow would have been unphysiological and this could have led to an adverse outcome in any one perfusion experiment. A further obvious but nonetheless important experimental improvement is to manufacture duplicate apparatus that allows one to run two perfusions in parallel, thus enabling one to act as a control. Clearly *exactly* matching all the potential experimental variables is impossible but at least two perfusions undertaken at the same time adjacent to one another on the same day permits more reliable comparisons to be made than those conclusions one may draw by comparing separate perfusions on different days.

3.5.1 Additional improvements

Bile volume production has been reported to be the most sensitive indicator of hepatic function (Gores *et al.* 1986) and a reduction in bile volume production by 4 hours has been reported, likely representing a decline in hepatic function. Cannulating the bile duct in the rat liver perfusions undertaken here and measuring bile production would be a further important improvement to the experimental design. In future the portal pressure may also be accurately measured by using a pressure transducer during a perfusion experiment to more accurately control the rate and constancy of fluid flow and hence perfusion pressure. Furthermore regular and more frequent measurements of perfusate biochemical parameters may lead to a better understanding of which other experimental variables can be more accurately controlled in future.

Turning to the actual composition of the perfusate, it may be worthwhile to consider the use of perfluorocarbon emulsions as a perfusion medium (Kamada *et al.* 1980). Perfluorochemicals are chemically inert synthetic molecules that consist primarily of carbon and fluorine atoms, and are clear, colourless liquids. They have the ability to physically dissolve significant quantities of many gases including oxygen and carbon dioxide. Perfluorochemicals are hydrophobic, and are therefore not miscible with water and thus have to be emulsified for intravenous use. With sophisticated technology, it is possible to generate a stable perfluorocarbon emulsion with exceptionally small particles (median diameter < 0.2 μm) and the future use of these agents may allow more efficient tissue perfusion and oxygen delivery with less parenchymal disruption.

3.5.2 Future work

There is clearly enormous scope for perfecting and improving upon the technique of liver perfusion described in this Chapter. In parallel with this it would be very worthwhile trying to pursue another means of *in vitro* modelling of the T_3 mitogenic effect, and this could be achieved through the use of the tissue slice (Martin *et al.* 2002). Liver slices would provide the more sophisticated hepatic architectural tissue platform required to study the effects of mitogens and several unique characteristics are attributed to precision-cut liver slices. By contrast with other *in vitro* models, the preparation of tissue slices does not require the use of proteolytic enzymes that disturb cell-cell interactions and may be damaging for cells (Lerche-Langrand and Toutain 2000). Additionally, with many *in vitro* systems, the conditions of organ preparation or isolation vary from species to species. In contrast, a similar and convenient procedure is

used to prepare and incubate tissue slices of several organs from different species, including humans, making this model particularly suitable to perform inter-organ and inter-species studies. The maintenance of cell heterogeneity and cell-cell interactions within the original tissue matrix contained in a slice of tissue better reflects the high level of biological organization of the organ. The first attempts to maintain intact liver slices *in vitro* were made as early as 1923 (Warburg O. 1923) but the liver slice has been used to study the hepatic response to toxins more recently and it has been used as a model to study liver fibrosis in the animal and human (van de *et al.* 2006a; van de *et al.* 2006b; van de *et al.* 2007b; van de *et al.* 2007a).

There are now available commercial units such as the Krumdieck tissue slicer, which enable fully automated tissue slicing with pieces of uniform thickness in a reliable and reproducible manner. For the purposes of modelling the mitogenic effects of T_3 the use of this technology would seem a logical next step. A sensitive and early marker (within 6 hours) of the mitogenic T_3 effect which can then be used *in vitro* and *in vivo* to measure mitogenic T_3 effect needs to be found. Such a marker can then be employed to measure the mitogenic response in perfused liver as well as in precision cut liver slice experiments.

In summary, the perfusion experiments described in this chapter have shown how difficult it is to obtain a reliable system in which mitogenic effects can be modelled on rodent and human liver. Under these current experimental conditions, short perfusions of up to 6 hours are the most successful but this does not allow the more conventional methods of measuring a proliferative response using BrdU and Ki-67. Therefore in the next chapter this research thesis turns to identify early mediators of the T_3 proliferative response in the *in vivo* rodent model which could then be used in the *in vitro* scenario of organ perfusion and precision cut liver slices.

Chapter 4 Investigating Cyclin D1 and Bcl-3 as Mediators of the T_3 Mitogenic Response

4.1 Background

As outlined in the previous chapter the liver tissue which underwent perfusion could only be maintained in a satisfactory histological state for up to 6 hours and therefore traditional means of measuring DNA synthesis, in response to growth factors, such as by way of BrdU incorporation, was not possible. The search therefore for a 'marker' of the *early* mitogenic effects of T_3 becomes important.

Others have shown the cell cycle associated protein cyclin D1 is up regulated *in vivo* after T_3 within 4 hours at the mRNA level in the rodent model (Pibiri *et al.* 2001). Cyclin D1 protein content was increased at 4 hours after T_3, further elevated at 12 hours and maintained for 24 hours in their study. It was decided therefore to investigate cyclin D1 as a potential early marker of the hepatic T_3 response *in vivo* before using it to measure the *in vitro* response. The first part of this Chapter sets about characterising the *in vivo* rodent response of hepatic cyclin D1 to T_3 in this laboratory.

In the second part of the Chapter a further set of *in vivo* experiments are reported and investigate the hypothesised role of a novel candidate mediator, Bcl-3, of the mitogenic T_3 response using a Bcl-3 knock out murine model. The starting point for this analysis was the murine cDNA microarray data published by Feng et al, analysing hepatic genes expressed 6 hours after treating hypothyroid mice with a single high dose of T_3 (Feng *et al.* 2000). The data revealed that expression of 10 genes involved in cell proliferation was altered, including up-regulation of three genes – B61, Bcl-3 and kinesin-like protein. Bcl-3 is an IkB-related protein that can act as a co-activator for NFkB homodimers and for the liver-enriched transcription factor AP-1 which is relevant to hepatocyte proliferation and may therefore be a plausible candidate as an early mediator of hepatocyte proliferation.

The analysis is in two parts:

a) 'cyclin D1 as an early mediator of the mitogenic T_3 effect'

b) 'Bcl-3 as a mediator of the mitogenic T_3 effect'

4.1.1 Cell Cycle

The eukaryotic cell cycle is divided into four stages: G1, S, G2 and M (Figure 22). The G1 and G2 phases represent the 'gaps' in the cell cycle that occur between the Mitotic phase and the DNA Synthesis phase (Schafer 1998).

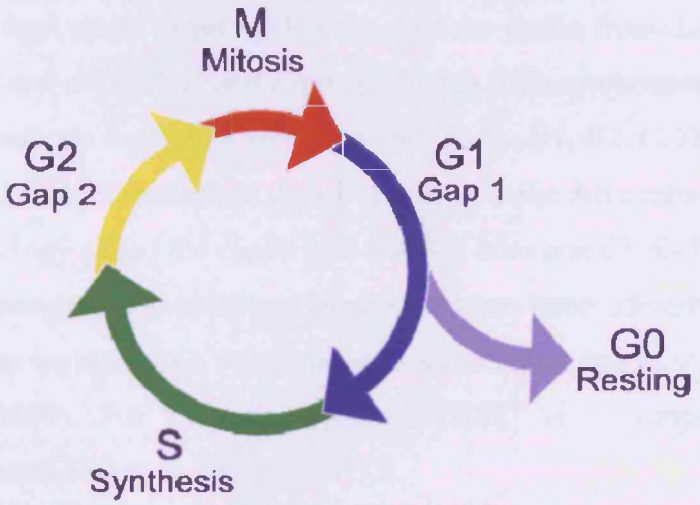

Figure 22 Diagram of the eukaryotic cell cycle indicating the different stages. In quiescent liver most hepatocytes are in the G_0 or resting phase. To undergo DNA synthesis they have to emerge from G_0 and enter the active G_1 phase prior to DNA synthesis in S phase.

In G1 the cell is preparing for DNA synthesis and in G2 it is preparing for mitosis. G_0 describes cells that are not within the active phases of the cell cycle but which have the potential for division. During G1 phase the cell integrates mitogenic and growth inhibitory signals and becomes committed to either proceeding with or exiting the cell

cycle (Johnson and Walker 1999). In the quiescent state the vast majority of hepatocytes exist in G_0 but have the ability to enter the cell cycle readily, given the correct conditions and stimuli (Sherr and Roberts 2004).

The serine/threonine protein kinases called cyclin dependent kinases (CDKs) complex with proteins called cyclins and this association catalyses progression of the cell cycle. Each CDK has a cyclin partner and binding to a cyclin is necessary for CDK activation. CDK inactivation prevents mitosis and the phosphorylation state of the CDK determines whether cycle progression can occur or not. Phosphorylation at certain residues can either stimulate or inhibit activity of the CDKs and other protein kinases can bring this about, for example the kinases *wee1* and *mik1*.

The cyclins are so called because they undergo cyclic expression. Part of the cyclic expression of cyclins is due to regulated degradation as they contain specific protein sequences that target them for ubiquitination at very specific times (Lu *et al.* 1992). Cyclin binding to CDKs is necessary for CDK activation and nuclear localisation and a cell enters the next phase of the cycle only once the cyclin from the previous phase has been degraded and the cyclin for the next phase has been synthesised.

In mammals there are more than 16 known cyclins (A, B1, B2, C, D1, D2, D3, E, F, G1, G2, H, I, K, T1 and T2) and more than 10 known CDKs. All cyclins contain a common region of homology called the cyclin box and it is here that CDKs bind and can then be activated. However other additional functions have been identified for cyclins and CDKs and these include DNA repair, apoptosis and regulation of transcription (Johnson and Walker 1999). For example, cyclin H/CDK7 is a component of the basal transcription machinery as is cyclin C/CDK8.

The CDKs phosphorylate a variety of substances allowing the cell cycle to progress. For example in G2 and M phases, nuclear laminins and microtubules act as substrates. Retinoblastoma protein in G1 (pRb) is another very important CDK substrate and it is described next.

4.1.1.1 D-type cyclins and pRb

The human cyclin D1 gene was initially cloned as a break point rearrangement in parathyroid adenoma. The murine homologue was identified as a colony-stimulating factor-1 responsive gene in macrophages (Fu *et al.* 2004). The cyclin D1 gene is over expressed in 30-50% of primary human breast cancers and a number of other human neoplasms show cyclin D1 up-regulation including squamous carcinoma of the head

and neck as well as several leukaemias and cyclin D1 has become well known for its prominent role in driving tumourogenesis. However the biological function of cyclin D1 when investigated in transgenic species is surprisingly redundant. In cyclin D1 deficient mice one sees retinal apoptosis, altered fat metabolism, hepatic steatosis and defects in macrophage migration.

D type cyclins associate with and activate the kinases CDK4 and CDK6 (Boylan and Gruppuso 2005; Rickheim *et al.* 2002) and the retinoblastoma protein (pRb) is the primary substrate for D-type cyclin kinases. Many oncogenic signals induce cyclin D1 expression and do this through distinct DNA sequences in the cyclin D1 promoter; these include: Ras, Src, ErbB2, and STATs.

pRb is very important as a gatekeeper of the G1 phase and its cell cycle inhibiting function is inactivated by cyclin D1 acting as the regulatory subunit of the holoenzymes that phosphorylate it (Nelsen *et al.* 2001). There is a point in G1 beyond which cells no longer respond to the withdrawal of growth factors and so it is termed the *restriction point.* So, if the growth factors are withdrawn prior to this the cell can revert to G_0 but after the restriction point the cell will go on into the DNA synthesis phase of the cycle. pRb is an important controlling factor of this restriction point (Loyer *et al.* 1996; Albrecht and Hansen 1999). Once the cyclin-CDK complex phosphorylates pRb, the transcription factor E2F is released and is free to transactivate genes necessary for cell cycle progression. Hypophosphorylated pRb binds E2F and prevents it from acting as a transcription factor. E2F factors regulate the expression of many genes that encode proteins involved in cell cycle progression and DNA synthesis, including cyclins E and A, CDK1 and DNA polymerase alpha (

Figure 23). After activation of E2F, cyclin E is the next cyclin to be induced and after it associates with its kinase, CDK2, the cell can now make the crucial transition from G1 into S phase (Moroy and Geisen 2004; Calbo *et al.* 2002).

Genes that are active in S phase are silenced by pRb by active repression of E2F transcriptional activity and this is reduced by cyclin D1. pRb acts as a tumour suppressor and loss of function results in loss of the restriction point check and therefore loss of cell cycle control.

Figure 23 Functions of cyclin D1. Cyclin D1 forms a complex with its kinase partner CDK4 and this activation step leads to phosphorylation of retinoblastoma protein Rb. The transcription factor E2F is released and can transactivate genes necessary for cell cycle progression (Fu et al. 2004).

There are many negative regulators of the cell cycle and they occur at different stages: In the G1 and S phase the most extensively investigated cell cycle inhibitors are the p16 and p21 families. These proteins form stable complexes with the CDKs before they are bound to cyclins, and excess expression of cyclin will not dissociate them from the CDK. p16 inactivates CDK4 and CDK6 in G1 and thereby prevents phosphorylation and inactivation of pRb. The p21 family is of primary importance in G1 regulation where family members can bind cyclins thereby preventing the CDK from phosphorylating pRb and inducing its dissociation from E2F (Albrecht *et al.* 1999; Albrecht *et al.* 1995). Unlike p16, cell cycle inhibition by p21 can be prevented by increasing cellular concentrations of cyclins.

4.1.1.2 Bcl-3

Feng (Feng *et al.* 2000) used a quantitative fluorescent cDNA microarray to identify genes regulated by thyroid hormone. Fluorescent labelled cDNA was prepared from the hepatic RNA of T_3-treated hypothyroid mice and hypothyroid mice within 6 hours of stimulation. Following array hybridisation relative changes in gene expression were analysed. 55 genes, 45 not previously known to be thyroid responsive genes, were found to be regulated by thyroid hormone. Of these 41 were negatively regulated and 14 were positively regulated.

Bcl-3 was striking as one of the T_3 regulated genes up-regulated in this array study and it is of interest given its involvement in control of cell proliferation. Bcl-3 belongs to a family of Iκβ proteins, originally identified as a candidate proto-oncogene over expressed in certain cases of B-cell chronic lymphocytic leukemia as a consequence of a t(14;19) chromosomal translocation and its involvement in the pathogenesis of solid tumors such as nasopharyngeal carcinoma is now well recognised (Brocke-Heidrich 2006).

Through an ankyrin repeat domain, the activity of NFκβ transcription factors can be regulated. In mammals there are five members of the NFκβ family RelA (p65), RelB, c-Rel, p50 and p52. Bcl-3 can either activate or repress gene transcription by forming complexes with p50 and p52 homodimers. Thus, Bcl-3 over-expression is proposed to cause dysregulation of genes normally regulated by NFκβ transcription factors implicated in cell proliferation, differentiation and apoptosis. Given the oncogenic potential of Bcl-3 and its likely effects on proliferative pathways, the hypothesis tested in this chapter is whether it acts as a critical mediator of the mitogenic hepatic effects of T_3. To this end the acquisition of a Bcl-3 knockout mouse from the University of Tubingen in Germany made the testing of this hypothesis possible.

4.2 Hypotheses and Experiments

Hypothesis (a) Cyclin D1 is an early mediator of the hepatic T_3 mitogenic effect

Experiments used to investigate this hypothesis:

i. Measure the mRNA expression of cyclin D1 in liver *in vivo* in adult euthyroid Sprague-Dawley rats, following mitogenic stimulation with the hepatomitogen T_3 using quantitative Real Time PCR.

ii. Use an immunohistochemical technique with a novel rabbit monoclonal anti cyclin D1 antibody to measure the *in vivo* protein expression of cyclin D1 in T_3 treated rat liver over time.

iii. Use the same technique to study the pattern of staining for cyclin D1 in quiescent rat liver, partial hepatectomy rat liver and human liver specimens.

Hypothesis (b) There is a reduced hepatocyte proliferative response to T_3 in Bcl-3 knock out mice

Experiments used to investigate this hypothesis:

i. Administer T_3 at a mitogenic dose to a group of Bcl-3 knock-out mice, to determine whether this protein is a critical mediator of the hepatic T_3 mitogenic effect.

4.3 Materials and Methods

4.3.1 Animal Protocols

Adult male Sprague Dawley rats weighing 200-250g were used. Animal care and all procedures were compatible with the Animals (Scientific Procedures) Act 1986 (see *General Methods* Chapter 2).

a) *First time course experiment*:

Rats (n=3) were injected with a single sub-cutaneous dose of 5μg T_3 (5μl of 1μg/μl T_3 dissolved in 1M NaOH added to 35μl 1M NaOH made up to 1ml with normal saline) and sacrificed at 1, 3, 14, 18, 22, 26 and 30 hours post dose.

A group of animals (n=3) were injected with vehicle only and sacrificed at 1 and 3 hours to act as a control.

The liver was sectioned after sacrifice, snap frozen in liquid nitrogen and stored at -80°C until use. Sections were also placed in formalin and after 24 hours sent for routine histological processing prior to embedding in paraffin blocks in readiness to cut 4μm paraffin sections for immunohistochemistry.

Second time course experiment:

A male SD rat (n=1) was injected with a dose of 5μg T_3 and sacrificed at 1, 3, 6, 9, 12, 14 and 18 hours post dose. A second animal was injected with vehicle only and sacrificed at the same time points. Tissue was collected in the same manner as before.

b) *Bcl-3 protocol*

Bcl-3 knock out (KO) mice were obtained in collaboration with Professor Schmidt at the University of Tubingen, Germany. The animals were imported into the United Kingdom and all animal care procedures were adhered to according to the Animals (Scientific Procedures) Act 1986. After a period of a few days following their arrival the animals had adapted to their new environment and were deemed in a healthy state permitting the experiment to be undertaken.

C57 Black 6 mice of a similar age were used as wild type controls. These were bred within the animal house at the Royal Free hospital.

Bcl-3 KO mice (n=4) were administered a mitogenic dose of T_3 (5μg) subcutaneously and sacrificed 24 hours later. One hour prior to sacrifice BrdU was administered

intraperitoneally at a dose of 50mg/kg to identify those hepatocytes undergoing DNA synthesis (flash labelling).

Bcl-3 KO mice (n=2) were administered vehicle only and sacrificed 24 hours later with flash labelling with BrdU at 23 hours post dose.

C57 Black 6 mice (n=4) were administered a mitogenic dose of 5μg T_3 and sacrificed 24 hours later with flash labelling with BrdU at 23 hours post dose.

C57 Black 6 mice (n=2) were administered vehicle only and sacrificed 24 hours later with flash labelling with BrdU at 23 hours post dose.

Following animal sacrifice, livers were harvested, sectioned and placed in formalin prior to histological processing for further analysis *(General Methods Chapter 2).*

4.3.2 Isolation of RNA

Please refer to *General Methods* Chapter 2.

4.3.2.1 Determination of RNA yield

Please refer to *General Methods* in Chapter 2.

A ratio above 1.8 (A_{260}/A_{280}) was obtained for all samples analysed.

4.3.2.2 RNA Gel Electrophoresis

Please refer to *General Methods* in Chapter 2.

The RNA obtained was of good quality as shown on RNA gel electrophoresis (Figure 24).

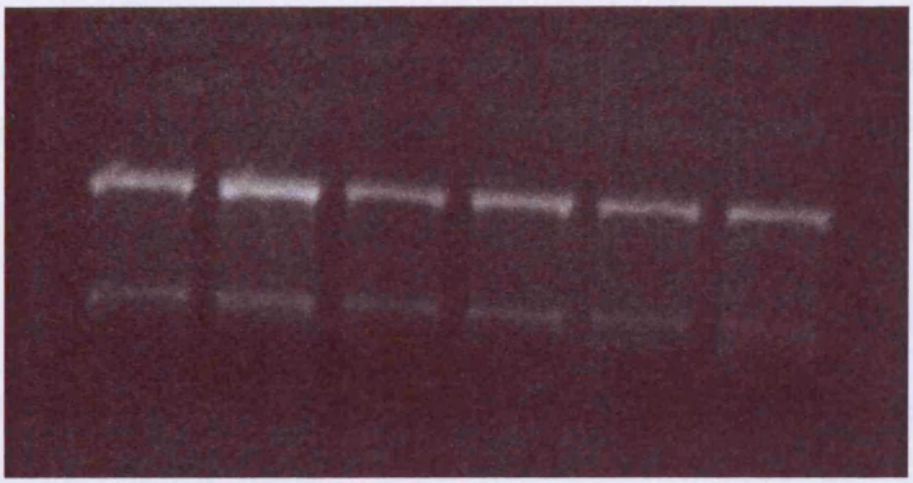

Figure 24 A 1.5% agarose gel showing intact RNA from liver samples 1 to 6. This is a representative example of all the samples obtained. The RNA is intact as shown by the sharp 28S (top) and 18S (bottom) bands and the 2:1 ratio of 28S:18S.

4.3.3 cDNA synthesis

Please refer to *General Methods* Chapter 2.

4.3.4 Primer design for cyclin D1 and 18S

Please refer to *General Methods* Chapter 2.

4.3.5 Primer design rules that were applied

Please refer to *General Methods* Chapter 2.

Using GeneBank (http://www.ncbi.nlm.nih.gov) the complete mRNA sequences for cyclin D1 and rat 18S were obtained. For both these targets forward and reverse primers were designed to comply with the rules set out above with the additional requirement

for real-time PCR that the size of the amplicon should be no more than 150bp in length. Using the computer software Vector NTI the proposed primers were assessed to ensure that an intron-exon boundary was spanned (to minimize genomic DNA amplification), no potential formation of primer-dimers or secondary structures was predicted, and similar annealing temperatures were appropriate for each primer pair. The primer pairs were screened against the Blast database to ensure specificity to the gene of interest.
cyclin D1 and 18S primer sequences were purchased from SigmaGenosys. An appropriate volume of DEPC-MilliQ water was added to the lyophilized primers to make 100μM stock concentrations from which 10μM working concentrations of primers were made. All primers were stored at -20°C at 100μM concentration for long term storage. Primer sequences are shown in Table 6.

Table 6 Primer sequences for cyclin D1 and 18S.

Target	Primer	Sequence	Temp (^{0}C)
Cyclin D1	Cyclin D1 forward	5'- AGGAGTTGCTGCAAATGG -3'	61.2
	Cyclin D1 reverse	5'- CTGGCATTTTGGAGAGGAAG-3'	61.4
18S	18S forward	5'-CTTAGAGGGACAAGTGGCG-3'	62.4
	18S reverse	5'-GGACATCTAAGGGCATCACA-3'	62.5

A set of primers was designed to amplify a sequence of DNA from the cyclin D1 coding region.
Forward position 560-577
Reverse position 645-664
Predicted PCR product is 104 bases.

A set of primers was designed to amplify a sequence of DNA from the 18S coding region.
Forward position 1488-1466
Reverse position 1517-1498
Predicted PCR product is 69 bases.

4.3.6 Conventional PCR to check primers (for cyclin D1 and 18S)

Please refer to *General Methods* Chapter 2.

4.3.7 DNA gel Electrophoresis

Please refer to *General Methods* Chapter 2.

The cyclin D1 PCR product was 104 base pairs when measured against a lane containing 7µl of Hyperladder IV (Figure 25).

The 18S PCR product was 69 base pairs when measured against a lane containing 7µl of Hyperladder IV (Figure 25).

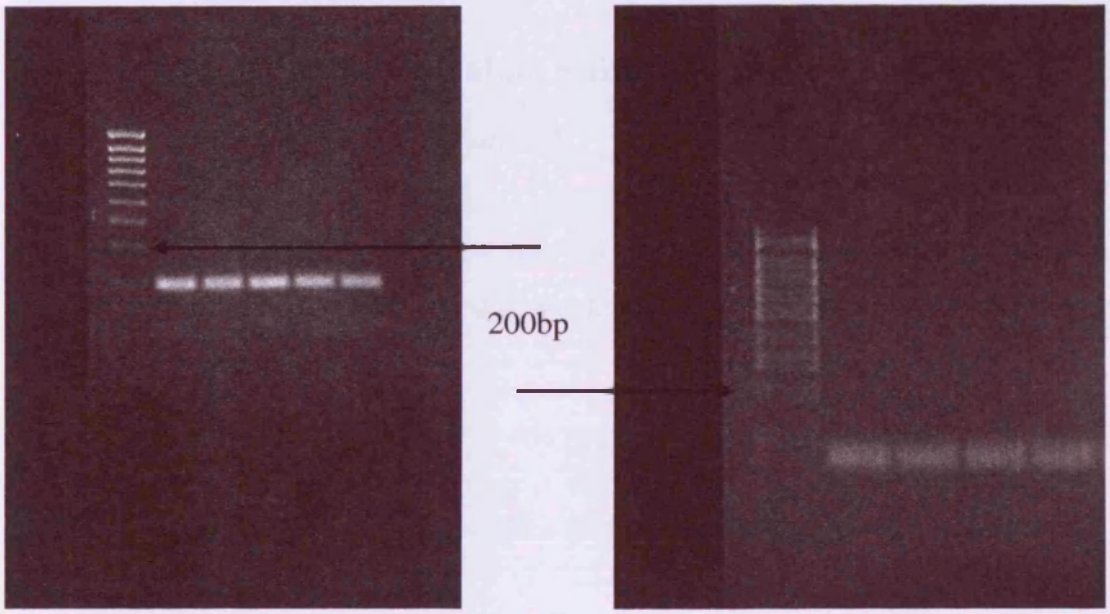

a) cyclin D1 b) 18S

Figure 25 2% agarose gel electrophoresis of the PCR products. (a) a single band of 104 nucleotides is seen in the samples (5 lanes) consistent with the size of the cyclin D1 amplicon and (b) a single band of 69 nucleotides is seen in the second gel samples (4 lanes) consistent with the size of the 18S amplicon. The 200 base pair marker (first lane in each gel) is indicated by the arrows.

4.3.8 Preparation of standards

Please refer to *General Methods* Chapter 2.

Method:

5µl of cDNA from a sample was used to make cyclin D1 product so as standards could be made for the real time PCR analysis for both cyclin D1 and 18S.

4.3.9 Amplicon Excision from DNA Agarose Gel

Please refer to *General Methods* Chapter 2.

4.3.9.1 Amplicon extraction from agarose gel

Please refer to *General Methods* Chapter 2.

4.3.9.2 Amount of specific product estimation using Avogadro's number

Please refer to *General Methods* Chapter 2.

The number of amplicon molecules was calculated using Avogadro's number (6.022 $x10^{23}$), the molecular weight of the amplicon and the estimated concentration of amplicon.

For cyclin D1:

Product 104 bp

Molecular weight of the amplicon = 330 x (length of the amplicon x 2)

1 mole = 68,640g = 6.022 $x10^{23}$

1ng = $8.77x10^{9}$

From the gel, 2µl = 20ng = 1.75 $x10^{11}$ copies

Standard = 8.75 $x10^{10}$ copies/µl

4.3.9.3 Developing a real time PCR protocol to quantify the expression of cyclin D1 mRNA in the liver

Please refer to *General Methods* Chapter 2.

4.3.9.3.1 Optimisation Steps

Please refer to *General Methods* Chapter 2.

4.3.9.3.2 **Standard Curve**

Please refer to *General Methods* Chapter 2.

4.3.9.3.3 **Samples**

With acceptable standard curves, all samples could then be run for cyclin D1 followed by 18S to which the copy numbers per reaction can be normalised. Accuracy of the assay was demonstrated by showing reproducibility across more than two separate real time runs.

Reaction Mix for cyclin D1:	Hotstar Mix	10µl
	Forward primer	2µl
	Reverse primer	2µl
	SYBR Green	1.5µl
	H_2O	2.5µl
	cDNA	2µl
	TOTAL	20µl

Reaction Mix for 18S:	Hotstar Mix	10µl
	Forward primer	0.5µl
	Reverse primer	0.5µl
	SYBR Green	1.5µl
	H_2O	6.5µl
	cDNA	1µl
	TOTAL	20µl

Within each individual real time PCR run the appropriate non template controls (NTCs) were included as well as the standards. The standards chosen would lie between the range of fluorescences of the experimental samples and were run in duplicate. At least three standards were included in each reaction. At the completion of each reaction the appropriate standard curve, either for cyclin D1 or 18S, was imported to allow the software to calculate the copy number of amplicon per reaction. This number was then normalised to the 18S copy number per reaction. Figure 26 shows an example of the raw data generated for cyclin D1 standards and the standard curve can then be constructed (Figure 27).

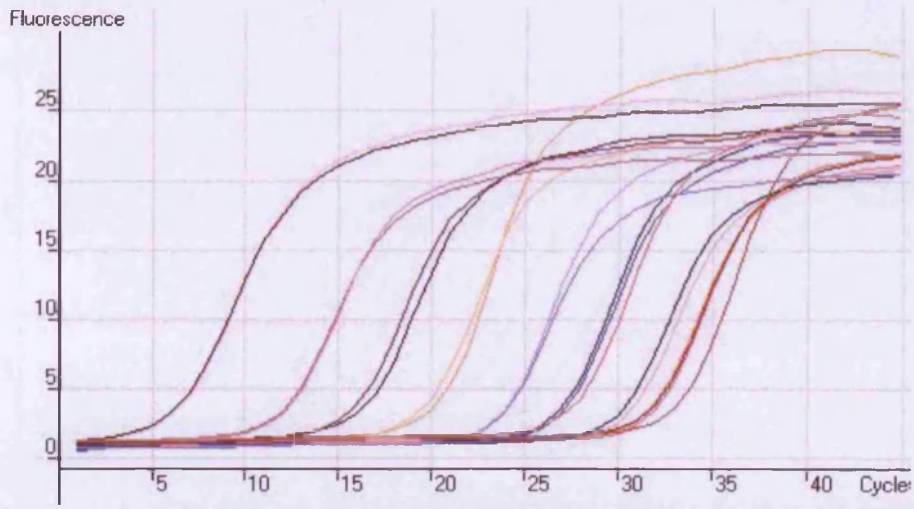

Figure 26 Raw Real Time PCR data for cyclin D1 standards. The sigmoid curves reflecting target amplification during the Real Time PCR reaction can be seen for each standard with the most concentrated standard with the lowest C_T value appearing first. Each standard is in duplicate.

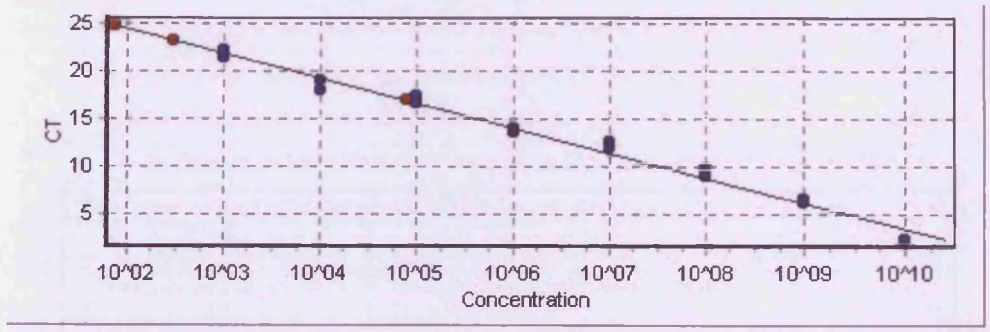

Figure 27 Cyclin D1 standard curve with C_T values for standards plotted ranging from 10^2 to 10^{10}.

Figure 28 shows raw data for 18S standards and from these the 18S standard curve can be constructed (Figure 29).

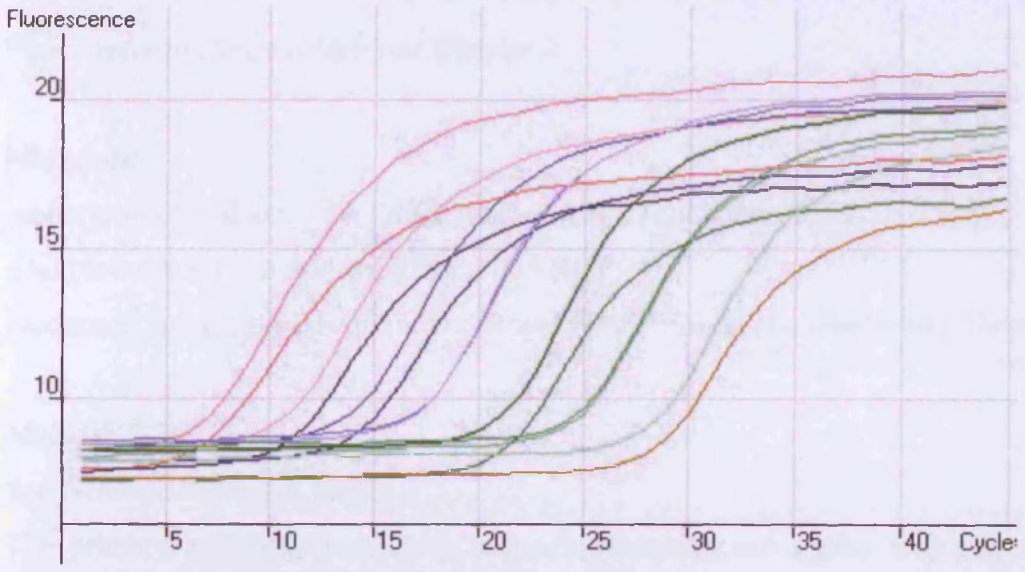

Figure 28 Raw Real Time PCR data for 18S standards. The sigmoid curves reflecting target amplification during the Real Time PCR reaction can be seen for each standard with the most concentrated standard with the lowest C_T value appearing first. Each standard is in duplicate.

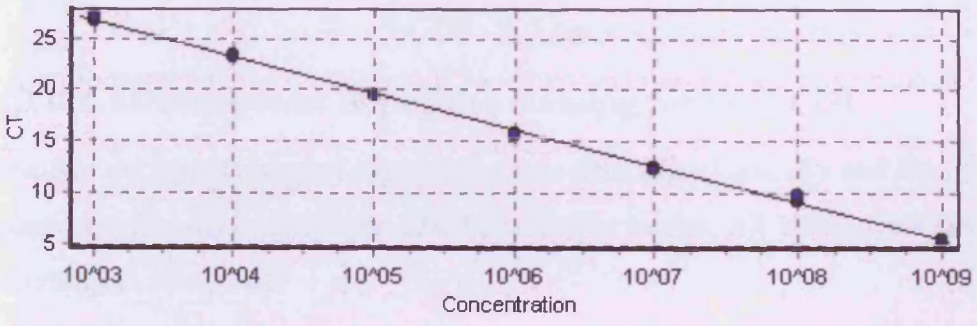

Figure 29 Rat 18S standard curve with C_T values for standards plotted ranging from 10^3 to 10^9.

4.3.10 Immunohistochemical analysis of cyclin D1 in the liver

Please refer to *General Methods* Chapter 2.

Materials:

rabbit monoclonal anti - cyclin D1 antibody SP4 (Labvision, UK)

goat biotinylated anti rabbit antibody (DAKO)

sections of human breast carcinoma (Royal Free Hospital Histopathology Department)

Method:

See *General Methods* Chapter 2

The primary antibody (LabVision monoclonal rabbit anti cyclin D1) was applied to tissue sections at an optimal dilution of 1:50 for a 1 hour incubation in a humid incubator (Cheuk *et al.* 2004).

Sections of human breast carcinoma acted as a positive control and a section without the primary antibody but instead incubated with the appropriate concentration of rabbit IgG acted as a negative control. The sections were washed for ten minutes in x1 PBS and incubated with the secondary antibody (DAKO goat biotinylated anti rabbit) for thirty minutes at an optimal dilution of 1:400.

The primary antibody used initially required optimising, varying its concentration to obtain optimal staining results at the dilutions defined above.

4.3.10.1 Measurement of positive staining for cyclin D1

Positive nuclear staining of hepatocytes was determined visually and then the number of positive cells was counted per 2,000 hepatocyte nuclei. All slides were blinded prior to counting to avoid bias.

4.3.10.2 H & E staining

Please refer to *General Methods* Chapter 2.

4.3.10.3 Immunohistochemistry for BrdU in mice

Please refer to *General Methods* Chapter 2.

Monoclonal Rat anti-BrdU supernatant (OBT 0030S) acted as the primary antibody.

4.4 Results

4.4.1 Quantifying the level of expression of cyclin D1 *in vivo* in rat liver following mitogenic stimulation with T_3 over time

Real Time PCR was used to quantify levels of cyclin D1 per unit 18S ribosomal RNA in all samples. There was an increase in the hepatic expression of cyclin D1 at 14 hours after T_3 was administered (Figure 30).

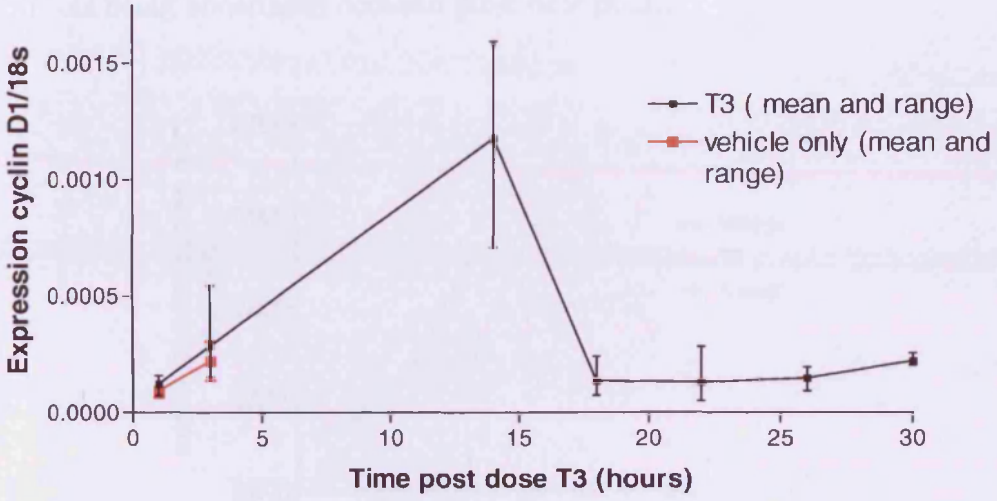

Figure 30 Time course of expression of cyclin D1 after T_3 in male adult SD rats as measured by Real Time PCR and normalised to 18S copy number per reaction. Data is presented as the mean and range for each time point (n=3). Vehicle only is indicated in red at 1 hour and at 3 hours.

At the early time point of 3 hours there was no significant increase in expression of cyclin D1 after a mitogenic dose of T_3 when compared to vehicle only treated animals.

4.4.2 Quantifying the level of expression of cyclin D1 *in vivo* in rat liver following mitogenic stimulation with T_3- a preliminary experiment looking at early time points

A further time course experiment was undertaken to examine more early time points between 0 and 14 hours post dose (Figure 31). This experiment included only one animal in each group (T_3 or vehicle only) as a preliminary indication of change in cyclin D1 expression was sought prior to consideration of larger and more expensive animal experiments being undertaken between these time points.

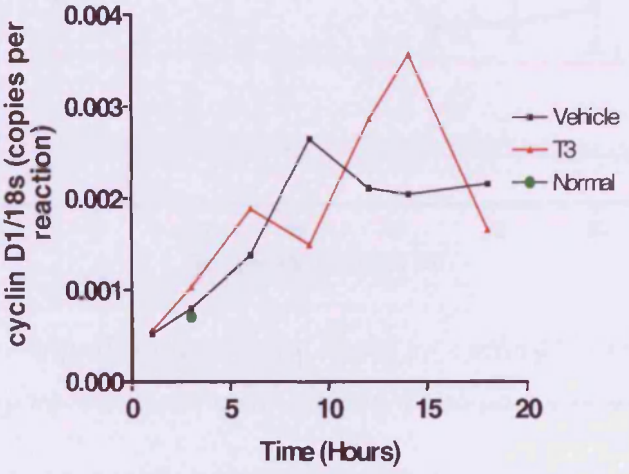

Figure 31 Cyclin D1 expression over time after a mitogenic dose of T_3 in male adult SD rats measured by Real Time PCR and normalised to 18S copy number per reaction. n = 1 at each time point and 'normal' represents an animal that received neither T_3 nor vehicle only.

There was no difference in expression of cyclin D1 between T_3 and vehicle only treated animals over the first ten hours. The expression in both groups rises over this time period. At 12 and 14 hours the expression was greater in the T_3 treated animal compared to vehicle only but the vehicle only response is still greater than the response at time 0.

4.4.3 Quantifying the level of cyclin D1 protein expression *in vivo* in T_3 treated Rat Liver

An immunohistochemical technique was used to determine hepatic cyclin D1 protein expression in response to T_3 and the number of positive hepatocyte nuclei were counted per tissue section (Figure 32).

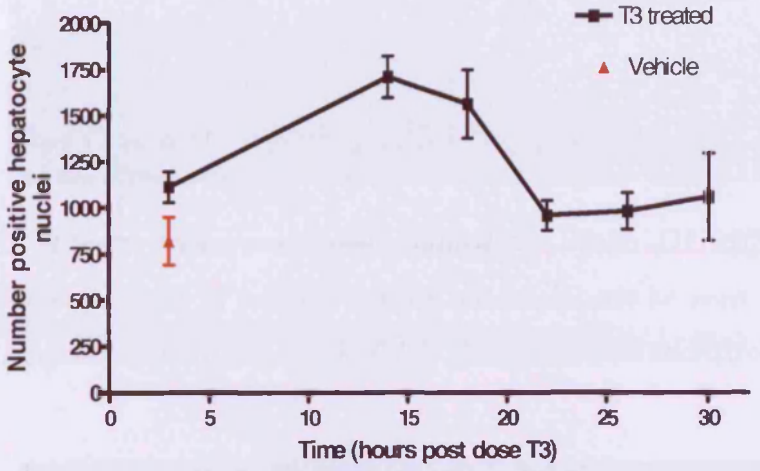

Figure 32 Number of positive hepatocyte nuclei for cyclin D1 over time after T_3 in male SD rats. 2,000 hepatocyte nuclei were counted. Data points represent mean and range, n=3.

There is an increase in the number of positively stained hepatocytes which is maximal at fourteen hours after stimulation with T_3.

4.4.3.1 The immunohistochemical pattern for cyclin D1 observed in rat and human liver

Staining for cyclin D1 in human breast cancer tissue sections was used as a positive control (Figure 33). An example of a section of rat liver incubated without primary antibody is shown, and this acted as a negative control (Figure 34).

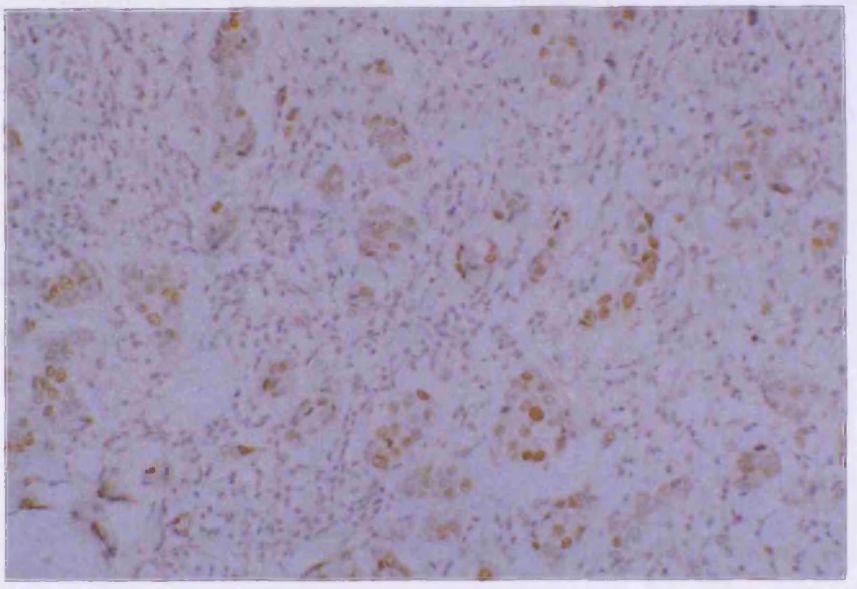

Figure 33 Human breast carcinoma stained for cyclin D1 x20 objective. The dark brown nuclear staining of positive cancer cell nuclei can be seen. These tissue sections acted as a positive control for cyclin D1 in the rodent immunohistochemical analysis.

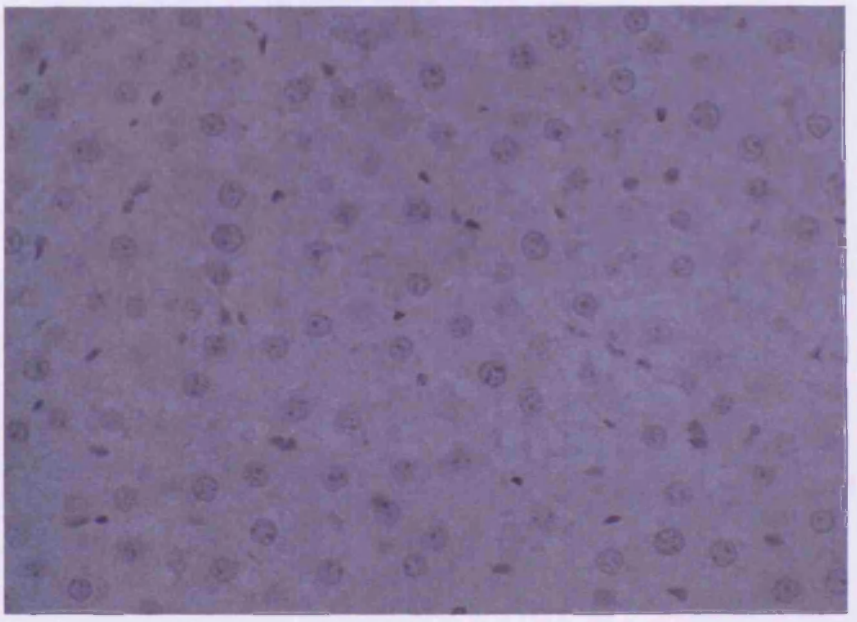

Figure 34 Rat liver section x40 objective, stained without primary antibody acts as a negative control for cyclin D1.

Further immunohistochemical examination of rat and human liver sections revealed interesting patterns of staining. Comparisons were made between quiescent rat liver, rat liver after partial hepatectomy at 24 hours and BS human liver placed in formalin on

arrival in the laboratory. The sections of partial hepatectomy rat liver were donated by a colleague in the laboratory.

In quiescent rat liver there is marked staining of hepatocyte nuclei but with notable sparing around the central veins (Figure 35), and when a comparison is made with rat liver after partial hepatectomy at 24 hours the observed staining is more widespread and intense with many more non parenchymal cells staining positive (Figure 35), however the marked sparing around the central veins is still seen to occur.

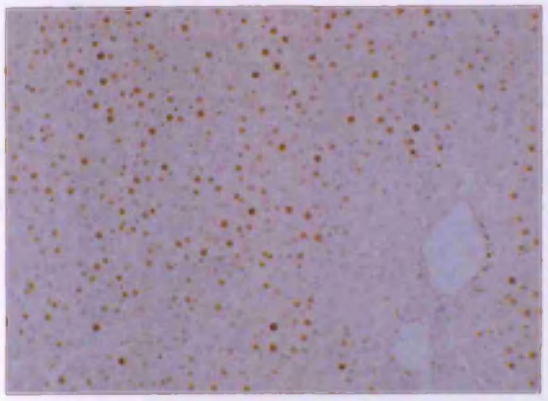

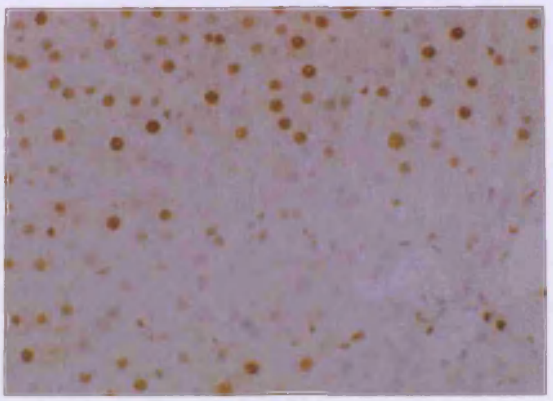

(a) rat liver quiescent x20 objective,
(Note sparing around the central vein)

x40 objective

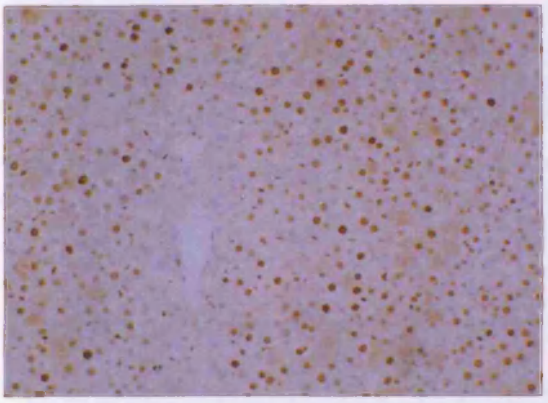

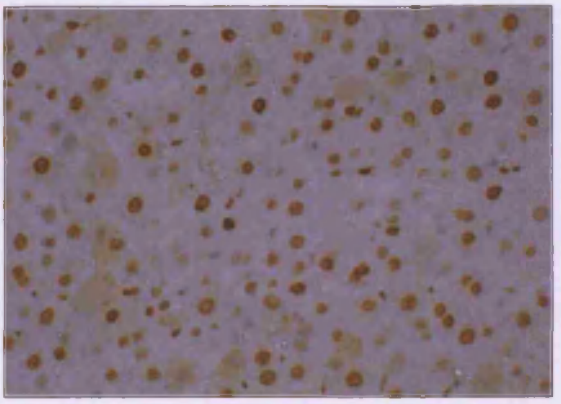

(b) rat liver after partial hepatectomy at 24 hours

x20 objective

x40 objective

(Note sparing around the central vein)

Figure 35. Rat liver stained for cyclin D1 in (a) quiescent state and (b) after partial hepatectomy at 24 hours, where more NPCs are stained positive for cyclin D1 and the staining intensity appears to be increased generally across the tissue section.

In BS human liver, the staining for cyclin D1 is much less intense and not as widespread with only a few small groups of cells neighbouring one another staining positive (Figure 36).

Figure 36. Human liver section (BS sample) x40 objective stained for cyclin D1. A few hepatocytes stain positive but most are negative. Compare this to quiescent rat liver where there are many more hepatocytes stained and the staining is more intense.

4.4.4 The T_3 Hepatic Proliferative Response in Bcl-3 Knock-out Mice

The result of administering a mitogenic T_3 dose to Bcl-3 knock-out mice is detailed in Figure 37.

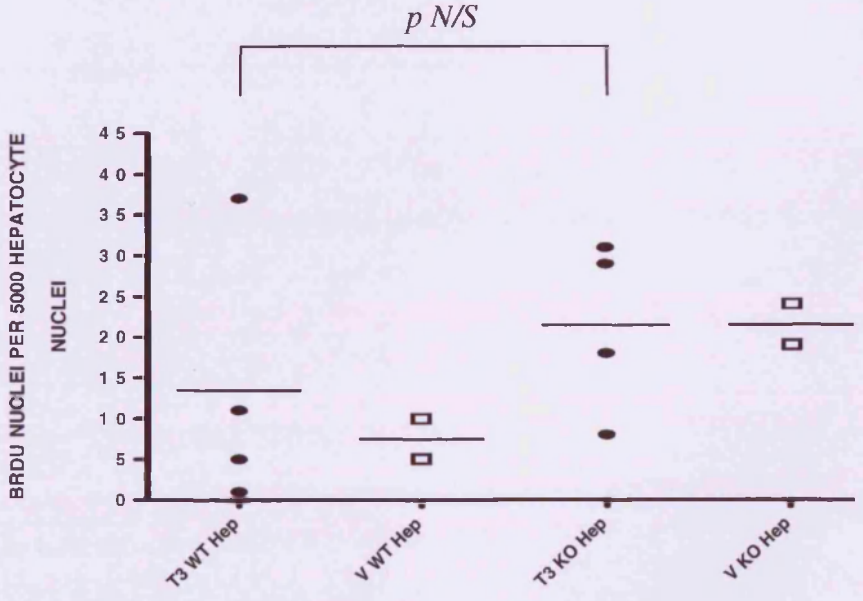

Figure 37 BrdU positive hepatocyte nuclei per 5,000 hepatocyte nuclei in T_3 treated wild type (WT) and Bcl-3 Knock out (KO) mice. V = vehicle only. Hep = hepatocyte.

The p value when comparing T_3 treated wild type and T_3 treated Bcl-3 knock-out mice does not reach statistical significance (p N/S).

The most striking result is that the hepatocyte proliferative response to T_3 in the Bcl-3 knockout animals is no less than in the wild type mice suggesting that Bcl-3 is not a critical mediator of the T_3 hepatocyte proliferative response seen in mice.
It is interesting to note that the overall hepatocyte proliferative response is less in mice at 24 hours (up to 0.1% hepatocytes positive for BrdU) post stimulus when compared to the rat model (approximately 5-7% BrdU positive hepatocyes at 24 hours after T_3). This observation is consistent with the published literature where it is also noted that the cell cycle is of a longer duration in mice and the proliferative response to partial hepatectomy is also more latent (Fausto 2000).

4.5 Discussion

Work by Pibiri (Pibiri *et al.* 2001) indicates the important role cyclin D1 may have in mediating the effects of T_3. The hepatic response to T_3 and partial hepatectomy (PH) was compared in their study. An increase in cyclin D1 mRNA (using Northern blot analysis) occurred much more rapidly after T_3 than after PH. The increase was evident as early as 2 hours after treatment and reached a maximum at 4 hours, however no change in cyclin D1 mRNA was seen in rats which had undergone PH at this time. Western blot analysis showed that cyclin D1 protein was increased at 4 hours after T_3, elevated further at 12 hours and maintained for up to 24 hours. The increase in cyclin D1 protein after hepatectomy was much delayed, being evident at only 12 hours. The changes described in cyclin D1 at 4 hours were however *not* compared with a control group of animals at the same time point in the Western blot analysis in their study.

Pibiri then considered whether this T_3 action may be common to the group of mitogens that act on nuclear receptors. Nafenopin, a peroxisome proliferator (a PPAR-alpha ligand member of the steroid/thyroid nuclear receptor superfamily) also caused a rapid increase in cyclin D1 protein content evident 2 hours after treatment, thereby indicating this group of mitogens may act in a similar way. The activation of cyclin D1 by T_3 and nafenopin may, they hypothesise, be a direct action of thyroid hormone and nafenopin on the cyclin D1 gene promoter. The hypothesis that cyclin D1 is an absolutely necessary factor in mediating these mitogenic effects is disputed in follow up work (Ledda-Columbano *et al.* 2002). Loss of cyclin D1 in knock out mice suggests it is not mandatory for development of most mouse tissues and during development other mechanisms compensate for its loss and this makes perfect evolutionary sense. Columbano used the powerful mitogen 1,4-bis [2-(3,5-dichloropyridyloxy)] benzene (TCPOBOP), a ligand of the constitutive androstane receptor, to see if lack of cyclin D1 in knock out mice, had an effect on the hepatic proliferative response (Ledda-Columbano *et al.* 2003). Entry into S phase was delayed but there was no effect on proliferation. The study suggests that other cyclins such as cyclin E may take over the role of cyclin D1, but further work is yet to be done to confirm this hypothesis.

The research undertaken in this thesis demonstrated a rise in cyclin D1 by 14 hours in rat liver at the mRNA level and at the protein level after a mitogenic dose of T_3. The much earlier rise (maximal at 4 hours) evident in Pibiri's work is not conclusively replicated here using the method of Real Time PCR analysis, as opposed to Northern blot analysis which was used in the Pibiri study. At the early time point of 3 hours there

is no difference in cyclin D1 expression between T_3 treated and vehicle only treated rat liver in this thesis.

However, when more of the early time points were examined, cyclin D1 expression is seen to rise in T_3 treated and vehicle only animals and this corresponds to the change in time of day when the animals were sacrificed. Indeed the trend in the extended time course experiment may reveal a change in cyclin D1 expression due to diurnal variation in the rat liver transcriptome. This complicates the analysis as to whether what is being observed is due to the specific effects of T_3 or due to a diurnal variation in expression i.e. a circadian rhythm or a combination of these two. The initial time course experiment was carried out using a group of vehicle only treated animals at 1 hour. This time point of animal sacrifice corresponded with a time in the morning of 10:00 and the 14 hour time point corresponded with animal sacrifice at 22:00 when levels of cyclin D1 are seen to rise again. Further possible evidence for a diurnal pattern of expression is the fall at the next time point of animal sacrifice of 18 hours which corresponds to 10:00 in the morning.

The question of a diurnal variation was partially addressed in the third time course experiment with a single animal at each time point paired with a control animal. Increased levels of cyclin D1 expression corresponded with the evening at 22:00 and lower levels with the morning at 10:00. This experiment may support the existence of a diurnal variation in hepatic cyclin D1 expression but clearly a further experiment needs to be undertaken which is powered with enough animals to answer this question definitively. Such an experiment was not done for the purposes of this research project given the considerable additional costs involved and it remains a future aim. The physiology of circadian rhythms is however briefly discussed next as it raises relevant issues regarding experimental design, important when examining the hepatic transcriptome under any experimental conditions.

4.5.1 Circadian rhythms

Circadian rhythms are endogenous rhythms of physiology and behaviour occurring in a majority of organisms (Desai *et al.* 2004). In mammals the central regulator of the cycle is the suprachiasmatic nucleus of the hypothalamus, affected by the light/dark cycle through the retinohypothalamic tract. At the molecular level, the clock functions as a result of interacting positive and negative transcriptional-translational feedback loops that govern the expression of specific clock control genes (Morgan *et al.* 2005). Some

peripheral tissues show tissue-specific rhythms regulated by many of the same clock control genes. Since some of these clock control genes encode transcription factors, the expression of a whole host of genes may be tied to the daily rhythm of the molecular clock (Akhtar *et al.* 2002).

Since tissue collection may occur throughout the day, understanding hepatic gene expression over time is critical (Boorman *et al.* 2005). Most work thus far has documented circadian effects on the mouse transcriptome and the rat has not been extensively studied.

Microarrays have been used to perform direct day/night 12h offset comparisons of rat hepatic transcripts and also compared transcripts of livers collected at different times of the day, notably comparing expression between 4 hours after lights on and 10 hours after lights on (6 hours apart) (Boorman *et al.* 2005). This study demonstrated the rat transcriptome exhibits significant circadian variation in expression and there was a marked difference in gene expression in livers collected 6 hours apart during the light period using quantitative reverse transcription PCR. Hepatic expression of many of the circadian genes rises during the day and the magnitude of variation of these was greater than those genes involved in metabolic pathways. There is no comment specifically on cyclin D1 in this study but given a whole host of hepatic transcripts rise or fall over a 6 hour period during the day, it is not inconceivable that cyclin D1 may be subject to the same circadian variation in expression.

4.5.2 Patterns of cyclin D1 staining in rat and human liver

Immunohistochemical analysis for cyclin D1 of T_3 treated rat liver over time was undertaken to see if at the protein level cyclin D1 could be used as a marker of the effects of T_3 in the *in vitro* conditions of the organ perfusion preparation of Chapter Three. At 14 hours post mitogenic stimulus a maximal response was observed as measured by hepatocyte staining for cyclin D1 protein. This is too late a time for the purposes of an early marker of T_3 effects in the liver perfusion experiments described in the previous chapter where changes within the first six hours are sought. Furthermore the marked basal staining in quiescent rat liver would make it difficult to detect small and subtle changes in cyclin D1 protein expression. Beyond these limitations, the pattern and intensity of staining in rat and human BS liver samples raises further interesting questions given that a measurable hepatic response to T_3 is ultimately sought in human liver.

The differences in staining for cyclin D1 between rat and human liver are borne out by some other but rather limited work in the literature. The expression of cyclin D1 protein in regenerating human liver is of interest although little work exists in the literature on this. Some comparisons between species and also quiescent and regenerating human liver have been made (Albrecht *et al.* 1995). In this study there was no detectable cyclin D1 in resting mouse liver, but significant basal protein expression in rat liver using Western blot analysis. There was some protein expression in resting human liver and certainly more than was seen in the quiescent mouse liver. Furthermore when samples of regenerating human liver were looked at, one year post transplant, there was a < 2 fold increase in the expression of cyclin D1 protein compared to normals. In the 8 to 21 days after transplantation cyclin D1 protein levels were 2 to 10 fold higher.

The results presented in this thesis demonstrated marked staining for cyclin D1 in resting rat liver with much less in resected human liver samples and this observation supports the findings in the Albrecht study where Western blot analysis was used to measure cyclin D1 protein expression.

4.5.2.1 Distribution of staining

4.5.2.1.1 *Rat Liver*

The *distribution* of staining for cyclin D1 in quiescent rat liver, with notable sparing of cells around the central veins, poses several questions. In addition the staining following PH is markedly more intense and many more NPCs stain positive. This increase is consistent with the changes that will be taking place with regards to hepatocyte regeneration after hepatectomy. Partial hepatectomy provides the strongest stimulus to hepatic regeneration and the up-regulation of cyclin D1 at 24 hours after surgery is expected and Pibiri confirmed that cyclin D1 was increased by 12 hours and remained elevated at 24 hours following PH (Pibiri *et al.* 2001).

After partial hepatectomy, hepatocyte proliferation starts in the area of the lobules surrounding the portal triads and proceeds to the pericentral areas by 36 to 48 hours. The peak rat proliferative response is 24 hours in the hepatocytes but more latent in the mouse after PH. The other liver cell populations enter into DNA synthesis at 48 hours or even later, in the rat and enhanced expression of cyclin D1 occurs before the onset of DNA synthesis. Increased cyclin D1 expression in this situation is known to occur late in G1 (12 hours in rat liver). The increased staining demonstrated in this Chapter at 24

hours after PH is consistent therefore with a persistent earlier rise in cyclin D1 protein expression.

The pattern of staining in quiescent liver is intriguing and one possible yet controversial explanation for it is the 'streaming liver hypothesis'.

After partial hepatectomy the majority of new hepatocytes are formed in the periportal region as shown by (3H) thymidine autoradiography (Grisham 1962). The 'streaming liver hypothesis' suggests that parenchymal cells located in the periportal region give rise to daughter cells that stream slowly toward the central vein (Zajicek *et al.* 1985). It proposes that new hepatocytes are constantly produced at the outer rim of the portal space and these cells move along the sinusoid toward the central vein where they are eventually eliminated. The hepatocytes mature as they get older and as a consequence they may display different enzymatic patterns and replicative potential.

The staining pattern for cyclin D1 may provide some support for this hypothesis, in that there is less staining for cyclin D1 within the hepatocytes located around the central veins. Since cyclin D1 is associated with progression in the cell cycle and subsequent DNA synthesis and cell replication, its absence may support the idea that these cells are no longer dividing or able to do so. However on-going controversy surrounds cell renewal in the adult liver and more recent work refutes the streaming liver model. Magami et al used 3H-thymidine incorporation to study hepatic cell kinetics in the adult mouse (Magami *et al.* 2002). They found that hepatocytes are supplied by postnatal replication and that streaming of hepatocytes from periportal to pericentral regions did not occur.

A more plausible approach to understanding this differential gradient for cyclin D1 staining would be to consider the known heterogeneity that exists amongst hepatocytes across the zones of the hepatic lobule and there is considerable published work describing this (Jungermann and Katz 1982; Jungermann *et al.* 1982; Jungermann and Katz 1989). The sophisticated techniques of microchemistry and microdissection and separation of periportal and perivenous hepatocytes were used in these studies. The periportal and perivenous hepatocytes have different metabolic capacities and each cell's metabolism and physiology may change as one moves from the periportal zone to the pericentral zone, and some of these changes may be controlled by different signal inputs. During passage through the liver the concentrations of hormones will change according to how they are metabolised or synthesised. The ratio of humoral signals changes from the periportal to the perivenous zone and therefore the net effect in any one area across the hepatic lobule will change. Similarly neural inputs are not equally

distributed across the hepatocytes. Many other factors should be taken into consideration such as individual receptor densities on hepatocytes which also may change across the zones. All in all these factors may combine to explain why there is a gradient of expression of cyclin D1 across the lobule consistent with the different metabolic capacities of the hepatocytes as one moves from pericentral to perivenous areas.

4.5.2.1.2 ***Human Liver***

In the quiescent human liver there is some staining for cyclin D1 although it is variable and much less intense and very few cells stain positive. Cyclin D1 protein may therefore be a useful marker of T_3 effects in *in vitro* human liver perfusions but its rise is most likely too latent for the human liver perfusions described in Chapter Three where once again a much earlier marker of the proliferative response is needed given the inability at present to maintain the liver tissue in a reasonable histological condition beyond six hours.

4.5.3 Bcl-3

The hepatocyte proliferative response to T_3 is notably much less in mice than rats, with approximately 4 hepatocyte nuclei per 5000 positive for BrdU in the mouse and 350 per 5000 (up to 7%) positive at 24 hours in the rat (*see Chapter Three*). This highlights the already known to exist species differences in the duration of the cell cycle (Michalopoulos 2007). The peak hepatocyte proliferative response after two thirds PH in the rat is 24 hours and in the mouse model it is 36 hours. The time course and magnitude of the proliferative response to T_3 is not known in mice but others have described the response to a single dose of the more powerful hepatomitogen TCPOBOP (Ledda-Columbano *et al.* 2004a). In that study there were a significant number of hepatocytes positive for BrdU by 24 hours with a peak response at 30 hours. It was thought reasonable in this thesis to compare identical time points between rats and mice given that there is a measurable response in mice by 24 hours after T_3, however the magnitude of this response is less than in rats. Given the small numbers of hepatocytes which are undergoing DNA synthesis at 24 hours in the mouse model, it would be an important future aim to undertake a full time course experiment in the future to ascertain the exact peak proliferative hepatocyte response in the mouse model after T_3 stimulation. For the purposes of this thesis this experiment has not yet been done as all

other *in vivo* work was consolidated and reliably replicated in the rat model. Despite the notable differences in response between species, the data presented here clearly shows that the response to T_3 in the Bcl-3 knock out mice was no less than that in the wild type age matched control animals.

In conclusion this chapter investigated cyclin D1 and Bcl-3 as mediators of the T_3 hepatocyte proliferative response. The peak of expression of cyclin D1 mRNA and protein was found to be at 14 hours which is a later time point than others have demonstrated in the published literature. A further preliminary experiment highlighted the complexities in interpreting these data as the variation in expression may be affected by a diurnal variation in the hepatic transcriptome. Cyclin D1 protein was expressed abundantly in hepatocytes in quiescent rat liver at the immunohistochemistry level. For these reasons it could not be used as an early marker of the T_3 proliferative response in the organ perfusion experiments described in Chapter 3. In the second part of the analysis Bcl-3 was found not to be a critical mediator of the mitogenic T_3 effect using a murine knock out model for the Bcl-3.

Given these results it is logical to apply a more generic approach and this is the strategy pursued in the next chapter where gene array studies are used for the first time to identify novel plausible mediators of the hepatic T_3 response in the rat.

Chapter 5 Affymetrix Whole Rat Genome Expression Array

5.1 Background

The hepatic rat expression profile after *in vivo* administration of T_3 is examined in this chapter to identify expression changes in potential novel candidate genes which may act as early markers of the T_3 mitogenic signal in the organ perfusion experiments outlined in Chapter 3. Cyclin D1 was not used to this end as its rise at 14 hours after T_3 demonstrated in the previous chapter is too late a time point to prove useful in the organ perfusion experiments.

The use of an expression gene chip array is a powerful means by which one can interrogate rodent liver tissue that has been stimulated with T_3 and this Chapter describes novel work examining the euthyroid rat hepatic expression profile within three hours of T_3 stimulation using expression array gene chip technology.

5.1.1 Micro-arrays

The principles of microarray technology were conceived over 20 years ago based on developments made from Southern blotting, but it was not to be for at least another decade that high quality slides and precision robotics made them into more of a commercial success (Jaluria *et al.* 2007; Brown and Botstein 1999). In recent years there has been a huge surge in the amount of papers published in the scientific literature based on data generated from microarray experiments.

A DNA microarray is a collection of microscopic DNA spots attached to a solid surface. These so called 'chips' are fabricated by high speed robotics on glass or nylon substances. The array therefore provides an orderly arrangement of samples against which the experimental sample of cDNA can be hybridised according to base pair rules. The attached oligonucleotides are hybridised with cDNA from 2 different experimental conditions for example normal vs. diseased state where the 2 different samples are labelled with 2 different fluorophores. After appropriate incubation and hybridisation the chip can be scanned so a comparison of expression across thousands of genes between the 2 experimental samples can be made in just one go. Gene microarray

systems differ in terms of material used- short oligonucleotides, long oligonucleotides or cDNA. Oligonucleotide arrays typically are used for genome-wide (tens of thousands of genes) screening and cDNA arrays for the investigation of smaller sets of genes.

The use of microarrays for gene expression profiling was first published in 1995 in Science (Schena *et al.* 1995) and the first complete eukaryotic gene on an array was published in 1997. The applications of array technology in modern biology are large and growing and they have provided a powerful tool in areas of gene discovery, disease diagnosis, pharmacogenomics and toxicogenomics. Six of the most popular commercially available platforms include Codelink, Affymetrix, Agilent, NimbleGen, Febit and Applied Biosystems. For the purposes of this PhD project, an Affymetrix expression array has been used to determine the rodent hepatic expression profile after *in vivo* stimulation with T_3.

A typical gene expression array experiment involves (Figure 38):

1. RNA isolation from the samples to be compared
2. Converting the RNA samples to labelled cDNA via reverse transcription
3. Hybridising the labelled cDNA to a glass side array
4. Remove the unhybridised cDNA
5. Detecting and quantitating the hybridised cDNA
6. Comparing the quantitative data from the various samples.

Affymetrix's GeneChips are glass slide arrays manufactured using special photolithographic methods and combinatorial chemistry, which allow the oligonucleotide spots to be synthesised directly onto the array substrate. The analysis procedure specifies that the RNA samples are converted to biotin-labelled cDNA, and each sample is hybridized to a separate GeneChip. The hybridized cDNA is then stained with a streptavidin-phycoerythrin conjugate and visualized with an array scanner.

A single array experiment can generate thousands of data points and so the challenge lies now in accurate interpretation of this data and to this end there are many commercially available software packages to aid the investigator in making sense of their data.

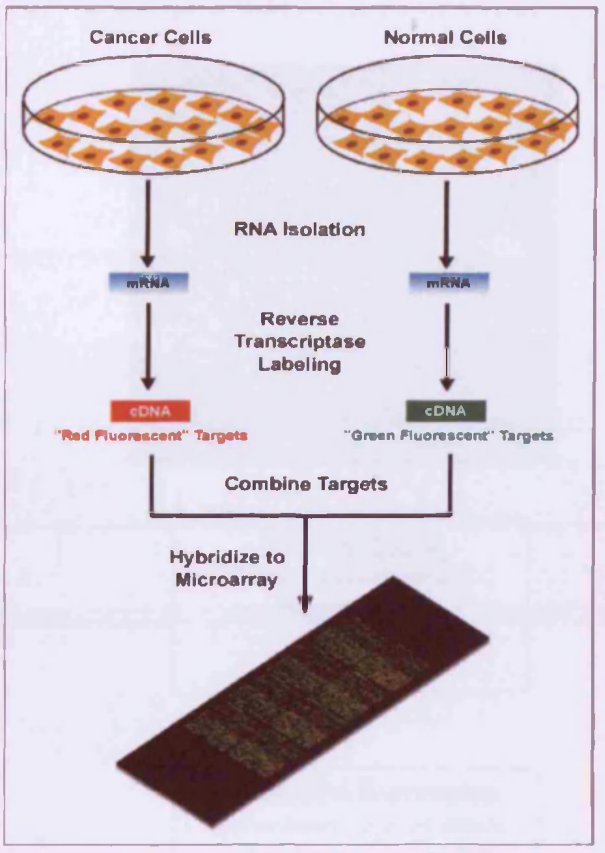

Figure 38 Schematic outline of sample preparation for an array experiment. Here the example compares gene expression differences between cancer cells and normal cells. cDNA from the cancer cells is labelled red and that from normal cells is labelled green prior to chip hybridisation.

Any discussion about microarrays must touch on the limitations and complexities inherently present. Both dual channel (these are hybridised with 2 different samples) and single channel arrays exist. The former generates relative expression values while the latter generates absolute expression values because only one sample has been hybridised.

Once a scanned image has been obtained there can be an initial visual inspection of the data prior to normalisation. An example of what is seen on the hybridised chip and the subsequent steps in analysis is shown in

Figure 39. Normalisation accounts for labelling efficiencies and detection levels for the fluorescent dyes as well as differences in the quantity/quality of RNA samples. In this

way it acts as the first level of filtering applied to the data. A number of institutions provide free software to enable this analysis to be performed.

Figure 39 An actual gene array chip (top) and the basic steps of raw data analysis (bottom). Two differently labelled probes, green and red, have been applied to this chip. Red spots indicate greater binding of the red labelled probe and green of the green labelled probe. Yellow spots indicate equal binding and black spots reflect no signal because of no hybridisation (Verducci et al. 2006).

Microarrays are imaged using an optical scanner and then these must be subjected to background correction to adjust for non specific binding and fluorescence from any other chemicals on the slide. The array contains multiple probes for each gene and these are scattered over the surface of the array and so variations in intensity from probe to probe for the same sample need to be resolved. Observed intensities are modified based on comparison with nearby background probes whose level of expression is known. On the Affymetrix array, each gene probe has a single nucleotide mismatch probe mate and the MAS 5.0 (Microarray Suite) of Affymetrix uses paired probes for adjustment and there is also the RMA or robust multichip average which uses quantile adjustment. The GC RMA method pools probes with comparable numbers of G-C bonds to achieve a stable mismatch adjustment.

After normalisation has taken place both within an array and between arrays, statistical techniques are used to evaluate and decipher the array data. The aims of these are to identify clusters of genes that are up or down regulated following the experimental stimulus. Thus normalisation forms part of the low level analysis and the high level analysis involves gene filtering then gene clustering before final gene annotation analysis.

5.1.1.1 Differential Expression

Fold change is used to compare differences in the level of expression between the two experimental samples. The disadvantage is it does not take into consideration the variability in the data. So, genes with low expression values yet large fold changes may be identified as differentially expressed but genes that display small but reproducible changes in expression may be missed. Since tens of thousands of genes are compared, many genes can be false positives. The False Discovery Rate or FDR has been proposed to handle the multiple comparison issues in the context of microarray data and the FDR is the expected proportion of false positives among all the rejected hypotheses. The FDR instead of trying to avoid any false positives controls the proportion of positive calls that are false positives. Put another way, the FDR is the ratio of the typical number (over all permutations) of transcripts 'discovered' at random (false discoveries) versus the number detected in the experiment.

5.1.1.2 Clustering Genes

Clustering is a data mining technique used to group genes which have similar expression patterns. A heat map represents a common approach to present expression data. Genes index the rows and chips the columns. The variation in colour across the row reflects the expression pattern of the gene. An example from the 1 hour array in this thesis is shown in Figure 40.

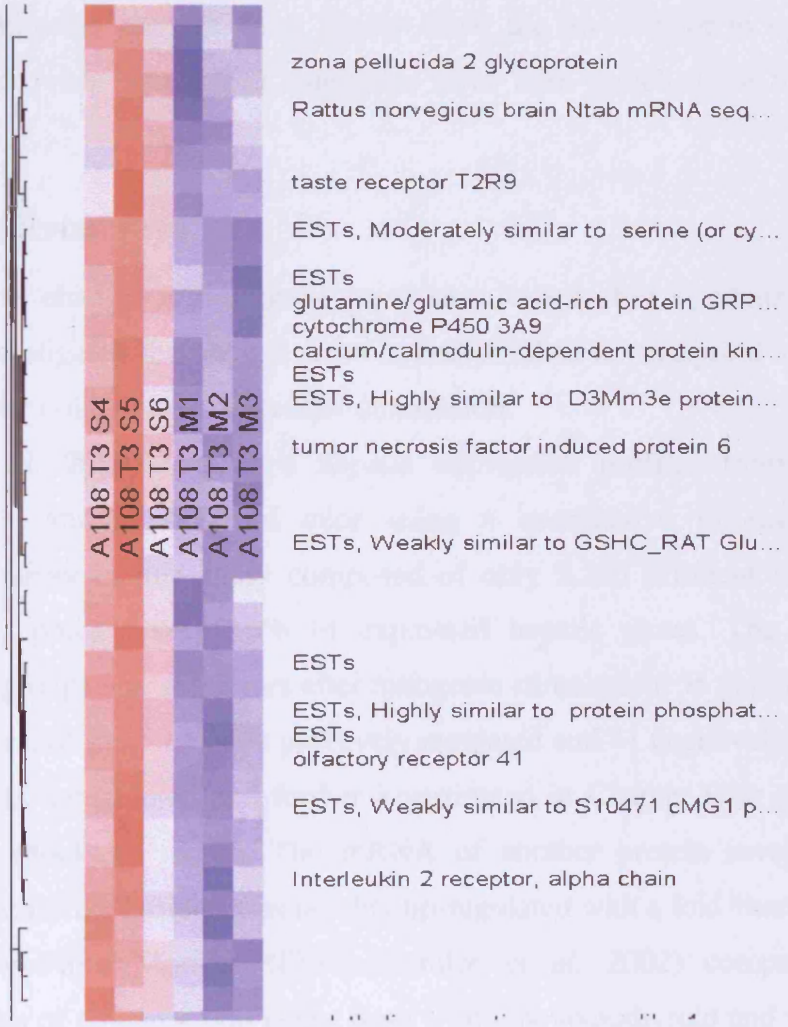

Figure 40 An example of higher level data analysis. Part of the dChip cluster hierarchical map for the 1 hour array in this thesis. The three chips on the left are labelled S for submitogenic and the three on the right are labelled M for mitogenic. Red indicates greater expression in the submitogenic group for each gene of interest shown here. EST = expressed sequence tags.

5.1.1.3 Annotation and functional characterisation

The final stage of higher level analysis is gene annotation. The current most relevant source of information for relating newly acquired gene expression level data to known functional and partial pathway information is the Gene Ontology GO database www.geneontology.org. It is a collaborative effort to address the need for a consistent description of gene products in different databases. Its three organising principles are molecular function, biological process and cellular component. Various tools such as GoMiner, Onto-Express and Go Term Finder allow the investigator to upload a full gene set and then view which GO categories have been enriched for the genes of interest.

5.1.2 T_3 and Microarrays

Previous reports of changes in liver gene expression *in vivo* after T_3 administration are available and investigated the change from hypothyroid to hyperthyroid status and/or looked at later time points (> 6 hours) after stimulation.

Feng (Feng *et al.* 2000) compared hepatic expression profiles from T_3 treated hypothyroid mice and hypothyroid mice using a quantitative fluorescent cDNA microarray. The array in this study composed of only 2,225 different mouse genes which represent approximately 10% of expressed hepatic genes. The comparison between the two groups was at 6 hours after mitogenic stimulation. 55 genes were found to be T_3 responsive, of these 14 were positively regulated and 41 negatively. Bcl-3 (fold change + 2.5) was upregulated and further investigated in Chapter Four of this thesis using a murine knock-out model. The mRNA of another protein involved in cell proliferation, kinesin-like protein, was notably up-regulated with a fold change of + 2.0.

In another study Flores-Morales (Flores-Morales *et al.* 2002) compared hepatic expression profiles of around 4,000 genes from wild type hypothyroid and wild type T_3 treated hypothyroid mice. A further comparison was between T_3 treated hypothyroid TRβ deficient mice and hypothyroid TRβ deficient mice. The time points examined were at 2 hours after mitogenic stimulation and at 5 days. T_3 was found to regulate more than 200 genes and of these 60% were dependent on the TRβ gene for T_3 regulation. The study showed a clear functional distinction between rapid (2 hours) and late T_3 effects in the mouse liver.

Weitzel (Weitzel *et al.* 2003) looked at hepatic expression in hypothyroid and T_3 treated hypothyroid rats using a DNA microarray. The time points of 6, 24 and 48 hours after T_3 administration were examined. 62 of 4,608 genes displayed a reproducible T_3

response. Representative examples of differentially regulated genes from each of six different gene profile clusters were further characterised by either Northern blot analysis or quantitative real time PCR. The study identified several genes already known to be T_3 responsive and involved in metabolic pathways: ANT2, myelin basic protein and ATP synthase β subunit. However the majority of differentially regulated genes were not primarily involved in metabolic functions, instead they encompassed translation, protein turnover, apoptosis and cell structure pathways.

Yen (Yen *et al.* 2003) studied the effects of ligand and thyroid receptor isoforms on hepatic gene expression profiles of thyroid receptor knockout mice. 48 complimentary DNA microarrays were used to examine hepatic gene expression profiles in wild type and TRα and TRβ knockout mice under different conditions: no treatment, treatment with T_3, propylthiouracil (PTU) induced hypothyroidism and treatment with a combination with PTU and T_3. Hierarchical clustering analyses showed that the 57 positively regulated genes fit into three main expression patterns: i) a pattern of basal repression during thyroid hormone deprivation and transcriptional activation after acute treatment with T_3 (includes Bcl-3 in cluster 2) ii) little or no basal repression during thyroid hormone deprivation but strong transcriptional activation after T_3 treatment. iii) basal repression in the absence of thyroid hormone with little activation after acute T_3 administration.

Stahlberg (Stahlberg *et al.* 2005) compared hepatic gene expression in hypothyroid mice and T_3 treated hypothyroid mice 2 hours after a 5μg dose of T_3. Malic enzyme I was up-regulated with a fold change of + 7.86 and cytochrome P450 4A3 was up-regulated with a fold change of + 9.77.

Finally Moeller (Moeller *et al.* 2005) examined the effect of T_3 on the expression of more than 15, 000 genes in cultured human fibroblasts from normal individuals and individuals with resistance to thyroid hormone (RTH) to confirm the specificity of the hormonal effect. Incubation of cells for microarray analysis was for 24 hours. 148 genes were induced with a fold change of 1.4 or more. These represented 91 up-regulated and five down regulated genes. A number of genes not previously known to be induced by thyroid hormone were indentified in this study and include member RAS oncogene family brain antigen RAB3B and platelet phosphofructokinase.

As yet therefore the response after T_3 in euthyroid rat liver at early time points has not been described in the worldwide literature and this strategy is usefully pursued in this Chapter.

5.2 Aims

To determine the *in vivo* rat hepatic expression profile after stimulation with

i) mitogenic dose T_3 versus vehicle only at 3 hours post dose.

ii) mitogenic dose T_3 versus sub-mitogenic dose T_3 at 1 hour post dose.

The first array experiment compared the response between T_3 and vehicle only at an early time point of 3 hours post stimulation. The results demonstrated a number of cell cycle genes and prominently a number of transcription factors (Kruppel Factors) which were up-regulated. A further targeted analysis was performed of their expression time course profile (outlined in Chapter Six) which indicated that 60 minutes post T_3 was of interest and therefore a second array experiment was performed at 60 minutes but now comparing a mitogenic with a *sub-mitogenic* doses of T_3. The *sub-mitogenic* dose does not bring about cell proliferation but does reflect the more general T_3 effects on metabolism. Any differences therefore between these two stimuli would highlight changes in genes specific to the T_3 *mitogenic* effect. The calculation of the sub-mitogenic dose is described in the Methods section of this chapter.

5.3 Materials and Methods

5.3.1 Animal Protocols

Please refer to *General Methods* Chapter 2.

Protocol one: Adult male SD rats, were administered a subcutaneous dose of 5μg T_3, or vehicle only (n = 3), and sacrificed at 3 hours post dose for hepatic microarray analysis.

Protocol two: Adult male SD rats, were administered a subcutaneous dose of 5μg T_3, or a sub-mitogenic dose of 0.1μg per animal (n=3), and sacrificed at 1 hour post dose for hepatic microarray analysis.

Liver was harvested and sectioned and pieces were snap frozen in liquid nitrogen and stored at -80°C for later analysis and RNA isolation.
The threshold at which the mitogenic effects of T_3 are apparent was established (2μg per animal) in Chapter Three. The proliferative effect of T_3 was only manifest at doses greater than 2μg per animal, with the peak at 5μg T_3 per whole rat. A comparison was therefore made between the 5μg mitogenic dose and a sub-mitogenic, although supra-physiological dose of 0.1μg per animal, to allow changes in gene expression specific to the mitogenic effect to be observed. At this lower T_3 dose, it is anticipated that the more general effects on metabolism will still occur, therefore if changes in expression are found these may be specifically due to the *mitogenic* effects of T_3 on the liver.

5.3.2 RNA preparation

Please refer to *General Methods* Chapter 2.

Materials:

Promega RNAgents® Total RNA Isolation System (# Z5110)
RNAgents® Denaturing solution (Promega #Z5651)
2M Sodium acetate pH 4.0
Phenol:chloroform:isoamyl alcohol 125:24:1 (Sigma #P1944)
Ice cold 75% ethanol
RNase free water
1.5ml centrifuge tubes

Method:

500µl denaturing solution for 50mg liver tissue was chilled. The liver sample was disrupted using a pestel and mortar in liquid nitrogen and on ice. It was then added to a 1.5ml centrifuge tube with the denaturing solution. 60 µl 2M sodium acetate was added and mixed. 600 µl phenol:chloroform:amyl alcohol was added and the tube was inverted 3 to 5 times. It was chilled on ice for 15 minutes and then centrifuged at 10,000g at 4^0C for 20 minutes. The top aqueous phase was transferred to a fresh DEPC treated tube.
An equal volume of the isopropanol was added and then incubated at -20^0C for 5 minutes. An RNA pellet was created by centrifugation at 10,000g for 10 minutes at 4^0C. The pellet was then washed by adding at least 1ml of ice cold 75% ethanol. The pellet was broken up with a sterile pipette tip and then a further spin was undertaken at 10,000g for 10 minutes at 4^0C. The pellet was dried in a vacuum desiccator for 10 minutes. The RNA was then dissolved in RNase free water and stored at -80^0C.

5.3.2.1 RNA Cleanup

Materials:

Qiagen RNeasy Mini kit (Qiagen, UK Cat. No. 74104)

Components of Buffer RLT, RW1 and RPE:

RLT- contains a guanidine thiocynate

RWL-contains guanidium thiocynate and ethanol

DNase I (Pharmacia)

10X DNase buffer

1M Tris pH 7.5

1M $MgCl_2$

1M DTT

Recombinant RNasin Ribonuclease Inhibitor (Promega)

β-Mercaptoethanol 14.3M (Sigma Aldrich)

Method:

RNA samples were subjected to DNase digestion to prevent any carry over of contaminating DNA. 72.5µl of sample containing 1-2µg/µl of RNA, nuclease free water, 1X DNase buffer, 2 units of DNase, 100 units of recombinant RNasin

Ribonuclease Inhibitor, was mixed gently with a pipette, and incubated at 37°C for 30 minutes. The samples were placed on ice, prior to loading onto spin columns supplied with the Qiagen RNeasy Mini kit as per *General Methods Chapter 2.*

The total RNA in solution was quantitated and analysed for purity by measuring its optical density at 260nm and 280nm. RNA was aliquotted and stored at –80°C.

5.3.2.2 RNA Integrity/Yield

Assessed as described in *General Methods Chapter 2.* RNA gel electrophoresis for the samples obtained is shown in Figure 41 and Figure 42.

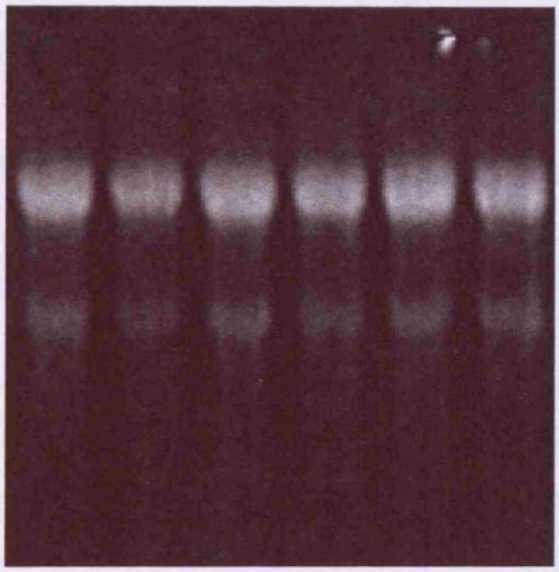

Figure 41 Denaturing RNA gel electrophoresis for the 3 hour array RNA samples. The RNA is intact in all the samples as shown by the sharp 28S (top) and 18S (bottom) bands and the 2:1 ratio of 28S:18S.

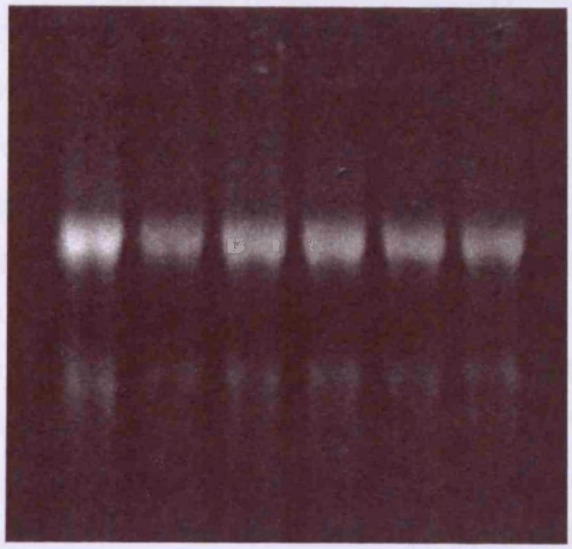

Figure 42 Denaturing RNA gel electrophoresis for the 1 hour array RNA samples. The RNA is intact in all the samples as shown by the sharp 28S (top) and 18S (bottom) bands and the 2:1 ratio of 28S:18S.

An absorbance A_{260}/A_{280} ratio of above 1.8 was obtained for all the samples.

5.3.3 Microarray analysis

Array analysis was performed with Dr. M. Hubank at the Institute for Child Health Gene Microarray Centre, University College London. Double stranded cDNA was synthesised from 5μg total RNA, labelled with biotin by an *in vitro* transcription reaction (IVT), and hybridised to Affymetrix Rat Genome arrays, RAE230v2 (Affymetrix, Santa Clara, CA) following standard procedures (www.affymetrix.com). The chip provides data on more than 30,200 transcripts including over 28,000 well substantiated rat genes. The chip is comprised of more than 31,000 probe sets and 681,012 distinct oligonucleotide features. Quality of hybridisation was determined using Affymetrix.rpt files (background < 100). Probe level values (.CEL files) were obtained using Affymetrix GCOS. Two separate microarray experiments were conducted using a total of 12 genechips.

5.3.3.1 Data Analysis

Probe set summary values were generated from CEL files using dChip (C. Li 2001) software (www.dchip.org). Groups were compared by unpaired Welch t-test, $p < 0.05$.

Empirical False Discovery Rate was estimated by permutation analysis. Data was filtered to remove genes with lower than 1.3 fold change. The final gene list fulfilling these statistical criteria can then be further interrogated using a number of freely available data mining tools. The ones used in this thesis are described next.

The genes with significant fold changes were functionally categorised using NetAffx™ (Affymetrix) www.affymetrix.com, KEGG and GenMapp www.genmapp.org. The NetAffx™ free online analysis centre enables correlation of results with annotation information which is constantly updated providing the very latest information for probe set IDs and much Gene Ontology information.

KEGG (www.genome.jp/kegg) is the Kyoto Encyclopaedia of Genes and Genomes. It is a bioinformatics resource from the Kanehisa Laboratories in the Bioinformatics Centre of Kyoto University and the Human Genome Centre of the University of Tokyo. The KEGG gene catalogue contains 2 million genes from 32 eukaryotes and 420 bacteria so far.

The Gene Annotator and Pathway finder (GenMAPP) has been developed at the Gladstone Institutes, University of California at San Francisco. The user chooses any map that may be of interest to them, for example cell cycle control. The expression dataset in the correct file format is then imported into the program and the data is displayed on the map with nominated colour changes reflecting up or down regulated genes. There are additional hyperlinks to more online information for each gene that may be of interest to the investigator.

In compliance with MIAME standards, Affymetrix data files (CHP and CEL) have been deposited in the ArrayExpress database at the European Bioinformatics Institute (EBI) http://www.ebi.ac.uk/arrayexpress/. MIAME (Minimum Information About a Microarray Experiment) describes the minimum information that is needed to enable the interpretation of the results of the experiment unambiguously and potentially to reproduce the experiment.

5.4 Results

5.4.1 T_3 treated rat liver versus vehicle only rat liver at 3 hours

2,259 transcripts exhibited a change in expression of Fold Change (FC) greater than +1.3 or less than -1.3 ($\leq \geq \pm$ 1.3) with p value <0.05. 1,554 regulated transcripts corresponded to identified genes, of which 1,111 were negatively regulated and 443 positively regulated. Regulated genes related to growth and transcription and general metabolic and signal transduction pathways are shown in Table 7. Genes with more marked changes (> 2 fold) with p values < 0.10 are also included.

5.4.2 Mitogenic T_3 treated rat liver versus Sub-mitogenic T_3 rat liver at 1 hour

As expected there were significantly fewer differences between the array data between the two groups.

230 transcripts exhibited a change in expression of FC $\leq \geq \pm$ 1.3 with p value < 0.05. 160 regulated transcripts corresponded to identified genes, of which 65 were negatively regulated and 95 positively regulated. They are grouped as before and displayed in functionally related categories in Table 8.

Table 7 Functionally related hepatic genes up- and down regulated on the Affymetrix RAE230v2 expression array, 3 hours after T_3 stimulation (negatively regulated genes in italics).

Probe ID	Description	Fold Change	P value
	METABOLIC EFFECTS/SIGNAL TRANSDUCTION		
	Thyroid		
1387852_at	Thyroid hormone responsive protein	1.52	0.028
1367726_at	*Thyroid hormone receptor alpha*	*-1.59*	*0.015*
1387983_at	*Thyroid receptor beta*	*-1.61*	*0.0134*
1369744_at	*Thyroglobulin*	*-2.37*	*0.06*
1371010_at	*Thyroid transcription factor*	*-2.44*	*0.06*
	Gluconeogenesis		
1372264_at	Phosphoenolpyruvate carboxykinase 1	1.74	0.013
	Glycolysis/gluconeogenesis		
1380045_at	Pyruvate dehydrogenase phosphatase isoenzyme 2	5.8	0.0003
1370725_a_at	Glucose 6 phosphatase	2.14	0.007
1369510_at	*Glyceraldehyde 3 phosphate dehydrogenase (glycolysis)*	*-1.94*	*0.009*
1369006_at	*Hexokinase 2*	*-2.28*	*0.029*
	Glycogen metabolism		
1369357_at	*Phosphorylase kinase alpha 1*	*-1.4*	*0.0068*
1381756_at	*Alcohol dehydrogenase 6A class V*	*-13.36*	*0.014*
	Krebs cycle		
1381671_at	Succinate coenzyme A ligase	3.82	0.02
1367911_at	Isocitrate dehydrogenase 3	1.75	0.004
1372790_at	Malate dehydrogenase	1.49	0.041
1375290_at	*Citrate synthase*	*-7.74*	*0.038*
	Fatty acid / lipid metabolism		
1388373_at	Adiponectin receptor 1	1.36	0.002
1375033_at	*Carnitine palmitoyltransferase 1c*	*-1.69*	*0.047*
1387065_at	*Phospholipase c delta 4*	*-25.17*	*0.018*

	Fatty acid degradation		
1369666_at	Glycerol 3 phosphate dehydrogenase 2	2.44	0.034
1394763_at	*Hydroxyacyl-coenzyme A dehydrogenase*	*-1.7*	*0.038*
	Fatty acid synthesis		
1369328_at	*Acetyl-coenzyme A carboxylase beta*	*-1.63*	*0.01*
	Insulin action & signalling		
1370114_a_at	Phosphoinositide 3-kinase polypeptide 1 (p85alpha)	2.54	0.037
1387847_at	Phosphatidylinositol 3-kinase catalytic subunit beta isoform	1.79	0.037
1369655_at	Phosphatidylinositol 3-kinase class 3	1.35	0.045
1368019_at	mTOR (FK506 binding protein 12)	1.34	0.026
1369050_at	Phosphatidylinositol 3-kinase C2	1.31	0.04
1386888_at	*4EBP1*	*-1.35*	*0.048*
1368056_at	*TSC 2*	*-1.37*	*0.044*
1369357_at	*Phosphorylase kinase alpha 1*	*-1.4*	*0.007*
1370605_a_at	*Leptin receptor*	*-2.06*	*0.047*
	Signal transduction		
1368958_at	Protein kinase C and casein kinase substrate in neurons 1	10.09	0.053
1387708_at	Adrenergic receptor alpha 2a	4.99	0.031
1370114_a_at	Phosphatidylinositol 3-kinase regulatory subunit	2.54	0.037
1379207_at	JNK/SAPK inhibitory kinase	2.37	0.04
1388066_a_at	G protein receptor kinase 6	2.36	0.025
1368700_at	Phospholipase C-like1	1.82	0.017
1388066_a_at	Mitogen activated protein kinase 6	1.67	0.036
1387907_at	Inositol 145-triphosphate receptor	1.43	0.01
1376039_at	*Serine/threonine kinase 6*	*-1.3*	*0.044*
1370585_at	*Protein kinase C beta 1*	*-1.33*	*0.012*
1371158_at	*Eph receptor A8*	*-1.64*	*0.037*
1369741_at	*Potassium inwardly rectifying channel subfam. j*	*-1.72*	*0.012*
1378997_at	*Eph receptor B6 predicted*	*-2.27*	*0.036*
1371219_a_at	*Phosphodiesterase 1C*	*-5.37*	*0.02*
1387065_at	*Phospholipase C delta 4*	*-25.17*	*0.012*
	Protein dephosphorylation		
1380045_at	Pyruvate dehydrogenase phosphatase isoenzyme 2	5.8	0.00031

1379191_x_at	Protein tyrosine phosphatase receptor type R	1.93	0.045
	G protein coupled receptor		
1368638_at	*147*	*-1.63*	*0.041*
1368796_at	*54*	*-1.67*	*0.045*
1368299_at	*83*	*-2.28*	*0.03*
1387182_at	*37*	*-2.41*	*0.012*
	Bile acid biosynthesis		
1368458_at	Cytochrome p450 family 7 subfamily a	3.81	0.005
	Cellular immunity		
1369529_at	*CSF 3*	*-2.82*	*0.043*
1371227_at	*CSF 2*	*-8.32*	*0.018*
	Cytoskeleton		
1378197_at	*Kinesin family member C2*	*-1.36*	*0.037*
1384885_at	*Tektin 2*	*-1.49*	*0.022*
1377799_at	*Microtubule associated protein 6*	*-1.5*	*0.016*
	Cation Transport		
1368746_a_at	ATPase H+/K+ transporting non-gastric alpha polypeptide	3.48	0.029
1369222_at	*Potassium channel subunit*	*-4.08*	*0.024*
	HSP/protein folding		
1370018_at	Heat shock 27kDa 2	2.32	0.023
1397502_at	Peptidylprolyl isomerase B	1.97	0.049
	Cell adhesion		
1383783_at	Protocadherin 9 (predicted)	5.88	0.04
1368320_at	Neural cell adhesion molecule 1	4.17	0.02
1373487_at	*Spondin 1*	*-1.51*	*0.03*
1368381_at	*Cartilage acidic protein 1*	*-4.19*	*0.006*
	GROWTH/TRANSCRIPTION		
	Kruppel Factors		
1368877_at	Zinc finger 354A	7.64	0.079
1381395_at	KF 15	1.66	0.019
1384432_at	Zinc finger protein 96	1.57	0.016
1370209_at	KF 9 / BTEB 1	1.36	0.047

1368067_at	Zinc finger 148	1.35	0.0328
1368228_at	Zinc finger 265	1.3	0.044
1380363_at	*Kruppel like factor 7*	*-1.46*	*0.016*
1379880_at	*Kruppel like factor 3*	*-1.86*	*0.037*
1375013_at	*Zinc finger protein 335*	*-2.29*	*0.041*
	Transcription factors		
1372639_at	Ring finger protein 30	2.95	0.009
1393278_at	cAMP responsive element binding protein 3	2.13	0.024
1369853_at	*Transcriptional regulator relax*	*-5.44*	*0.026*
1382637_at	*E74 like factor 2*	*-6.59*	*0.043*
	Apoptosis		
1372016_at	GADD 45 beta predicted	2.74	0.029
1369995_at	*Fas associated factor 1*	*-1.5*	*0.02*
1370625_at	*FAS apoptotic inhibitory molecule 2*	*-1.64*	*0.044*
1369198_at	*Apoptotic protease activating factor 1*	*-1.79*	*0.005*
1370787_at	*Bcl-2 like 11 apoptosis facilitator*	*-1.84*	*0.024*
	Cell cycle/proliferation		
1397126_at	Minichromosome maintenance deficient domain	2.7	0.046
1367725_at	PIM-3	2.34	0.045
1371150_at	Cyclin D1	2.14	0.1
1386299_at	Cullin 5	1.80	0.014
1399100_at	Cyclin T2	1.63	0.016
1390343_at	Cyclin C	1.48	0.013
1382664_at	Cell division cycle 27 homolog	1.33	0.021
1367780_at	*Pituitary tumour transforming protein 1*	*-1.32*	*0.044*
1375996_at	*Septin 1*	*-1.43*	*0.045*
1370233_at	*Fibroblast growth factor 12*	*-1.53*	*0.028*
1370788_at	*Fibroblast growth factor 4*	*-1.55*	*0.035*
1370116_at	*Septin 3*	*-1.6*	*0.04*
1382370_at	*Cyclin F*	*-1.69*	*0.003*
1377702_at	*Retinoblastoma 1*	*-1.7*	*0.017*
1370294-a_at	*Cell division cycle 20 homolog*	*-1.85*	*0.01*
1369884_at	*Fibroblast growth factor 7*	*-1.86*	*0.043*
1369608_at	*Fibroblast growth factor 16*	*-1.9*	*0.02*
1387647_at	*Trefoil factor 1 (neg. reg. of prolif.)*	*-2.2*	*0.023*
1370042_at	*Stathmin-like 2*	*-3.73*	*0.048*
1368388_at	*v-maf musculoaponeurotic fibrosarcoma avian*	*-4.14*	*0.042*

	RAS oncogene		
1383089_at	RAB21	1.56	0.04
1397839_at	*RAB15*	*-1.49*	*0.04*
1368847_at	*RAB10*	*-1.52*	*0.02*
	Nuclear receptors		
1386935_at	*Nuclear receptor subfamily 4 group A member 1*	*-1.65*	*0.03*
1369007_at	*Orphan nuclear receptor*	*-1.65*	*0.03*

Table 8 Functionally related hepatic genes up- and down- regulated on the Affymetrix RAE230v2 expression array, 1 hour after mitogenic vs. sub-mitogenic T_3 stimulation (negatively regulated genes in italics).

Probe ID	Description	Fold Change	P value
	METABOLIC EFFECTS/SIGNAL TRANSDUCTION		
	Insulin signalling		
1376011_at	MAPK 13	2.44	0.09
	MAPK signalling		
1369255_at	Interleukin 1 receptor type 1	1.77	0.03
1368592_at	Interleukin 1 alpha	1.47	0.015
	Lipid metabolism		
1370387_at	*Cytochrome p450 subfamily 3*	*-2.12*	*0.01*
1377407_at	*Aa2-174*	*-6.04*	*0.003*
	Proteolysis		
1390018_at	Dipeptidylpeptidase 10	2.11	0.048
1387819_at	*Pancreatic elastase 1*	*-2.61*	*0.00078*
	Ion transport		
1375877_at	Synaptotagmin 4	5.33	0.07
1388263_at	*Potassium voltage gated channel shaker related subfamily*	*-1.77*	*0.02*
	Cytoskeleton		
1395485_s_at	Myosin 1b	1.35	0.039
1376124_at	*Wiskott-aldrich syndrome like (human)*	*-1.39*	*0.031*
	Immune response		
1371015_at	*Myxovirus resistance 2*	*-17.31*	*0.1*
	GROWTH/TRANSCRIPTION		
	Kruppel Factors		
1369363_at	Sp4	4.15	0.04

	Transcription		
1393571_at	SRY-box containing gene 4	6.05	0.0093
1389909_at	Nuclear receptor co activator	3.35	0.03
1369544_a_at	Homeobox A1	1.4	0.025
1385837_at	*Homeobox D3*	*-3.85*	*0.027*
	Apoptosis		
1389506_x_at	FAS associated factor 1	1.62	0.035
1387521_at	Programmed cell death 4	1.35	0.015
	Cell cycle		
1372685_at	Cyclin dependent kinase inhibitor 3	2.22	0.023
1373722_at	Kinesin family member 20A	1.96	0.04
1379582_a_at	Cyclin A2	1.93	0.017
1393848_at	Ribonucleotide reductase M2 (DNA replication)	1.83	0.04
1368260_at	Aurora kinase b	1.82	0.026
1370294_a_at	Cell division cycle 20 homolog	1.68	0.03
1383747_at	ect 2 oncogene	1.63	0.021
1398482_at	Bcl-3 (predicted)	1.48	0.007
1386857_at	Stathmin 1	1.37	0.019

5.5 Discussion

The transcriptome data presented here illustrate two facets of T_3's actions in rat liver *in vivo* – the effects of sudden elevation of circulating T_3 above normal, and the more limited changes specific to administration of T_3 above the dosage at which liver mitogenesis is initiated. The initial data set at three hours after administration of T_3 adds to the observations on rodent liver made by Yen et al (Yen 2001; Feng *et al.* 2000) and Stahlberg et al (Stahlberg *et al.* 2005) , specifically by investigating rats rather than mice and in looking at an earlier time point, reflecting interest in the early events that rapidly lead to the initiation of DNA synthesis. Yen et al defined specific clusters of up-regulated and down regulated genes (their clusters 2 & 5) the expression of which was specifically associated with the response of the euthyroid rather than the hypothyroid liver to T_3 administration; they and others (Flores-Morales *et al.* 2002; Wikenheiser-Brokamp 2006) also addressed the changes seen on thyroid replacement in hypothyroid mice.

There is no overlap between either the positively responding cluster (27 genes) or the negative (21 genes) identified by Yen at 6 hours in mice and in rats at 3 hours after single high dose T_3 in this thesis. Even the genes affected most prominently in their 6 hours array - lipocalin2 (14-fold) and Bcl-3 (>3 fold) were unchanged according to the array data presented here at 3 hours.

At the three hour time point there are firstly physiologically plausible alterations in directly T_3-related proteins, with up-regulation of thyroid-responsive protein, and down-regulation of thyroid receptor alpha and beta, thyroid transcription factor, and the transport protein thyroglobulin, the latter changes appropriate to the initiation of a negative feedback following over-stimulation of the T_3 pathway.

As anticipated there were multiple changes in the expression of enzymes of intermediary metabolism. A major function of thyroid hormone is regulation of thermogenesis, hyperthyroid states being associated with an elevation of basal metabolic rate reflecting stimulation of futile cycles of intermediary metabolism, with both increased synthesis and degradation of proteins, lipids and carbohydrates, and enhanced cation shuttling across cell membranes (Brent 1994). The known up-regulation of the rate-limiting enzyme of gluconeogenesis, phosphoenolpyruvate carboxykinase 1 (Barthel and Schmoll 2003), is shown here to be initiated by gene expression within 3 hours of stimulation, as is glucose-6-phosphatase. Changes in Krebs cycle enzyme expression are divergent, with a marked down-regulation of citrate synthase but up-regulation of other components. A dominant decrease in citrate

synthase activity would imply decreased capacity to divert acetyl coenzyme A to fatty acid synthesis, and there is a decrease in expression of some enzymes mediating fatty acid synthesis. The changes however are highly complex, and their proper interpretation would require serial observations linked with metabolic studies initiated to elucidate changes potentially relevant to cell proliferation.

5.5.1 Proliferative response

A set of cell-cycle related genes were up-regulated by 3 hours, including cyclin D1 (FC +2.14), the early expression of which has been associated with both T_3 induced liver proliferation and that induced by other primary mitogens. The fold change however did not reach statistical significance with a p value of < 0.1. As set out in Chapter Four the rise at the expression level of cyclin D1 after T_3 in rat liver studied in this thesis was observed at a later time point of 14 hours post dose and it may be that this is when the greatest and most significant fold change would be observed to occur.

The greatest fold change was in the serine-threonine kinase PIM-3 (FC + 2.34) – a gene initially identified as a depolarisation induced gene in a rat phaeochromocytoma cell line (Amaravadi and Thompson 2005), and more recently shown to be aberrantly expressed in human hepatocellular carcinoma tissues and cell lines derived there from (Fujii *et al.* 2005), with a role both in cell cycle progression and in negative regulation of apoptosis. PIM-3 is selectively expressed in malignant lesions but not normal tissues of endoderm-derived organs such as liver (Li *et al.* 2006). Studies suggest that PIM-3 promotes carcinogenesis as a negative regulator of apoptosis, most recently in human colon cancer cells (Popivanova *et al.* 2007).

There was also significant down-regulation of some of the genes governing expression of pro-apoptotic processes such as Fas-associated 1, apoptotic protease activating factor, and 'Bcl-2 like 11' apoptosis facilitator but reflecting the complexity of the system other anti-apoptotic genes are also down regulated e.g. Fas apoptotic inhibitory molecule 2.

Interestingly, Bcl-3 is up-regulated on the 1 hour array with a modest fold change of +1.48 and yet in Chapter Four it was shown that the T_3 proliferative response was not diminished in knockout mice for this gene. The up regulation is small and of course a rise in expression does not necessarily lead to an increase in protein expression and thereafter a rise in functional activity of the protein.

Other notable genes linked to cell cycle control and importantly cycle progression are also up-regulated at 1 hour. The Aurora kinases play a critical role in mitosis and have been suggested as promising targets for cancer therapy due to their frequent over expression in a variety of tumours (Andrews 2005). Aurora kinase B is a regulator of kinetochore-microtubule attachment and has a number of substrates during mitosis. Proper functioning is required for faultless mitosis and hence cell proliferation.

Stathmin 1 (FC + 1.37) has some known functions but it is still to be fully described in the literature. Levels are noted to be elevated in various tumour cells and it is known to be a microtubule-destabilising phosphoprotein (Rowlands *et al.* 1995; Mistry and Atweh 2001). When stathmin 1 is phosphorylated by cyclin dependent kinase 2, its microtubule-depolymerizing activity is lost and the mitotic spindle is formed. Thus, regulation of Stathmin 1 expression is important for cell cycle progression.

Mammalian ECT-2 (FC +1.63 on the 1h array) is a proto-oncogene that forms an actomyosin contractile ring that separates the plasma membrane of two forming daughter cells during cell division (Saito *et al.* 2003). Amino-terminally truncated ECT-2 shows transforming activity in some cultured cells.

A further analysis of the 3 hour array data relevant to proliferative events is summarised in Table 9 and additional hypotheses can be generated.

Cell membrane signal transduction and signal amplification	**Protein Chaperoning**	**RAS Proto-oncogene**	**Translation machinery Purine/pyrimidine synthesis**
Phosphatidylinositol 3-kinase, gamma polypeptide (+1.57)	HSPC210 (+1.8)	v-ras (+1.99)	Mouse methionyl-tRNA formyltransferase (+1.5)
MAP associated Protein 1 (+1.74)	HSPC021 (+1.79)	RAB6 (+1.75)	Lysyl-tRNA synthetase (+1.57)
PIM 3 (+2.1)	HSP 105 (+1.61)	RAB 2 (+1.59)	Phosphoribosylpyrophosphate symthetase (+1.58)
Phospholipase C, beta 4 (+1.52)	HSPC182 (+1.5)	RAB4A (+1.57)	5-aminoimidazole-4-carboxamide ribonucleotide formyltransferase (+1.56)

Table 9 Additional up-regulated genes involved in the proliferative response. Fold change is indicated in brackets. (HSP = Heat Shock Protein)

The T_3 mitogenic signal upstream of membrane phospholipids may be mediated by PI3K (a proto-oncogene) and the MAP (Mitogen Activated Protein) kinase cascade is then activated via phospholipase C and PI3K leading to nuclear phosphorylation events and gene transcription. RAS family proto-oncogene products also contribute to the proliferative response. HSPs (Heat Shock Proteins) assist in protein chaperoning in readiness for cell division and translational proteins are expressed, necessary for the up regulated response (Didelot *et al.* 2006). Enzymes involved in purine/pyrimidine synthesis are produced permitting DNA synthesis.

5.5.2 GADD45beta

The key up-regulated genes after T_3 can be compared with those up-regulated by the primary mitogen 1, 4-bis-[2-(3, 5,-dichloropyridyloxy) benzene (TCPOBOP) in mice, which initiates proliferation via the constitutive androstenedione receptor (Columbano *et al.* 2001). Interestingly it is a much stronger mitogen in mice than rats, and it is also a more powerful mitogen than T_3. The highest change in expression at 3 hours in TCBOPOP treated mice was in the Gadd45beta/MyD118 gene, up-regulated >3 fold at 3 hours. There was a similar up-regulation over a similar time course after partial hepatectomy, and Columbano et al subsequently demonstrated that two distinct pathways can up-regulate Gadd45beta/MyD118 – one activated during partial hepatectomy dependent on NFkB, and another enlisted by TCPOBOP via the CAR receptor (Columbano *et al.* 2005). In the 3 hour array it was found that T_3 also appears to recruit this gene with +2.74 fold up-regulation. The full role of Gadd45beta remains to be defined, but it has an anti-apoptotic role (De Smaele *et al.* 2001), and Columbano has suggested its expression at the onset of the cell cycle in different models of hepatocyte proliferation may indicate a role in the protection of hepatocytes from apoptosis.

5.5.3 Kruppel Factor Response

The Kruppel Factor transcription factors were notably up-regulated on the 3 hour array and therefore these are further investigated as plausible mediators of the T_3 mitogenic signal in Chapter Six.

Chapter 6 Kruppel Factors

6.1 Background

In an effort to demonstrate a mitogenic effect of T_3, early markers of its action have been pursued in this research thesis. In Chapter Four it was found that the rise in cyclin D1 occurred too late for it to be useful in measuring early T_3 effects in the organ perfusion system described in Chapter Three. Furthermore another plausible candidate, Bcl-3, was found not to be a critical mediator of the mitogenic T_3 signal in a murine knockout model.

The previous chapter therefore outlined novel work using microarray technology to identify which genes are up or down regulated after T_3 administration in euthyroid rat liver. The hepatic expression profile after T_3 over time of plausible candidates is further pursued in this chapter.

The greatest change in expression on the 3 hour array was the up-regulation of a Kruppel factor, Zinc finger protein 354A (FC + 7.64). Indeed there was a cluster of changes amongst the Kruppel transcription factors, and this chapter therefore investigates these more closely. Using Real Time-PCR analysis, the expression of a panel of these evolutionarily conserved transcription factors is described, reflecting their known involvement in proliferation and differentiation and thus their biologically plausible candidature as mediators of the T_3 mitogenic effect.

To elucidate further changes in gene expression associated with the proliferative effect of T_3 the second expression microarray, comparing mitogenic and sub-mitogenic T_3 doses was performed at 1 hour post dose time point and as anticipated the largest cluster of function-associated genes demonstrating significant change after mitogenic T_3 was amongst cell cycle genes. The only Kruppel factor for which differential expression was detected at 1 hour after T_3 was Sp4.

6.1.1 Kruppel Factors

Zinc Finger proteins exhibit very diverse functions, including RNA packaging, transcriptional activation, apoptosis regulation, protein folding, lipid binding and DNA recognition (Laity *et al.* 2001). Classically the zinc finger comprises of 2 cysteine and 2 histidine residues organised around a zinc atom. It was first recognised 15 years ago and since then many more such proteins have been defined. The name Kruppel is derived

from the fact that they exhibit homology to the *Drosophila melanogaster* segmentation gene product, Kruppel (Ghaleb *et al.* 2005). Many of the Kruppel factors exhibit tissue-selective expression and a range of regulatory functions. They typically regulate expression of genes which have GC rich promoters. At least 21 members of the Kruppel family of proteins are encoded in the human genome which encompasses over 700 genes that contain C_2H_2- type zinc fingers, equating to approximately 1% of the human genome.

The Kruppel family's 21 members show ~65% homology between members, of which at least 11 homologs have been identified in the rat (Kaczynski *et al.* 2003). Their defining feature is a highly conserved DNA-binding domain (with more than 65% sequence identity among family members) at the carboxyl terminus. The amino acid sequences in the zinc finger domains of the Kruppel Factors are closely related to one another but the regions outside the zinc fingers are usually unique (Figure 43).

The Kruppel Factors investigated here are ZFP354A, KF 15, KF 9, KF 4 and Sp4.

The greatest change in expression at 3 hours (FC + 7.64) on the first microarray was the up-regulation of the Zinc finger protein 354A. ZFP354A (also known as Kid-1, transcription factor 17) gene product plays a role in the establishment of a differentiated phenotype and proliferative control in rat proximal kidney tubule, and can be induced by membrane depolarization (Witzgall *et al.* 1998). It was the first KRAB-zinc finger protein for which a transcriptional repressor activity was demonstrated and contains 13 C_2H_2 zinc fingers in groups of 4 and 9 separated by a 32 amino acid spacer. Its mRNA accumulates with age and is detected predominantly in the kidney. ZFP354A mRNA levels decline after renal injury secondary to ischaemia, an insult which results in epithelial cell dedifferentiation, followed by regenerative hyperplasia and differentiation. In the Witzgall study it was noted to be predominantly expressed in kidney with very little rodent hepatic expression on Northern blot analysis.

KF15 (Fold change + 1.66 on 3h array) was first identified as a protein that binds to the promoter of the gene for CLC-K1, a kidney specific chloride channel (Uchida *et al.* 2000). Later it was shown to regulate the genes for the glucose transporter GLUT4 in adipocytes (Gray *et al.* 2002) and for acetyl-CoA synthase in muscle cells (Yamamoto *et al.* 2004). Among the organs KF15 is expressed at the highest level in the liver where in mice it has been shown that KF15 expression is up-regulated in the fasted state and down-regulated by feeding (Teshigawara *et al.* 2005). The same study showed that forced expression of KF15 in cultured hepatocytes increased the expression of phosphoenolpyruvate carboxykinase (PEPCK).

KF9 (Fold change + 1.36 on 3 h array) is otherwise known as Basic Transcription Element-binding protein (BTEB). It is noted to be a T_3 regulated gene in developing rat brain (Denver *et al.* 1999) where T_3 rapidly up-regulates BTEB mRNA in neuro-2a cells engineered to express TRβ1 but not in cells expressing TRα1. In neuronal cells at least over expression of KF9 increases the number and length of neurites but has no effect on the rate of cell proliferation.

The only Kruppel factor for which differential expression was detected 1 hour after T_3 (Fold change + 4.15) was Sp4 (trans-acting transcription factor 4 or Specificity Protein 4), a member of the Sp-1 family, highly expressed in developing brain in the mouse, in which its absence is associated with early post-natal mortality (Lerner *et al.* 2005; Kolell and Crawford 2002). The range of its functions remains to be defined, but in general it appears to be an activator, and it presents one potential candidate for mediating T_3's mitogenic effects (Supp *et al.* 1996). Sp-4 shows a complex expression pattern but it is most abundant in neuronal tissue. In mice with targeted disruption of the Sp4 gene there are severe consequences for post natal development. $Sp4^{null}$ mice develop until birth without severe consequences but after birth two thirds die within 4 weeks (Gollner *et al.* 2001). Male $Sp4^{null}$ mice do not breed and have a reduced testis size.

KF4 is discussed in more detail in the conclusions to this chapter. There was no change in its expression level on either of the array experiments but given its known role in cell proliferation it was thought prudent to investigate its expression over time after T_3.

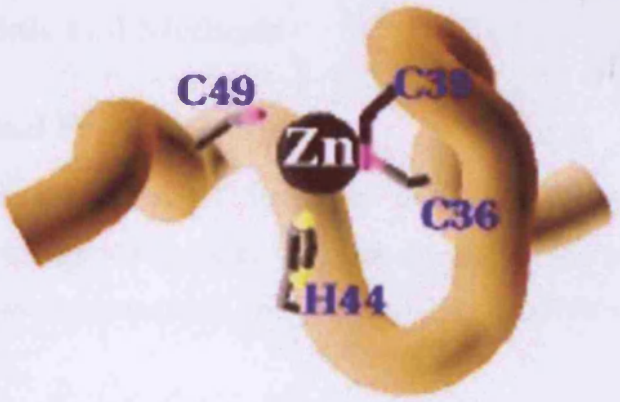

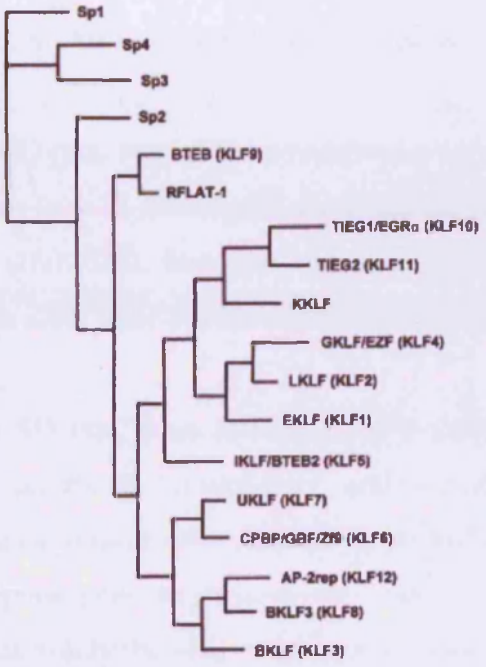

Figure 43 The zinc finger motif common to the Kruppel Factors- 2 cysteine and 2 histidine residues organised around a zinc atom, and an unrooted phylogram of the human Kruppel Factors. Branch changes are proportional to amino acid changes.

6.2 Aims

i) To measure the expression of novel candidates (Kruppel Factor transcription factors) as potential mediators of the mitogenic effects of T_3 over time in mitogenic versus sub-mitogenic T_3 treated rat liver using quantitative Real Time PCR.

ii) To determine whether or not observed changes in gene expression are due to the time of day of animal sacrifice.

6.3 Materials and Methods

6.3.1 Animal Procedures

Male Sprague-Dawley rats (250g) were housed in a temperature- and light-controlled room (12-hour light/dark cycle) with free access to food and water. Animal care and all procedures were compatible with the Animal (Scientific Procedures) Act 1986, UK Home Office.

Animals were sacrificed at the appropriate time points by a schedule one procedure. Liver was harvested and sectioned for histology and pieces were snap frozen in liquid nitrogen and stored at -80°C for later analysis and RNA isolation.

Protocol 1: Male SD rats, were administered a subcutaneous dose of either mitogenic T_3 (5μg per animal) or (n = 3) sub-mitogenic T_3 (0.1μg per animal) and sacrificed at 0, 20, 40, 60, 90, 120, 150, 180, and 480 minutes post dose to provide RNA for serial assessment of individual gene expression (n=3 per time point).

Protocol 2: Male SD rats, were administered a subcutaneous dose of vehicle only at 0900 (n=4) and sacrificed immediately and a second group were administered a subcutaneous dose of vehicle only at 0900 (n=4) and sacrificed 60 minutes later to look for changes in hepatic gene expression that may be due to the time of day of animal sacrifice rather than solely the effects of T_3 on the hepatic transcriptome.

6.3.2 RNA preparation

Please refer to *General Methods* Chapter 2.

Frozen liver samples (-80°C) were homogenised with a Rotastar homogeniser in buffer containing guanidine thiocyanate and β-Mercaptoethanol and the total RNA was isolated using RNA MidiKit reagents (Qiagen, UK) following manufacturer's guidelines.

6.3.2.1 RNA Integrity and Quantitation

Please refer to *General Methods* Chapter 2.

A 260:280 nm absorbance ratio above 1.8 was obtained for all samples. RNA quality was assessed by denaturing formaldehyde gel electrophoresis. The 28S:18S ratio was 2:1 for all samples.

6.3.2.2 Preparing for Quantitative Real Time PCR/Preparation of standards

Please refer to *General Methods* Chapter 2.

6.3.2.3 cDNA synthesis

Please refer to *General Methods* in Chapter 2.

cDNA was prepared from 0.5μg total RNA using a QuantiTect Reverse Transcription reaction mixture following manufacturer's guidelines (Qiagen, UK).

6.3.2.4 Primer Design

Please refer to *General Methods* Chapter 2.

Primers were designed for KF15, ZFP354A, KF9, KF4, Sp4 and 18S (sequences in Table 10). The primer design rules outlined in Chapter Two were adhered to.

6.3.2.5 Conventional PCR to check primers

Please refer to *General Methods* Chapter 2.

6.3.2.6 DNA gel Electrophoresis

Please refer to *General Methods* Chapter 2.

Conventional PCR was undertaken to check the primers and then to produce sufficient target amplicon for use in making necessary standards for the subsequent real time PCR reactions. Representative gels are shown in Figure 44 and Figure 45.

Table 10 Primer sequences used for the Real Time PCR and the size of the amplicon for each sequence

KF15	F 5'- CCAATGCCAAACCTAT -3' R 5'- CTACATGTGGTTCTCGTCGGTGGAG -3' Amplicon length 161 base pairs
ZFP354A	F 5'- GAGCTCCTCACGTATAGCAC -3' R 5'- GGTTGGTAAGGGATGACCTA -3' Amplicon length 103 base pairs
KF4	F 5'- TGATGGTGCTTGGTGAGT -3' R 5'- TTGCACATCTGAAACCACAG -3' Amplicon length 201 base pairs
KF9	F 5'- ATACAGGTGAACGGCCCTT -3' R 5'- TCCGAGCGCGAGAACTTTT -3' Amplicon length 63 base pairs
Sp4	F 5'- ATGAGCGATCAGAAGAAGGAGG -3' R 5'- GAGTCCCTATTTTGCTGCAAGT -3' Amplicon length 175 base pairs
18S	F 5'- CTTAGAGGGACAAGTGGCG -3' R 5'- GGACATCTAAGGGCATCACA -3' Amplicon length 69 base pairs

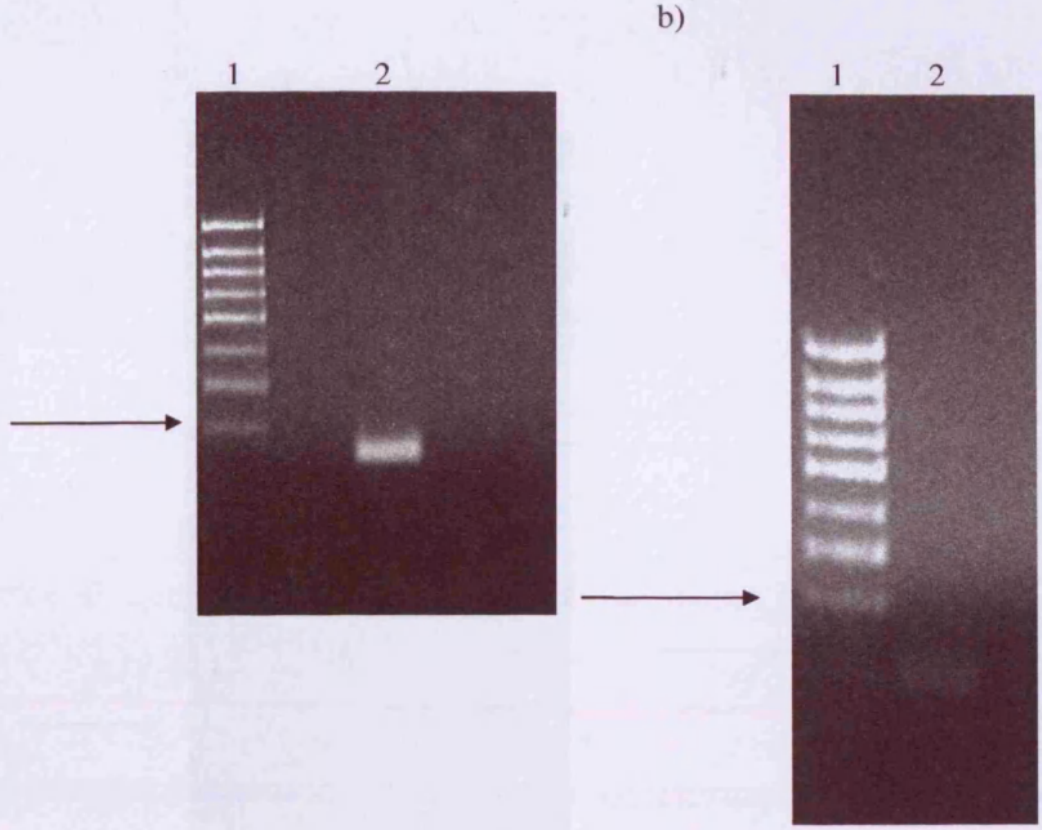

Figure 44 2% agarose gel electrophoresis of the PCR products. (a) Kruppel factor 15 (201 base pair amplicon) and (b) ZFP354A (103 base pair amplicon) on agarose gels after conventional PCR. Lane 1 in each gel contains 7µl of Hperladder IV and Lane 2 contains either Kruppel Factor 15 or ZFP354A DNA. The arrows indicate the position of the 200 base pair marker in Lane 1.

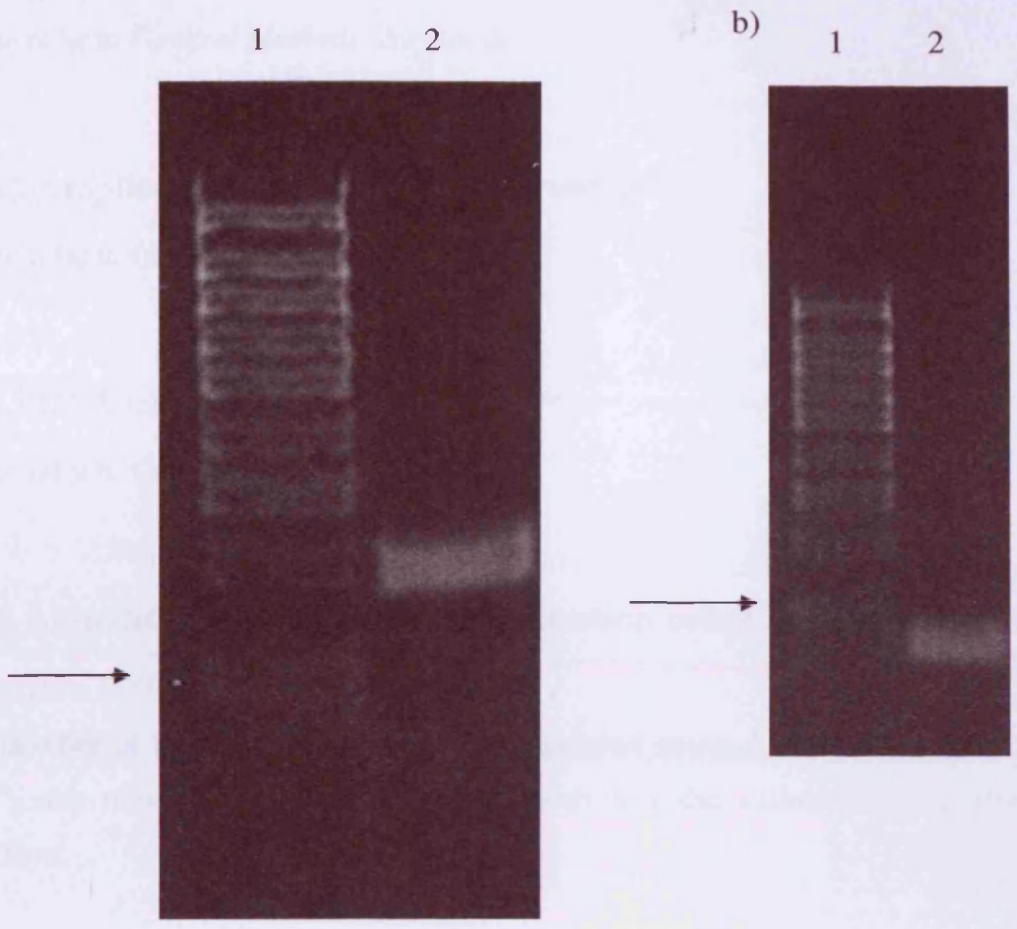

Figure 45 2% agarose gel electrophoresis of the PCR products. (a) Kruppel factor 4 (161 base pair amplicon) and (b) 18S (69 base pair amplicon) on agarose gels after conventional PCR. Lane 1 in each gel contains 7µl of Hperladder IV and Lane 2 contains either Kruppel Factor 4 or 18S DNA. The arrows indicate the position of the 100 base pair marker in Lane 1.

6.3.3 Preparation of standards

Please refer to *General Methods* Chapter 2.

Method

5µl of cDNA from a sample was used to make specific product so as standards could be made for the real time PCR analysis for both all Kruppel Factors and 18S.

6.3.3.1 Amplicon Excision from DNA Agarose Gel

Please refer to *General Methods* Chapter 2.

6.3.3.2 Amplicon extraction from agarose gel

Please refer to *General Methods* Chapter 2.

6.3.3.3 DNA estimation

Please refer to *General Methods* Chapter 2.

6.3.4 Amount of specific product estimation using Avogadro's number

Please refer to *General Methods* Chapter 2.

The number of amplicon molecules was calculated using Avogadro's number (6.022 $x10^{23}$), the molecular weight of the amplicon and the estimated concentration of amplicon.

6.3.5 Real Time PCR

Please refer to *General Methods* Chapter 2.

Real Time PCR was performed on a Rotor-Gene 3000 Real Time PCR machine in 0.1mL strip tubes. A QuantiTect SYBR Green Master Mix (Qiagen) was used (See *Chapter 2*).

The PCR reaction utilised an initial activation step for 15m at 95°C, then 45 cycles of 95°C for 30s, 60°C for 30s, 72°C for 30s, finally 72°C for 10 minutes.

Relative quantitation was used to determine amount of target with external standards (Bustin 2005) after initial generation of suitable standard curves for each Kruppel Factor. The copy number was normalised to 18S RNA. Accuracy of the assay is demonstrated by showing reproducibility across more than one real time run; and this is what was done (two separate real time runs were performed) (*See General Methods Chapter Two).*

6.4 Results

For ZFP354A, KF 15, and KF 9 there were marked transient rises in gene expression, peaking 60 minutes after T_3 administration, but no differences between animals receiving mitogenic or sub-mitogenic doses. These Kruppel Factors are therefore clearly T_3 responsive (Figure 46-48).

a)

b)

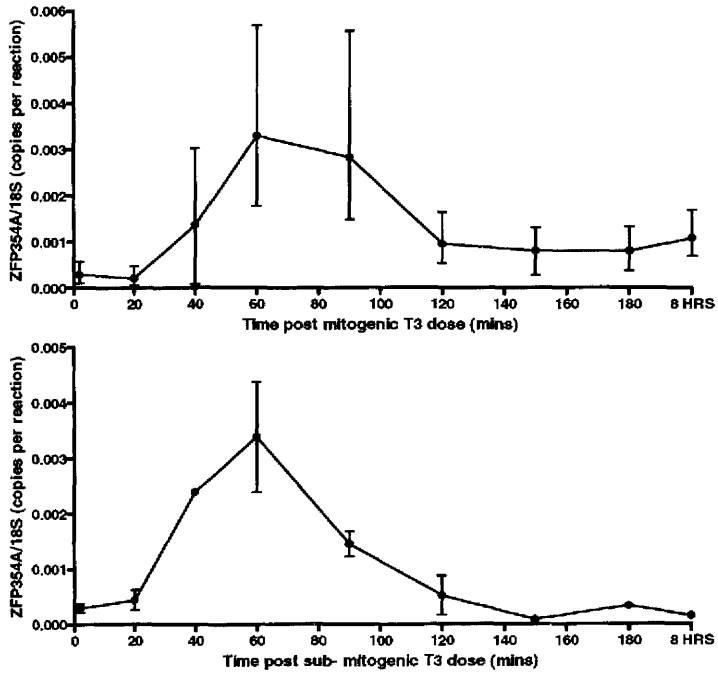

Figure 46 The hepatic ZFP354A response to T_3 over time comparing (a) mitogenic with (b) sub-mitogenic doses of T_3. The expression analysis used real time PCR with copy number per reaction normalised to 18S copy number. Each time point represents n=3 mean and range.

a)

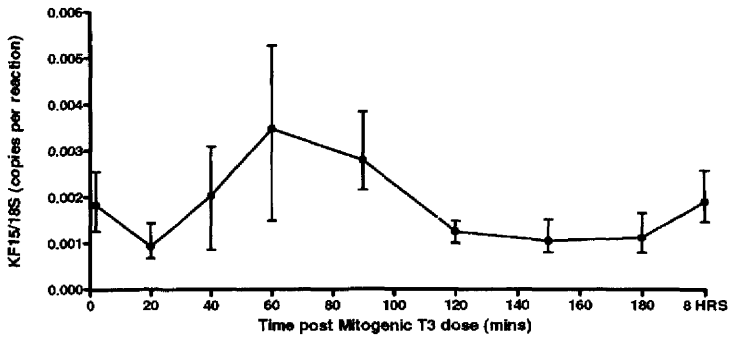

b)

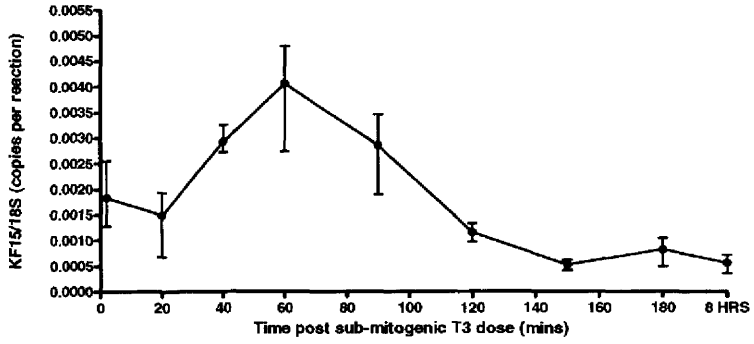

Figure 47 The hepatic KF15 response to T_3 over time comparing (a) mitogenic with (b) sub-mitogenic doses of T_3. The expression analysis used real time PCR with copy number per reaction normalised to 18S copy number. Each time point represents n=3 mean and range.

a)

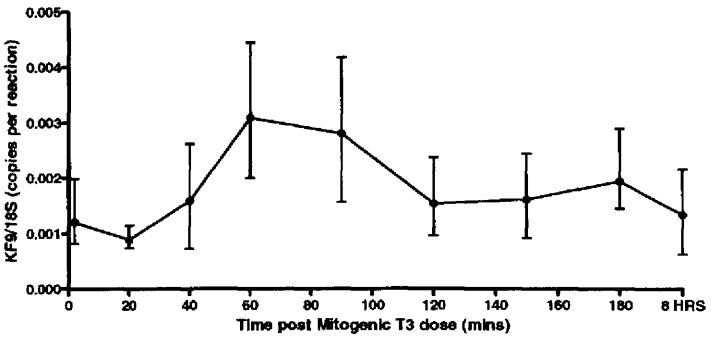

b)

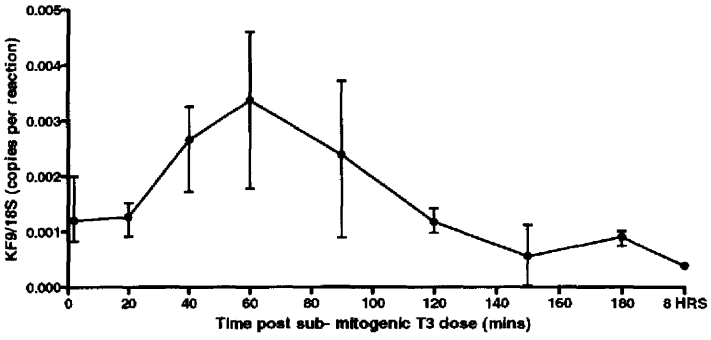

Figure 48 The hepatic KF9 response to T_3 over time comparing (a) mitogenic with (b) sub-mitogenic doses of T_3. The expression analysis used real time PCR with copy number per reaction normalised to 18S copy number. Each time point represents n=3 mean and range.

Interestingly, there was a divergence of expression of KF4 between mitogenic and sub-mitogenic dose of T_3 with a fall in expression at 20 minutes after a mitogenic dose, not observed in the sub-mitogenic liver (Figure 49).

a)

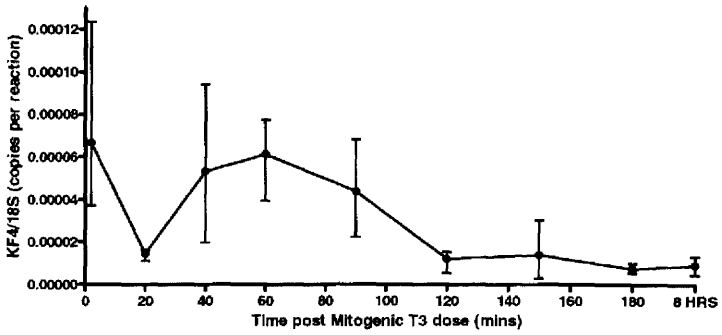

b)

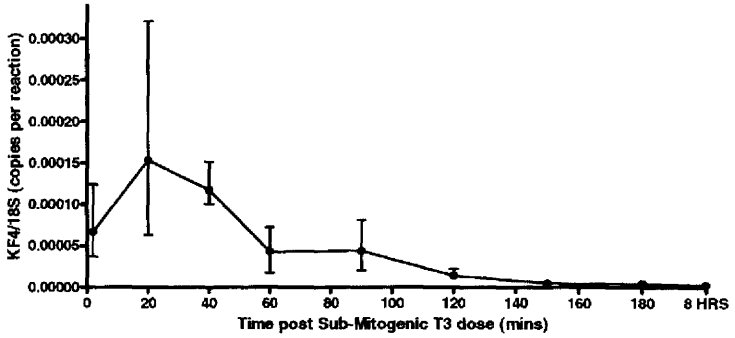

Figure 49 The hepatic KF4 response to T_3 over time comparing (a) mitogenic with (b) sub-mitogenic doses of T_3. The expression analysis used real time PCR with copy number per reaction normalised to 18S copy number. Each time point represents n=3 mean and range.

For Sp4 (Figure 50) expression there was no evident trend that emerged over time, although there was greater expression at 60 minutes after mitogenic T_3 and this confirms the up-regulation noted on the 1 hour array where a fold change of + 4.15 was found.

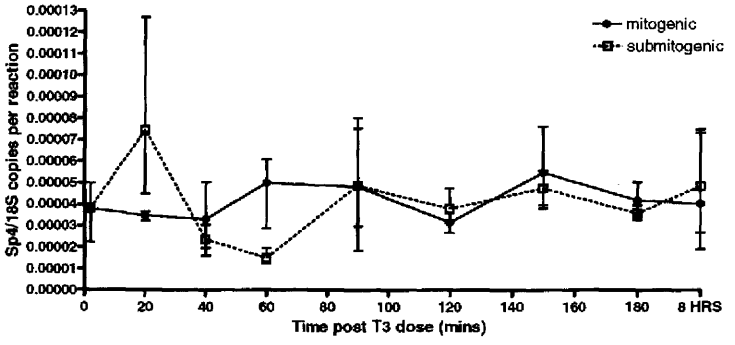

Figure 50 The hepatic Sp4 response to T_3 over time comparing mitogenic with sub-mitogenic doses of T_3. The expression analysis used real time PCR with copy number per reaction normalised to 18S copy number. Each time point represents n=3 mean and range.

6.4.1 Changes in gene expression are not due to time of day of animal sacrifice

Figure 51 shows that between the time points of 0900 and 1000 there was no change in the hepatic expression of the Kruppel Factors KF 15 and ZFP354A. For the Kruppel Factors 4 and 9 the same result was obtained. The increase in expression of the Kruppel factors at 60 minutes post dose seen previously is not therefore due to a change in the hepatic transcriptome according to the time of day of animal sacrifice.

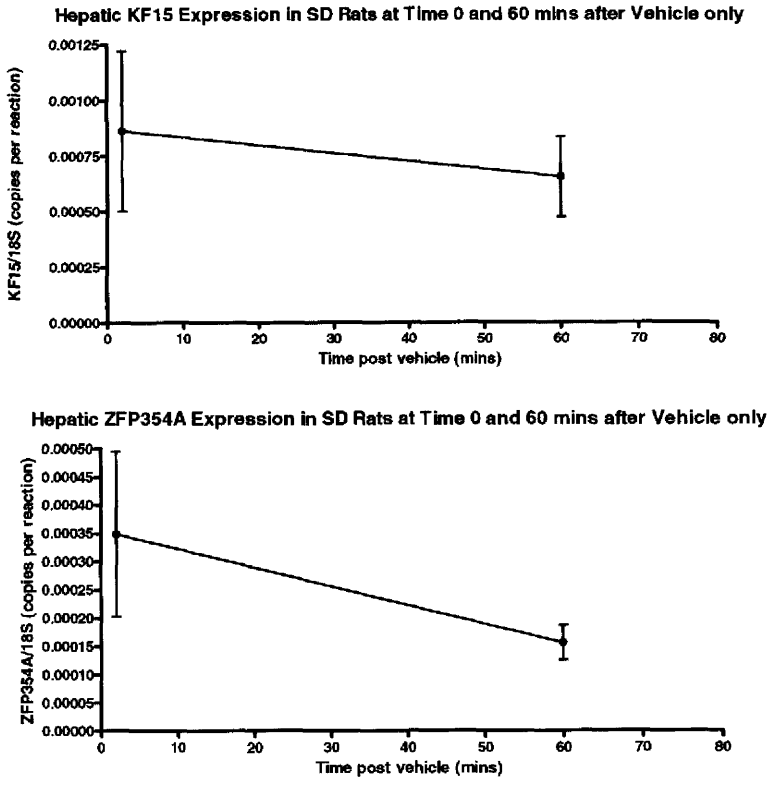

Figure 51 Real Time PCR analysis of the Kruppel Factor response (copy number per reaction normalised to 18S copy number) for KF 15 and ZFP354A after vehicle only at 0900 (time of animal sacrifice) and sixty minutes later at 1000 (time of animal sacrifice).

6.5 Discussion

The analysis performed here is based on gene expression profiles at the mRNA level of the Kruppel Factors ZFP354A, KF 15 and KF 9. These were shown to be T_3 responsive but no differences were found between mitogenic and sub-mitogenic treated liver and consequently they do not appear to critically mediate the mitogenic T_3 response. However this study did not examine effects T_3 may have at the protein level on pre-formed transcription factors. Another possible pathway of T_3 action might be through rapid 'non-genomic' activation of pools of transcription factors which can then go about activating downstream pro-proliferative signalling pathways leading to DNA synthesis and cell division. A proteomics based approach in the future may identify those involved and is a future aim of this project.

Proteomics encompasses diverse techniques that allow different aspects of protein structure and function to be analysed. Among the proteomic techniques mass spectrometry has emerged as the main method for analysing the production and function of proteins in biological systems (Cravatt *et al.* 2007). Recent published work has described the use of a proteomics based approach in the analysis of the hepatic regenerative response in the rat (Sun *et al.* 2007). Twenty four proteins were noted to be differentially expressed one hour after partial hepatectomy and these were functionally grouped to together. These evolving and powerful protemic techniques should be used to examine the hepatic response to mitogens including T_3.

6.5.1 KF 4

While the majority of the Kruppel factors showed no difference in response to mitogenic and sub-mitogenic doses of T_3, there was however a transient fall in Kruppel Factor 4 expression seen at 20 minutes only after a mitogenic dose of T_3. KF4 also known as Gut enriched Kruppel Factor, plays a role as a tumour suppressor gene, exerting an inhibitory effect on cyclins and their cyclin dependent kinase partners, and blocks G1/S phase progression (Shields *et al.* 1996; Rowland *et al.* 2005). In gut epithelium, its down-regulation is associated with cell hyper-proliferation (Ghaleb *et al.* 2005). Among the KF4 regulated cell cycle genes many up-regulated genes are inhibitors of proliferation whereas genes that promote proliferation are repressed. KF4 levels rise following DNA damage, cell-cycle arrest in response to serum withdrawal and contact inhibition (Chen *et al.* 2001). These observations established KF4 as a stress and differentiation associated inhibitor of proliferation and confirm its tumour

suppressor function. Indeed its expression is lost in various human cancers and recently it has been shown to undergo promoter methylation and loss of heterozygosity in gastrointestinal cancer (Wei *et al.* 2005). KF4 mRNA and protein is over expressed in 70% of mammary carcinomas.

In a human colonic adenocarcinoma cell line (HT-29), KF4 over-expression significantly inhibited cyclin D1 mRNA levels as well as cyclin D1 promoter activity. As discussed previously the activation of cyclin D1 early in the hepatic mitogenic response to T_3 has been described. In transient transfection experiments KF4 was found to decrease cyclin D1 promoter activity by 55% (Shie *et al.* 2000). Sequential deletion and site-directed mutation analysis of the cyclin D1 promoter have identified the sequence in a region containing an Sp1 response element, to be essential for KF4 function. The inhibitory effect of KF4 on cyclin D1 promoter activity was completely abolished by an excessive amount of Sp1 DNA and KF4 significantly reduced the stimulatory function of Sp1 suggesting that KF4 and Sp1 may compete for the same binding site on the cyclin D1 promoter. These results indicate that KF4 is a transcriptional repressor of the cyclin D1 gene and that the inhibitory effect of KF4 is, in part, mediated by an interaction with the Sp1 binding domain on its promoter.

Thus it is plausible to hypothesise that T_3 might exert its effect on inducing proliferation, at least in part by suppression of KF4 transcription. A number of companies produce commercially available antibodies to KF4 and it would therefore be interesting to investigate T_3 stimulated liver samples to look for changes in KF4 expression at the protein level using either an enzyme linked immunosorbant assay (ELISA) or Western blot approach.

6.5.2 Sp-4

Sp-4 showed differential expression 60 minutes after a mitogenic compared to a sub-mitogenic dose of T_3. Recent work using RNA interference has revealed that Sp-4 is expressed in pancreatic cancer cells and plays an important role in regulating expression of VEGF (vascular endothelial derived growth factor) in these cells (Abdelrahim *et al.* 2004). The allied molecule Sp-3 was shown to be a key regulator of G1 to S phase cell cycle progression in these cells and there clearly remain as yet unidentified roles for Sp-4 and its involvement in control of proliferation. The commercial availability of antibodies to Sp-4 means it may be further analysed in the setting of T_3 induced hepatocyte proliferation.

In conclusion, this chapter describes the response to T_3 amongst important transcription factors- the Kruppel Factors, however no one transcription factor has conclusively emerged as a likely critical early mediator of the mitogenic T_3 response. In the next chapter therefore analysis turns to investigating early events by examining the signalling pathway upstream of cyclin D1 activation, in an effort to find a new critical early mediator of the hepatic mitogenic T_3 response.

Chapter 7 mTOR Mediates the Mitogenic T_3 Response

7.1 Background

7.1.1 Signalling upstream of cyclin D1

In an effort to understand what may precede cyclin D1 activation after T_3 stimulation, it is important to explore the web of signalling interactions that are involved (Davis *et al.* 2000). This approach could lead to identifying earlier mediators of the hepatic proliferative response to T_3.

An important pathway that merits interrorgation in this context involves 'mTOR' or the mammalian target of rapamycin. In this chapter the hypothesis 'mTOR mediates the hepatic mitogenic T_3 response' is investigated on the basis that the target of rapamycin (TOR) plays a pivotal role in integrating signals from mitogens and nutrients that regulate cell growth (Nelsen *et al.* 2003a). The importance of mTOR in mediating proliferation signals is supported by a number of published studies, one of which noted that in the liver mTOR mediates the hepatocyte proliferative response to amino acid infusion (Ijichi *et al.* 2003; Nelsen *et al.* 2003b). In another it was shown that mTOR can also provide an alternative pathway of liver regeneration following partial hepatectomy as revealed in animals in which the ability to respond to tyrosine growth factor receptors is deficient e.g. STAT3 deficient mice (Haga *et al.* 2005).

Rapamycin is already known to inhibit liver regeneration *in vivo* in rats in a dose dependent manner up to 1.0 mg/kg where one sees elimination of the normal regenerative response (Francavilla *et al.* 1991) and it can also inhibit hepatocyte proliferation under cell culture conditions (Francavilla *et al.* 1992).

Furthermore, several studies conducted in mammalian cells have shown that rapamycin inhibits the expression of cyclin D1, important in cell cycle progression and proliferation as described in Chapter 4 (Hidalgo and Rowinsky 2000). In cultured rat hepatocytes rapamycin prevents the up-regulation of cyclin D1 and it inhibits regeneration in the mouse after partial hepatectomy but this can be overcome by transfection with cyclin D1 (Nelsen *et al.* 2003a). To assess whether there was an *in vivo* as opposed to just an *in vitro* effect, rapamycin-treated mice were transfected with

cyclin D1 using an adenoviral system and the result was an increase of DNA synthesis measured by BrdU incorporation of 14% compared to 0% in control-transfected mice.

7.1.2 mTOR pathways

Rapamycin is a macrolide produced by the bacterium *Streptomyces hygroscopicus* and derives its name from the island of *Rapa Nui* from where it was discovered in a soil sample in 1970. Its initial use was as an anti-fungal agent but its potent immunosuppressant properties were quickly realised and as a result it went relatively unexploited for a number of years until the early 1990s when its target was identified. The mTOR gene was described in 1994 and it was as late as 1997 that the drug was approved by the Federal Drug Administration as an anti-rejection agent in renal transplantation. Now there has been an explosion of interest in rapamycin and its newer analogues and many are now in clinical trials for uses as varied as combating cancer and treating coronary artery disease.

The mammalian target of rapamycin is a well conserved 289 kDa serine-threonine kinase (Figure 52) that regulates cell-cycle progression and is specifically inhibited by rapamycin (Wullschleger *et al.* 2006). Every eukaryote genome examined contains a TOR gene. mTOR regulates cell growth by integrating four major inputs: growth factors, nutrients (especially amino acids), and energy and stress, (for example hypoxia) (Rohde *et al.* 2001; Martin and Hall 2005). Commercial antibodies are able to detect total mTOR and also the active form of the kinase, phosphorylated mTOR. Phosphorylation at serine residue 2448 leads to mTOR activation (Kenessey and Ojamaa 2006).

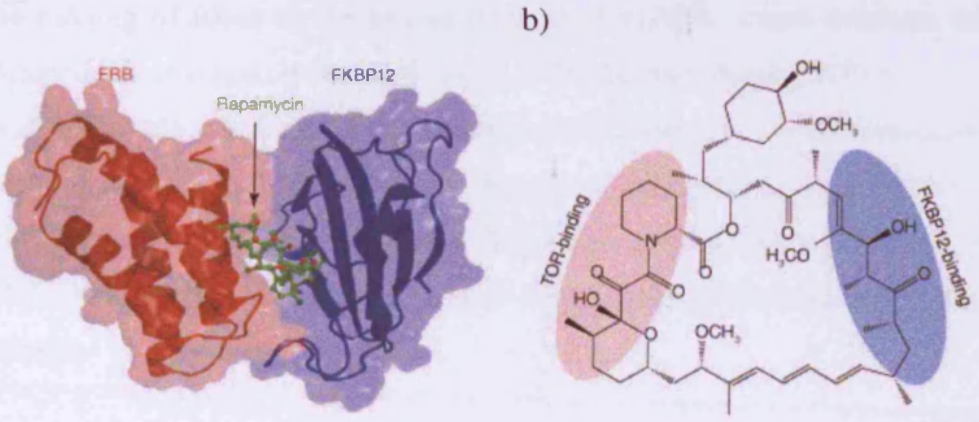

Figure 52 (a) The structure of the ternary complex of FKB12- rapamycin binding domain (FRB) (red), rapamycin (green) and FKBP12 (blue) (Choi et al. 1996). (b) Chemical structure of rapamycin and its binding sites for FKBP12 (blue region) and mTOR (red region).

Rapamycin includes two separate moieties, the TOR-binding and the FKBP12-binding regions. To be active biologically, rapamycin must form a ternary complex with mTOR and FKBP12, which is a cytosolic binding protein collectively called immunophilin. Therefore, rapamycin acts to induce the dimerization of mTOR and FKBP12. The formation of a rapamycin–FKBP12 complex results in a gain-of-function because the complex binds directly to mTOR and inhibits the function of mTOR and the mTOR-mediated signalling network (Tsang *et al.* 2007).

7.1.2.1 mTOR Activation- Upstream Events

Among the signal inputs, growth factor- and hormone (e.g. insulin)-induced mTOR activation is the best characterized, and is mediated by the activation of phosphatidylinositol-3-kinase, PI3K. Active PI3K localizes to the cell membrane and catalyzes the conversion of phosphatidylinositol (4,5)-biphosphate [PtdIns(4,5)P_2] into phosphatidylinositol (3,4,5)-triphosphate [PtdIns(3,4,5)P_3]. Subsequently PtdIns(3,4,5)P_3 recruits and activates AKT, which, in turn, phosphorylates and inactivates the tuberous sclerosis protein complex (TSC), which is a heterodimer composed of TSC1 and TSC2. TSC2 acts as a GTPase-activating protein (GAP) for the small GTPase Rheb, and the action of TSC is thought to be mediated by Rheb, possibly

by the binding of Rheb to the kinase domain of mTOR, which activates mTOR in a GTP-dependent manner (Inoki *et al.* 2002; Nobukini and Thomas 2004).

Several studies also show that GTP-loading of Rheb induces a conformational change in mTOR that results in activation of mTOR and phosphorylation of downstream effector proteins. Other studies have shown that AKT phosphorylates mTOR directly at Ser2448, but the functional significance of phosphorylation of this remains to be established.

7.1.2.2 mTOR Activation- Downstream Events

Growth and development require mTOR, and disruption of mTOR results in embryonic lethality and severe developmental defects (Gangloff *et al.* 2004). At the cellular level, mTOR is central to the regulation of both catabolic and anabolic processes. In response to optimal growth stimuli, mTOR promotes the synthetic capabilities of the cell by up-regulating key processes such as ribosome biogenesis and protein translation, which lead to an increase in cell mass and size, and, thus, accelerated proliferation. The best characterized downstream effectors of mTOR are the ribosomal protein S6 kinases (S6K) and 4E-BP1 (also called PHAS-I). S6K1 is phosphorylated directly by mTOR during stimulation with either nutrients or growth factors, which results in a selective increase in the translation of mRNA transcripts that contain a 5′ tract of oligopyrimidine (5′-TOP) motif. The 5′-TOP mRNAs encode components of the translation apparatus such as elongation factors and ribosomal proteins. Thus, mTOR-dependent activation of S6K1 promotes an overall increase in protein synthesis. However, S6 phosphorylation and translation of 5′-TOP mRNAs are still responsive to mitogens in a rapamycin-dependent manner in a S6K1/S6K2 double-knockout mutant, which indicates that an alternative effector is also present. 4E-BP1 is an inhibitor of eukaryotic translation initiation factor 4E (eIF4E). After hyperphosphorylation by mTOR, 4E-BP1 dissociates from eIF4E, which allows eIF4E to associate with the 5′-CAP of mRNAs and initiate translation.

7.1.3 Elaboration of Hypothesis

The hypothesis underlying this chapter is that T_3 recruits the mTOR pathway and the potential means by which this may work is through a non-genomic effect. In addition there is evidence for mTOR involvement fom the gene array experiment of Chapter

Five where mTOR is up-regulated (FC + 1.34) at the mRNA level after administration of T_3.

The extra-nuclear or 'non-genomic' T_3 actions were discussed in detail in Chapter 1 but to re-capitulate, T_3 is well known to classically ligand with its nuclear receptor β isoform in the liver to effect gene transcription (Aranda and Pascual 2001; Yen 2001). However a number of T_3 actions occur too rapidly to be explained by this 'genomic' pathway and hence a set of 'non- genomic' actions have been increasingly described (Bassett *et al.* 2003; Davis *et al.* 2007). The site of these non-genomic actions may be the plasma membrane, cytosol or cellular organelles. They include the regulation of ion channels for example and involve the generation of intracellular secondary messengers and induction of signalling cascades such as cyclic AMP or the protein kinase cascades (Davis and Davis 2002).

There is some recent evidence that T_3 in human cells can activate the mTOR pathway (Cao *et al.* 2005). This group showed that in human fibroblasts T_3 activates mTOR by way of phosphatidylinositol 3-kinase which is activated first by the liganded TRβ1 receptor in a non-genomic mechanism of activation. The kinase then activates Akt/protein kinase B which phosphorylates the mTOR at S2448 bringing about its rapid activation and subsequent phosphorylation of $p70^{s6k}$ which is involved in translation initiation.

A diagram summarising the proposed T_3 - mTOR signalling pathway is shown in Figure 53.

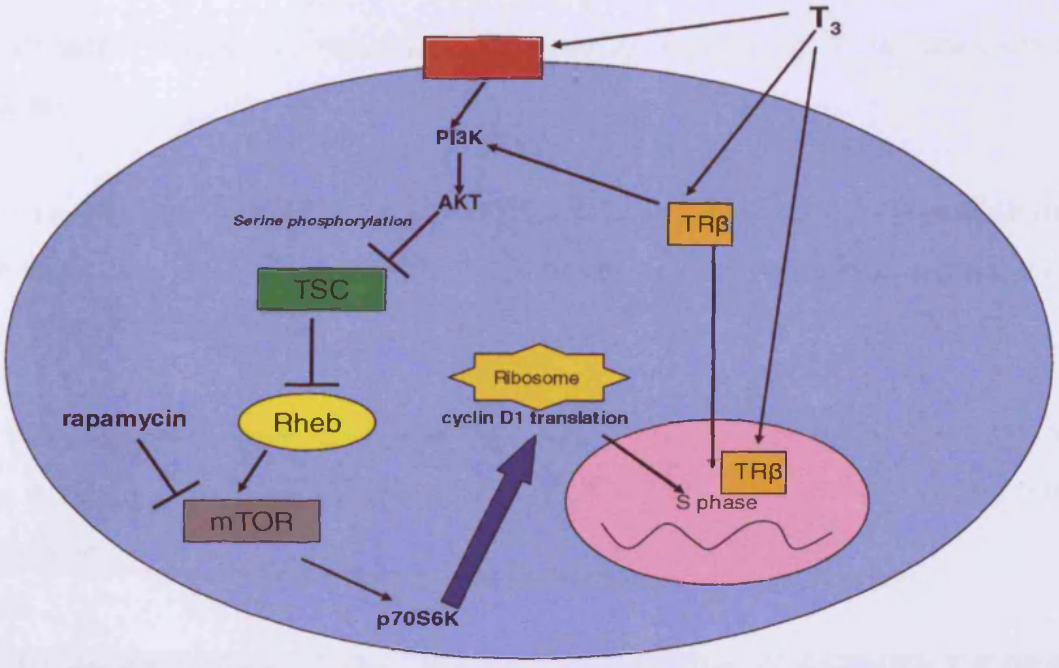

Figure 53 The signalling mTOR network and its relationship to T_3 and cell cycle progression. T_3 receptors are located either at the cell membrane or in the cell nucleus (classical genomic mechanism). By acting at the cell membrane (non classical mode of thyroid hormone action) a signal transduction cascade is activated that brings about AKT activation by PI3K and this then allows mTOR activation by inhibition of the TSC complex and subsequent Rheb activation. mTOR activation leads to translation of genes necessary for cell cycle progression. Most important amongst these is cyclin D1 which acts with CDK4 to phosphorylate Rb and allow release of E2F transcription factors which transactivate further genes necessary for S phase to progress.

7.2 Aims

a) To assess the *in vivo* hepatocyte proliferative response to T_3 in rapamycin treated rodents.

b) To examine the change in phosphorylated mTOR in mitogenic T_3 treated rat liver and sub-mitogenic T_3 treated rat liver over time using an immunohistochemical technique and Western blot analysis.

c) To examine T_3 treated rodent liver for phosphorylated AKT (upstream of mTOR) and the downstream effector phosphorylated p70S6kinase using an immunohistochemical technique.

d) To stimulate primary human hepatocytes with T_3 and monitor the phosphorylated mTOR response using Western blot analysis and to stain human liver sections for phosphorylated mTOR and study the pattern of staining.

e) To administer the PI3K inhibitor wortmannin to rats *in vivo* and assess the hepatocyte proliferative response to T_3 to determine whether the hepatic mTOR pathway is activated by T_3 through PI3K.

7.3 Materials and Methods

7.3.1 Animal Procedures and Protocols

Adult male Sprague Dawley rats (200-250g) were housed in a temperature- and light-controlled room (12-hour light/dark cycle) with free access to food and water. Animal care and all procedures were compatible with the Animal (Scientific Procedures) Act 1986, UK Home Office.

T_3 was obtained from Sigma (Poole, England) and dissolved in 1M NaOH at a concentration of 1mg/ml. It was administered to rats by subcutaneous injection at a dose of 5μg per whole animal in 1ml total volume diluent (960μl NaCl and 40μl 1M NaOH).

Protocol 1

Rats (n=4) were administered an i/p dose of rapamycin (proetinkinase.de GmbH) 1.5mg/kg solubilised in Dimethylsulfoxide (DMSO) and delivered in a volume of 500μl normal saline two hours before 5μg of T_3 was administered subcutaneously. Thirteen hours later a second dose of rapamycin 0.75mg/kg i/p was administered.

A second group of control rats (n=4) were administered an i/p dose of vehicle only at the same time points followed by 5μg T_3.

One hour prior to sacrifice all animals received an intra-peritoneal injection of BrdU (Sigma, Poole England) 50 mg/kg solubilised in normal saline at a concentration of 12.5mg/ml.

Animals were sacrificed 24 hours after the dose of T_3 was administered by a schedule one procedure and livers were immediately removed, sectioned and placed in formalin before processing ready for immunohistochemical analysis of the BrdU hepatocyte proliferative response.

Protocol 2

Rats were administered a subcutaneous dose of either mitogenic T_3 (5μg per animal) or sub-mitogenic T_3 (0.1μg per animal) and sacrificed at (n=3 per time point) 0, 20, 40, 60, 90, 120, 150 ,180 and 480 minutes post dose for immunohistochemical assessment of the hepatocyte phosphorylated mTOR response, phosphorylated AKT and phosphorylated p70S6kinase response. Liver samples were snap frozen in liquid nitrogen then stored at -80^{0}C for later protein isolation for Western blot analysis. The sub-mitogenic dose still brings about the metabolic consequences of T_3 administration

but crucially does not lead to proliferation of the hepatocytes (see *Results Chapter Three*).

Protocol 3

Adult male SD rats (n=7) were injected i/p with 100μg/kg wortmannin in 0.5mls normal saline (Cell Signalling Tech. # 9951 from stock 5mg/ml in methanol) and 30 minutes later injected with 5μg T_3 subcutaneously. Twenty three hours later BrdU was administered to flash label hepatocytes undergoing DNA synthesis and 1 hour later animals were sacrificed in the usual manner.

A second group of rats (n=5) were administered vehicle only i/p and then a 5μg mitogenic dose of T_3 prior to BrdU flash labelling twenty three hours later and one hour later sacrifice by a schedule one method.

Livers were removed, sectioned and placed into formalin for 24 hours, prior to routine histological processing.

The dose and timing of administration of wortmannin was based on that other workers have used to bring about successful PI3K inhibition *in vivo* in the rat (Pustylnyak *et al.* 2005). The approximate half life of the drug is 2 hours.

7.3.2 Immunohistochemistry

Please refer to *General Methods* Chapter 2.

Formalin fixed tissues were embedded in paraffin and 4μm thick sections were cut. Incorporation of BrdU into hepatocyte nuclei was detected using a mouse monoclonal antibody (Dako Ltd., Cambridge, UK) followed by a biotinylated rabbit anti-mouse IgG secondary antibody (Dako Ltd., Cambridge , UK).

Phosphorylated mTOR was localised using a rabbit monoclonal anti phospho-mTOR serine-2448 antibody (Cell Signalling Tech., MA) followed by a biotinylated goat anti-rabbit IgG secondary antibody (Dako, Cambridge UK). Visualisation was by the indirect peroxidase technique using 3,3'–diaminobenzidine (Sigma, Poole England) as a substrate.

Phosphorylated p70S6kinase and phosphorylated AKT were detected in rat liver using the appropriate antibodies (see *Chapter 2).*

7.3.3 Statistical Analyses

Hepatocytes positive for phosphorylated mTOR were counted over a low power x100 original magnification which equates to a tissue section area of 3.14mm^2. The mean of 4 such fields was taken and plotted as the mean ± range.

The statistical difference between the means was determined using a Student's t test; $p < 0.05$ was considered significant.

7.3.4 Primary Human Hepatocyte Culture

The harvested human hepatocytes (work done by other colleagues) were plated into 6 well plates at a density of 2 million cells per well (see *General Methods Chapter 2*).

Each experimental sample was designated 'BS' and then given a sequential number.

For each time point 2 6-well plates were prepared; one for vehicle only stimulated cells and one for T_3 stimulated cells. Cells were incubated in medium made with T_3 deplete FCS (See *General Methods Chapter Two*).

On the morning of day 1 cells were either treated with T_3 (final concentration 100 nM derived by adding 1.34µl T_3 stock at 1µg/µl to 20mls of medium) or vehicle only (from 1.34 µl 1M NaOH to 20mls medium) and harvested at time points 0, 15, 25, 40, 60, and 90 minutes post stimulation.

A volume of 2mls medium was used per well of a 6 well plate.

At the end of each time point plates were placed in a -80^{0}C freezer to terminate the experiment and shortly thereafter protein lysates were made using 500µl RIPA lysis buffer per 6 well plate. Cells were lysed with the help of a cell scraper (see *Chapter 2*).

The human livers examined were BS43, BS44, BS45 and BS47.

7.3.5 Western Blot analysis

Rat and human protein lysate samples were quantitated using the BCA method and stored aliquoted out in smaller volumes at -80^{0}C (see *Chapter Two General Methods*).

Lysates were run on SDS-PAGE gels prior to protein membrane transfer and subsequent probing with primary antibodies to phosphorylated mTOR and total mTOR.

50µg of protein was loaded per lane. The mean protein concentration of the rat liver lysates was 10 mg/ml and for the human hepatocyte lysates it was 11 mg/ml.

Following incubation with primary antibody to phosphorylated mTOR (p-mTOR) and then the appropriate secondary antibody, the membrane was stripped using Pierce Stripping Buffer to enable re-probing of the membrane with an antibody to total mTOR. Total mTOR acted as a loading control against which p-mTOR could be normalised.

7.4 Results

7.4.1 Rapamycin inhibits the peak proliferative response to T_3

Rapamycin significantly inhibits the proliferative hepatocyte response brought about by T_3 ($p < 0.04$) (Figure 54). A striking reduction by almost 50% is seen in the number of positive BrdU hepatocytes at 24 hours in the animals which received T_3 and rapamycin.

a)

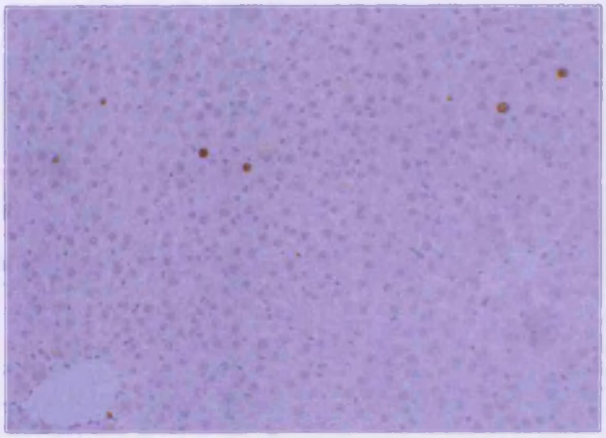

b)

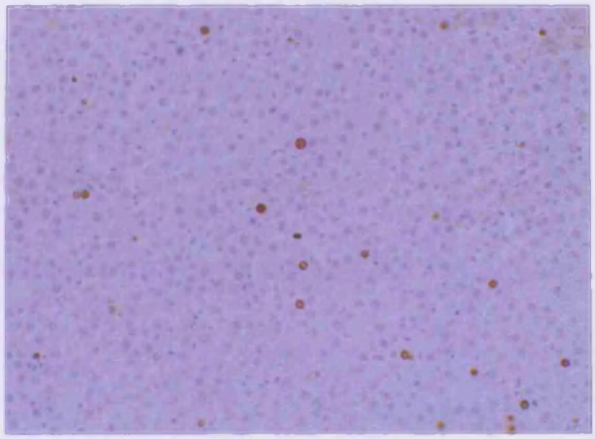

c)

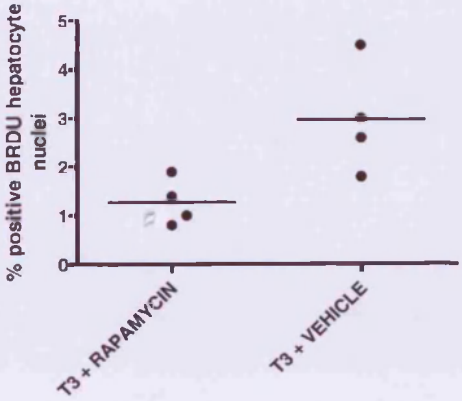

Figure 54 Photomicrographs comparing the maximum hepatocyte proliferative BrdU response at 24 hours after 5μg T_3 in adult male SD rats by immunohistochemistry after (a) rapamycin and (b) vehicle only, x10 objective. (c) BrdU proliferative response comparing rapamycin and T_3 treated animals with T_3 and vehicle only treated animals ($p < 0.04$). 2,000 hepatocyte nuclei were scored.

7.4.2 Positive control for phosphorylated mTOR

Sections of human colon cancer (donated by the Royal Free histopathology department) were used as positive controls for phosphorylated mTOR (Figure 55). The antibody used reacts with human and rat phosphorylated mTOR.

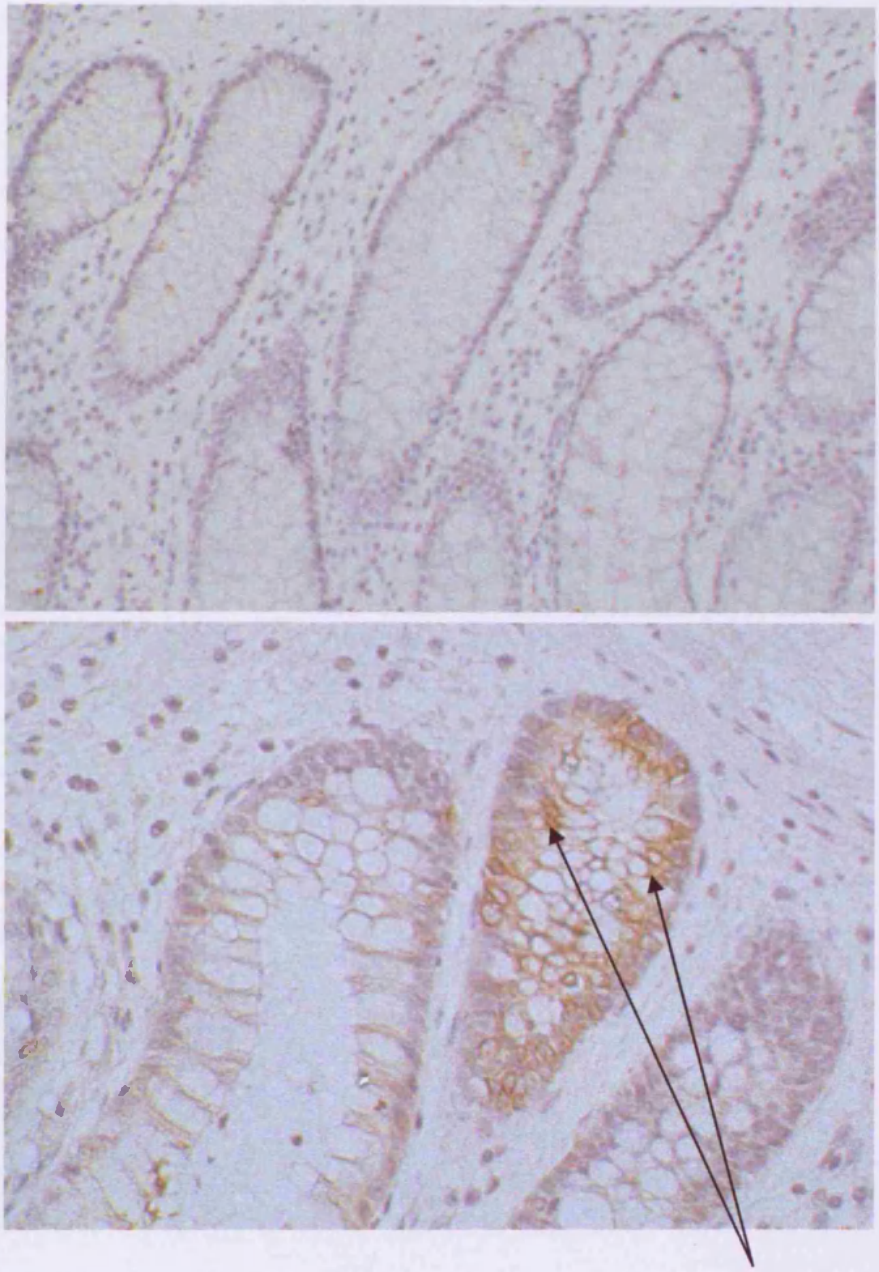

Figure 55 Sections of human colon carcinoma stained for phosphorylated mTOR to act as positive controls for the subsequent immunohistochemistry experiments. The top section is incubated with no primary antibody and stains negative for phosphorylated mTOR (negative control). The bottom section is a positive control and positive brown staining (see arrows) can be seen in some cells at the base of a colonic crypt, x40 objective.

7.4.2.1 Mitogenic but not sub-mitogenic T_3 induces a surge in mTOR phosphorylation

There is a clear surge in the number of hepatocytes staining positive for phosphorylated mTOR at 90 minutes after mitogenic T_3 but no such response is seen after the sub-mitogenic dose. There is a return to baseline by 3 hours post T_3 (Figure 56). The sub-mitogenic dose is still more than 2,500 times supra-physiological but does not result in the proliferation of hepatocytes (see *Results Chapter 3*).

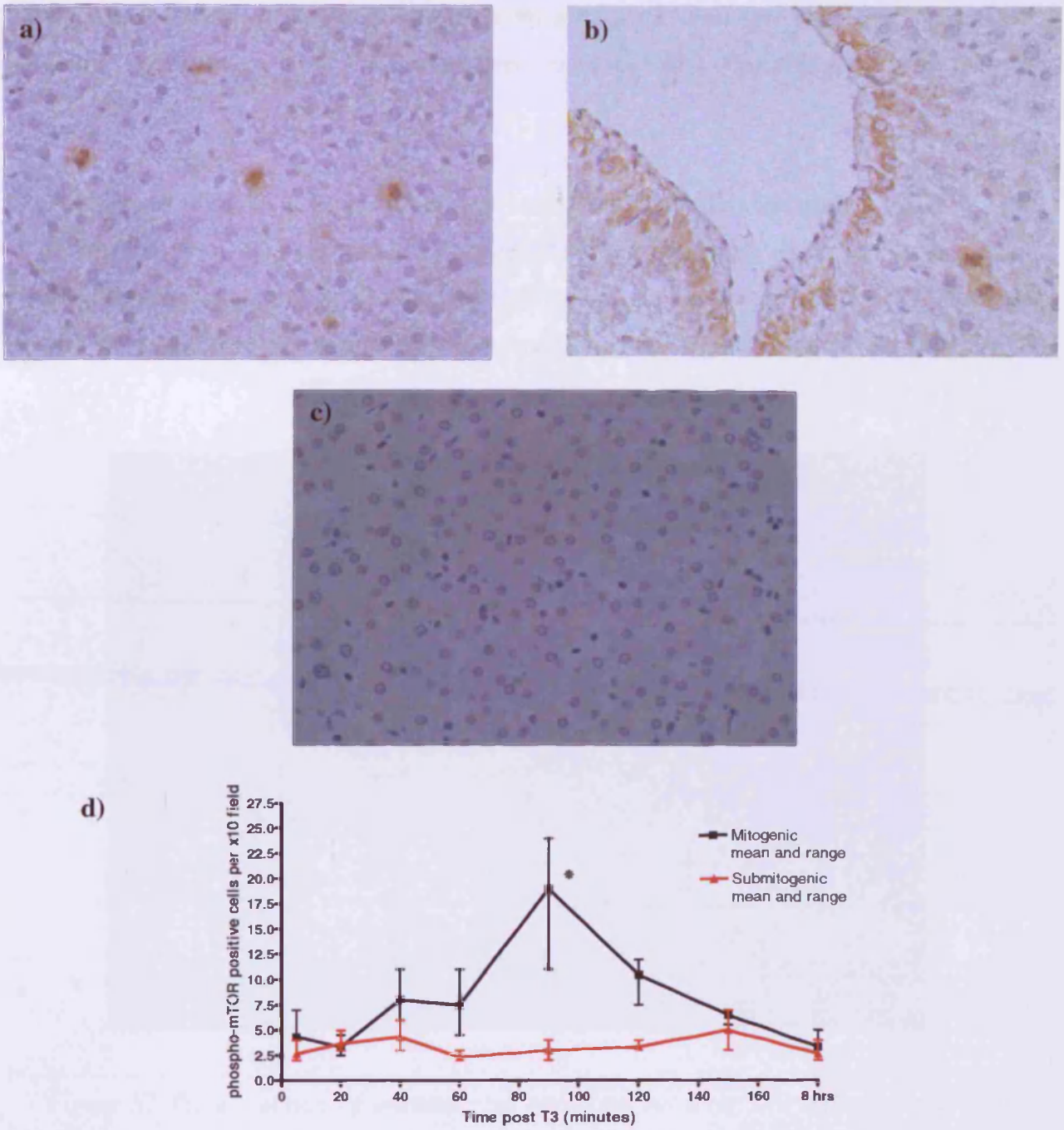

Figure 56 (a-b) Photomicrographs showing the peak phosphorylated mTOR hepatocyte response at 90 minutes after mitogenic T_3, x40 objective. Cells surrounding vessels stain strongly positive but this is also seen in unstimulated liver.

(c) the response is compared with sub-mitogenic T_3 at 90 minutes where very few hepatocytes stain positive for phospho- mTOR, x10 objective

(d) the time course of phospho-mTOR expression in mitogenic versus sub-mitogenic T_3 *treated rat liver. There is a surge in the number of positive hepatocytes for phospho-mTOR at 90 minutes after mitogenic* T_3 *but not in the sub-mitogenic treated group. (*p*

< 0.05 vs vehicle only treated liver at 90 minutes). Numbers of positive cells were scored over the area of tissue visualised using the x10 objective, which equates to 3.14mm^2.

The pattern of staining for p-mTOR was striking in that cells surrounding major vessels stained positive. This can be seen in Figure 56b and Figure 57 where the cytoplasm of cells surrounding this major vessel is clearly positive. This was seen both in quiescent and T_3 treated rat liver and these cells were not scored when assessing the response to T_3.

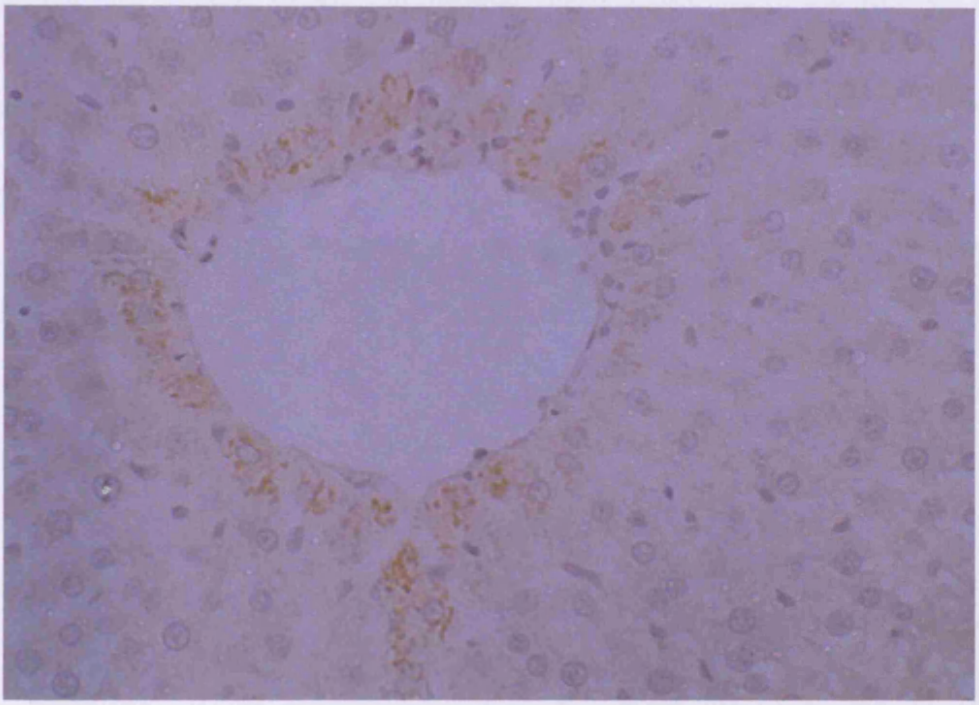

Figure 57 Tissue section of unstimulated quiescent rat liver x40 objective stained for phosphorylated mTOR. Note positive staining in cells surrounding a major vessel.

7.4.2.2 The induced phosphorylation is localised to the midzone

It has been previously demonstrated that the T_3 mitogenic effect is localised to the midzone although the reason for this is not known (Malik *et al.* 2003). Interestingly the phosphorylated mTOR hepatocyte response is localised to the same area in the hepatic lobule and this would be consistent with these cells later undergoing DNA synthesis and eventual replication in response to the initial mitogenic T_3 signal.

7.4.3 Investigating AKT and p70S6kinase

7.4.3.1 Rat phosphorylated AKT

AKT activation may precede that of mTOR in a T_3 sensitive pathway. The signalling network was further probed using an antibody directed against phosphorylated AKT (pAKT). Tissue sections from the entire mitogenic T_3 time course in the rat were examined for pAKT. Evident was subtle membranous (Figure 58) and occasional cytoplasmic staining that did not alter in distribution or intensity over time following T_3 stimulation. Given the nature and distribution of the staining, any increase in staining after T_3 may be difficult to see. On blinded visual inspection of the sections no overall change in staining was observed. This is in contrast to the well established method of counting discretely stained nuclei positive for BrdU described elsewhere in this thesis.

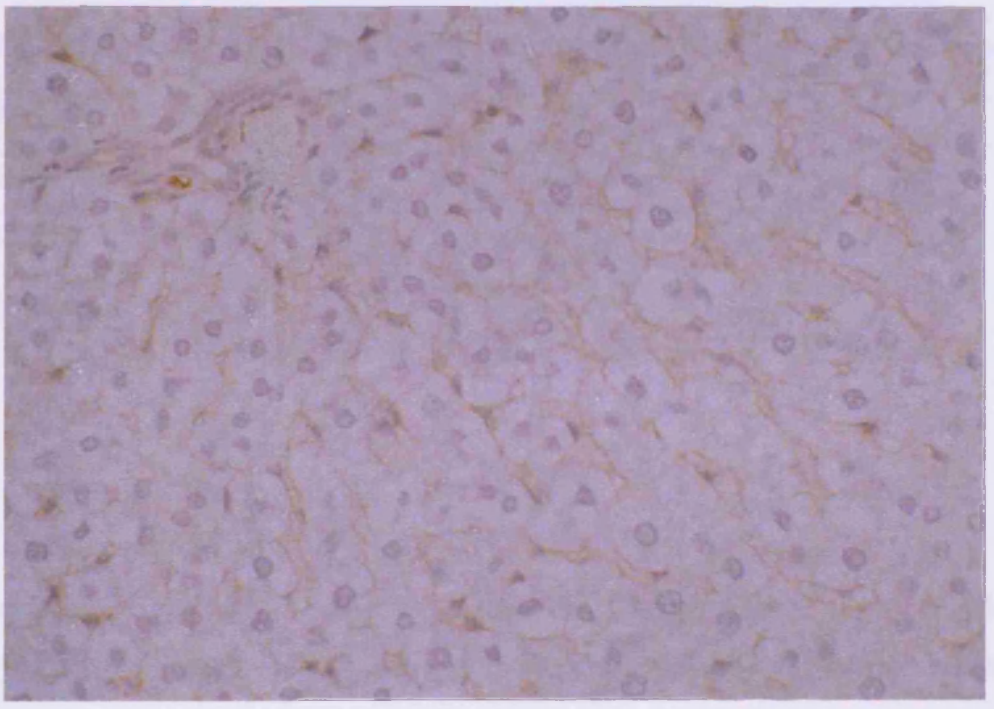

Figure 58 Tissue section of unstimulated rat liver x40 objective stained for phosphorylated AKT. The staining is subtle and restricted to the cell membranes across most tissue sections. There was no change in this pattern of staining over time following T_3 stimulation.

7.4.3.2 Rat p70S6kinase liver immunohistochemistry

One known downstream effector of p-mTOR is p70S6kinase. To investigate whether this became activated following T_3 stimulation, rat liver tissue sections from the mitogenic T_3 time course experiment were examined for phosphorylated p70S6kinase (Figure 59). The pattern of staining was very similar to that seen for pAKT and no increase in staining was observed over time after T_3.

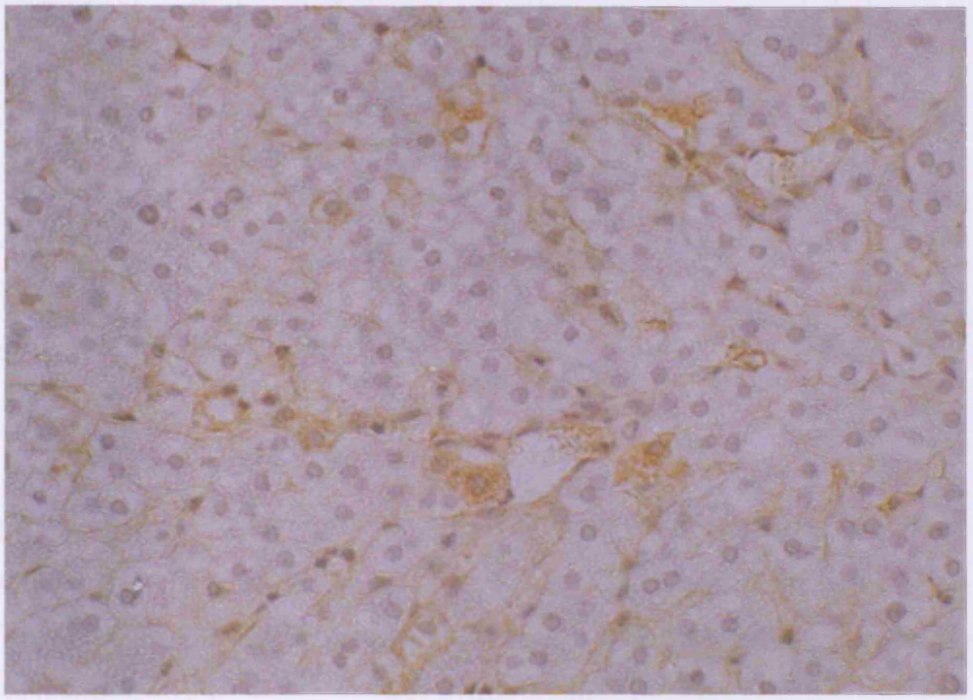

Figure 59 Tissue section of unstimulated rat liver x40 objective stained for phosphorylated p70S6kinase. The staining is subtle and predominantly restricted to the hepatocyte cell membranes. Some hepatocyte cytoplasmic staining can also be seen. There was no increase in distribution and/or intensity of staining following mitogenic T_3 stimulation.

7.4.4 Phosphorylated mTOR in T_3 treated rat liver over time- Western Blot Analysis

There was no significant change in the amount of phosphorylated mTOR over time in T_3 stimulated rat liver as measured by Western lot analysis (Figure 60). Indeed the peak seen in the immunohistochemical analysis at 90 minutes post mitogenic T_3 dose is not replicated in the Western blot analysis. This may well reflect the fact that in

unstimulated rat liver there is a basal level of phosphorylated mTOR seen particularly around the hepatic vasculature and therefore subtle increases or decreases in the amount of this active enzyme may not be detected using the Western blot technique which may not be sensitive enough to detect small changes in p-mTOR.

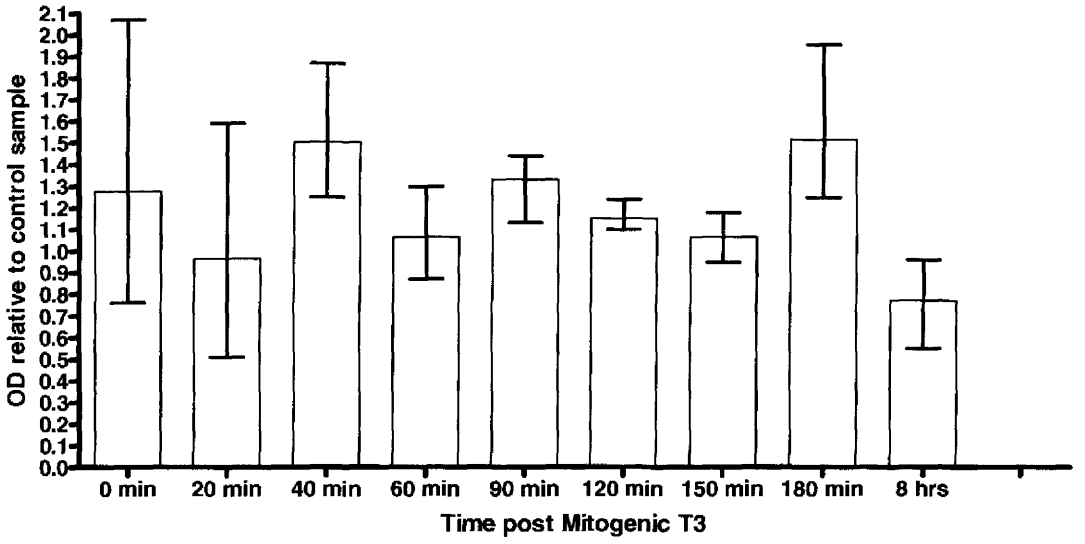

Figure 60 Western blot analysis of the hepatic phosphorylated mTOR response over time after T_3 in vivo in the adult male SD rat. The graph represents optical density of the p-mTOR protein bands relative to total mTOR protein bands when each blot was probed with the relevant antibodies. (Mean and range n=3).

7.4.5 The phosphorylated mTOR response in Primary Human Hepatocytes

Collagen coated wells were examined using phase microscopy on Day 1 to assess quality and extent of cell attachment before and after washing and prior to undertaking the T_3 time course experiments (Figure 61). In all cases there was good cell attachment. The hepatocyte yield per perfusion was between 138 million to 400 million cells with a mean viability of 70% as measured by trypan blue exclusion (See *General Methods Chapter Two*).

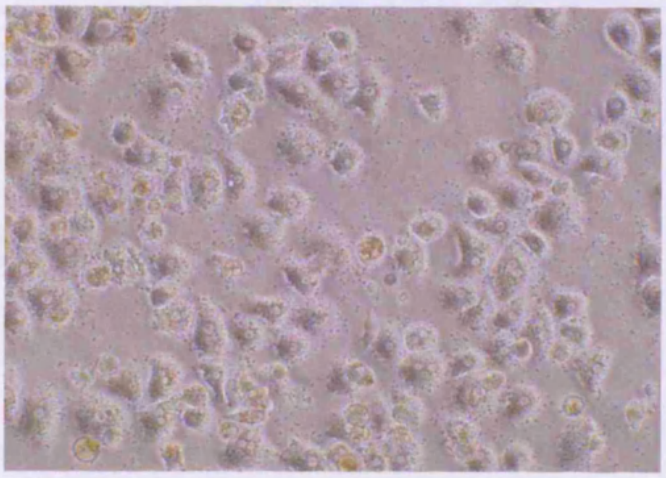

Figure 61 BS 43 phase x 20 objective Day 1. There is good cell attachment to the well after washing and a reasonable monolayer of hepatocytes can be seen.

Representative films after a Western blot was probed for phosphorylated mTOR and then total mTOR (after the membrane was stripped and re-probed) are shown in Figure 62. Positive and negative controls using 293 cell lysates are also shown.

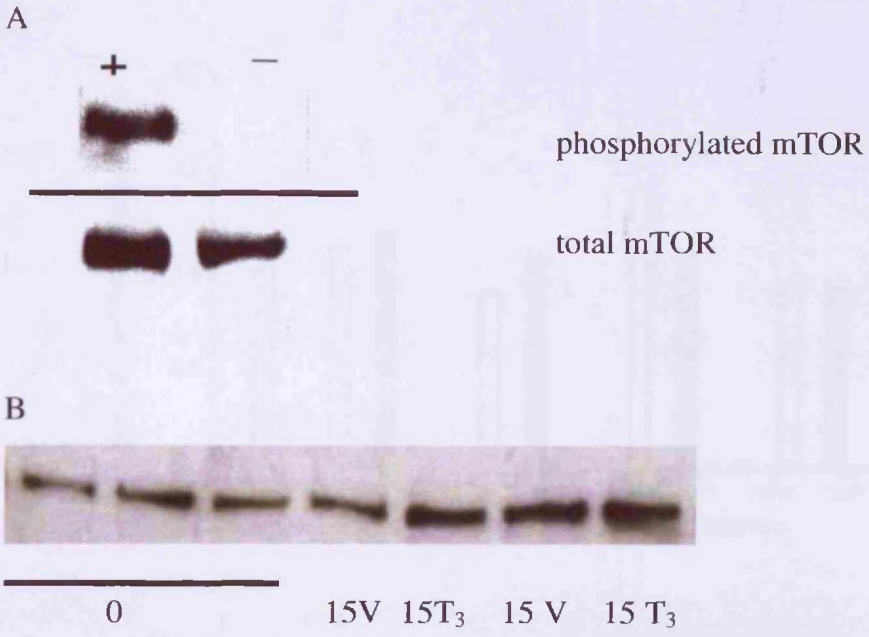

Figure 62 (A) Western blot of 293 cell positive and negative control lysates for phosphorylated mTOR (upper half) and re-probed for total mTOR (lower half) (B) BS43 Western blot for phosphorylated mTOR at time 0 and 15 minutes after T_3 and vehicle only using primary human hepatocyte cell lysate. The membrane was re-probed for total mTOR after stripping. An equal amount of protein lysate was loaded in each lane (50µg). Lanes with no primary antibody were negative and the mTOR bands are of the correct molecular weight when measured against a rainbow marker confirming specificity for mTOR detection.

7.4.5.1 BS 43

In this human hepatocyte experiment the amount of phosphorylated mTOR is greater in the T_3 treated hepatocytes at all time points, except at 40 minutes post stimulation where the amount is greater in the vehicle only treated cells (Figure 63).

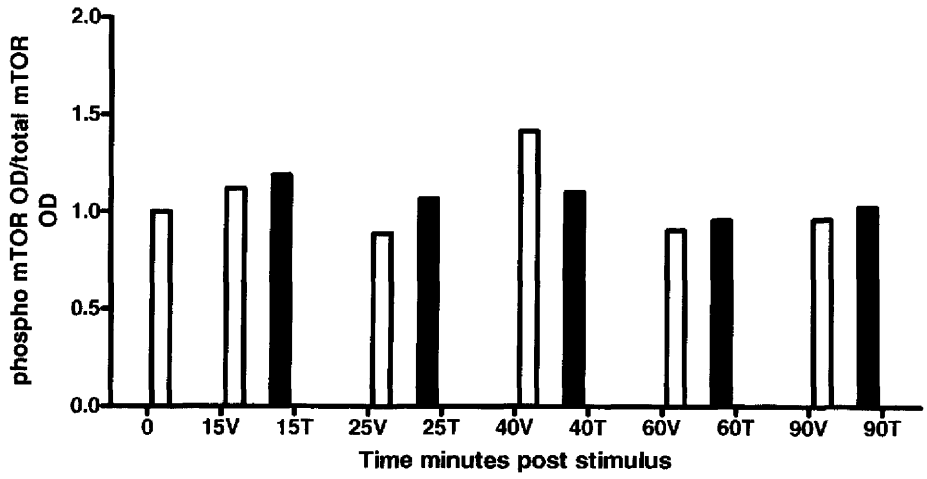

Figure 63 Western blot analysis of the BS43 phosphorylated mTOR response over time after stimulation of primary human hepatocytes with T_3 (T) or vehicle only (V). The optical density (OD) of the phospho-mTOR protein band is relative to the optical density for the total mTOR protein band.

7.4.5.2 BS44

In BS44 an increase in mTOR hepatocyte phosphorylation is seen at each time point after T_3 stimulation apart from at 40 minutes where less p-mTOR than is seen when compared to the vehicle only treated cells (Figure 64).

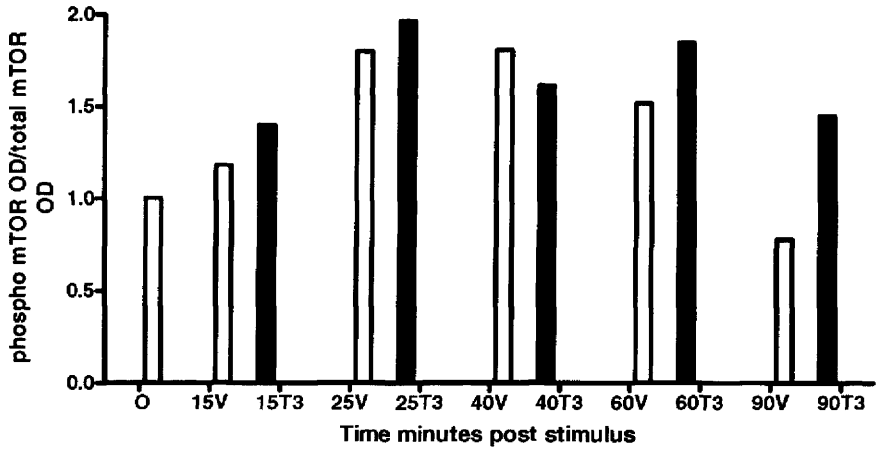

Figure 64 Western blot analysis of the BS44 phosphorylated mTOR response over time after stimulation of primary human hepatocytes with T_3 (T) or vehicle only (V). The optical density (OD) of the phospho-mTOR protein band is relative to the optical density for the total mTOR protein band.

7.4.5.3 BS45

The trend seen in BS 43 and BS 44 is replicated in BS45 (Figure 65).

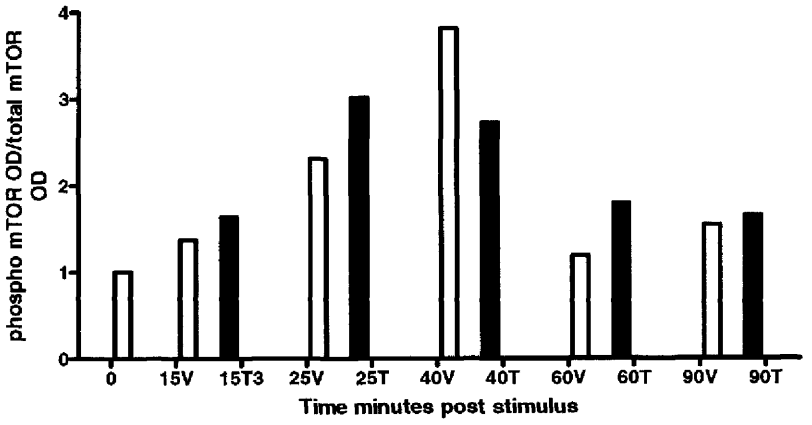

Figure 65 Western blot analysis of the BS45 phosphorylated mTOR response over time after stimulation of primary human hepatocytes with T_3 (T) or vehicle only (V). The optical density (OD) of the phospho-mTOR protein band is relative to the optical density for the total mTOR protein band.

7.4.5.4 BS47

BS 47 was examined. The T_3 stimulated hepatocytes contained greater amounts of phosphorylated mTOR at the time points examined (Figure 66) including 40 minutes post stimulation.

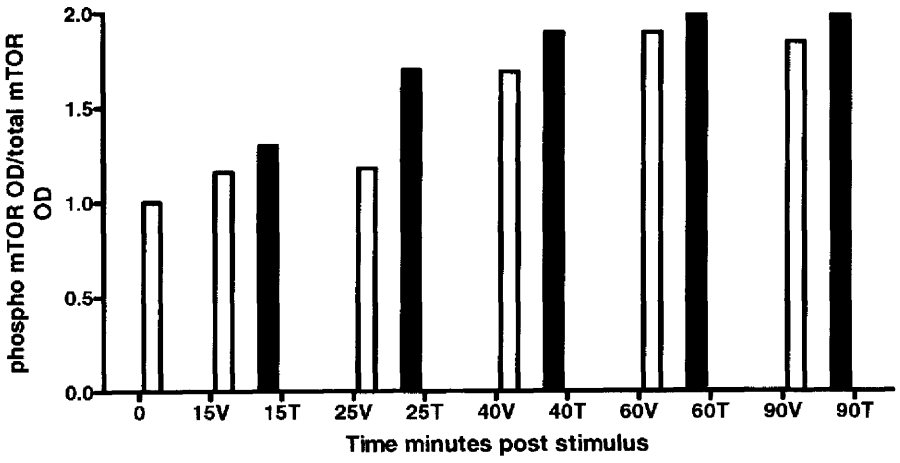

Figure 66 Western blot analysis of the BS47 phosphorylated mTOR response over time after stimulation of primary human hepatocytes with T_3 (T) or vehicle only (V). The optical density (OD) of the phospho-mTOR protein band is relative to the optical density for the total mTOR protein band.

7.4.6 Mean of Western blots for BS Livers

The mean result of the Western blot analysis of the response to T_3 in primary human hepatocyte culture is shown in Figure 67. There is a greater amount of p-mTOR at every time point when compared to vehicle only apart from at 40 minutes post stimulation when there is a greater amount in the vehicle only treated cells. The results however do not reach statistical significance.

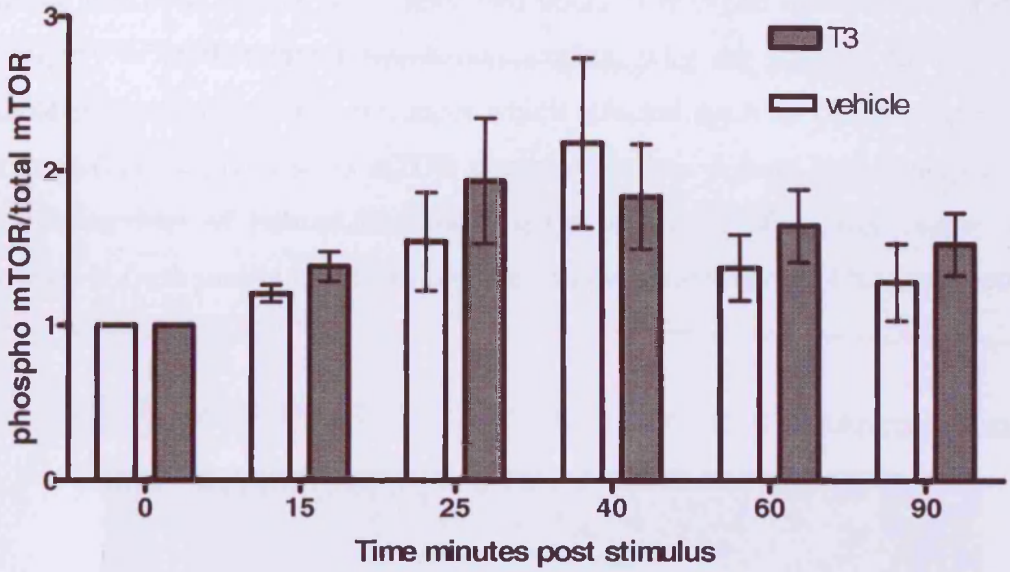

Figure 67 The primary human hepatocyte response to T_3 over time as measured by Western blot protein band densitometry analysis for p-mTOR normalised to total mTOR. Mean of all four BS livers is plotted +/- SD. There is an increase in the amount of p-mTOR every time point apart from at 40 minutes when there is more in the vehicle only treated cells. The differences do not reach statistical significance.

7.4.7 Human Liver phosphorylated mTOR immunohistochemistry

Initial immunohistochemical analysis was performed on human liver to assess the pattern of mTOR staining with a view to using this as a future marker of the T_3 response in the perfused human liver samples described in Chapter Three.

An interesting pattern of staining for phosphorylated mTOR was noted in a random number of BS livers that were examined. These histological sections are from pieces of liver which were placed into formalin soon after resection and are not those from liver pieces which underwent organ perfusion as described in the experiments of Chapter 3.

In some, very little staining is noted (Figure 70) while in others the staining is quite dramatic in its intensity and distribution. In these samples such as BS39, there is avid staining around vessels (Figure 68) but then there are large areas where one sees the hepatic parenchyma also staining positive. This is in contrast to that which one sees in the rat where there is still notable staining around the vessels but not in large areas of the parenchyma as seen in BS39.

Clearly this liver tissue was fixed once it had arrived back at the laboratory and therefore had been *ex-vivo* for at least two hours. The organ manipulation alone during the surgery is another factor which may explain why the staining for p-mTOR is so variable and any one of these instances which affected the liver (for example an episode of hypoxia) could give rise to mTOR phosphorylation. A next logical step would be to examine sections of human liver obtained at the time of a liver biopsy when the specimen is fresh and is fixed in formalin almost immediately. This may better reflect the true *in vivo* scenario.

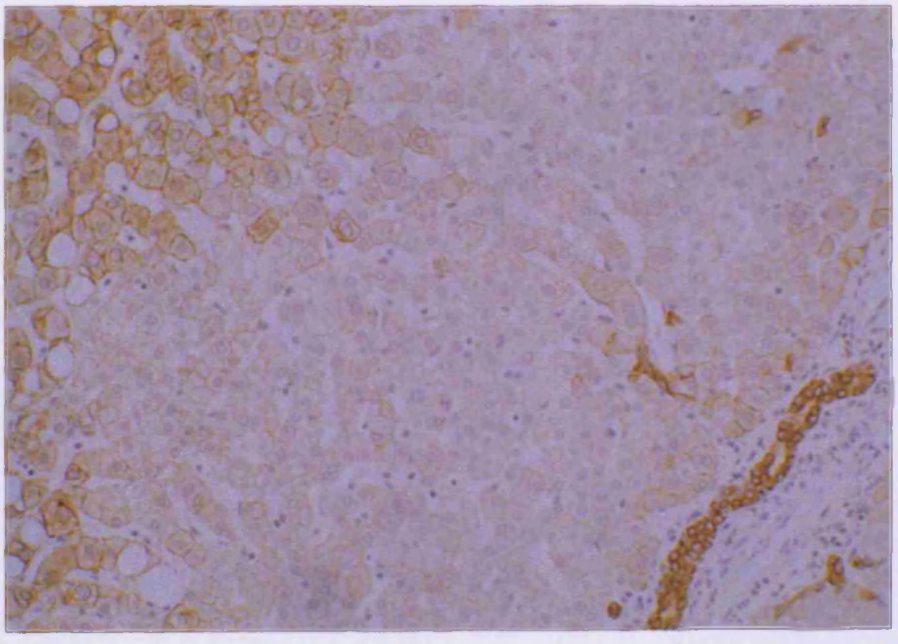

Figure 68 Tissue section of BS39 x 20 objective stained for phosphorylated mTOR. Note the positive cytoplasmic staining of hepatocytes to the left of the tissue section and the biliary cells staining strongly positive to the right of the tissue section.

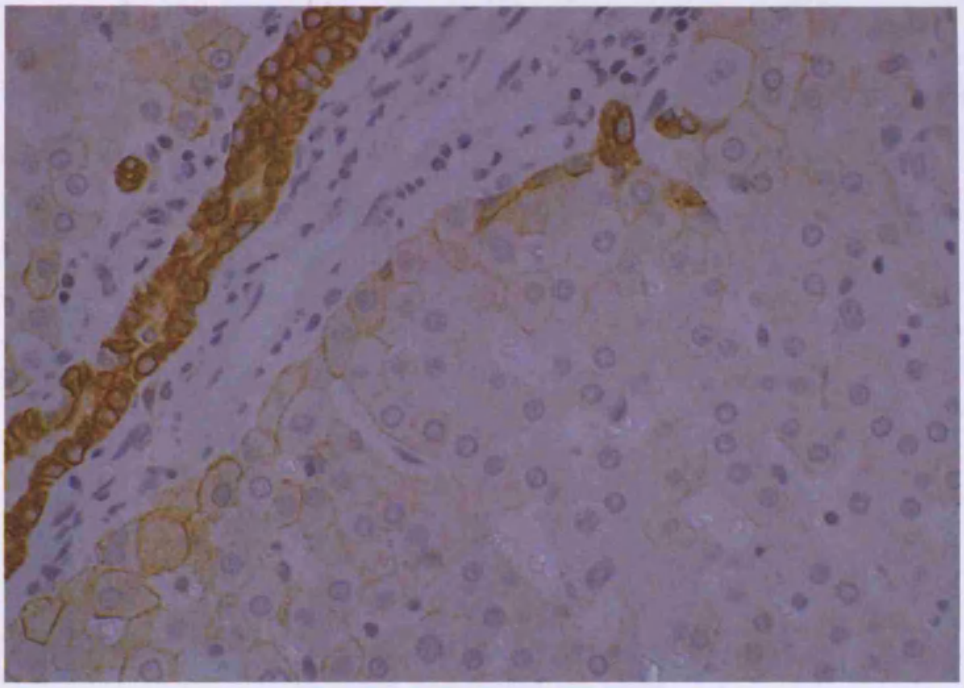

Figure 69 Tissue section of BS39 x40 objective. A similar area of liver is now shown under higher magnification and non parenchymal cells (biliary in origin) stain strongly positive to the left of the tissue section.

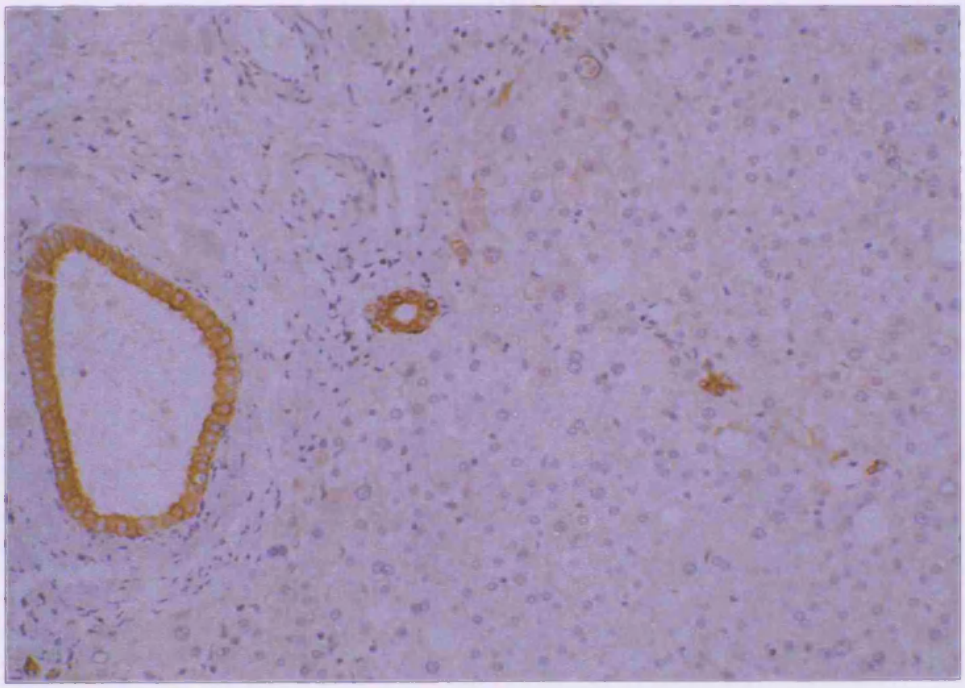

Figure 70 Tissue section of BS29 stained for phosphorylated mTOR x20 objective. Most hepatocytes stain weakly positive in this tissue section but strong staining is only seen in structures in the portal tract.

7.4.8 The *in vivo* response to T_3 in wortmannin treated SD rats

To assess whether the mTOR phosphorylation comes about as a result of the involvement of the upstream signalling enzyme PI3kinase, the PI3K inhibitor wortmannin was administered to rats *in vivo* to see if it reduced the T_3 hepatocyte proliferative response (Figure 71).

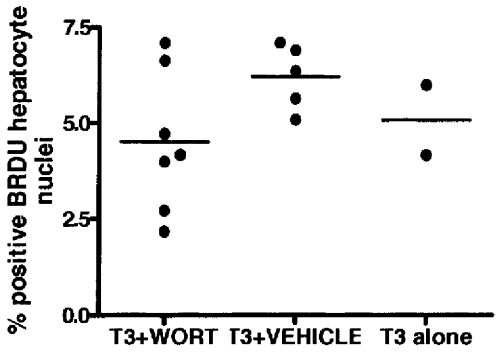

Figure 71 The male SD rat hepatocyte T_3 proliferative response measured by BrdU incorporation after pre-treatment with wortmannin or vehicle only in vivo prior to administration of a mitogenic dose of T_3. (WORT = wortmannin).

A reduction in the percentage of BrdU positive hepatocyte nuclei in those animals pre-treated with wortmannin at a dose of 100µg/kg can be seen. The difference however does not reach statistical significance.

7.5 Discussion

In summary, in this study inhibition by rapamycin of the T_3 proliferative hepatocyte response was demonstrated *in vivo* in rats. Immunohistochemistry demonstrated a surge in mTOR phosphorylation in midzone hepatocytes 90 minutes after a mitogenic dose of T_3 and it is already known that T_3 brings about eventual proliferation of the midzone hepatocytes. Western blot analysis did not confirm a change in phosphorylated mTOR at the same time points after T_3 in rat liver. Immunohistochemical examination of the other likely involved enzymes p70S6kinase and AKT was undertaken but there was no change in the intensity of staining for these phosphorylated enzymes after T_3.

The mTOR response in T_3 treated human hepatocytes was then investigated using the technique of Western blot analysis and human liver sections were stained for phosphorylated mTOR to determine the pattern and extent of staining in unstimulated human liver samples. The Western blot experiments did not confirm the involvement of mTOR at early time points in T_3 treated primary human hepatocytes. Finally, the involvement of PI3K upstream of mTOR was investigated by the *in vivo* rodent wortmannin experiment. The difference in the BrdU proliferative index between animals pre-treated with wortmannin and vehicle only did not reach statistical significance although there was an interesting trend suggesting a real biological effect. For this to be confirmed a further experiment needs to be undertaken which uses a greater number of animals in each experimental group.

Turning to the technique of Western blot analysis, a clear protein band for p-mTOR in unstimulated liver is seen and the immunohistochemistry confirms the presence of p-mTOR in cells surrounding the major vessels in quiescent rat liver. There was no change in the intensity of the protein bands for p-mTOR as measured by densitometry after T_3 over time in rat liver, but this likely reflects a lack of sensitivity using Western blot analysis where an increase over the basal amount is not detectable using densitometry measurements of the protein bands. It must be remembered that the increase in mTOR phosphorylation is restricted to a small number of midzonal hepatocytes after T_3 at 90 minutes post dose and this increase in the amount of p-mTOR may not be detectable using a Western blot approach. To overcome this problem the future use of an ELISA technique may better detect these subtle changes more satisfactorily.

The BS human liver sections examined stained strongly positive for p-mTOR in many areas and therefore using immunohistochemical or Western blot techniques to detect changes in response to T_3 may not be sensitive enough as is the case in the rat liver

scenario. Indeed a strong protein band is seen for p-mTOR in unstimulated human hepatocytes at time 0. There is little published in the worldwide literature on p-mTOR expression in human liver. One group has examined human hepatocellular carcinoma liver samples using an immunohistochemical technique with the same manufacturer's antibodies as used in this thesis (Sahin *et al.* 2004). Analysis was on formalin fixed paraffin embedded samples collected over a period of sixteen years. Increased expression of p-mTOR was found in 15% of hepatocellular carcinoma but p-mTOR was negative in non neoplastic liver tissue but no actual immunohistochemistry photomicrographs are shown to demonstrate this finding. This is in contrast to the marked staining shown in this thesis for p-mTOR in human liver. These BS samples were however only formalin fixed after they were transported by road stored on ice in USW solution to the laboratory and clearly the handling of the tissue may have brought about activation of mTOR phosphorylation.

A recent study examined PTEN expression in human and rodent liver samples and found that unsaturated fatty acids inhibited PTEN expression in HepG2 cells via activation of a signalling complex formed by mTOR and NF-κβ (Vinciguerra *et al.* 2008). As part of the analysis p-mTOR expression was studied using Western blot analysis in ZDF, male Wistar and Lou/C rats. A strong basal protein band on Western blot analysis can be seen in all three species for p-mTOR, but it was particularly strong in the Lou/C rat and comparable to the band seen in unstimulated male SD rat liver found in this thesis.

The primary human hepatocyte work presented here is therefore suggestive but not conclusive of T_3 increasing the levels of human phosphorylated mTOR. If there is a subtle effect it needs to be confirmed with a greater number of experimental replicates and it is necessary to measure the change in p-mTOR using a more sensitive method than Western blot analysis, such as ELISA. It is also not clear if the time course chosen is the correct one as the T_3 may be exerting its effect on hepatocytes within seconds or minutes and this change may not be seen when examining the time points chosen in this thesis.

Another possible explanation for why a significant effect was not observed is that in monolayer hepatocyte cell culture the co-operation of other cells which may be necessary to bring about the observed *in vivo* mitogenic response is lacking. In addition the hepatocytes have been through a host of mechanical and biochemical handling procedures before they are plated out and it is not known if this handling alone is

enough to stimulate mTOR phosphorylation and this is perhaps why a strong protein band at time 0 is seen for p-mTOR.

It is also important to note that the T_3 concentration used *in vitro* (100nM) may be inadequate as if 5μg is distributed in all of the 15mls of the rat's circulating blood volume this equates to a concentration of about 500 nM *in vivo*. The choice of 100nM was based on the fact that published data used this concentration of T_3 to bring about successful activation of PI3K and mTOR in fibroblasts and cardiomyocytes (Kenessey and Ojamaa 2006)

In future it would be highly desirable to isolate the hepatocytes that undergo proliferation in response to T_3 and this could be achieved by utilising the technique of laser capture microdissection to specifically study the midzone hepatocytes; indeed it is in these cells that the surge in mTOR phosphorylation is seen 90 minutes post mitogenic T_3 and it is in the midzone that the T_3 exerts its proliferative effect. Laser microdissection can be performed on cryostat liver to isolate 3,000 to 5,000 hepatocytes and then mRNA and/or protein expression analysis can be performed on these cells (Melle *et al.* 2004; Melle *et al.* 2007). Although technically demanding a number of studies now report the use of laser microdissection to study just single cells.

7.5.1 The Non-Genomic Effect

The results in this Chapter indicate that mTOR phosphorylation is an important early event in mediating the mitogenic effects of T_3 on rat liver. Due to the rapidity of this response, it is hypothesised that this T_3 effect is acting through a so-called 'non-genomic' mechanism via phosphatidylinositol 3-kinase activation followed by AKT phosphorylation acting through the intermediates Rheb and TSC complex with subsequent activation of the mTOR downstream effectors p70S6 kinase and 4E-BP1, the mammalian translational regulators (Figure 72). These would effect important downstream cell cycle regulators such as cyclin D1 enabling cell cycle progression and published work has clearly demonstrated that rapamycin inhibits expression of cyclin D1 (Hidalgo and Rowinsky 2000).

Figure 72 The T_3 activation of proliferative pathways acting through mTOR via a 'non-genomic' mechanism. T_3 activates PI3K which brings about downstream activation of AKT then mTOR leading to nuclear transcription events (Moeller et al. 2006).

There is gathering evidence from the literature for T_3 acting through the hypothesised pathway. Cao (Cao *et al.* 2005) shows that T_3 increased ZAKI 4 alpha expression in human skin fibroblasts and this was through Serine 2448 mTOR phosphorylation leading to p70S6 kinase phosphorylation. The pathway acted through AKT phosphorylation and PI3K, as PI3K inhibitors blocked the T_3 effect. They showed an association between thyroid hormone receptor β1 and the PI3K-regulatory sub-unit p85α (Moeller *et al.* 2006).

Kenessey (Kenessey and Ojamaa 2006) shows T_3 acts through the PI3K pathway in rat cardiomyocytes where it increases 3H-leucine incorporation at 24 hours in cultured cells. The study demonstrated a direct interaction between cytosolic TRα1 and the p85α

subunit of PI3K and also further downstream activation of AKT then mTOR leading to p70S6K activation. The T_3 effects were blocked by PI3K inhibitors and rapamycin.

Coutant et al (Coutant *et al.* 2002) examined the role of this pathway in primary rat hepatocyte culture. They showed a dose dependent inhibition of DNA replication by the PI3K inhibitor LY294002, in EGF stimulated hepatocytes. A dose dependent inhibition was also shown with rapamycin up to complete abolition of the DNA replicative response with EGF. In addition a link to cyclin D1 protein expression and its inhibition by LY294002 and rapamycin was demonstrated.

Recently further evidence has emerged showing that the mTOR pathway is thyroid hormone responsive. Thyroid hormone activates AKT to bring about cardiac hypertrophy in mice and there is activation of the pathway seen in cardiomyocyte cell culture. The induced cardiac hypertrophy was completely inhibited by rapamycin (Kuzman *et al.* 2007). Furthermore it is now known that the thyroid hormone receptor TRβ, mediates AKT activation by T_3 in pancreatic beta cells (Verga *et al.* 2007).

Chapter 8 General Discussion

8.1 What was achieved

The long term goal pursued in this research thesis is therapeutic, enabling the use of T_3 in the setting of human liver disease to augment and improve a patient's functioning hepatic mass and the overall original aim of this thesis was to demonstrate a mitogenic effect of T_3 on human liver which no-one else has yet been able to achieve. Furthermore workers have not been able to demonstrate a mitogenic effect on rodent liver cells *in vitro*, but the *in vivo* model has been well characterised up to now.

The work presented here has significantly contributed to our understanding of the mitogenic mechanism of action of T_3 on hepatocytes however a direct mitogenic effect was not conclusively demonstrated in primary human hepatocytes or in rodent or human liver pieces which underwent organ perfusion. Nonetheless results from this research project offer some novel insights into the mechanism of action of T_3 when acting as a direct hepatic mitogen.

The experiments sought to identify an early marker (within 6 hours) of the T_3 mitogenic effect which could be utilised firstly in the organ perfusion experiments of Chapter 3 and later in the primary human hepatocyte work undertaken in Chapter 7. In pursuit of such an early marker, cyclin D1, important in cell cycle progression, was first investigated in Chapter 4. Its levels were found to rise after T_3 stimulation (at 14 hours) at both the mRNA and protein levels, however this rise is not as early as others have described (within 2 to 4 hours). Its use therefore as a marker of early T_3 effects in the organ perfusion experiments was not pursued further. A second likely mediator of the mitogenic response, the oncogene Bcl-3, was next probed by examining the hepatocyte proliferative response to T_3 in Bcl-3 knockout mice. The proliferative response was no less in the knockout animals and so Bcl-3 was not investigated any further.

Work moved forward to try and identify novel mediators of the T_3 response using the powerful technique of expression based gene array technology in Chapter 5. A host of genes potentially associated with proliferation and cell cycle control were identified and most notable amongst these were the Kruppel like transcription factors which were shown to be T_3 responsive using Real Time PCR technology in Chapter 6. Their rise at the expression level was common to both mitogenic and sub-mitogenic T_3 treated liver, confirming their T_3 responsiveness, except in the case of the tumour suppressor Kruppel

Factor 4 where a fall in expression was noted after the mitogenic T_3 dose at 20 minutes. This Kruppel factor remains a candidate as a mediator of the proliferative hepatocyte response.

In Chapter 7, the mTOR pathway was explored as an early mediator of the T_3 proliferative response and a clear rise in active phosphorylated mTOR after 90 minutes at the immunohistochemical level following a dose of mitogenic but not sub-mitogenic T_3 was shown. In the remainder of that chapter experiments were undertaken which attempted to demonstrate a T_3 effect on mTOR activation in primary human hepatocytes. There is a trend seen using Western blot analysis with a greater amount of p-mTOR in the T_3 treated hepatocytes over early time points but the increase across 4 different human liver primary hepatocyte preparations did not reach statistical significance when compared to vehicle only treated cells. The involvement of PI3K upstream of mTOR in mediating the T_3 signal is suggested by the reduction in the hepatocyte proliferative response in rodents pre-treated *in vivo* with the PI3K inhibitor wortmannin. The change however did not reach statistical significance, nonetheless may be biologically significant and an experiment with more replicates needs to be conducted.

8.2 Signalling, receptors and PI3K

Based on this collection of experimental observations it is clear that the mitogenic mechanism of action of T_3 in the liver is complex, probably utilising more than one signalling pathway with effects attributable to 'genomic' and 'non-genomic' pathways to bring about the proliferation of midzone hepatocytes. The work underscores the emerging importance of the 'non-genomic' signalling pathways involved as it is about 10 years ago that reports began to tentatively describe membrane or cytosol forms of nuclear receptors that could mediate rapid responses following ligand binding which could not be explained by slower nuclear transcriptional events. Now in 2008 it is well established that many nuclear receptor family members are coupled to the rapid activation of cytoplasmic signal transduction pathways that generally emanate from membrane-associated or membrane-integral receptors and ion channels. Novel new receptors have been identified that bind ligand and these receptors are distinct from their nuclear counterparts (Revankar *et al.* 2005). Nuclear and non-nuclear receptors represent two integrated arms of the same signalling pathway. As outlined in Chapter 7's introduction it is likely that the mTOR mediated response is via T_3 binding to the TRβ receptor isoform which is most prevalent in the liver. The receptor may be cytosol

or membrane associated or both but clearly other as yet to be identified receptors may be involved in mediating the T_3 effect.

PI3K may be involved in the upstream regulation of the T_3 response and dysregulation of PI3K signalling is increasingly shown to contribute to the development of abnormal cell growth and a variety of neoplasms (Engelman *et al.* 2006). There is further recent evidence to suggest that the AKT-mTOR-p70S6kinase pathway is thyroid hormone responsive and involved in the control of cell proliferation via PI3K activation. Kaneshige (Kaneshige *et al.* 2000) developed a TRβ mutant knockin mouse harbouring a frame-shift mutation in carboxyl-terminal 16 amino acids, termed TRβPV. This type of mutation was identified in a patient with the syndrome of thyroid hormone resistance termed RTH. The TRβPV mouse reproduces the RTH phenotype one sees in humans with elevated levels of thyroid hormone and non-suppressible TSH levels. PV interferes with the transcriptional activity of TRs leading to repression of the positively regulated T_3 genes. However as these $TR\beta^{PVPV}$ mice age they develop follicular thyroid carcinoma. Mutant PV increases the phosphorylation of AKT in the thyroid lesions (Furuya *et al.* 2007) and this comes about through activation of PI3K in $TR\beta^{PVPV}$ mice. The p85α subunit of PI3K binds to PV three times more strongly than to TRβ.

8.3 Species differences

The *in vivo* hepatic response to T_3 is well characterised in the rodent but as a direct mitogenic response has not been shown in human hepatocytes consideration has to be given to the likely differences in response between species and how these differences can quickly be recognised so the ultimate goal of using mitogenic T_3 in humans can be realised.

Most of the detailed work conducted in the field of liver regeneration has been performed in the rodent model and this is indeed the case when examining the mitogenic action of T_3 on the liver. It is highly likely there will be inter-species variation in the hepatic proliferative response to T_3 just as there is in the response to partial hepatectomy between rats and mice where the duration of the cell cycle in the latter species is longer hence resulting in a more latent peak in hepatocyte proliferation. It is difficult to allow for these differences in the interpretation of the experiments undertaken in this thesis but there are obvious differences between species and their response to primary mitogens. For example when taking into consideration the response to PPAR ligands, these cause peroxisome proliferation in rodents but not in human liver

where they are crucially not hepatocarcinogenic whereas they can cause liver tumours in rodents.

There is limited data on the physiological and molecular processes underlying human liver regeneration as most of the work has been carried out in rodents, dogs, pigs, frogs and zebra fish (Hata *et al.* 2007). The regeneration of human liver has been studied in patients with hepatocellular injury such as in fulminant hepatic failure but also in patients who have undergone partial hepatectomy. An intermediate step therefore is the use of a primate model and this needs to be considered but there is little published data on studies of hepatic regeneration in a primate model. In human patients with right lobe allografts there is an increase in the amount of Ki-67 staining of hepatocytes compared with cadaveric allografts and by 3 weeks there is restoration of liver volume in the right lobe allograft group of patients due to this proliferation of the hepatocytes (Huang *et al.* 2004). By contrast Gaglio et al (Gaglio *et al.* 2002) describe some pilot work in the Macaca mulatta monkey. The proliferative response was studied in 3 animals that underwent partial hepatectomy, by examining serial liver biopsies in the days following surgery. The peak in expression of the cell cycle antigen Ki-67 occurred after 3 weeks and this is dramatically different to the peak seen in rats following PH which is seen to occur within a matter of hours.

Studying the effects of mitogens in a primate model, although extremely useful and informative would nonetheless present numerous difficulties, notably the great costs involved in such experiments and the sensitive ethical issues surrounding the use of primates. A more plausible route to pursue with regards to this thesis is further intensive work on perfecting the organ perfusion technique in Chapter 3 and to begin tissue slice experiments which may better reflect the *in vivo* scenario in humans. These techniques will reduce the ethical and economic costs of animal experiments and once perfected in a robust system could prove very valuable in modelling the T_3 mitogenic hepatic response across many different species.

8.4 The Dose in Humans

A potential criticism in trying to extrapolate the use of T_3 from the rodent model to man, is that the dose required in man may be potentially toxic and therefore clinically inappropriate. This needs to be addressed as it is central to the future use of this hormone in man. The main instance in which T_3 is currently administered to humans acutely is in the setting of myxoedema coma due to hypothyroidism. Due to the earlier recognition of the hypothyroid state this is a rare clinical entity however patients do still

present to hospital and in England in 2004 there were 11 such cases. Endocrinologists would treat this condition with a dose of intravenous T_3 of 75μg in the first 24 hours (Kearney and Dang 2007). This equates to about 1μg/kg in the human and the dose used in the animal model in this thesis is 20μg/kg. The similarity between these doses means it is very likely T_3 will be used safely in the future in humans to act as a primary liver mitogen. Furthermore the cardiovascular effects of T_3 in healthy male volunteers has been studied (Schmidt *et al.* 2002) when 100μg is injected intravenously into a forearm vein over 1 minute. Simultaneous infusion of a β adrenergic blocking drug was administered to limit the cardiovascular side effects but the T_3 exhibited excellent tolerability and there were no adverse events.

In conclusion therefore, this thesis has described interesting new hepatic signalling pathways that are T_3 responsive as well as the importance of mTOR in mediating the proliferative T_3 effect. To enable an effect to be demonstrated in human hepatocytes further work still needs to be done and this will be best achieved using the techniques of liver slice technology prior to the necessary clinical trials being undertaken of mitogenic T_3 in humans with liver diease.

REFERENCES

Abdelrahim M, Smith R, III, Burghardt R, Safe S (2004) Role of Sp proteins in regulation of vascular endothelial growth factor expression and proliferation of pancreatic cancer cells. *Cancer Res.* **64,** 6740-6749.

Akhtar RA, Reddy AB, Maywood ES, Clayton JD, King VM, Smith AG, Gant TW, Hastings MH, Kyriacou CP (2002) Circadian cycling of the mouse liver transcriptome, as revealed by cDNA microarray, is driven by the suprachiasmatic nucleus. *Curr.Biol.* **12,** 540-550.

Albrecht JH, Hansen LK (1999) Cyclin D1 promotes mitogen-independent cell cycle progression in hepatocytes. *Cell Growth Differ.* **10,** 397-404.

Albrecht JH, Hu MY, Cerra FB (1995) Distinct patterns of cyclin D1 regulation in models of liver regeneration and human liver. *Biochem.Biophys.Res.Commun.* **209,** 648-655.

Albrecht JH, Rieland BM, Nelsen CJ, Ahonen CL (1999) Regulation of G(1) cyclin-dependent kinases in the liver: role of nuclear localization and p27 sequestration. *Am.J.Physiol* **277,** G1207-G1216.

Alexander B, Aslam M, Benjamin IS (1995) Hepatic function during prolonged isolated rat liver perfusion using a new miniaturized perfusion circuit. *J.Pharmacol.Toxicol.Methods* **34,** 203-210.

Alexander B, Aslam M, Benjamin IS (1998) The dependence of hepatic function upon sufficient oxygen supply during prolonged isolated rat liver perfusion. *J.Pharmacol.Toxicol.Methods* **39,** 185-192.

Alexander B, Von AT, Aslam M, Kolhe PS, Benjamin IS (1984) Practical miniaturized membrane oxygenator for isolated organ perfusion. *Lab Invest* **50,** 597-603.

Alisi A, Demori I, Spagnuolo S, Pierantozzi E, Fugassa E, Leoni S (2005) Thyroid status affects rat liver regeneration after partial hepatectomy by regulating cell cycle and apoptosis. *Cell Physiol Biochem.* **15,** 69-76.

Alisi A, Spagnuolo S, Napoletano S, Spaziani A, Leoni S (2004) Thyroid hormones regulate DNA-synthesis and cell-cycle proteins by activation of PKCalpha and p42/44 MAPK in chick embryo hepatocytes. *J.Cell Physiol* **201,** 259-265.

Amaravadi R, Thompson CB (2005) The survival kinases Akt and Pim as potential pharmacological targets. *J.Clin.Invest* **115,** 2618-2624.

Andrews PD (2005) Aurora kinases: shining lights on the therapeutic horizon? *Oncogene* **24,** 5005-5015.

Aranda A, Pascual A (2001) Nuclear hormone receptors and gene expression. *Physiol Rev.* **81,** 1269-1304.

Band CJ, Mounier C, Posner BI (1999) Epidermal growth factor and insulin-induced deoxyribonucleic acid synthesis in primary rat hepatocytes is phosphatidylinositol 3-kinase dependent and dissociated from protooncogene induction. *Endocrinology* **140,** 5626-5634.

Barrass NC, Price RJ, Lake BG, Orton TC (1993) Comparison of the acute and chronic mitogenic effects of the peroxisome proliferators methylclofenapate and clofibric acid in rat liver. *Carcinogenesis* **14,** 1451-1456.

Barthel A, Schmoll D (2003) Novel concepts in insulin regulation of hepatic gluconeogenesis. *Am.J.Physiol Endocrinol.Metab* **285,** E685-E692.

Bassett JH, Harvey CB, Williams GR (2003) Mechanisms of thyroid hormone receptor-specific nuclear and extra nuclear actions. *Mol.Cell Endocrinol.* **213,** 1-11.

Bergh JJ, Lin HY, Lansing L, Mohamed SN, Davis FB, Mousa S, Davis PJ (2005) Integrin alphaVbeta3 contains a cell surface receptor site for thyroid hormone that is linked to activation of mitogen-activated protein kinase and induction of angiogenesis. *Endocrinology* **146,** 2864-2871.

Bernard PS, Wittwer CT (2000) Homogeneous amplification and variant detection by fluorescent hybridization probes. *Clin.Chem.* **46,** 147-148.

Berridge MJ (1993b) Cell signalling. A tale of two messengers. *Nature* **365,** 388-389.

Berridge MJ (1993a) Inositol trisphosphate and calcium signalling. *Nature* **361,** 315-325.

Bessems M, 't Hart NA, Tolba R, Doorschodt BM, Leuvenink HG, Ploeg RJ, Minor T, van Gulik TM (2006) The isolated perfused rat liver: standardization of a time-honoured model. *Lab Anim* **40,** 236-246.

Bianco AC, Salvatore D, Gereben B, Berry MJ, Larsen PR (2002) Biochemistry, cellular and molecular biology, and physiological roles of the iodothyronine selenodeiodinases. *Endocr.Rev.* **23,** 38-89.

Bockhorn M, Frilling A, Benko T, Best J, Sheu SY, Trippler M, Schlaak JF, Broelsch CE (2007) Tri-iodothyronine as a stimulator of liver regeneration after partial and subtotal hepatectomy. *Eur.Surg.Res.* **39,** 58-63.

Boorman GA, Blackshear PE, Parker JS, Lobenhofer EK, Malarkey DE, Vallant MK, Gerken DK, Irwin RD (2005) Hepatic gene expression changes throughout the day in the Fischer rat: implications for toxicogenomic experiments. *Toxicol.Sci.* **86,** 185-193.

Bottaro DP, Rubin JS, Faletto DL, Chan AM, Kmiecik TE, Vande Woude GF, Aaronson SA (1991) Identification of the hepatocyte growth factor receptor as the c-met proto-oncogene product. *Science* **251,** 802-804.

Boylan JM, Gruppuso PA (2005) D-type cyclins and G1 progression during liver development in the rat. *Biochem.Biophys.Res.Commun.* **330,** 722-730.

Brauer RW, Pessotti RL, Pizzolato P (1951) Isolated rat liver preparation; bile production and other basic properties. *Proc.Soc.Exp.Biol.Med.* **78,** 174-181.

Brent GA (1994) The molecular basis of thyroid hormone action. *N.Engl.J.Med.* **331,** 847-853.

Brown KE, Mathahs MM, Broadhurst KA, Weydert J (2006) Chronic iron overload stimulates hepatocyte proliferation and cyclin D1 expression in rodent liver. *Transl.Res.* **148,** 55-62.

Brown PO, Botstein D (1999) Exploring the new world of the genome with DNA microarrays. *Nat.Genet.* **21,** 33-37.

Bustin SA (2000) Absolute quantification of mRNA using real-time reverse transcription polymerase chain reaction assays. *J.Mol.Endocrinol.* **25,** 169-193.

Bustin SA (2005) Real-time, fluorescence-based quantitative PCR: a snapshot of current procedures and preferences. *Expert.Rev.Mol.Diagn.* **5,** 493-498.

Calbo J, Parreno M, Sotillo E, Yong T, Mazo A, Garriga J, Grana X (2002) G1 cyclin/cyclin-dependent kinase-coordinated phosphorylation of endogenous pocket proteins differentially regulates their interactions with E2F4 and E2F1 and gene expression. *J.Biol.Chem.* **277,** 50263-50274.

Cao X, Kambe F, Moeller LC, Refetoff S, Seo H (2005) Thyroid hormone induces rapid activation of Akt/protein kinase B-mammalian target of rapamycin-p70S6K cascade through phosphatidylinositol 3-kinase in human fibroblasts. *Mol.Endocrinol.* **19,** 102-112.

Cattley RC (2003) Regulation of cell proliferation and cell death by peroxisome proliferators. *Microsc.Res.Tech.* **61,** 179-184.

Cattori V, Hagenbuch B, Hagenbuch N, Stieger B, Ha R, Winterhalter KE, Meier PJ (2000) Identification of organic anion transporting polypeptide 4 (Oatp4) as a major full-length isoform of the liver-specific transporter-1 (rlst-1) in rat liver. *FEBS Lett.* **474,** 242-245.

Chen X, Johns DC, Geiman DE, Marban E, Dang DT, Hamlin G, Sun R, Yang VW (2001) Kruppel-like factor 4 (gut-enriched Kruppel-like factor) inhibits cell proliferation by blocking G1/S progression of the cell cycle. *J.Biol.Chem.* **276,** 30423-30428.

Cheuk W, Wong KO, Wong CS, Chan JK (2004) Consistent immunostaining for cyclin D1 can be achieved on a routine basis using a newly available rabbit monoclonal antibody. *Am.J.Surg.Pathol.* **28,** 801-807.

Cheung K, Hickman PE, Potter JM, Walker NI, Jericho M, Haslam R, Roberts MS (1996) An optimized model for rat liver perfusion studies. *J.Surg.Res.* **66,** 81-89.

Chevalier S, Macdonald N, Roberts RA (1999) Induction of DNA replication by peroxisome proliferators is independent of both tumour necrosis factor (alpha) priming and EGF-receptor tyrosine kinase activity. *J.Cell Sci.* **112 (Pt 24),** 4785-4791.

Choi J, Chen J, Schreiber SL, Clardy J (1996) Structure of the FKBP12-rapamycin complex interacting with the binding domain of human FRAP. *Science* **273,** 239-242.

Cody V, Davis PJ, Davis FB (2007) Molecular modeling of the thyroid hormone interactions with alpha v beta 3 integrin. *Steroids* **72,** 165-170.

Columbano A, Ledda GM, Sirigu P, Perra T, Pani P (1983) Liver cell proliferation induced by a single dose of lead nitrate. *Am.J.Pathol.* **110,** 83-88.

Columbano A, Ledda-Columbano GM (2003) Mitogenesis by ligands of nuclear receptors: an attractive model for the study of the molecular mechanisms implicated in liver growth. *Cell Death.Differ.* **10 Suppl 1,** S19-S21.

Columbano A, Ledda-Columbano GM, Coni PP, Vargiu M, Faa G, Pani P (1984) Liver hyperplasia and regression after lead nitrate administration. *Toxicol.Pathol.* **12,** 89-95.

Columbano A, Ledda-Columbano GM, Pibiri M, Concas D, Reddy JK, Rao MS (2001) Peroxisome proliferator-activated receptor-alpha mice show enhanced hepatocyte proliferation in response to the hepatomitogen 1,4-bis [2-(3,5-dichloropyridyloxy)] benzene, a ligand of constitutive androstane receptor. *Hepatology* **34,** 262-266.

Columbano A, Ledda-Columbano GM, Pibiri M, Cossu C, Menegazzi M, Moore DD, Huang W, Tian J, Locker J (2005) Gadd45beta is induced through a CAR-dependent, TNF-independent pathway in murine liver hyperplasia. *Hepatology* **42,** 1118-1126.

Columbano A, Ledda-Columbano GM, Pibiri M, Piga R, Shinozuka H, De L, V, Cerignoli F, Tripodi M (1997) Increased expression of c-fos, c-jun and LRF-1 is not required for in vivo priming of hepatocytes by the mitogen TCPOBOP. *Oncogene* **14,** 857-863.

Columbano A, Pibiri M, Deidda M, Cossu C, Scanlan TS, Chiellini G, Muntoni S, Ledda-Columbano GM (2006) The thyroid hormone receptor-{beta} agonist GC-1 induces cell proliferation in rat liver and pancreas. *Endocrinology* **147(7),** 3211-3218.

Columbano A, Shinozuka H (1996) Liver regeneration versus direct hyperplasia. *FASEB J.* **10,** 1118-1128.

Coni P, Simbula G, de Prati AC, Menegazzi M, Suzuki H, Sarma DS, Ledda-Columbano GM, Columbano A (1993) Differences in the steady-state levels of c-fos, c-jun and c-myc messenger RNA during mitogen-induced liver growth and compensatory regeneration. *Hepatology* **17,** 1109-1116.

Corton JC, Lapinskas PJ, Gonzalez FJ (2000) Central role of PPARalpha in the mechanism of action of hepatocarcinogenic peroxisome proliferators. *Mutat.Res.* **448,** 139-151.

Coutant A, Rescan C, Gilot D, Loyer P, Guguen-Guillouzo C, Baffet G (2002) PI3K-FRAP/mTOR pathway is critical for hepatocyte proliferation whereas MEK/ERK supports both proliferation and survival. *Hepatology* **36,** 1079-1088.

Cravatt BF, Simon GM, Yates JR, III (2007) The biological impact of mass-spectrometry-based proteomics. *Nature* **450,** 991-1000.

Cressman DE, Diamond RH, Taub R (1995) Rapid activation of the Stat3 transcription complex in liver regeneration. *Hepatology* **21,** 1443-1449.

D'Arezzo S, Incerpi S, Davis FB, Acconcia F, Marino M, Farias RN, Davis PJ (2004) Rapid nongenomic effects of 3,5,3'-triiodo-L-thyronine on the intracellular pH of L-6 myoblasts are mediated by intracellular calcium mobilization and kinase pathways. *Endocrinology* **145,** 5694-5703.

Davis FB, Mousa SA, O'connor L, Mohamed S, Lin HY, Cao HJ, Davis PJ (2004) Proangiogenic action of thyroid hormone is fibroblast growth factor-dependent and is initiated at the cell surface. *Circ.Res.* **94,** 1500-1506.

Davis FB, Tang HY, Shih A, Keating T, Lansing L, Hercbergs A, Fenstermaker RA, Mousa A, Mousa SA, Davis PJ, Lin HY (2006) Acting via a cell surface receptor, thyroid hormone is a growth factor for glioma cells. *Cancer Res.* **66,** 7270-7275.

Davis PJ, Davis FB (2002) Nongenomic actions of thyroid hormone on the heart. *Thyroid* **12,** 459-466.

Davis PJ, Davis FB (1996) Nongenomic actions of thyroid hormone. *Thyroid* **6,** 497-504.

Davis PJ, Davis FB, Cody V (2005) Membrane receptors mediating thyroid hormone action. *Trends Endocrinol.Metab* **16,** 429-435.

Davis PJ, Leonard JL, Davis FB (2007) Mechanisms of nongenomic actions of thyroid hormone. *Front Neuroendocrinol* **29,** 211-218.

Davis PJ, Shih A, Lin HY, Martino LJ, Davis FB (2000) Thyroxine promotes association of mitogen-activated protein kinase and nuclear thyroid hormone receptor (TR) and causes serine phosphorylation of TR. *J.Biol.Chem.* **275,** 38032-38039.

de Jong M, Visser TJ, Bernard BF, Docter R, Vos RA, Hennemann G, Krenning EP (1993) Transport and metabolism of iodothyronines in cultured human hepatocytes. *J.Clin.Endocrinol.Metab* **77,** 139-143.

De Smaele E, Zazzeroni F, Papa S, Nguyen DU, Jin R, Jones J, Cong R, Franzoso G (2001) Induction of gadd45beta by NF-kappaB downregulates pro-apoptotic JNK signalling. *Nature* **414,** 308-313.

del Rincon SV, Rousseau C, Samanta R, Miller WH, Jr. (2003) Retinoic acid-induced growth arrest of MCF-7 cells involves the selective regulation of the IRS-1/PI 3-kinase/AKT pathway. *Oncogene* **22,** 3353-3360.

Denver RJ, Ouellet L, Furling D, Kobayashi A, Fujii-Kuriyama Y, Puymirat J (1999) Basic transcription element-binding protein (BTEB) is a thyroid hormone-regulated gene in the developing central nervous system. Evidence for a role in neurite outgrowth. *J.Biol.Chem.* **274,** 23128-23134.

Desai VG, Moland CL, Branham WS, Delongchamp RR, Fang H, Duffy PH, Peterson CA, Beggs ML, Fuscoe JC (2004) Changes in expression level of genes as a function of time of day in the liver of rats. *Mutat.Res.* **549,** 115-129.

Didelot C, Schmitt E, Brunet M, Maingret L, Parcellier A, Garrido C (2006) Heat shock proteins: endogenous modulators of apoptotic cell death. *Handb.Exp.Pharmacol.* 171-198.

DiStefano JJ, III, Jang M, Malone TK, Broutman M (1982) Comprehensive kinetics of triiodothyronine production, distribution, and metabolism in blood and tissue pools of the rat using optimized blood-sampling protocols. *Endocrinology* **110,** 198-213.

Engelman JA, Luo J, Cantley LC (2006) The evolution of phosphatidylinositol 3-kinases as regulators of growth and metabolism. *Nat.Rev.Genet.* **7,** 606-619.

Escher P, Wahli W (2000) Peroxisome proliferator-activated receptors: insight into multiple cellular functions. *Mutat.Res.* **448,** 121-138.

Evans RM (1988) The steroid and thyroid hormone receptor superfamily. *Science* **240,** 889-895.

Fausto N (2000) Liver regeneration. *J.Hepatol.* **32,** 19-31.

Fausto N, Campbell JS, Riehle KJ (2006) Liver regeneration. *Hepatology* **43,** S45-S53.

Fausto N, Laird AD, Webber EM (1995) Liver regeneration. 2. Role of growth factors and cytokines in hepatic regeneration. *FASEB J.* **9,** 1527-1536.

Fausto N, Riehle KJ (2005) Mechanisms of liver regeneration and their clinical implications. *J.Hepatobiliary.Pancreat.Surg.* **12,** 181-189.

Feng X, Jiang Y, Meltzer P, Yen PM (2000) Thyroid hormone regulation of hepatic genes in vivo detected by complementary DNA microarray. *Mol.Endocrinol.* **14,** 947-955.

Flores-Morales A, Gullberg H, Fernandez L, Stahlberg N, Lee NH, Vennstrom B, Norstedt G (2002) Patterns of liver gene expression governed by TRbeta. *Mol.Endocrinol.* **16,** 1257-1268.

Forbes SJ, Themis M, Alison MR, Shiota A, Kobayashi T, Coutelle C, Hodgson HJ (2000) Tri-iodothyronine and a deleted form of hepatocyte growth factor act synergistically to enhance liver proliferation and enable in vivo retroviral gene transfer via the peripheral venous system. *Gene Ther.* **7,** 784-789.

Forrest D, Hallbook F, Persson H, Vennstrom B (1991) Distinct functions for thyroid hormone receptors alpha and beta in brain development indicated by differential expression of receptor genes. *EMBO J.* **10,** 269-275.

Francavilla A, Carr BI, Azzarone A, Polimeno L, Wang Z, Van Thiel DH, Subbotin V, Prelich JG, Starzl TE (1994) Hepatocyte proliferation and gene expression induced by triiodothyronine in vivo and in vitro. *Hepatology* **20,** 1237-1241.

Francavilla A, Carr BI, Starzl TE, Azzarone A, Carrieri G, Zeng QH (1992) Effects of rapamycin on cultured hepatocyte proliferation and gene expression. *Hepatology* **15,** 871-877.

Francavilla A, Starzl TE, Carr B, Azzarone A, Carrieri G, Zeng QH, Porter KA (1991) The effects of FK 506, cyclosporine, and rapamycin on liver growth in vitro and in vivo. *Transplant.Proc.* **23,** 2817-2820.

Friesema EC, Docter R, Moerings EP, Verrey F, Krenning EP, Hennemann G, Visser TJ (2001) Thyroid hormone transport by the heterodimeric human system L amino acid transporter. *Endocrinology* **142,** 4339-4348.

Friesema EC, Ganguly S, Abdalla A, Manning Fox JE, Halestrap AP, Visser TJ (2003) Identification of monocarboxylate transporter 8 as a specific thyroid hormone transporter. *J.Biol.Chem.* **278,** 40128-40135.

Friesema EC, Jansen J, Heuer H, Trajkovic M, Bauer K, Visser TJ (2006) Mechanisms of disease: psychomotor retardation and high T3 levels caused by mutations in monocarboxylate transporter 8. *Nat.Clin.Pract.Endocrinol.Metab* **2,** 512-523.

Friesema EC, Jansen J, Milici C, Visser TJ (2005a) Thyroid hormone transporters. *Vitam.Horm.* **70,** 137-167.

Friesema EC, Jansen J, Visser TJ (2005b) Thyroid hormone transporters. *Biochem.Soc.Trans.* **33,** 228-232.

Fu M, Wang C, Li Z, Sakamaki T, Pestell RG (2004) Minireview: Cyclin D1: normal and abnormal functions. *Endocrinology* **145,** 5439-5447.

Fujii C, Nakamoto Y, Lu P, Tsuneyama K, Popivanova BK, Kaneko S, Mukaida N (2005) Aberrant expression of serine/threonine kinase Pim-3 in hepatocellular carcinoma development and its role in the proliferation of human hepatoma cell lines. *Int.J.Cancer* **114,** 209-218.

Fujiwara K, Nagoshi S, Ohno A, Hirata K, Ohta Y, Mochida S, Tomiya T, Higashio K, Kurokawa K (1993) Stimulation of liver growth by exogenous human hepatocyte growth factor in normal and partially hepatectomized rats. *Hepatology* **18,** 1443-1449.

Furuya F, Ying H, Zhao L, Cheng SY (2007) Novel functions of thyroid hormone receptor mutants: beyond nucleus-initiated transcription. *Steroids* **72,** 171-179.

Gaglio PJ, Liu H, Dash S, Cheng S, Dunne B, Ratterree M, Baskin G, Blanchard J, Bohm R, Jr., Theise ND, LaBrecque D (2002) Liver regeneration investigated in a non-human primate model (Macaca mulatta). *J.Hepatol.* **37,** 625-632.

Galletti PM (1971) Applications of plastics in membrane oxygenators. *J.Biomed.Mater.Res.* **5,** 129-134.

Gangloff YG, Mueller M, Dann SG, Svoboda P, Sticker M, Spetz JF, Um SH, Brown EJ, Cereghini S, Thomas G, Kozma SC (2004) Disruption of the mouse mTOR gene leads to early postimplantation lethality and prohibits embryonic stem cell development. *Mol.Cell Biol.* **24,** 9508-9516.

Gerlach C, Sakkab DY, Scholzen T, Dassler R, Alison MR, Gerdes J (1997) Ki-67 expression during rat liver regeneration after partial hepatectomy. *Hepatology* **26,** 573-578.

Germain P, Staels B, Dacquet C, Spedding M, Laudet V (2006) Overview of nomenclature of nuclear receptors. *Pharmacol.Rev.* **58,** 685-704.

Ghaleb AM, Nandan MO, Chanchevalap S, Dalton WB, Hisamuddin IM, Yang VW (2005) Kruppel-like factors 4 and 5: the yin and yang regulators of cellular proliferation. *Cell Res.* **15,** 92-96.

Gibson UE, Heid CA, Williams PM (1996) A novel method for real time quantitative RT-PCR. *Genome Res.* **6,** 995-1001.

Gollner H, Bouwman P, Mangold M, Karis A, Braun H, Rohner I, Del RA, Besedovsky HO, Meinhardt A, van den BM, Cutforth T, Grosveld F, Philipsen S, Suske G (2001) Complex phenotype of mice homozygous for a null mutation in the Sp4 transcription factor gene. *Genes Cells* **6,** 689-697.

Gores GJ, Kost LJ, LaRusso NF (1986) The isolated perfused rat liver: conceptual and practical considerations. *Hepatology* **6,** 511-517.

Gray S, Feinberg MW, Hull S, Kuo CT, Watanabe M, Sen-Banerjee S, DePina A, Haspel R, Jain MK (2002) The Kruppel-like factor KLF15 regulates the insulin-sensitive glucose transporter GLUT4. *J.Biol.Chem.* **277,** 34322-34328.

Grisham JW (1962) A morphologic study of deoxyribonucleic acid synthesis and cell proliferation in regenerating rat liver; autoradiography with thymidine-H3. *Cancer Res.* **22,** 842-849.

Gruters A, Krude H (2007) Update on the management of congenital hypothyroidism. *Horm.Res.* **68 Suppl 5,** 107-111.

Haga S, Ogawa W, Inoue H, Terui K, Ogino T, Igarashi R, Takeda K, Akira S, Enosawa S, Furukawa H, Todo S, Ozaki M (2005) Compensatory recovery of liver mass by Akt-mediated hepatocellular hypertrophy in liver-specific STAT3-deficient mice. *J.Hepatol.* **43,** 799-807.

Hata S, Namae M, Nishina H (2007) Liver development and regeneration: from laboratory study to clinical therapy. *Dev.Growth Differ.* **49,** 163-170.

Hennemann G, Docter R, Friesema EC, de Jong M, Krenning EP, Visser TJ (2001) Plasma membrane transport of thyroid hormones and its role in thyroid hormone metabolism and bioavailability. *Endocr.Rev.* **22,** 451-476.

Hidalgo M, Rowinsky EK (2000) The rapamycin-sensitive signal transduction pathway as a target for cancer therapy. *Oncogene* **19,** 6680-6686.

Higgins, G. M. (1933) Effects of feeding desiccated thyroid gland on restoration of the liver. Archives in Pathology **16,** 227-231.

Higgins GM, Anderson RM (1931) Experimental pathology of liver; restoration of liver of white rat following partial surgical removal. *Archives in Pathology* **12,** 186-202.

Higuchi R, Fockler C, Dollinger G, Watson R (1993) Kinetic PCR analysis: real-time monitoring of DNA amplification reactions. *Biotechnology (N.Y.)* **11,** 1026-1030.

Huang R, Schiano TD, Amolat MJ, Miller CM, Thung SN, Saxena R (2004) Hepatocellular proliferation and changes in microarchitecture of right lobe allografts in adult transplant recipients. *Liver Transpl.* **10,** 1461-1467.

Ijichi C, Matsumura T, Tsuji T, Eto Y (2003) Branched-chain amino acids promote albumin synthesis in rat primary hepatocytes through the mTOR signal transduction system. *Biochem.Biophys.Res.Commun.* **303,** 59-64.

Inoki K, Li Y, Zhu T, Wu J, Guan KL (2002) TSC2 is phosphorylated and inhibited by Akt and suppresses mTOR signalling. *Nat.Cell Biol.* **4,** 648-657.

Iocca HA, Isom HC (2003) Tumor necrosis factor-alpha acts as a complete mitogen for primary rat hepatocytes. *Am.J.Pathol.* **163,** 465-476.

Issemann I, Green S (1990) Activation of a member of the steroid hormone receptor superfamily by peroxisome proliferators. *Nature* **347,** 645-650.

Jaluria P, Konstantopoulos K, Betenbaugh M, Shiloach J (2007) A perspective on microarrays: current applications, pitfalls, and potential uses. *Microb.Cell Fact.* **6,** 4.

James NH, Gill JH, Brindle R, Woodyatt NJ, Macdonald N, Rolfe M, Hasmall SC, Tugwood JD, Holden PR, Roberts RA (1998) Peroxisome proliferator-activated receptor (PPAR) alpha-regulated growth responses and their importance to hepatocarcinogenesis. *Toxicol.Lett.* **102-103,** 91-96.

Johnson DG, Walker CL (1999) Cyclins and cell cycle checkpoints. *Annu.Rev.Pharmacol.Toxicol.* **39,** 295-312.

Jungermann K, Heilbronn R, Katz N, Sasse D (1982) The glucose/glucose-6-phosphate cycle in the periportal and perivenous zone of rat liver. *Eur.J.Biochem.* **123,** 429-436.

Jungermann K, Katz N (1982) Functional hepatocellular heterogeneity. *Hepatology* **2,** 385-395.

Jungermann K, Katz N (1989) Functional specialization of different hepatocyte populations. *Physiol Rev.* **69,** 708-764.

Kaczynski J, Cook T, Urrutia R (2003) Sp1- and Kruppel-like transcription factors. *Genome Biol.* **4,** 206.

Kamada N, Calne RY, Wight DG, Lines JG (1980) Orthotopic rat liver transplantation after long-term preservation by continuous perfusion with fluorocarbon emulsion. *Transplantation* **30,** 43-48.

Kaneshige M, Kaneshige K, Zhu X, Dace A, Garrett L, Carter TA, Kazlauskaite R, Pankratz DG, Wynshaw-Boris A, Refetoff S, Weintraub B, Willingham MC, Barlow C, Cheng S (2000) Mice with a targeted mutation in the thyroid hormone beta receptor

gene exhibit impaired growth and resistance to thyroid hormone. *Proc.Natl.Acad.Sci.U.S.A* **97,** 13209-13214.

Kavok NS, Krasilnikova OA, Babenko NA (2001) Thyroxine signal transduction in liver cells involves phospholipase C and phospholipase D activation. Genomic independent action of thyroid hormone. *BMC.Cell Biol.* **2,** 5.

Kearney T, Dang C (2007) Diabetic and endocrine emergencies. *Postgrad.Med.J.* **83,** 79-86.

Kenessey A, Ojamaa K (2006) Thyroid hormone stimulates protein synthesis in the cardiomyocyte by activating the Akt-mTOR and p70S6K pathways. *J.Biol.Chem.* **281,** 20666-20672.

Klemperer JD, Klein IL, Ojamaa K, Helm RE, Gomez M, Isom OW, Krieger KH (1996) Triiodothyronine therapy lowers the incidence of atrial fibrillation after cardiac operations. *Ann.Thorac.Surg.* **61,** 1323-1327.

Kohrle J (2000) The deiodinase family: selenoenzymes regulating thyroid hormone availability and action. *Cell Mol.Life Sci.* **57,** 1853-1863.

Kohrle J, Brabant G, Hesch RD (1987) Metabolism of the thyroid hormones. *Horm.Res.* **26,** 58-78.

Kolell KJ, Crawford DL (2002) Evolution of Sp transcription factors. *Mol.Biol.Evol.* **19,** 216-222.

Kuzman JA, O'connell TD, Gerdes AM (2007) Rapamycin prevents thyroid hormone-induced cardiac hypertrophy. *Endocrinology* **148,** 3477-3484.

Laity JH, Lee BM, Wright PE (2001) Zinc finger proteins: new insights into structural and functional diversity. *Curr.Opin.Struct.Biol.* **11,** 39-46.

Lakatos P, Stern PH (1991) Evidence for direct non-genomic effects of triiodothyronine on bone rudiments in rats: stimulation of the inositol phosphate second messenger system. *Acta Endocrinol.(Copenh)* **125,** 603-608.

Lazar MA (1993) Thyroid hormone receptors: multiple forms, multiple possibilities. *Endocr.Rev.* **14,** 184-193.

Ledda-Columbano GM, Columbano A, Coni P, Liguori C, Pani P (1987) Liver cell proliferation induced by the mitogen ethylene dibromide, unlike compensatory cell proliferation, does not achieve initiation of rat liver carcinogenesis by diethylnitrosamine. *Cancer Lett.* **36,** 247-252.

Ledda-Columbano GM, Columbano A, Coni PP, Vargiu M, Liguori C, Pani P (1984) Stimulation of DNA synthesis after a single administration of cadmium nitrate. *Toxicol.Lett.* **23,** 267-272.

Ledda-Columbano GM, Columbano A, Pani P (1983) Lead and liver cell proliferation. Effect of repeated administrations. *Am.J.Pathol.* **113,** 315-320.

Ledda-Columbano GM, Coni P, Columbano A (1994) Cell proliferation and cell death in rat liver carcinogenesis by chemicals. *Arch.Toxicol.Suppl* **16,** 271-280.

Ledda-Columbano GM, Coni P, Simbula G, Zedda I, Columbano A (1993) Compensatory regeneration, mitogen-induced liver growth, and multistage chemical carcinogenesis. *Environ.Health Perspect.* **101 Suppl 5,** 163-168.

Ledda-Columbano GM, Molotzu F, Pibiri M, Cossu C, Perra A, Columbano A (2006) Thyroid hormone induces cyclin D1 nuclear translocation and DNA synthesis in adult rat cardiomyocytes. *FASEB J.* **20,** 87-94.

Ledda-Columbano GM, Perra A, Loi R, Shinozuka H, Columbano A (2000a) Cell proliferation induced by triiodothyronine in rat liver is associated with nodule regression and reduction of hepatocellular carcinomas. *Cancer Res.* **60,** 603-609.

Ledda-Columbano GM, Perra A, Pibiri M, Molotzu F, Columbano A (2005) Induction of pancreatic acinar cell proliferation by thyroid hormone. *J.Endocrinol.* **185,** 393-399.

Ledda-Columbano GM, Pibiri M, Concas D, Cossu C, Tripodi M, Columbano A (2002) Loss of cyclin D1 does not inhibit the proliferative response of mouse liver to mitogenic stimuli. *Hepatology* **36,** 1098-1105.

Ledda-Columbano GM, Pibiri M, Concas D, Molotzu F, Simbula G, Cossu C, Columbano A (2003) Sex difference in the proliferative response of mouse hepatocytes to treatment with the CAR ligand, TCPOBOP. *Carcinogenesis* **24,** 1059-1065.

Ledda-Columbano GM, Pibiri M, Cossu C, Molotzu F, Locker J, Columbano A (2004a) Aging does not reduce the hepatocyte proliferative response of mice to the primary mitogen TCPOBOP. *Hepatology* **40,** 981-988.

Ledda-Columbano GM, Pibiri M, Loi R, Perra A, Shinozuka H, Columbano A (2000b) Early increase in cyclin-D1 expression and accelerated entry of mouse hepatocytes into S phase after administration of the mitogen 1, 4-Bis[2-(3,5-Dichloropyridyloxy)] benzene. *Am.J.Pathol.* **156,** 91-97.

Ledda-Columbano GM, Pibiri M, Molotzu F, Cossu C, Sanna L, Simbula G, Perra A, Columbano A (2004b) Induction of hepatocyte proliferation by retinoic acid. *Carcinogenesis* **25,** 2061-2066.

Lee SS, Pineau T, Drago J, Lee EJ, Owens JW, Kroetz DL, Fernandez-Salguero PM, Westphal H, Gonzalez FJ (1995) Targeted disruption of the alpha isoform of the peroxisome proliferator-activated receptor gene in mice results in abolishment of the pleiotropic effects of peroxisome proliferators. *Mol.Cell Biol.* **15,** 3012-3022.

Lehmann JM, Moore LB, Smith-Oliver TA, Wilkison WO, Willson TM, Kliewer SA (1995) An antidiabetic thiazolidinedione is a high affinity ligand for peroxisome proliferator-activated receptor gamma (PPAR gamma). *J.Biol.Chem.* **270,** 12953-12956.

Leonard DM, Stachelek SJ, Safran M, Farwell AP, Kowalik TF, Leonard JL (2000) Cloning, expression, and functional characterization of the substrate binding subunit of rat type II iodothyronine 5'-deiodinase. *J.Biol.Chem.* **275,** 25194-25201.

Lerche-Langrand C, Toutain HJ (2000) Precision-cut liver slices: characteristics and use for in vitro pharmaco-toxicology. *Toxicology* **153,** 221-253.

Lerner LE, Peng GH, Gribanova YE, Chen S, Farber DB (2005) Sp4 is expressed in retinal neurons, activates transcription of photoreceptor-specific genes, and synergizes with Crx. *J.Biol.Chem.* **280,** 20642-20650.

Li W, Liang X, Kellendonk C, Poli V, Taub R (2002) STAT3 contributes to the mitogenic response of hepatocytes during liver regeneration. *J.Biol.Chem.* **277,** 28411-28417.

Li YY, Popivanova BK, Nagai Y, Ishikura H, Fujii C, Mukaida N (2006) Pim-3, a proto-oncogene with serine/threonine kinase activity, is aberrantly expressed in human

pancreatic cancer and phosphorylates bad to block bad-mediated apoptosis in human pancreatic cancer cell lines. *Cancer Res.* **66,** 6741-6747.

Lin HY, Davis FB, Gordinier JK, Martino LJ, Davis PJ (1999) Thyroid hormone induces activation of mitogen-activated protein kinase in cultured cells. *Am.J.Physiol* **276,** C1014-C1024.

Lin HY, Yen PM, Davis FB, Davis PJ (1997) Protein synthesis-dependent potentiation by thyroxine of antiviral activity of interferon-gamma. *Am.J.Physiol* **273,** C1225-C1232.

Locker J, Tian J, Carver R, Concas D, Cossu C, Ledda-Columbano GM, Columbano A (2003) A common set of immediate-early response genes in liver regeneration and hyperplasia. *Hepatology* **38,** 314-325.

Locksley RM, Killeen N, Lenardo MJ (2001) The TNF and TNF receptor superfamilies: integrating mammalian biology. *Cell* **104,** 487-501.

Losel R, Wehling M (2003) Nongenomic actions of steroid hormones. *Nat.Rev.Mol.Cell Biol.* **4,** 46-56.

Loyer P, Cariou S, Glaise D, Bilodeau M, Baffet G, Guguen-Guillouzo C (1996) Growth factor dependence of progression through G1 and S phases of adult rat hepatocytes in vitro. Evidence of a mitogen restriction point in mid-late G1. *J.Biol.Chem.* **271,** 11484-11492.

Lu XP, Koch KS, Lew DJ, Dulic V, Pines J, Reed SI, Hunter T, Leffert HL (1992) Induction of cyclin mRNA and cyclin-associated histone H1 kinase during liver regeneration. *J.Biol.Chem.* **267,** 2841-2844.

Lynch MA, Andrews JF, Moore RE (1985) Low doses of T3 induce a rapid metabolic response in young lambs. *Horm.Metab Res.* **17,** 63-66.

Magami Y, Azuma T, Inokuchi H, Kokuno S, Moriyasu F, Kawai K, Hattori T (2002) Cell proliferation and renewal of normal hepatocytes and bile duct cells in adult mouse liver. *Liver* **22,** 419-425.

Malik R, Habib M, Tootle R, Hodgson H (2005) Exogenous thyroid hormone induces liver enlargement, whilst maintaining regenerative potential--a study relevant to donor preconditioning. *Am.J.Transplant.* **5,** 1801-1807.

Malik R, Mellor N, Selden C, Hodgson H (2003) Triiodothyronine enhances the regenerative capacity of the liver following partial hepatectomy. *Hepatology* **37,** 79-86.

Marsman DS, Cattley RC, Conway JG, Popp JA (1988) Relationship of hepatic peroxisome proliferation and replicative DNA synthesis to the hepatocarcinogenicity of the peroxisome proliferators di(2-ethylhexyl)phthalate and [4-chloro-6-(2,3-xylidino)-2-pyrimidinylthio]acetic acid (Wy-14,643) in rats. *Cancer Res.* **48,** 6739-6744.

Martin DE, Hall MN (2005) The expanding TOR signaling network. *Curr.Opin.Cell Biol.* **17,** 158-166.

Martin H, Sarsat JP, Lerche-Langrand C, Housset C, Balladur P, Toutain H, Albaladejo V (2002) Morphological and biochemical integrity of human liver slices in long-term culture: effects of oxygen tension. *Cell Biol.Toxicol.* **18,** 73-85.

Melle C, Ernst G, Scheibner O, Kaufmann R, Schimmel B, Bleul A, Settmacher U, Hommann M, Claussen U, von EF (2007) Identification of specific protein markers in microdissected hepatocellular carcinoma. *J.Proteome.Res.* **6,** 306-315.

Melle C, Kaufmann R, Hommann M, Bleul A, Driesch D, Ernst G, von EF (2004) Proteomic profiling in microdissected hepatocellular carcinoma tissue using ProteinChip technology. *Int.J.Oncol.* **24,** 885-891.

Menegazzi M, Carcereri-De PA, Suzuki H, Shinozuka H, Pibiri M, Piga R, Columbano A, Ledda-Columbano GM (1997) Liver cell proliferation induced by nafenopin and cyproterone acetate is not associated with increases in activation of transcription factors NF-kappaB and AP-1 or with expression of tumor necrosis factor alpha. *Hepatology* **25,** 585-592.

Michalopoulos GK (2007) Liver regeneration. *J.Cell Physiol.* **213 (2),** 286-300.

Michalopoulos GK, Appasamy R (1993) Metabolism of HGF-SF and its role in liver regeneration. *EXS* **65,** 275-283.

Michalopoulos GK, DeFrances M (2005) Liver regeneration. *Adv.Biochem.Eng Biotechnol.* **93,** 101-134.

Michalopoulos GK, DeFrances MC (1997) Liver regeneration. *Science* **276,** 60-66.

Miller LL, Bly CG, Watson ML, Bale WF (1951) The dominant role of the liver in plasma protein synthesis; a direct study of the isolated perfused rat liver with the aid of lysine-epsilon-C14. *J.Exp.Med.* **94,** 431-453.

Mischinger HJ, Walsh TR, Liu T, Rao PN, Rubin R, Nakamura K, Todo S, Starzl TE (1992) An improved technique for isolated perfusion of rat livers and an evaluation of perfusates. *J.Surg.Res.* **53,** 158-165.

Mistry SJ, Atweh GF (2001) Stathmin inhibition enhances okadaic acid-induced mitotic arrest: a potential role for stathmin in mitotic exit. *J.Biol.Chem.* **276,** 31209-31215.

Moeller LC, Cao X, Dumitrescu AM, Seo H, Refetoff S (2006) Thyroid hormone mediated changes in gene expression can be initiated by cytosolic action of the thyroid hormone receptor beta through the phosphatidylinositol 3-kinase pathway. *Nucl.Recept.Signal.* **4,** e020.

Moeller LC, Dumitrescu AM, Walker RL, Meltzer PS, Refetoff S (2005) Thyroid hormone responsive genes in cultured human fibroblasts. *J.Clin.Endocrinol.Metab* **90,** 936-943.

Morgan KT, Jayyosi Z, Hower MA, Pino MV, Connolly TM, Kotlenga K, Lin J, Wang M, Schmidts HL, Bonnefoi MS, Elston TC, Boorman GA (2005) The hepatic transcriptome as a window on whole-body physiology and pathophysiology. *Toxicol.Pathol.* **33,** 136-145.

Moroy T, Geisen C (2004) Cyclin E. *Int.J.Biochem.Cell Biol.* **36,** 1424-1439.

Morrison TB, Weis JJ, Wittwer CT (1998) Quantification of low-copy transcripts by continuous SYBR Green I monitoring during amplification. *Biotechniques* **24,** 954-8, 960, 962.

Nachtomi E, Farber E (1978) Ethylene dibromide as a mitogen for liver. *Lab Invest* **38,** 279-283.

Nakamura T, Nawa K, Ichihara A (1984) Partial purification and characterization of hepatocyte growth factor from serum of hepatectomized rats. *Biochem.Biophys.Res.Commun.* **122,** 1450-1459.

Nelsen CJ, Rickheim DG, Timchenko NA, Stanley MW, Albrecht JH (2001) Transient expression of cyclin D1 is sufficient to promote hepatocyte replication and liver growth in vivo. *Cancer Res.* **61,** 8564-8568.

Nelsen CJ, Rickheim DG, Tucker MM, Hansen LK, Albrecht JH (2003a) Evidence that cyclin D1 mediates both growth and proliferation downstream of TOR in hepatocytes. *J.Biol.Chem.* **278,** 3656-3663.

Nelsen CJ, Rickheim DG, Tucker MM, McKenzie TJ, Hansen LK, Pestell RG, Albrecht JH (2003b) Amino acids regulate hepatocyte proliferation through modulation of cyclin D1 expression. *J.Biol.Chem.* **278,** 25853-25858.

Nelson CC, Faris JS, Hendy SC, Romaniuk PJ (1993) Functional analysis of the amino acids in the DNA recognition alpha-helix of the human thyroid hormone receptor. *Mol.Endocrinol.* **7,** 1185-1195.

Nobukini T, Thomas G (2004) The mTOR/S6K signalling pathway: the role of the TSC1/2 tumour suppressor complex and the proto-oncogene Rheb. *Novartis.Found.Symp.* **262,** 148-154.

Ohmura T, Ledda-Columbano GM, Piga R, Columbano A, Glemba J, Katyal SL, Locker J, Shinozuka H (1996) Hepatocyte proliferation induced by a single dose of a peroxisome proliferator. *Am.J.Pathol.* **148,** 815-824.

Ozeki A, Tsukamoto I (1999) Retinoic acid repressed the expression of c-fos and c-jun and induced apoptosis in regenerating rat liver after partial hepatectomy. *Biochim.Biophys.Acta* **1450,** 308-319.

Patijn GA, Lieber A, Schowalter DB, Schwall R, Kay MA (1998) Hepatocyte growth factor induces hepatocyte proliferation in vivo and allows for efficient retroviral-mediated gene transfer in mice. *Hepatology* **28,** 707-716.

Peters JM, Cheung C, Gonzalez FJ (2005) Peroxisome proliferator-activated receptor-alpha and liver cancer: where do we stand? *J.Mol.Med.* **83,** 774-785.

Pfaffl MW (2001) A new mathematical model for relative quantification in real-time RT-PCR. *Nucleic Acids Res.* **29,** e45.

Pibiri M, Ledda-Columbano GM, Cossu C, Simbula G, Menegazzi M, Shinozuka H, Columbano A (2001) Cyclin D1 is an early target in hepatocyte proliferation induced by thyroid hormone (T3). *FASEB J.* **15,** 1006-1013.

Popivanova BK, Li YY, Zheng H, Omura K, Fujii C, Tsuneyama K, Mukaida N (2007) Proto-oncogene, Pim-3 with serine/threonine kinase activity, is aberrantly expressed in human colon cancer cells and can prevent Bad-mediated apoptosis. *Cancer Sci.* **98,** 321-328.

Pustylnyak VO, Zakharova LY, Mikhailova ON, Rice RH, Gulyaeva LF, Lyakhovich VV (2005) In vivo effects of protein kinase and phosphatase inhibitors on CYP2B induction in rat liver. *Toxicology* **207,** 315-322.

Revankar CM, Cimino DF, Sklar LA, Arterburn JB, Prossnitz ER (2005) A transmembrane intracellular estrogen receptor mediates rapid cell signaling. *Science* **307,** 1625-1630.

Ribeiro RC, Apriletti JW, Wagner RL, West BL, Feng W, Huber R, Kushner PJ, Nilsson S, Scanlan T, Fletterick RJ, Schaufele F, Baxter JD (1998) Mechanisms of thyroid hormone action: insights from X-ray crystallographic and functional studies. *Recent Prog.Horm.Res.* **53,** 351-392.

Rickheim DG, Nelsen CJ, Fassett JT, Timchenko NA, Hansen LK, Albrecht JH (2002) Differential regulation of cyclins D1 and D3 in hepatocyte proliferation. *Hepatology* **36,** 30-38.

Riedel GL, Scholle JL, Shepherd AP, Ward WF (1983) Effects of hematocrit on oxygenation of the isolated perfused rat liver. *Am.J.Physiol* **245,** G769-G774.

Robb WL (1968) Thin silicone membranes--their permeation properties and some applications. *Ann.N.Y.Acad.Sci.* **146,** 119-137.

Roberts RA, Chevalier S, Hasmall SC, James NH, Cosulich SC, Macdonald N (2002) PPAR alpha and the regulation of cell division and apoptosis. *Toxicology* **181-182,** 167-170.

Roberts RA, Soames AR, Gill JH, James NH, Wheeldon EB (1995) Non-genotoxic hepatocarcinogens stimulate DNA synthesis and their withdrawal induces apoptosis, but in different hepatocyte populations. *Carcinogenesis* **16,** 1693-1698.

Rohde J, Heitman J, Cardenas ME (2001) The TOR kinases link nutrient sensing to cell growth. *J.Biol.Chem.* **276,** 9583-9586.

Rowland BD, Bernards R, Peeper DS (2005) The KLF4 tumour suppressor is a transcriptional repressor of p53 that acts as a context-dependent oncogene. *Nat.Cell Biol.* **7(11),** 1074-1082.

Rowlands DC, Harrison RF, Jones NA, Williams A, Hubscher SG, Brown G (1995) Stathmin is expressed by the proliferating hepatocytes during liver regeneration. *Clin.Mol.Pathol.* **48,** M88-M92.

Rubinacci A, Divieti P, Lodigiani S, De PA, Samaja M (1992) Thyroid hormones and active calcium transport of inside-out red cell membrane vesicles. *Biochem.Med.Metab Biol.* **48,** 235-240.

Sahin F, Kannangai R, Adegbola O, Wang J, Su G, Torbenson M (2004) mTOR and P70 S6 kinase expression in primary liver neoplasms. *Clin.Cancer Res.* **10,** 8421-8425.

Saito S, Tatsumoto T, Lorenzi MV, Chedid M, Kapoor V, Sakata H, Rubin J, Miki T (2003) Rho exchange factor ECT2 is induced by growth factors and regulates cytokinesis through the N-terminal cell cycle regulator-related domains. *J.Cell Biochem.* **90,** 819-836.

Sanders JP, Van der GS, Kaptein E, Darras VM, Kuhn ER, Leonard JL, Visser TJ (1997) Characterization of a propylthiouracil-insensitive type I iodothyronine deiodinase. *Endocrinology* **138,** 5153-5160.

Schafer KA (1998) The cell cycle: a review. *Vet.Pathol.* **35,** 461-478.

Schena M, Shalon D, Davis RW, Brown PO (1995) Quantitative monitoring of gene expression patterns with a complementary DNA microarray. *Science* **270,** 467-470.

Schmidt BM, Martin N, Georgens AC, Tillmann HC, Feuring M, Christ M, Wehling M (2002) Nongenomic cardiovascular effects of triiodothyronine in euthyroid male volunteers. *J.Clin.Endocrinol.Metab* **87,** 1681-1686.

Schmucker DL, Jones AL, Michielsen CE (1975) An improved system for hemoglobin-free perfusion of isolated rat livers. *Lab Invest* **33,** 168-175.

Schwabe RF, Bradham CA, Uehara T, Hatano E, Bennett BL, Schoonhoven R, Brenner DA (2003) c-Jun-N-terminal kinase drives cyclin D1 expression and proliferation during liver regeneration. *Hepatology* **37,** 824-832.

Segal J (1989b) Action of the thyroid hormone at the level of the plasma membrane. *Endocr.Res.* **15,** 619-649.

Segal J (1989c) Acute effect of thyroid hormone on the heart: an extranuclear increase in sugar uptake. *J.Mol.Cell Cardiol.* **21,** 323-334.

Segal J (1989a) A rapid, extranuclear effect of 3,5,3'-triiodothyronine on sugar uptake by several tissues in the rat in vivo. Evidence for a physiological role for the thyroid hormone action at the level of the plasma membrane. *Endocrinology* **124,** 2755-2764.

Segal J, Schwartz H, Gordon A (1977) The effect of triiodothyronine on 2-deoxy-D-(1-3H)glucose uptake in cultured chick embryo heart cells. *Endocrinology* **101,** 143-149.

Sherr CJ, Roberts JM (2004) Living with or without cyclins and cyclin-dependent kinases. *Genes Dev.* **18,** 2699-2711.

Shibata H, Spencer TE, Onate SA, Jenster G, Tsai SY, Tsai MJ, O'Malley BW (1997) Role of co-activators and co-repressors in the mechanism of steroid/thyroid receptor action. *Recent Prog.Horm.Res.* **52,** 141-164.

Shie JL, Chen ZY, Fu M, Pestell RG, Tseng CC (2000) Gut-enriched Kruppel-like factor represses cyclin D1 promoter activity through Sp1 motif. *Nucleic Acids Res.* **28,** 2969-2976.

Shields JM, Christy RJ, Yang VW (1996) Identification and characterization of a gene encoding a gut-enriched Kruppel-like factor expressed during growth arrest. *J.Biol.Chem.* **271,** 20009-20017.

Shih A, Lin HY, Davis FB, Davis PJ (2001) Thyroid hormone promotes serine phosphorylation of p53 by mitogen-activated protein kinase. *Biochemistry* **40,** 2870-2878.

Shinozuka H, Kubo Y, Katyal SL, Coni P, Ledda-Columbano GM, Columbano A, Nakamura T (1994) Roles of growth factors and of tumor necrosis factor-alpha on liver cell proliferation induced in rats by lead nitrate. *Lab Invest* **71,** 35-41.

Shinozuka H, Ohmura T, Katyal SL, Zedda AI, Ledda-Columbano GM, Columbano A (1996) Possible roles of nonparenchymal cells in hepatocyte proliferation induced by lead nitrate and by tumor necrosis factor alpha. *Hepatology* **23,** 1572-1577.

Shiota G, Wang TC, Nakamura T, Schmidt EV (1994) Hepatocyte growth factor in transgenic mice: effects on hepatocyte growth, liver regeneration and gene expression. *Hepatology* **19,** 962-972.

Short J, Brown RF, Husakova A, Gilbertson JR, Zemel R, Lieberman I (1972) Induction of deoxyribonucleic acid synthesis in the liver of the intact animal. *J.Biol.Chem.* **247,** 1757-1766.

Short J, Wedmore R, Kibert L, Zemel R (1980) Triidothyronine: on its role as a specific hepatomitogen. *Cytobios* **28,** 165-177.

Stahlberg N, Merino R, Hernandez LH, Fernandez-Perez L, Sandelin A, Engstrom P, Tollet-Egnell P, Lenhard B, Flores-Morales A (2005) Exploring hepatic hormone actions using a compilation of gene expression profiles. *BMC.Physiol* **5,** 8.

Sun Y, Deng X, Li W, Yan Y, Wei H, Jiang Y, He F (2007) Liver proteome analysis of adaptive response in rat immediately after partial hepatectomy. *Proteomics.* **7,** 4398-4407.

Supp DM, Witte DP, Branford WW, Smith EP, Potter SS (1996) Sp4, a member of the Sp1-family of zinc finger transcription factors, is required for normal murine growth, viability, and male fertility. *Dev.Biol.* **176,** 284-299.

Szanto A, Narkar V, Shen Q, Uray IP, Davies PJ, Nagy L (2004) Retinoid X receptors: X-ploring their (patho)physiological functions. *Cell Death.Differ.* **11 Suppl 2,** S126-S143.

Taga T, Kishimoto T (1997) Gp130 and the interleukin-6 family of cytokines. *Annu.Rev.Immunol.* **15,** 797-819.

Talarmin H, Rescan C, Cariou S, Glaise D, Zanninelli G, Bilodeau M, Loyer P, Guguen-Guillouzo C, Baffet G (1999) The mitogen-activated protein kinase kinase/extracellular signal-regulated kinase cascade activation is a key signalling pathway involved in the regulation of G(1) phase progression in proliferating hepatocytes. *Mol.Cell Biol.* **19,** 6003-6011.

Tang HY, Lin HY, Zhang S, Davis FB, Davis PJ (2004) Thyroid hormone causes mitogen-activated protein kinase-dependent phosphorylation of the nuclear estrogen receptor. *Endocrinology* **145,** 3265-3272.

Taub R (2004) Liver regeneration: from myth to mechanism. *Nat.Rev.Mol.Cell Biol.* **5,** 836-847.

Taub R (1996a) Liver regeneration 4: transcriptional control of liver regeneration. *FASEB J.* **10,** 413-427.

Taub R (1996b) Liver regeneration in health and disease. *Clin.Lab Med.* **16,** 341-360.

Taylor AH, Stephan ZF, Steele RE, Wong NC (1997) Beneficial effects of a novel thyromimetic on lipoprotein metabolism. *Mol.Pharmacol.* **52,** 542-547.

Teshigawara K, Ogawa W, Mori T, Matsuki Y, Watanabe E, Hiramatsu R, Inoue H, Miyake K, Sakaue H, Kasuga M (2005) Role of Kruppel-like factor 15 in PEPCK gene expression in the liver. *Biochem.Biophys.Res.Commun.* **327,** 920-926.

Tsang CK, Qi H, Liu LF, Zheng XF (2007) Targeting mammalian target of rapamycin (mTOR) for health and diseases. *Drug Discov.Today* **12,** 112-124.

Turmelle YP, Shikapwashya O, Tu S, Hruz PW, Yan Q, Rudnick DA (2006) Rosiglitazone inhibits mouse liver regeneration. *FASEB J.* **20,** 2609-2611.

Uchida S, Tanaka Y, Ito H, Saitoh-Ohara F, Inazawa J, Yokoyama KK, Sasaki S, Marumo F (2000) Transcriptional regulation of the CLC-K1 promoter by myc-associated zinc finger protein and kidney-enriched Kruppel-like factor, a novel zinc finger repressor. *Mol.Cell Biol.* **20,** 7319-7331.

Umesono K, Giguere V, Glass CK, Rosenfeld MG, Evans RM (1988) Retinoic acid and thyroid hormone induce gene expression through a common responsive element. *Nature* **336,** 262-265.

Umesono K, Murakami KK, Thompson CC, Evans RM (1991) Direct repeats as selective response elements for the thyroid hormone, retinoic acid, and vitamin D3 receptors. *Cell* **65,** 1255-1266.

van de Bovenkamp, Groothuis GM, Meijer DK, Olinga P (2006a) Precision-cut fibrotic rat liver slices as a new model to test the effects of anti-fibrotic drugs in vitro. *J.Hepatol.* **45,** 696-703.

van de Bovenkamp, Groothuis GM, Meijer DK, Olinga P (2007a) Liver fibrosis in vitro: cell culture models and precision-cut liver slices. *Toxicol.In Vitro* **21,** 545-557.

van de Bovenkamp, Groothuis GM, Meijer DK, Olinga P (2007b) Liver slices as a model to study fibrogenesis and test the effects of anti-fibrotic drugs on fibrogenic cells in human liver. *Toxicol.In Vitro.* **22(3),** 771-778.

van de Bovenkamp, Groothuis GM, Meijer DK, Slooff MJ, Olinga P (2006b) Human liver slices as an in vitro model to study toxicity-induced hepatic stellate cell activation in a multicellular milieu. *Chem.Biol.Interact.* **162,** 62-69.

Verducci JS, Melfi VF, Lin S, Wang Z, Roy S, Sen CK (2006) Microarray analysis of gene expression: considerations in data mining and statistical treatment. *Physiol Genomics* **25,** 355-363.

Verga FC, Petrucci E, Patriarca V, Michienzi S, Stigliano A, Brunetti E, Toscano V, Misiti S (2007) Thyroid hormone receptor TRbeta1 mediates Akt activation by T3 in pancreatic beta cells. *J.Mol.Endocrinol.* **38,** 221-233.

Vinciguerra M, Veyrat-Durebex C, Moukil MA, Rubbia-Brandt L, Rohner-Jeanrenaud F, Foti M (2008) PTEN down-regulation by unsaturated fatty acids triggers hepatic steatosis via an NF-kappaBp65/mTOR-dependent mechanism. *Gastroenterology* **134,** 268-280.

Wahlstrom GM, Sjoberg M, Andersson M, Nordstrom K, Vennstrom B (1992) Binding characteristics of the thyroid hormone receptor homo- and heterodimers to consensus AGGTCA repeat motifs. *Mol.Endocrinol.* **6,** 1013-1022.

Wang YG, Dedkova EN, Fiening JP, Ojamaa K, Blatter LA, Lipsius SL (2003) Acute exposure to thyroid hormone increases Na+ current and intracellular Ca2+ in cat atrial myocytes. *J.Physiol* **546,** 491-499.

Warburg O. Versuche an überlebendem Karzinomgewebe. Biochem.Z. 142, pp. 317-333. 1923.

Webber EM, Godowski PJ, Fausto N (1994) In vivo response of hepatocytes to growth factors requires an initial priming stimulus. *Hepatology* **19,** 489-497.

Wehling M, Losel R (2006) Non-genomic steroid hormone effects: membrane or intracellular receptors? *J.Steroid Biochem.Mol.Biol.* **102,** 180-183.

Wehling M, Schultz A, Losel R (2006) Nongenomic actions of estrogens: exciting opportunities for pharmacology. *Maturitas* **54,** 321-326.

Wei D, Gong W, Kanai M, Schlunk C, Wang L, Yao JC, Wu TT, Huang S, Xie K (2005) Drastic down-regulation of Kruppel-like factor 4 expression is critical in human gastric cancer development and progression. *Cancer Res.* **65,** 2746-2754.

Weitzel JM, Hamann S, Jauk M, Lacey M, Filbry A, Radtke C, Iwen KA, Kutz S, Harneit A, Lizardi PM, Seitz HJ (2003) Hepatic gene expression patterns in thyroid hormone-treated hypothyroid rats. *J.Mol.Endocrinol.* **31,** 291-303.

Wikenheiser-Brokamp KA (2006) Retinoblastoma family proteins: insights gained through genetic manipulation of mice. *Cell Mol.Life Sci.* **63,** 767-780.

Williams GR (2000) Cloning and characterization of two novel thyroid hormone receptor beta isoforms. *Mol.Cell Biol.* **20,** 8329-8342.

Witzgall R, Obermuller N, Bolitz U, Calvet JP, Cowley BD, Jr., Walker C, Kriz W, Gretz N, Bonventre JV (1998) Kid-1 expression is high in differentiated renal proximal tubule cells and suppressed in cyst epithelia. *Am.J.Physiol* **275,** F928-F937.

Wong ML, Medrano JF (2005) Real-time PCR for mRNA quantitation. *Biotechniques* **39,** 75-85.

Wullschleger S, Loewith R, Hall MN (2006) TOR Signaling in Growth and Metabolism. *Cell* **124,** 471-484.

Yamamoto J, Ikeda Y, Iguchi H, Fujino T, Tanaka T, Asaba H, Iwasaki S, Ioka RX, Kaneko IW, Magoori K, Takahashi S, Mori T, Sakaue H, Kodama T, Yanagisawa M, Yamamoto TT, Ito S, Sakai J (2004) A Kruppel-like factor KLF15 contributes fasting-

induced transcriptional activation of mitochondrial acetyl-CoA synthetase gene AceCS2. *J.Biol.Chem.* **279,** 16954-16962.

Yang SQ, Lin HZ, Mandal AK, Huang J, Diehl AM (2001) Disrupted signaling and inhibited regeneration in obese mice with fatty livers: implications for nonalcoholic fatty liver disease pathophysiology. *Hepatology* **34,** 694-706.

Yen PM (2001) Physiological and molecular basis of thyroid hormone action. *Physiol Rev.* **81,** 1097-1142.

Yen PM, Feng X, Flamant F, Chen Y, Walker RL, Weiss RE, Chassande O, Samarut J, Refetoff S, Meltzer PS (2003) Effects of ligand and thyroid hormone receptor isoforms on hepatic gene expression profiles of thyroid hormone receptor knockout mice. *EMBO Rep.* **4,** 581-587.

Zajicek G, Oren R, Weinreb M, Jr. (1985) The streaming liver. *Liver* **5,** 293-300.

Zhang J, Lazar MA (2000) The mechanism of action of thyroid hormones. *Annu.Rev.Physiol* **62,** 439-466.

Zimmers TA, McKillop IH, Pierce RH, Yoo JY, Koniaris LG (2003) Massive liver growth in mice induced by systemic interleukin 6 administration. *Hepatology* **38,** 326-334.

PUBLICATIONS

PAPERS

MICROARRAY ANALYSIS OF THE RODENT HEPATIC RESPONSE TO T3

Bungay A, Selden C, Brown D, Malik R, Hubank M, Hodgson H

UCL Institute of Hepatology, Royal Free & University College Medical School, Royal Free Campus, Rowland Hill Street, Hampstead, London NW3 2PF

Telephone: +4420 7433 2862 Fax: +4420 7433 2852

E-mail: a.bungay@medsch.ucl.ac.uk

The Journal of Gastroenterology and Hepatology

Accepted for publication April 2008

POSTER PRESENTATION BASL DUBLIN 2006

THE KRUPPEL FACTOR Sp4 HELPS MEDAITE THE HEPATIC T3 MITOGENIC RESPONSE

Anton Bungay, Clare Selden and Humphrey Hodgson.

UCL Institute of Hepatology, Royal Free & University College Medical School, Royal Free Campus, Rowland Hill Street, Hampstead, London NW3 2PF

Telephone: +4420 7433 2862 Fax: +4420 7433 2852

E-mail: a.bungay@medsch.ucl.ac.uk

Background: Tri-iodothyronine, T3, a primary hepatic mitogen offers exciting therapeutic opportunities in liver surgery and in acute liver disease to increase liver mass and function. It has been impossible to directly demonstrate an effect of T3 in humans. Its effects are modelled in rodents in vivo. An understanding of the mitogenic mechanism of action of T3 is crucial prior to its human use.

Kruppel Factors (evolutionarily conserved zinc finger containing transcription factors) are implicated in virtually all facets of cellular function, including proliferation, apoptosis, differentiation and neoplastic transformation. During a structured analysis of liver gene expression induced by T3 we investigated KF expression; in particular pursuing the hypothesis that alteration in expression of one of these may define a critical pathway involved in the T3 proliferative response.

Aim: To analyse the hepatic expression of T3 regulated genes using a whole-rat genome microarray, then to investigate the hepatic expression over time of some KFs using quantitative real time PCR.

Methods: An Affymetrix expression array compared RNA prepared from mitogenic T3 treated and submitogenic T3 treated rat liver at 1h. Real time PCR was used to measure the expression of Kruppel factors over time in mitogenic and submitogenic T3 treated rat liver.

Results: ZFP354A, KF15 and KF9 are not critical in mediating mitogenic T3 effects as their expression rises in both mitogenic and submitogenic T3 treated rat liver. Sp4 however exhibits a FC of +4.15 on the microarray and its expression is increased at 1h after mitogenic T3 using quantitative real time PCR, confirming the microarray result.

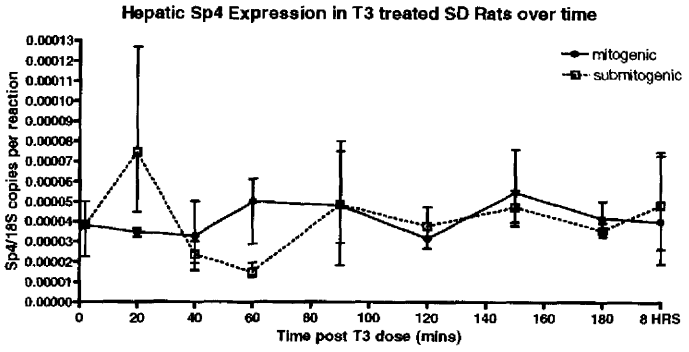

Conclusion: Sp Kruppel Factors contribute to a metastatic tumour phenotype and are known to be involved in cell cycle control but their exact roles are yet to be fully described and identified. Sp4's up-regulation as an early event in T3 induced liver proliferation (but not when T3 is at submitogenic doses) suggests it plays a critical role in the mitogenic action of T3 on the liver.

POSTER PRESENTATION AASLD 2006

STIMULATION OF HEPATOCYTE PROLIFERATION AND LIVER GROWTH BY TRI-IODOTHYRONINE AND ITS RELATIONSHIP TO BCL-3 EXPRESSION

Raza Malik, Anton Bungay, Marc Riemann, Roland Schmid, Mike Hubank, Clare Selden and Humphrey Hodgson.

UCL Institute of Hepatology, Royal Free & University College Medical School, Royal Free Campus, Rowland Hill Street, Hampstead, London NW3 2PF

Telephone: +4420 7433 2862 Fax: +4420 7433 2852

E-mail: a.bungay@medsch.ucl.ac.uk

Background: We and others have demonstrated the effects of thyroid hormone as a mitogen that induces hepatocyte proliferation and enhances liver mass. These experiments provide a potential strategy to use primary mitogens in the field of liver surgery, enhancing liver mass thus pre-conditioning the liver prior to resection or living-related transplants. We use Feng et al's data from a cDNA microarray of livers of hypothyroid mice subjected to T3 stimulation at mitogenic doses. There were 55/2225 mouse genes regulated by T3 and we used these to identify possible candidates for the proliferative pathway initiated by T3. The genes affecting cell proliferation included Kip1p, CHD-1 and Bcl-3. Bcl-3 appeared as a plausible candidate for the mitogenic effects of T3 – Bcl-3 is an IKB- related protein that enhances NF-KB activity resulting in the expression of a variety of cellular genes, including those regulating cell proliferation, and Bcl-3 mutations in human lymphocytes induce cellular proliferation. The first two proteins are mitotic spindle components.

Methods: We confirmed by microarray, in euthyroid rats subject to a mitogenic dose of T3, that Bcl-3 mRNA was also unregulated in rats within 3h of T3 administration. We then used real time PCR to quantify levels of Bcl-3 mRNA in the liver and SDS-PAGE electrophoresis/western blotting to demonstrate protein expression serially.

Results: Hepatocyte proliferation in rats peaked at 24 hours (7±1.1% cf. <1%) after T3. There was a progressive increase in expression of Bcl-3 in the livers of rats receiving T3, with the peak increase in mRNA expression (Bcl-3:18S ratio 0.63 ± 0.11 cf. 0.40 ± 0.03 in controls – $P < 0.01$) and protein expression ($P < 0.01$) also occurring 24 hours after T3 was given. However, comparing Bcl-3 knockout mice and the wild-type parental strain, there was no difference in the proportion of hepatocytes in DNA synthesis 28h after T3 administration.

Discussion: The potential use of primary mitogens in liver surgery in humans is dependant on identifying the underlying mechanism in rodents. Although there is an up-regulation of Bcl-3 in the livers of rodents stimulated with T3 this IKB-related protein does not appear to be critical to the process of T3 induced liver cell hyperplasia.